Investigations of the Reactivity of Bis(trichlorostannyl)organyl Compounds

DISSERTATION

zur Erlangung des akademischen Grades eines

DOKTORS DER NATURWISSENSCHAFTEN

(Dr. rer. nat.)

dem Fachbereich Chemie

der Philipps-Universität Marburg

vorgelegt von

Hari Pada Nayek, M.Sc.

aus Howrah, Indien

Marburg/Lahn 2009

Die vorliegende Arbeit entstand in der Zeit von August 2006 bis July 2009 unter der Anteitung von Frau Prof. Dr. Stefanie Dehnen am Fachbereich Chemie der Phillips-Universität Marburg.

1. Gutachter: Prof. Dr. S. Dehnen

2. Gutachter: Prof. Dr. J. Sundermeyer

Tag der mündlichen Prüfung:

Dedicated to my parents

The extraordinary does not happen on plain, ordinary ways

Johann Wolfgang von Goethe

Acknowledgements

The research presented in this thesis would not have been possible without the generous help and support of many people. In this section I would like to thank and acknowledge all of them.

Firstly, I would like to thank my advisor Prof. Dr. Stefanie Dehnen for her intellectual and professional guidance, for the opportunity to work in an exciting research group, for involving me in the preparation of many manuscripts, and especially for allowing me a large degree of independence and creative freedom to explore a wide range of synthetic aspirations.

I am grateful to Prof. Jörg Sundermeyer, who commented on my research and reviewed the thesis.

I would also like to express my thanks to Prof. Dr. Werner Massa and Dr. Klaus Harms for helping me in crystal structure analysis and Frau Geiseler for collecting single crystal data.

I would like to thank Dr. Frank Weller, Fritjof Schmock and Cornelia Mischke, who provided me with valuable results in the IR and Raman spectroscopy analyses.

I am grateful to Dr. Seema Agarwal for her help with thermogravimetric analyses.

I would like to thank Clemens Pietzonka for recording EDX spectra and for teaching me how to measure EDX.

I am grateful to my students, Stefanie Uhlmann, Leonid Schaaf, Stephan Hammer, Wang Di and Heinke Thrun for synthesizing a lot of compounds.

I would like to thank all past and present members of the Dehnen research group, Ursula Siepe, Dr. Maike Melullis, Dr. Eugen Ruzin, Dr. Sima Haddadpour, Dr. Zhien Lin, Dr. Reza Halvagar, Susanne Burtzlaff, Heiko Niedermeyer, Felicitas Lips, Zohre

Table of Contents

5   Crystallographic Data…………………………116

Chapter 1

Introduction

1.1 Tin

Tin, the element of the atomic number 50, is a member of Group 14 of the periodic table. People have been using tin for thousands of years in the form of alloys. Tin and its compounds have many important applications starting from small preparative to large industrial scales. Tin forms a large variety of different compounds in combination with other elements. Tin, organotin compounds and chalcogenostannates have been extensively studied due to interesting catalytic or biological activities, as well as their precursor function for the generation of tinchalcogenide films in opto-electronic applications [1].

1.1.1 Occurrence

Scientists believe that the atoms of the heavy elements (such as tin) are formed as the atoms of lighter elements (such as helium) fused during nuclear reactions occurring inside the supernovas. When supernovas run out of energy they explode. The blast sprays out the elements all over the universe. Billions of years ago, heavy elements from an exploding supernova reached Earth. Although, it is also possible to find native or pure tin, in most cases tin is available in the form of minerals, combined with other elements. The most important tin mineral is Cassiterite or Tinstone (tin oxide; SnO_2), containing about 80% of the metal on Earth. Other minerals are sulfidic in nature and include Stannite, $SnS_2 \cdot Cu_2S \cdot FeS$, a complex tin compound containing copper, iron and sulfur, Herzenbergite, SnS, Teallite, $SnS \cdot PbS$; Franckeite, $2SnS_2 \cdot Sb_2S_3 \cdot 5PbS$, Cylindrite, $Sn_6Pb_6Sb_2Sn$ and Plumbostannite, $2SnS_2 \cdot 2PbS \cdot 2(Fe.Zn)S \cdot Sb_2S_3$. Initially, Britain and Spain were the major sources of tin minerals. Now, Southeast Asia and China account for

more than 60 percent of the world's annual supply of tin minerals. Bolivia, Brazil, Peru, Australia, Russia, Zimbabwe also supply tin minerals as source of tin [2].

1.1.2 Physical Properties of Metallic Tin

Tin is a soft and malleable metal, which is easily transformable into different shapes. It has one of the lowest melting points of all the metals. It melts at 232 ºC and stays at liquid phase up to 2270 ºC. Tin exists in three different allotropes: Gray or alpha tin, white or beta tin and brittle or gamma tin. Gray tin is the semi-metallic form of the element and is stable below 14 ºC. White or beta tin is a silvery white metal and is stable between 14 ºC and 161 ºC, whereas gamma tin is stable between 161 ºC and 232 ºC. Tin has 10 stable isotopes (Table 1.1), the largest number of stable isotopes of any element. In addition, many unstable isotopes exist with half-lives in the range of 2.2 minutes to 10^5 years [3, 4].

Table 1.1 Stable isotopes of tin

Isotope	Mass	Abundance (%)
^{112}Sn	111.90494	0.95
^{114}Sn	113.90296	0.65
^{115}Sn	114.90353	0.34
^{116}Sn	115.90211	14.24
^{117}Sn	116.90306	7.57
^{118}Sn	117.90179	24.01
^{119}Sn	118.90339	8.58
^{120}Sn	119.90213	32.97
^{122}Sn	121.90341	4.71
^{124}Sn	123.90524	5.98

1.1.3 Chemical Properties

Tin is relatively unaffected by both water and oxygen at room temperature. It does not rust, corrode, or react normally. This explains one of its major uses as a coating material to protect other metals to prevent corrosion. At higher temperatures, however, the metal reacts with both water (as steam) and oxygen to form tin oxide. Tin dissolves easily in concentrated acids and in hot alkaline solutions, such as hot concentrated potassium hydroxide. The metal also reacts with the halogens to form compounds such as tin chloride and tin bromide. It also forms a wide variety of compounds with sulfur, selenium, and tellurium. Organotin compounds are also well established. The ground state of tin is ^3P according to the [Kr] $4d^{10}5s^25p^2$ configuration. A covalence two is expected from this ground state configuration. In order to form covalence four a ^5S state with four uncoupled electrons is required. Tin forms predominately covalent bonds with other elements but those bonds exhibit a high degree of ionic character [3].

1.2 Inorganic Tin Chalcogen Compounds

1.2.1 Chalcogenidostannates

Chalcogenidometallates of Group 14 (semi)metals have been an extensively explored research area during the last decades because of their unique properties and potential applications, such as semiconductivity, photoconductivity, non-linear optics, catalysis, and ion exchange capability [5-11]. A wide variety of chalcogenidostannates and their homologue chalcogenidogermanates have been reported starting from small SnE (S, Se, and Te) to larger polymeric frameworks. Table 1.2 shows the optical band gap of some of the binary and ternary chalgenidometallates indicating their semi-conducting nature [12].

The basic and most fundamental building block of this family (Figure 1.1) is the tetrahedral monomeric $[SnE]^{4-}$ anion. $[Sn_2E_7]^{6-}$ is composed of two *corner*-sharing tetrahedra, the structure of which correspond to familiar oxoanions such as $[Si_2O_7]^{6-}$, $[P_2O_7]^{4-}$, and represents the first step of the possible condensation reactions of the tetrahedron [13]. Another type of dimeric species is $[Sn_2E_6]^{4-}$ consisting of two *edge*-

Table 1.2 Band gaps of some chalcogenidometallates [12]

Binary Phase	Band Gap (eV)	Ternary Phase	Band Gap (eV)
Cu_2S	1.1-1.3	$CuInS_2$	1.5
Cu_2Se	0.9-1.1	$CuInSe_2$	1.0
Ag_2S	0.8-1.0	$CdIn_2Se_4$	1.4
Ag_2Se	0.2	Cu_2GeSe_3	0.9
$CdSe$	1.7-2.3	Ag_8GeSe_6	0.9
In_2S_3	2.6	Ag_8SnSe_6	0.8
In_2Se_3	1.4	$AgAsS_2$	2.0
$GeSe_2$	2.5		
$SnSe_2$	2.7		
As_2S_3	2.6		

$[SnS_4]^{4-}$ $[Sn_2S_7]^{6-}$ $[\{SnS_3\}^{2-}]_n$

$[Sn_2S_6]^{4-}$ $[Sn_4S_{10}]^{4-}$
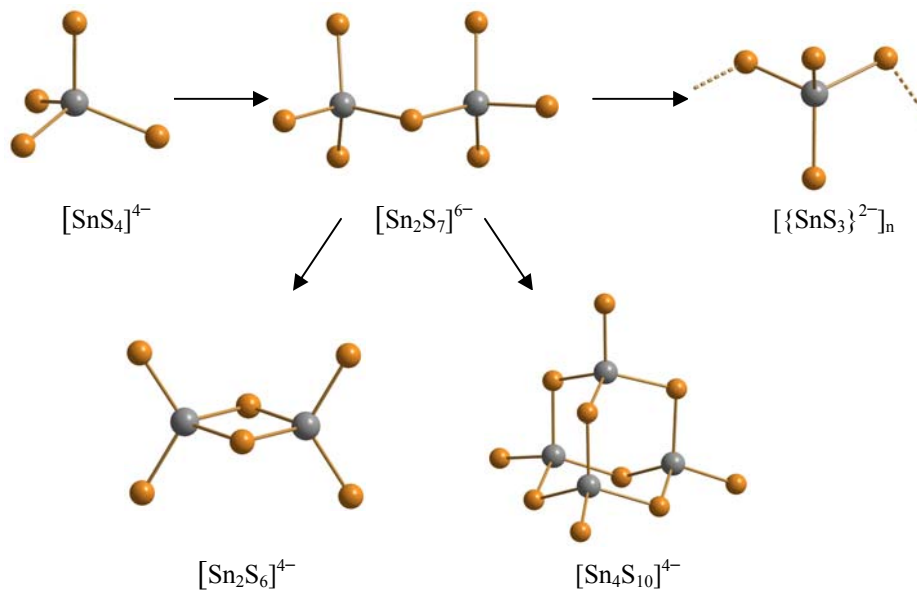
Figure 1.1 Condensation pathways of the $[SnS_4]^{4-}$ tetrahedron, color code: Sn, gray; S, yellow

sharing tetrahedra. Polymeric species $[(SnE_3)^{2-}]_n$ represent *corner*-sharing tetrahedral chains. Tetrameric adamantane-like species of the composition $[Sn_4E_{10}]^{4-}$ are produced as the predominant condensation products in solutions of lower pH-values, between pH = 7 and pH = 3. A large number of chalcogenidostannates have been discovered during last decades. The anionic charge is compensated either by alkali, alkaline metal ions or organic cations. For instances, A_4SnE_4 or $A_4Sn_2E_6$ (A = Na, K, Li, Cs, $[NR_4]^+$, $[enH]^+$; *en* = 1,2-diaminomethane and E = S, Se, Te) were synthesized by solid state reactions, solvothermal or hydrothermal reactions [14-26]. Also polychalcogenidostannates were reported. For instance, a polythiostanate, $A_2Sn_3E_7$ (A = Cs, NMe_4^+, NEt_4^+; E = S, Se) has been shown to consist of the framework of composition $[Sn_3E_7]^{2-}$ with two exchangeable A^+ ions occupying cavities in the structure (Figure 1.2); these cations can be exchanged with a variety of further alkali, alkaline earth or transition metal cation [27-28].
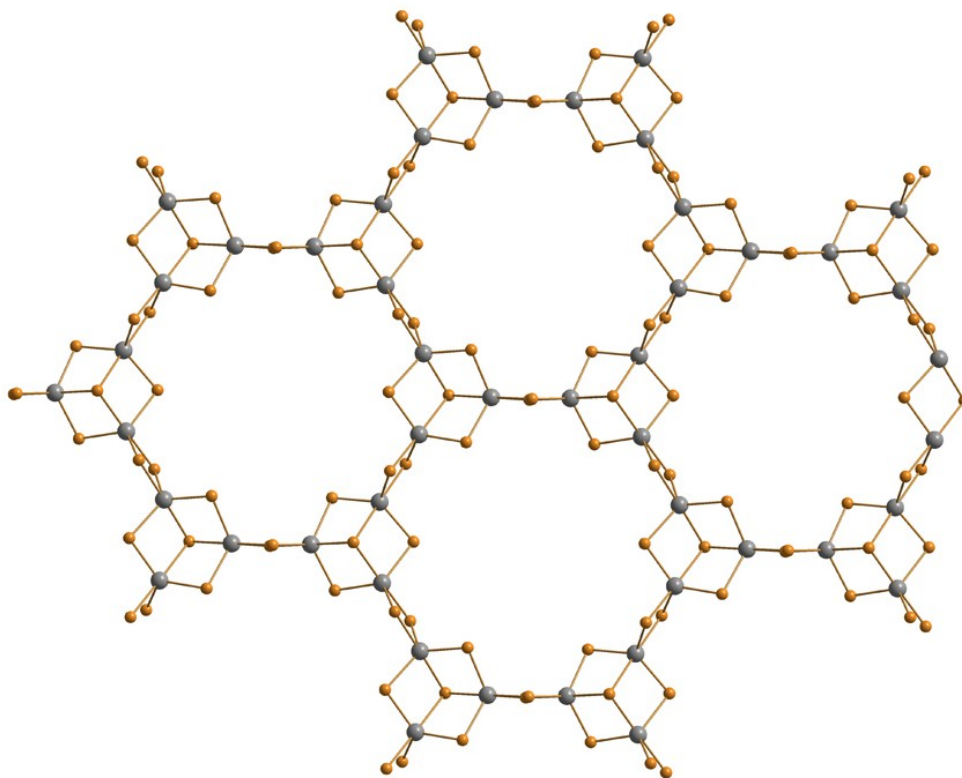
Figure 1.2 Fragment of one $[\{SnS_3\}^{2-}]_n$ layer in the crystal structure of $[NMe_4^+]_2[Sn_3S_7]\cdot H_2O$, color code: Sn, gray; S, yellow

A methanolothermal reaction of $SnSe_2$ and *en* (160 °C) ends up with the neutral polymeric phase [2SnSe$_2$·*en*], containing chain-type $^1_\infty$[2SnSe$_2$·*en*] aggregates which is based on alternating, *edge*-sharing [SnSe$_4$] tetrahedra and [SnSe$_4$(*en*)] octahedral (Figure 1.3) [29].
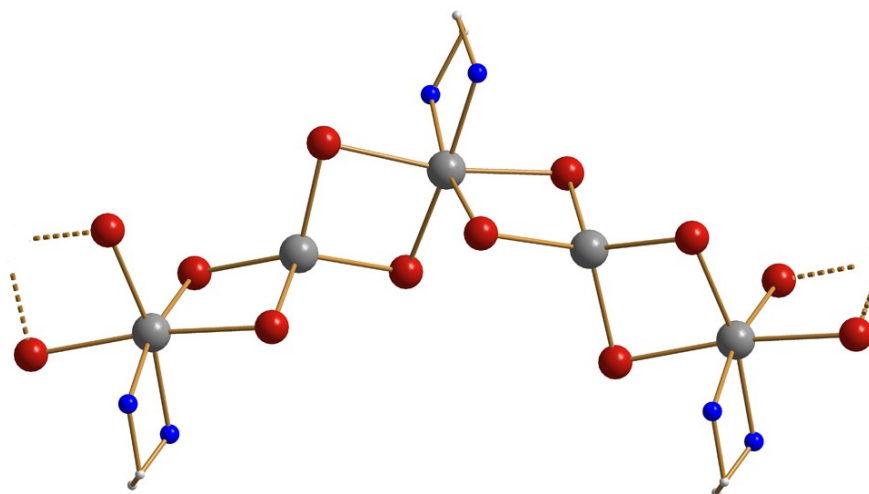
Figure 1.3 Fragment of the polymeric chain structure of [2SnSe$_2$·*en*]$_\infty$, color code: Sn, gray; Se, red; N, blue; C, light gray

1.2.2 Ternary Tin Chalcogenide Clusters

The formation of compounds that contain ternary heavy atom M/E'/E frameworks, in which binary aggregates of main group elements of group 14-16 are coordinated to transition metal ions M^{n+} are actively investigated by several research groups. This is the result both the multifaceted structural variety and the interesting optoelectronic and magnetic properties of the resulting ternary or multinary compounds that in some cases combine the properties of the formally underlying binary phases. *Dehnen et al.* reported among others a series of ternary T3 and P1 clusters, synthesized by reacting binary 14/16 anions with transition metal ions, [Na$_{10}$(H$_2$O)$_{32}$][M$_5$Sn(μ_3-S)$_4$(SnS$_4$)$_4$]·2H$_2$O (M = Zn, Co) and [K$_{10}$(H$_2$O)$_{20}$][M$_4$Sn(μ_4-Te)(SnTe$_4$)$_4$] (M = Zn, Mn, Cd), the magnetic and optical properties of which were investigated (Figure 1.4) [30-32]. Figure 1.5 shows the UV-vis spectra of the series of compounds [K$_{10}$(ROH)$_n$][M$_4$(μ_4-E)(SnE$_4$)$_4$] for M = Zn, Mn, Cd,

Hg, and E = Se, Te. The spectra show that with replacement of selenium by tellurium there is a sharp change in the band gap to lower energies. However, for a given chalcogenide, fine-tuning of the band gap is achieved by the choice of metal.
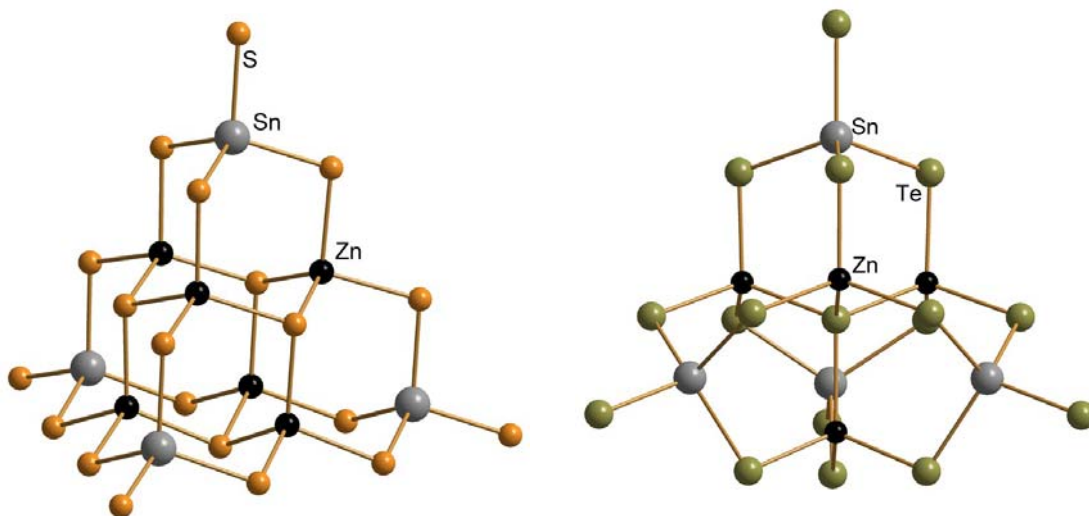
Figure 1.4 T3 and P1 ternary clusters
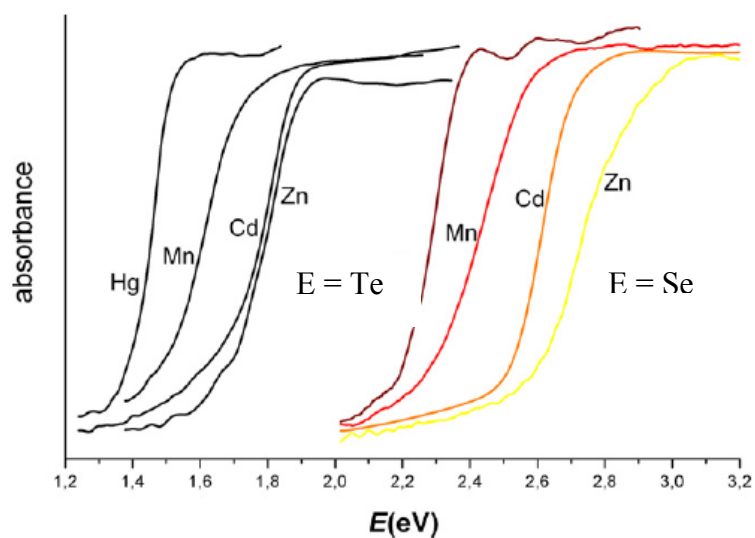
Figure 1.5 Solid state UV-vis spectra of compounds $[K_{10}(ROH)_n][M_4(\mu_4\text{-}E)(SnE_4)_4]$ for M = Zn, Mn, Cd, Hg; E = Se (right hand side) or Te (left hand side), R = H, (n = 20) or R = H, Me (n = 16.5, 0.5)

Kanatzidis et al. showed that various sulfide and selenide clusters $[ME_4]^{4-}$, $[M_2E_6]^{4-}$, and $[M_4E_{10}]^{4-}$ (M = Ge, Sn; E = S, Se), when bound to metal ions Pt^{2+}, yield gels having porous frameworks (eq. 1.1-1.3) [33]. These gels can be transformed to aerogels after supercritical drying with carbon dioxide. The aero gels possess a high internal surface area (up to 327 m^2/gm) and broad pore size distribution. The pores of these sulfide and selenide materials absorb heavy metals. The materials show narrow energy gaps between 0.2 and 2.0 electron volts and low densities, and they may be useful in optoelectronics, or in the removal of heavy metals from water.

$$(R_4N)_4[M_4E_{10}] + 2\ K_2PtCl_4 \rightarrow Pt_2[M_4E_{10}] + 4\ KCl + 4\ R_4NCl \tag{1.1}$$

$$K_4[M_2E_6] + 2\ K_2PtCl_4 \rightarrow Pt_2[M_2E_6] + 8\ KCl \tag{1.2}$$

$$A_4[ME_4] + 2\ K_2PtCl_4 \rightarrow Pt_2[ME_4] + 4\ KCl + 4\ ACl \tag{1.3}$$
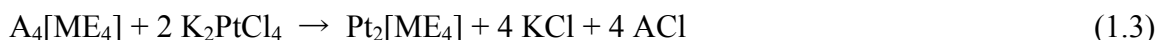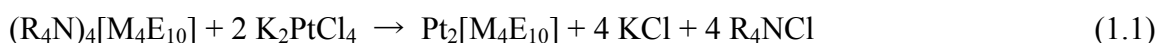
(R = Me, Et; M = Ge, Sn; E = S, Se; and A = Na, K)

In these reactions, all chloride ligands of $[PtCl_4]^{2-}$ can be replaced by the E terminal atoms of chalcogenido clusters, generating materials with a formula of $Pt_2[M_4E_{10}]$.
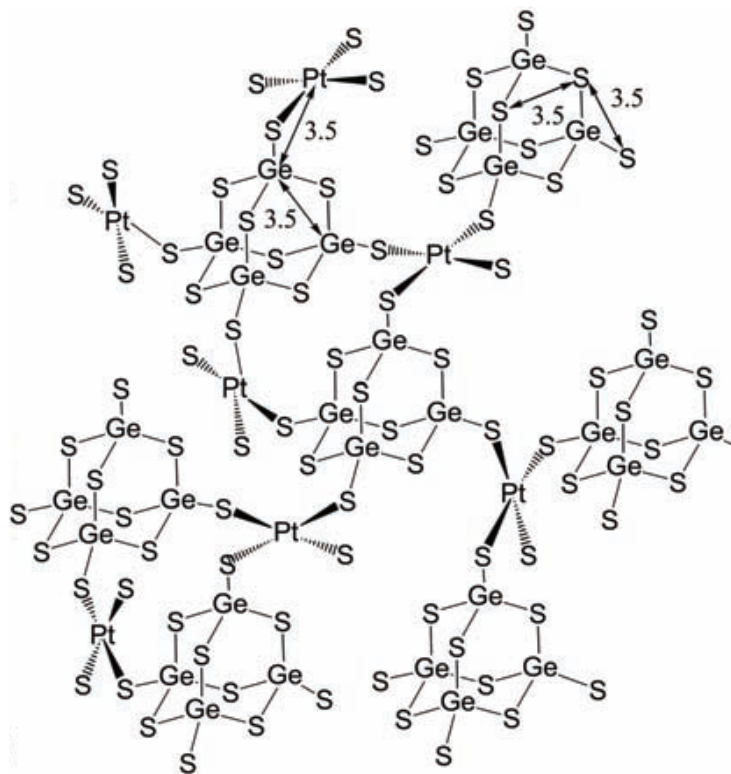
Figure 1.6 Polymeric structure of the chalcogel material $Pt_2[Ge_4S_{10}]$

Recently, *Trikalitis* and *Dehnen et al.* reported the synthesis of $(R_4N)_4[Sn_4E_{10}]$ (E = S, Se, Te) from $K_2Sn_2E_5$ with stoichiometric amounts of alkyl-ammonium bromides R_4NBr (R = Me or Et) in ethylenediamine (*en*). These salts were further used to synthesize a family of open-framework compounds $(Me_4N)_2[MSn_4Se_{10}]$ (M = Mn, Fe, Co, Zn) by reactions with transition metal salts. Depending on the transition metal in $(Me_4N)_2[MSn_4Se_{10}]$, the band gaps of these compounds vary from 1.27 to 2.23 eV. $(Me_4N)_2[MnGe_4Te_{10}]$ is the first telluride analogue and is a narrow band gap semiconductor with an optical absorption energy of 0.69 eV [34-35].
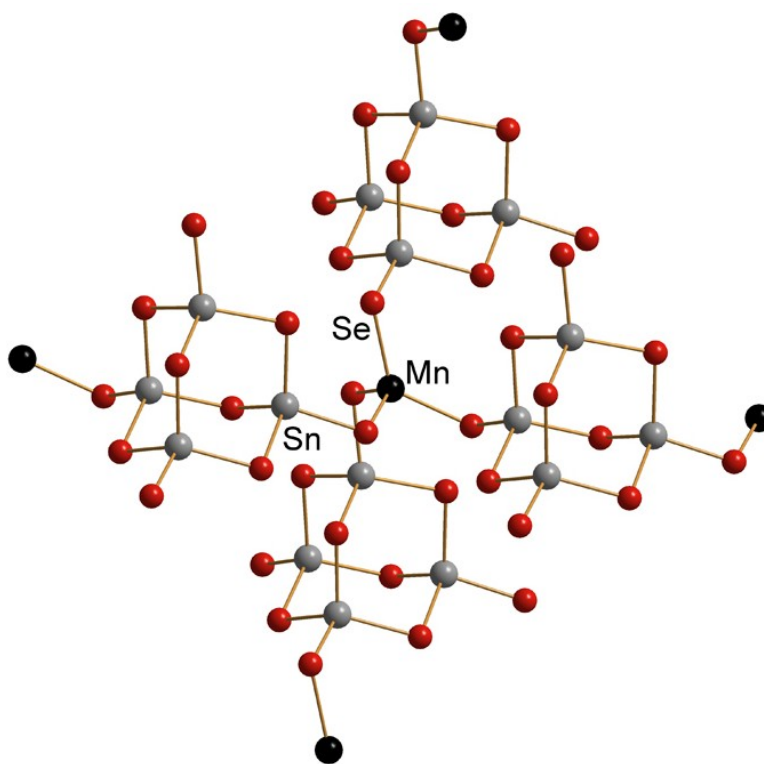
Figure 1.7 Fragment of the anionic open framework structure of $(R_4N)_4[MnSn_4Se_{10}]$

1.3 Organotin Compounds

Organotin compounds are substances comprising at least one tin–carbon bond. Organotin chemistry became a distinct area more than 150 years ago, when the first organotin compound, Et_2SnI_2 was discovered by *Frankland* on 1849 [36-37]. At present, a lot of organotin compounds have been synthesized and their multifunctional roles in different fields were investigated, for instance, in catalysis, materials sciences, biology and medicine [38].
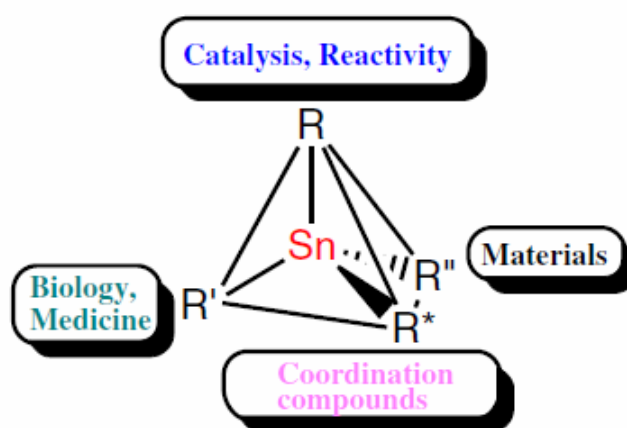
Figure 1.8 Application of organotin compounds (printed from ref. [38])

Methods for the synthesis of organotin compounds usually involve two principal steps. The first is the formation of a tetraorganotin compound of the type R_4Sn, followed by the reaction of R_4Sn with tin tetrachloride or hydrochloric acid to prepare organotin halides of the types R_3SnCl, R_2SnCl_2 or $RSnCl_3$. The most widely used route for the synthesis of tetraorganotin compounds is the reaction of an appropriate *Grignard* reagent RMgX (R = organic group, X = Cl, Br, I) with a tin(IV)halide, usually $SnCl_4$. For tetraalkyltin compounds with alkyl groups larger than R = Bu, a substantial excess of *Grignard* reagent is often used to obtain full conversion. In that case, a *Wurtz*-type reaction of $SnCl_4$ with an *in situ* prepared organosodium is more efficient. R_3Al is generally used as alkylating agent for the industrial preparation of tetraalkyltins to avoid distannate

formation. The formation of organotin and organotin halides are given in equations 1.4-1.7 [39].

$$SnCl_4 \xrightarrow[\substack{3.\ RM \\ (M=\ Na,\ Li)}]{\substack{1.\ RMgX \\ 2.\ R_3Al}} R_4Sn \xrightarrow{+\ SnCl_4} \begin{cases} R_3SnCl \\ R_2SnCl_2 \\ RSnCl_3 \end{cases} \tag{1.4}$$

$$R_4Sn + SnX_4 \longrightarrow R_3SnX + RSnX_3 \tag{1.5}$$

$$R_3SnX + SnX_4 \longrightarrow R_2SnX_2 + RSnX_3 \tag{1.6}$$

$$R_2SnX_2 + SnX_4 \longrightarrow 2\ RSnX_3 \tag{1.7}$$
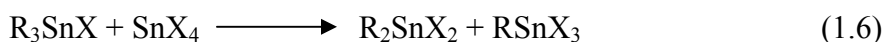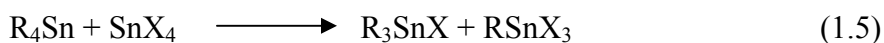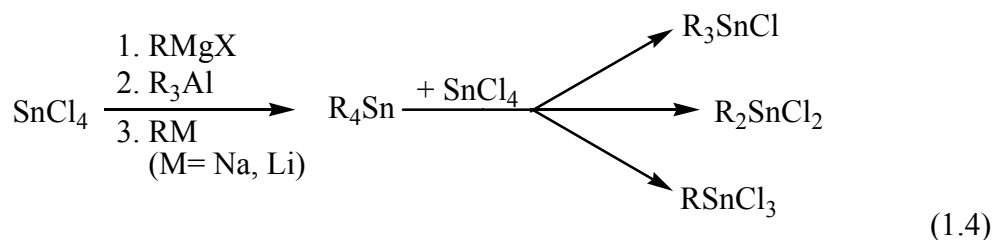
1.3.1 Organotin Chalcogenide Compounds

Organotin chalcogenide compounds have recently been shown to be useful precursors for the preparation of funtionized binary or ternary cluster compounds or frameworks. Binary organotin chalcogenolates, for example, are synthesized by reacting tin tetrahalides (SnX_4, X = Cl, Br) or organotin halides R_nSnX_{4-n} with alkyl or aryl chalcogenolates to form corresponding chalcogenolato complexes [40-41].

$$R_nSnX_{4-n} + (4\text{-}n)\ R'EH + (4\text{-}n)\ Et_3N \longrightarrow R_nSn(ER')_{4-n} + (4\text{-}n)\ Et_3NHX \tag{1.8}$$

$$R =\ R' =\ alkyl,\ aryl\ and\ E = S,\ Se$$
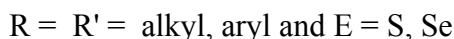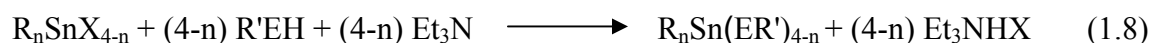
For instance, tin tetrachloride or triphenyltinchloride, reacts with thiophenol (PhSH) or selenophenol (PhSeH) in the presence of a base to yield tetra(arylchalcogenolato)tin or $Ph_3Sn(EPh)$ [40]. Figure 1.9 shows some mononuclear or dinuclear tin chalocogeolates.

Organotin halides smoothly react with chalcogenide anions to form organotin chalcogenide derivatives. The reactions are usually carried out using A_2E, e.g. H_2S, Li_2S, Na_2S, Li_2Se or Na_2Se in water, organic solvent or in liquid ammonia at room temperature or low temperature, depending on the reactivity of the reactants to form a variety of compounds [42-44].
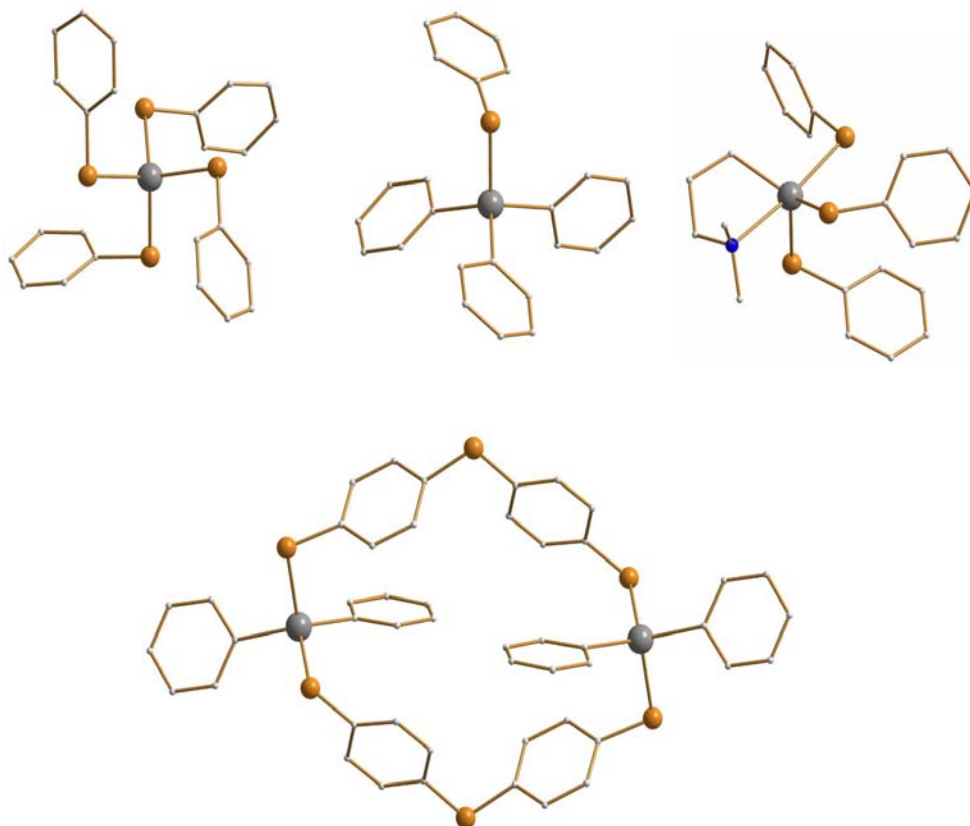
Figure 1.9 Examples for mononuclear (top) and dinuclear (bottom) tin chalcogenolates, color code: Sn, gray; S, yellow; N, blue; C, light gray

For instance, triorganotin halide R_3SnX (R = Me, Bu, Ph) are reacted with anhydrous sodium sulfide in absolute ethanol to result in dimeric compound $R_3Sn–S–SnR_3$, where sulfur acts as a bridge between two R_3Sn units. Diorganotin halides (R_2SnX_2) react with anhydrous Na_2E (S, Se) in dry THF to give trimeric $R_6Sn_3S_3$, which is widely used for the preparation of SnS films by thermolysis or chemical vapour deposition (CVD). $RSnX_3$ yields a tetrameric compound $R_4Sn_4S_6$ upon reaction with Na_2S in acetone/THF (eq. 1.9-1.11).

$$R_3SnX + E^{2-} \longrightarrow R_3Sn–S–SnR_3 + X^- \tag{1.9}$$

$$R_2SnX_2 + E^{2-} \longrightarrow R_4Sn_2S_2 \text{ or } R_6Sn_3S_3 \tag{1.10}$$

$$2\ RSnX_3 + 3\ E^{2-} \longrightarrow R_4Sn_4S_6 \tag{1.11}$$
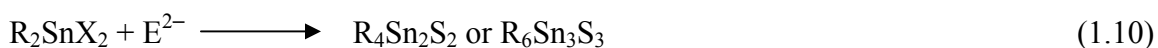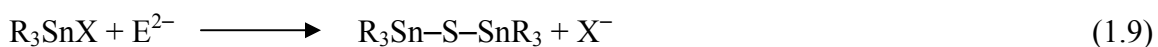
(R = Me, Bu, Ph and X = Cl, Br)

This tetrameric compound exists in two different topologies, namely a double-decker-type and an adamantane-type. For alkyl or aryl ligand R, the latter is the favourite one; however, functional groups at R, such as COR, COOH or CONH$_2$, lead to the formation of double-decker type isomers that are stabilized by back-bonding of the functional group to tin [45-47].

Single bridged dimer   Double bridged dimer

Adamantane   Double-decker
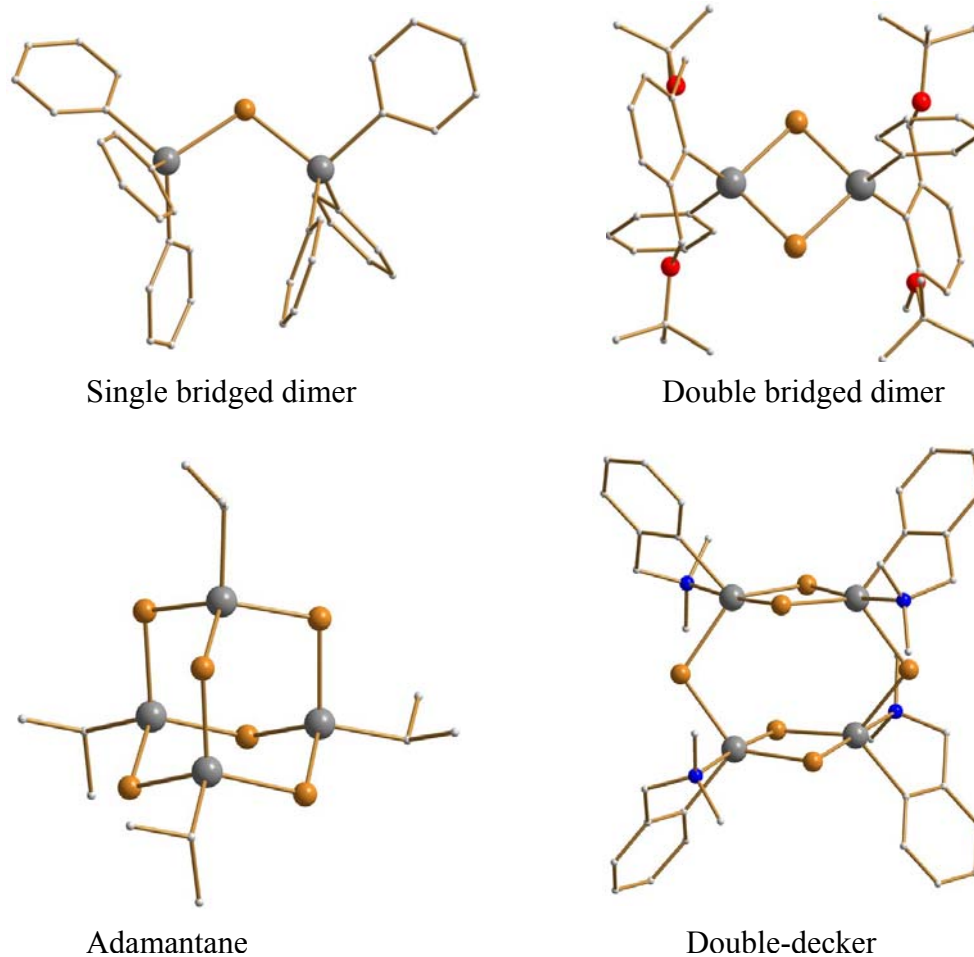
Figure 1.10 Organotin chalcogenide compounds, color code: Sn, gray; S, yellow; N, blue; C, light gray

1.3.2 Organotin Ternary Clusters

At present, synthesis of organo functionalized ternary clusters or functionalization of known ternary clusters is a challenging field in inorganic or organoelement chemistry at the border to materials science. However, so far only few organyl ligated compounds of the elemental combination Group 14/16 have been reported in combination with transition metal atoms. In 2002 *Merzweiler's* group synthesized the first example, $[(PhSn)_2(CuPMe_2Ph)_6S_6]$ (Figure 1.11) [48].
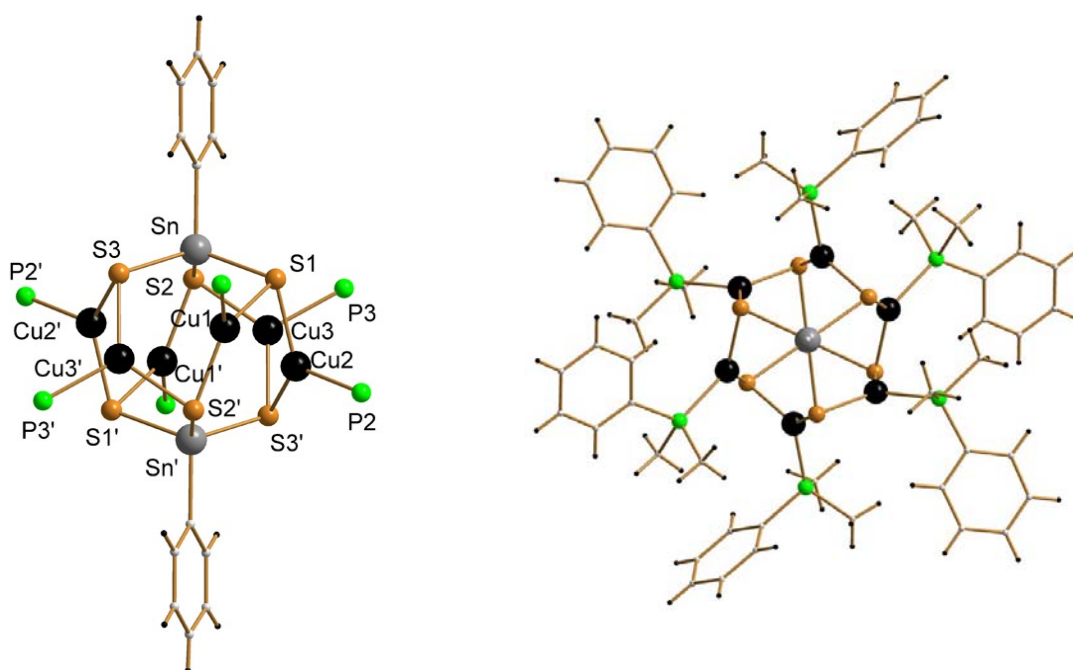
Figure 1.11 Molecular structure of $[(PhSn)_2(CuPMe_2Ph)_6S_6]$ in two different views. For clarity, ligands at P are not given on the left hand side

For its synthesis, $[PhSnS_3]^{3-}$, prepared from $Ph_4Sn_4S_6$ and Na_2S in aqueous THF, was reacted with the copper(I) complex $[(PhPMe_2)bipyCuCl]$ (bipy = 2,2'-Bipyridine). Recently, *Tatsumi et al.* reported two ternary Pd/Ge/S complexes, $[DmpGe(\mu-S)_2]_2[(\mu-S)_2Pd(dppe)]$ and $[DmpGe(\mu-S)_2]_2[(\mu-S)_2Pd(PPh_3)]$ (Dmp = 2,6-dimesitylphenyl). Here, $[DmpGe(SH)(\mu-S)_2Ge(SH)-Dmp]$ was reacted with *n*-BuLi (2 equivalents) to form a

dilithium salt *in situ*, which yielded the Ge_2PdS_4 clusters upon addition of $[Pd(dppe)Cl_2]$ or $[Pd(PPh_3)_2Cl_2]$ (Figure 1.12) [49].
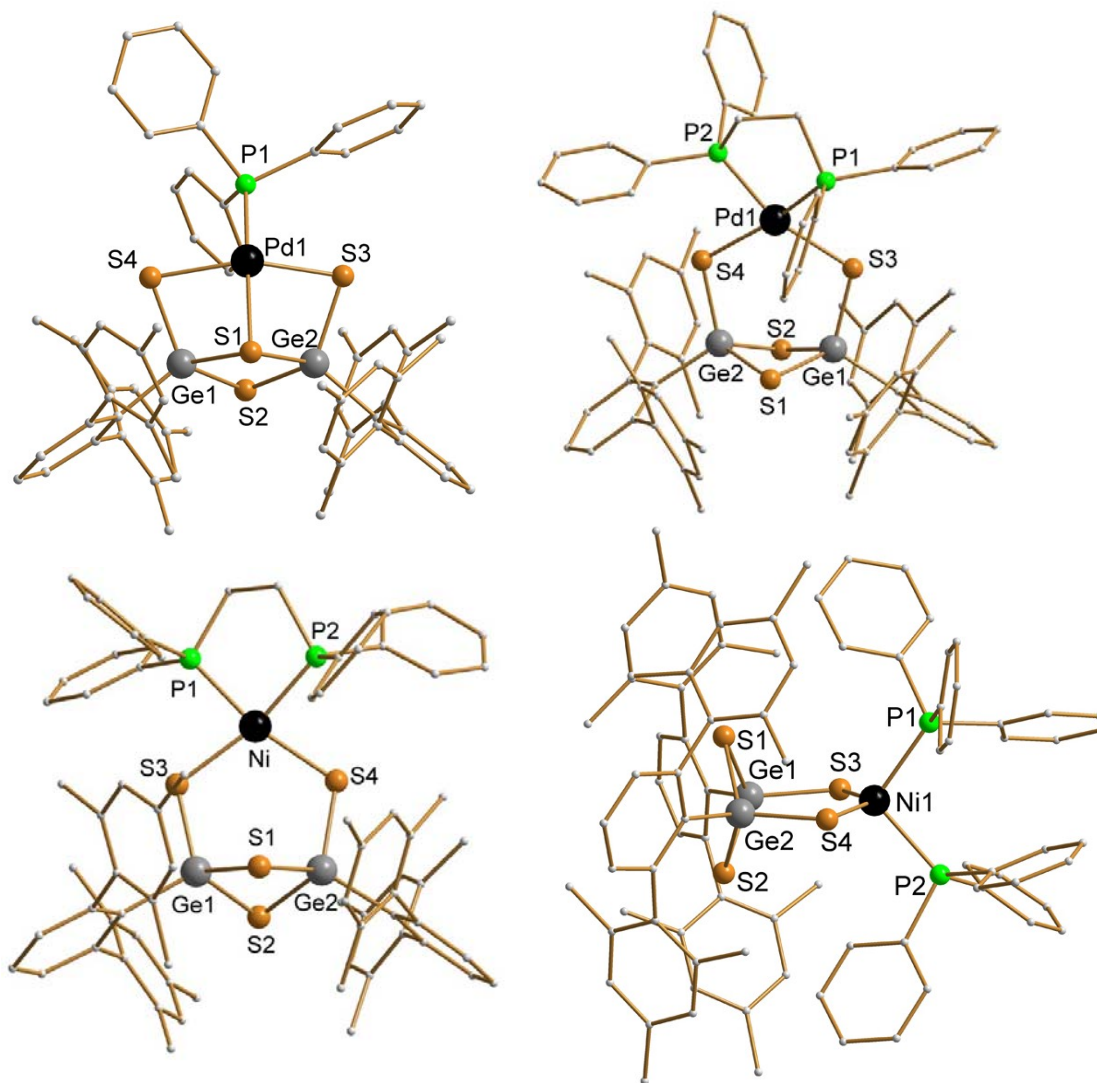
Figure 1.12 Molecular structures of organyl and phosphine ligated Ge_2PdS_4 and Ge_2NiS_4 clusters

Similarly, they have reported the synthesis of two Ge_2NiS_4 clusters, $[DmpGe(\mu-S)_2]_2[(\mu-S)_2Ni(dppe)]$ and $[DmpGe(\mu-S)_2]_2[(\mu-S)_2Ni(PPh_3)]$, by reaction of $[DmpGe(SLi)(\mu-S)_2Ge(SLi)-Dmp]$ with $[Ni(dppe)Cl_2]$ or $[Ni(PPh_3)_2Cl_2]$. When $[DmpGe(\mu-S)_2]_2[(\mu-S)_2Ni(PPh_3)]$ was heated to 120 °C in toluene, a novel $Ge_4Ni_6S_{12}$ cluster, $[\{DmpGe(\mu-S)_3\}_4Ni_6]$ (Figure 1.13) was obtained. In the $Ge_4Ni_6S_{12}$ cluster, six nickel atoms form an

octahedron and four DmpGeS$_3$ units cap four of the eight trigonal faces. So far, this has been the largest ligated ternary M/14/16 cluster [50].
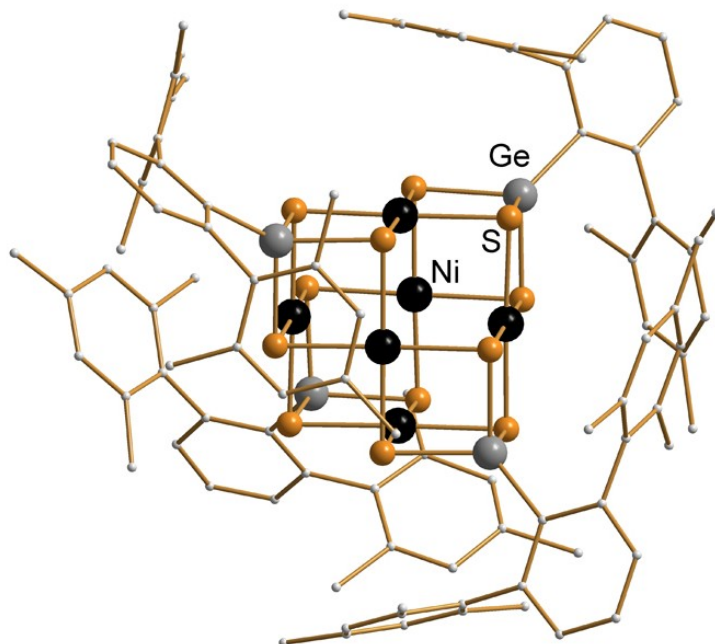
Figure 1.13 Molecular structure of [{DmpGe(μ- S)$_3$}$_4$Ni$_6$]

As stated before, a large variety of arylchalcogenolato complexes of Group 14 (semi)metals of the type Sn(ER)$_4$ have been synthesized. Although, they were used most frequently for the synthesis of tin chalcogenide materials, SnS or SnS$_2$, some arylchalcogenolate complexes of tin were recently used as metalloligands for the synthesis of organoclad ternary M/Sn/S complexes or clusters. For instance, Sn(SPh)$_4$ was reacted with CuCN and PPh$_3$ in dichloromethane to produce a linear [{(Ph$_3$P)Cu}$_2$Sn(SPh)$_6$] arrangement (Figure 1.14) that represents a distorted SnS$_6$ octahedron, sharing two opposite faces with two adjacent, slightly distorted CuS$_3$P tetrahedra. By using (Bu$_4$N)$_2$[Sn$_3$S$_4$(edt)$_3$] {edt = (SCH$_2$CH$_2$S)$^{2-}$} two further compounds have been obtained, [{(Ph$_3$P)$_2$Cu}$_2$SnS(edt)$_2$]·2CH$_2$Cl$_2$·H$_2$O and [{(Ph$_3$P)$_2$Cu}$_2$SnS(edt)$_2$]·2DMF·H$_2$O, based on the same neutral [{(Ph$_3$P)$_2$Cu}$_2$SnS(edt)$_2$] complex (Figure 1.15) [51].
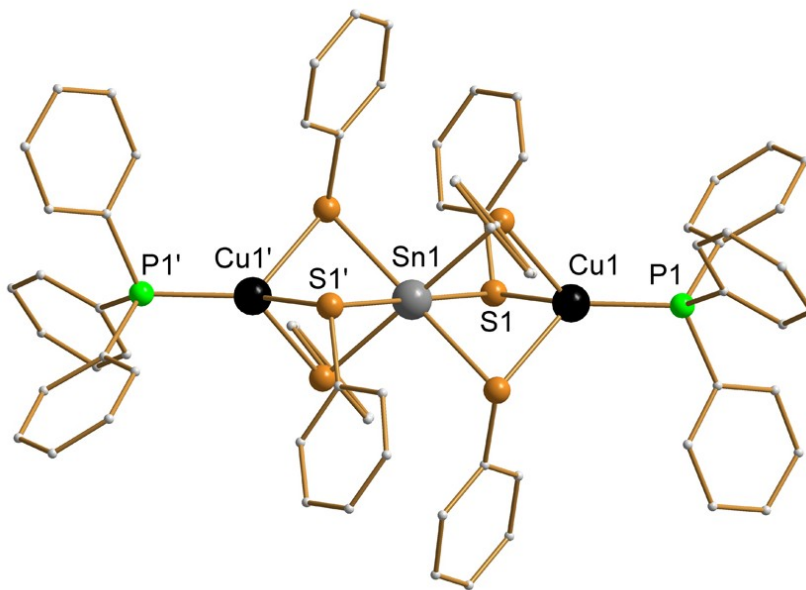
Figure 1.14 Molecular structure of $[\{(Ph_3P)Cu\}_2Sn(SPh)_6]$
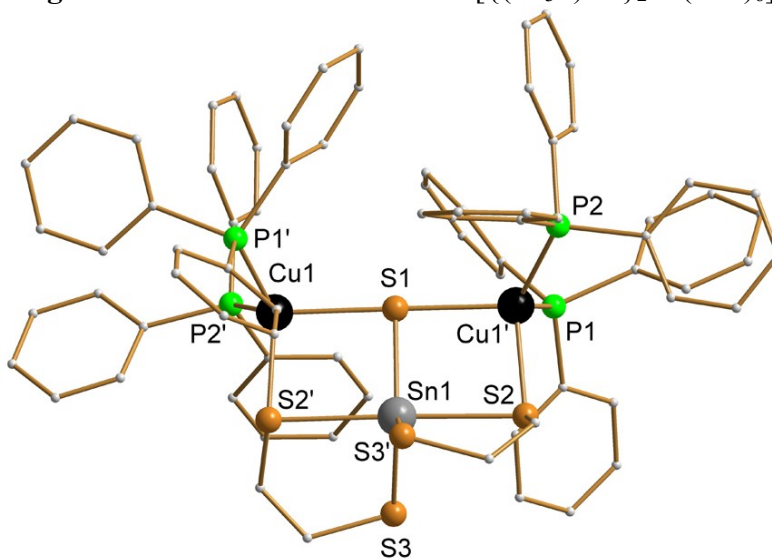
Figure 1.15 Molecular structure of $[\{(Ph_3P)_2Cu\}_2SnS(edt)_2]$ cluster

A reaction of $[Cu(PPh_3)_2(MeCN)_2]ClO_4$ and $Sn(edt)_2$ (edt = ethane-1,2-dithiolate) in DCM afforded another compound, $[Sn_3Cu_4(S_2C_2H_4)_6(\mu_3\text{-}O)(PPh_3)_4](ClO_4)_2 \cdot 3CH_2Cl_2$ (Figure 1.16), which was the first example of the heptanuclear Sn^{IV}–Cu^I oxosulfur complex. The complex, exhibiting a bottle-shaped cluster core shows a blue-green luminescent emission in the solid state [52].
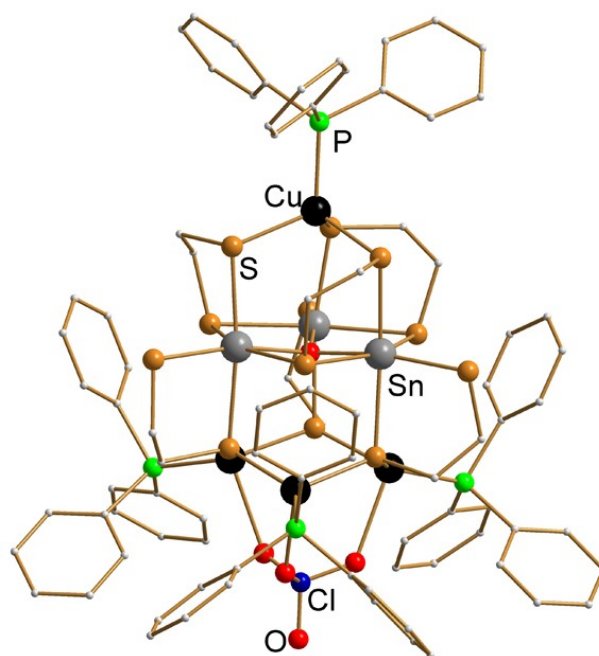
Figure 1.16 Molecular structure of $[Sn_3Cu_4(S_2C_2H_4)_6(\mu_3\text{-}O)(PPh_3)_4](ClO_4)_2$

Recently, *Tatsumi et al.* reported the usefulness of a related heterobimetallic organogermanium compound, $[(dmp)(dep)Ge(\mu\text{-}S)(\mu\text{-}O)Ru(PPh_3)]$, for the heterolytic cleavage of dihydrogen at 7.5-10 atm., and $[(dmp)(dep)Ge(\mu\text{-}S)(\mu\text{-}OH)Ru(PPh_3)]^+$ for reversible heterolytic cleavage of dihydrogen at 1 atm. Figure 1.17 shows the according pathway [53-55].
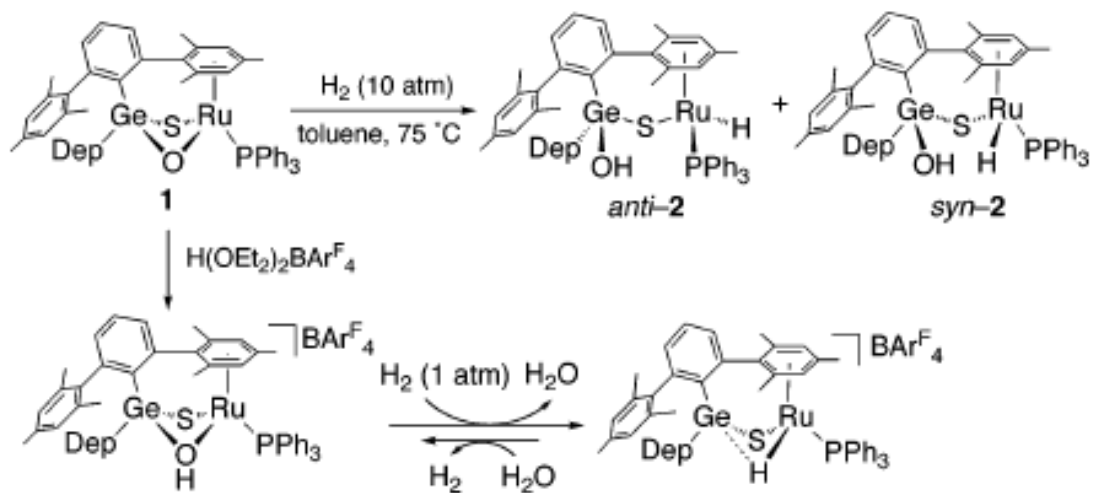
Figure 1.17 Heterolytic cleavage of dihydrogen by Ge/S/Ru compounds

Chapter 2

Research Objectives

The general aim of the work described in this thesis was the investigations of the reactivity of bis(trichlorostannyl)organyl compounds towards chalcogenides, chalcogenolates or a combination of chalcogenides or chalcogenolates with transition metal compounds for the synthesis of new organochalcogenidostannates and organo-clad binary or ternary complexes and clusters. As mentioned in the introduction, organotin or organogermanium chalcogenide chemistry has attracted much interest due to structural diversity and potential applications of the target compounds.

However, the chalcogenide chemistry of bis(trichlorostannyl)organyl compounds is completely unknown. Developements in the synthesis of bis(trichlorostannyl)organyl compounds, might open a novel approach to organotin chemistry. With or without resembles to organomonotin compounds bis(trichlorostannyl)organyl compounds are promising candidates for further derivatizations shown in scheme 2.1.
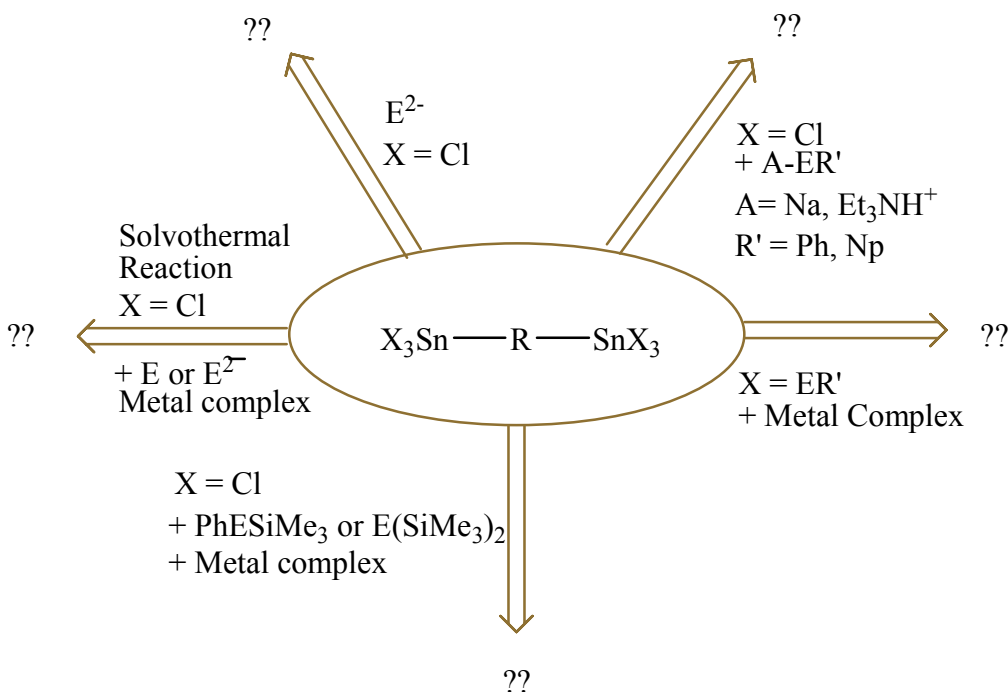
Scheme 2.1 Possible reactivities of bis(trichlorostannyl)organyl compounds, E = S, Se

Like oragnomonotin compounds, bis(trichlorostannyl)organyl compounds might react with chalcogenides or chalcogenolates resulting in functionalized binary frameworks or bis[tris(chalcogenolato)stannyl]organyl compounds, which again may be useful as synthons for the synthesis of tin chalcogenide (Sn/E) materials or metal chalcogenide binary or ternary complexes and clusters. Bis(trichlorostannyl)organyl compounds should also react with chalcogenide and/or transition metal to end up with organo-clad clusters or framework structures depending on the reaction conditions. Considering the background of organomonotin and organomonogermanium compounds, an effort was taken to contribute a pinch of light to the so far completely dark world of the chalcogenide (except oxygen) chemistry of bis(trichlorostannyl)organyls.

Chapter 3

Results and Discussion

3.1 Reactivity of Bis(trichlorostannyl)organyls toward Chalcogenides and Chalcogenolates

The bis(trichlorostannyl)organyl compounds 1,4-bis(trichlorostannyl)butane, 1,4-bis(trichlorostannylmethyl)benzene and 4,4'-bis(trichlorostannylmethyl)biphenyl were synthesized from their dibromo or dichloro (butyl or 1,4-dimethylbenzene and 4,4'-dimethylbiphenyl bridged respectively) adducts according to literature procedures [56-58]. 1,1'-bis(trichlorostannyl)ferrocene was prepared from ferrocene [59]. The major steps involved were (1) the formation of a digrignard reagent or dilithium salt from the corresponding dihalogeno organic compounds or ferrocene, respectively followed by the reaction with triphenyltin chloride, tricyclohexyltin chloride or trimethyltin chloride, respectively and (2) the reaction of the product of step (1) with tin tetrachloride to result in bis(trichlorostannyl)organyl compounds. The compounds were characterized by means of ^{1}H NMR, ^{13}C NMR and ^{119}Sn NMR spectroscopy and their cell parameters were also confirmed by X-ray diffraction. Over the past decades, there has been considerable interest in the synthesis and application of thiolate, selenolate or tellurolate complexes of tin due to their structural diversity, catalytic or biological activity and potential application as precursors for the synthesis of binary or ternary chalcogenide materials [60–71].

3.1.1 Reactivity of Bis(trichlorostannyl)organyls toward Chalcogenides

As mentioned in the introduction, organotin halides smoothly react with chalcogenide anions to form organotin chalcogenide derivatives. Some of these compounds were used for the synthesis of tin chalcogenide films by thermolysis or chemical vapor deposition. The reactions were usually carried out using H_2E, A_2E, $E(SiMe_3)_2$ (E = S, Se, Te; A = Li, Na) as chalcogenide source in water, an organic solvent or in liquid ammonia at room

temperature or low temperature, depending on the reactivity of the reactants to form a variety of compounds [42-44]. Trichloroorganotin compounds, $RSnCl_3$ (R = Me, Bu, Ph), for instance, are precursors to adamantane or double-decker type $R_4Sn_4E_6$ compounds (Scheme 3.1).
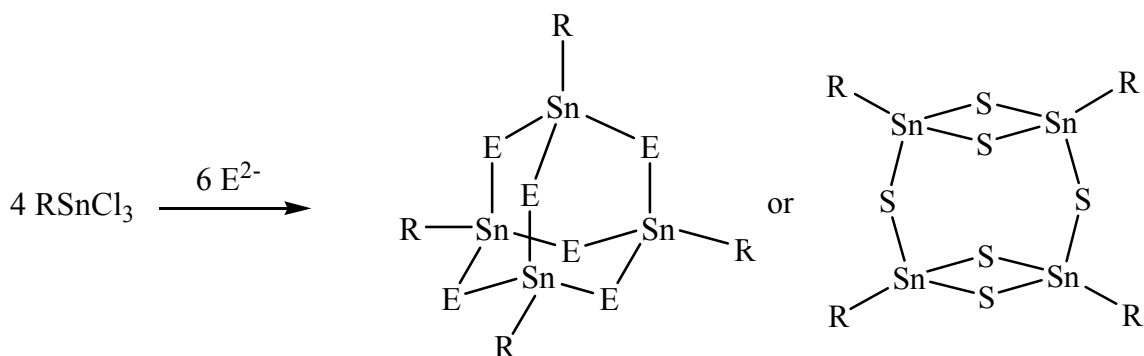
Scheme 3.1 Synthesis of adamantane or double-decker compounds

Here, bis(trichlorostannyl)organyls (Cl_3Sn–R–$SnCl_3$) were reacted with $Na_2S·9H_2O$ in water-acetone, Na_2E in THF, liquid ammonia or $E(SiMe_3)_2$ (E = S, Se) in THF, with the intention to prepare a three dimensional metal-chalcogenide framework, where each adamantane or double-decker will be connected to each other by four bridging organyls (Scheme 3.2). For instance, 1,4-bis(trichlorostannyl)butane was reacted with $Na_2S·9H_2O$ in water-acetone, with Na_2S in THF or liquid ammonia, or with $S(SiMe_3)_2$ in THF. All resulted in an immediate formation of white solids, all of which were insoluble at room temperature and even after refluxing for few hours, strongly indicating a polymeric nature of the products. Various efforts were taken to get some structural information of the obtained compounds. According to the elemental analysis, the compound obtained from the reaction of 1,4-bis(trichlorostannyl)butane with $S(SiMe_3)_2$ contains C: 14.91 %; H: 2.70 %. For a compound according to scheme 3.2, one would expect a ratio C: 12.33 %; H: 2.07 %, hence somewhat differents. Because of the amorphous nature, the X-ray powder diffractogram of the compound shows no informative signal in the powder (Figure 3.1). An EDX analysis confirms the presence of tin and sulphur in the solid with Sn:S; 1:1.25 (Figure 3.2), which again differs somewhat from the calculated value (Sn:S; 1:1.5) based on the above framework structure.

$$Cl_3Sn\text{-}R\text{-}SnCl_3$$

$$\downarrow\ E^{2-}$$

Scheme 3.2 Intended synthesis of tin chalcogenide framework
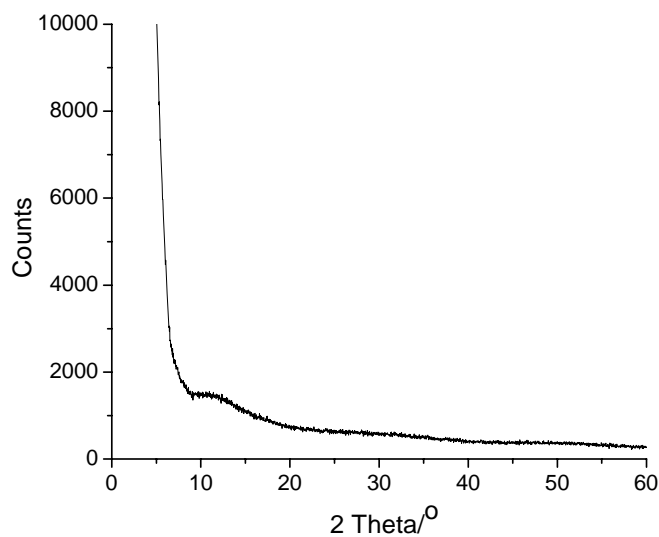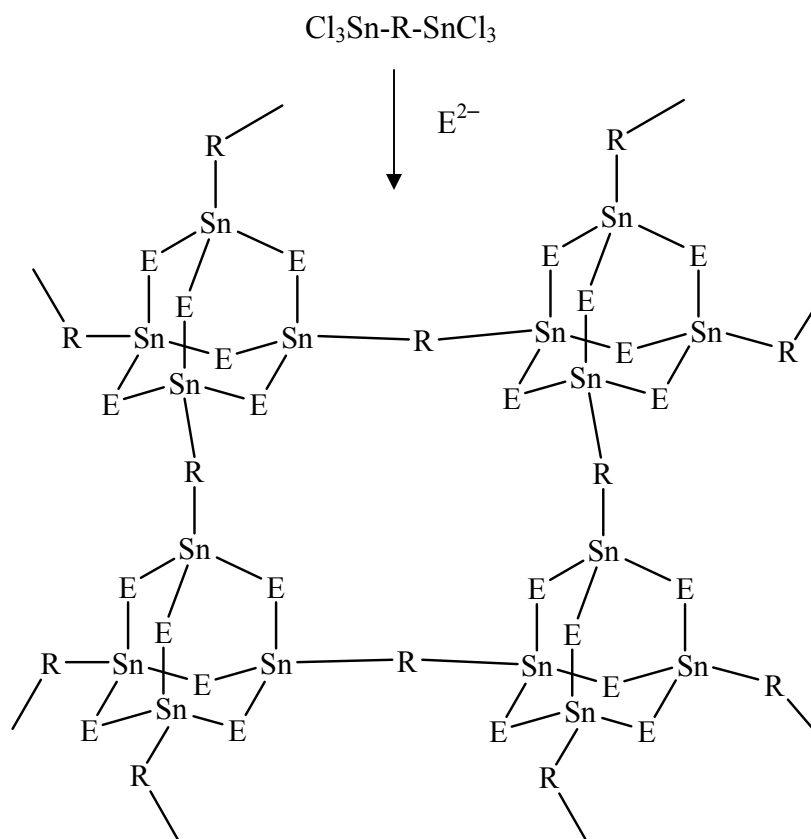
Figure 3.1 X-ray powder diffractogram of the obtained insoluble solid (see text)

However, it rationalizes the existance of Sn beside C and S atoms in the obtained polymer. This is additionally supported by solid state ^{119}Sn NMR (Figure 3.3). Solid state

^{119}Sn NMR analyses indicate the presence of different chemical environments around the tin atoms within the solid-may be due to a structure different from those sketched in scheme 3.2 or owing to a mixture of different polymers.
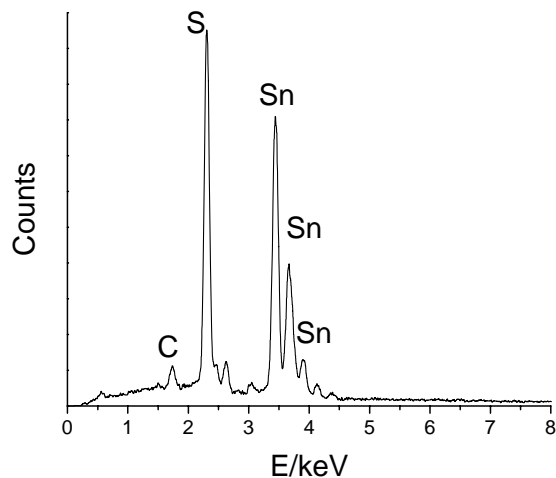
Figure 3.2 EDX spectrum of the obtained insoluble solid (see text)
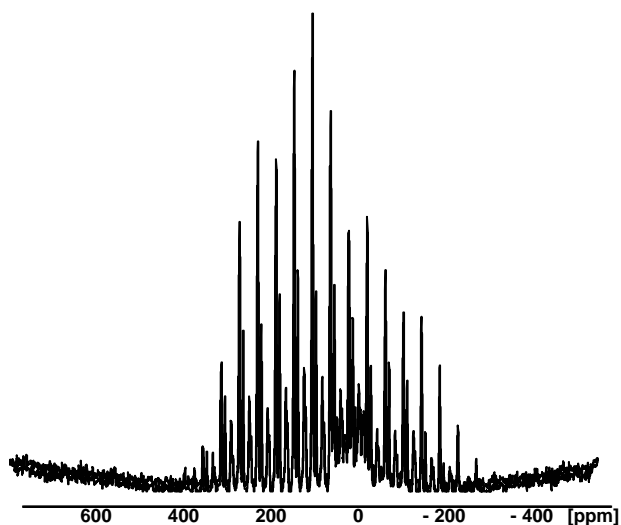
Figure 3.3 Solid state ^{119}Sn NMR spectrum of the obtained insoluble solid (see text)

None of the above analyses is capable of giving exact informations about the structure. However, it is very likely that method indeed led to the formation of hybride RSn/S network. Future investigations may characterize these compounds fully by functionalization in the organic residue, thus increasing solubility and chances of crystallization.

3.1.2 Reactivity of Bis(trichlorostannyl)organyls toward Thiolates

A wide variety of thiolate complexes of monotin and organomonotin compounds have been reported. For instance, $Sn(SPh)_4$, prepared by reacting tin tetrachloride with sodium thiophenolate under reflux in toluene, is a potential precursor for the synthesis of thin films of SnS or SnS_2, which are highly valuable materials for photovoltaic, holographic recording systems and solar control devices [72-73]. Moreover, in 2008 $Sn(SPh)_4$ was used as a precursor for the synthesis of a ternary Sn/Cu/S complex $[(Ph_3P)Cu]_2Sn(SPh)_6$ [46]. Organotin thiolates, of the type $R_nSn(SR')_{4-n}$ (n = 1-3, R = Me, *n*-Bu, *n*-heptane and R' = Ph, Np) have also been prepared in a similar way as $Sn(SPh)_4$, or by reacting organotin chlorides with corresponding thiols in the presence of a base. These compounds are well known for their activities in organic synthesis [74].

Here, bis(trichlorostannyl)organyls of the general formula $Cl_3Sn-R-SnCl_3$ (R = butyl, 1,4-dimethylbenzene and 4,4'-dimethylbiphenyl) were reacted with six equivalents of sodium thiophenolate in methanol to produce $(PhS)_3Sn-(CH_2)_4-Sn(SPh)_3$ (**1**), $(PhS)_3Sn-$ 1,4-dimethylbenzene-$Sn(SPh)_3$ (**2**) and $(PhS)_3Sn-4,4'$-dimethylbiphenyl-$Sn(SPh)_3$ (**3**) or with six equivalents of 2-thionaphthol in toluene in the presence of triethyl amine (Scheme 3.3). These reactions result in colorless (**1**, **4**, **5**) or light yellow solids (**2**, **3**).

Scheme 3.3 Synthesis of $(PhS)_3Sn-R-Sn(SPh)_3$

Pure crystalline products were obtained by recrystallization from a dichloromethane/*n*-hexane (1:1) mixture solution in 57-70% yield. The compounds were characterized by standard physical methods ^{1}H NMR, ^{13}C NMR, ^{119}Sn NMR and single-crystal X-ray diffraction except compound **2** due to poor crystal quality.

3.1.2.1 Characterization of Bis[tris(arylthiolato)stannyl]organyls (R'S)₃Sn–R–Sn(SR')₃ with R', R = Ph, 1,4-Bu (1), Ph, 1,4-Dimethylbenzene (2), Ph, 4,4'-Dimethylbiphenyl (3), 2-Naphthyl, 1,4-Bu (4) and 2-Naphthyl, 1,4-Dimethylbenzene (5)

Colorless blocks of **1**, light yellow crystals of **2**, light yellow needles of **3**, colorless needles or blocks of **4** or **5** are highly soluble in dichloromethane, chloroform and toluene. Crystals of **2** were not suitable for single-crystal X-ray diffraction. Therefore, **2** was characterized by means of NMR spectroscopy (see experimental section). Figure 3.4 shows the [119]Sn spectrum that shows a singlet at δ = 61.42, indicating both tin atoms to possess in the same average chemical environment.
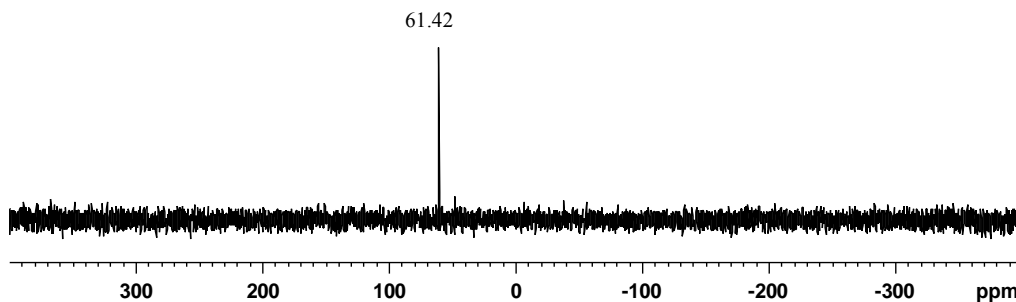
Figure 3.4 [119]Sn spectrum of compound **2**

According to single-crystal X-ray diffraction of **1** and **3-5**, compound **1** crystallizes in the triclinic space group $P\bar{1}$ (No. 2) with one formula unit in the unit cell, **3** crystallizes in the monoclinic space group $P\,2_1/c$ (No. 14) with two formula units in the unit cell. Colorless needles of **4** crystallize in the trigonal space group $R3$ (No.146) with three formula units in the unit cell and colorless blocks of **5** crystallize in the monoclinic space group $P\,2_1/n$ (No.14) with two formula units in the unit cell. The molecular structure of **1** and **3-5** are shown in figure 3.5.
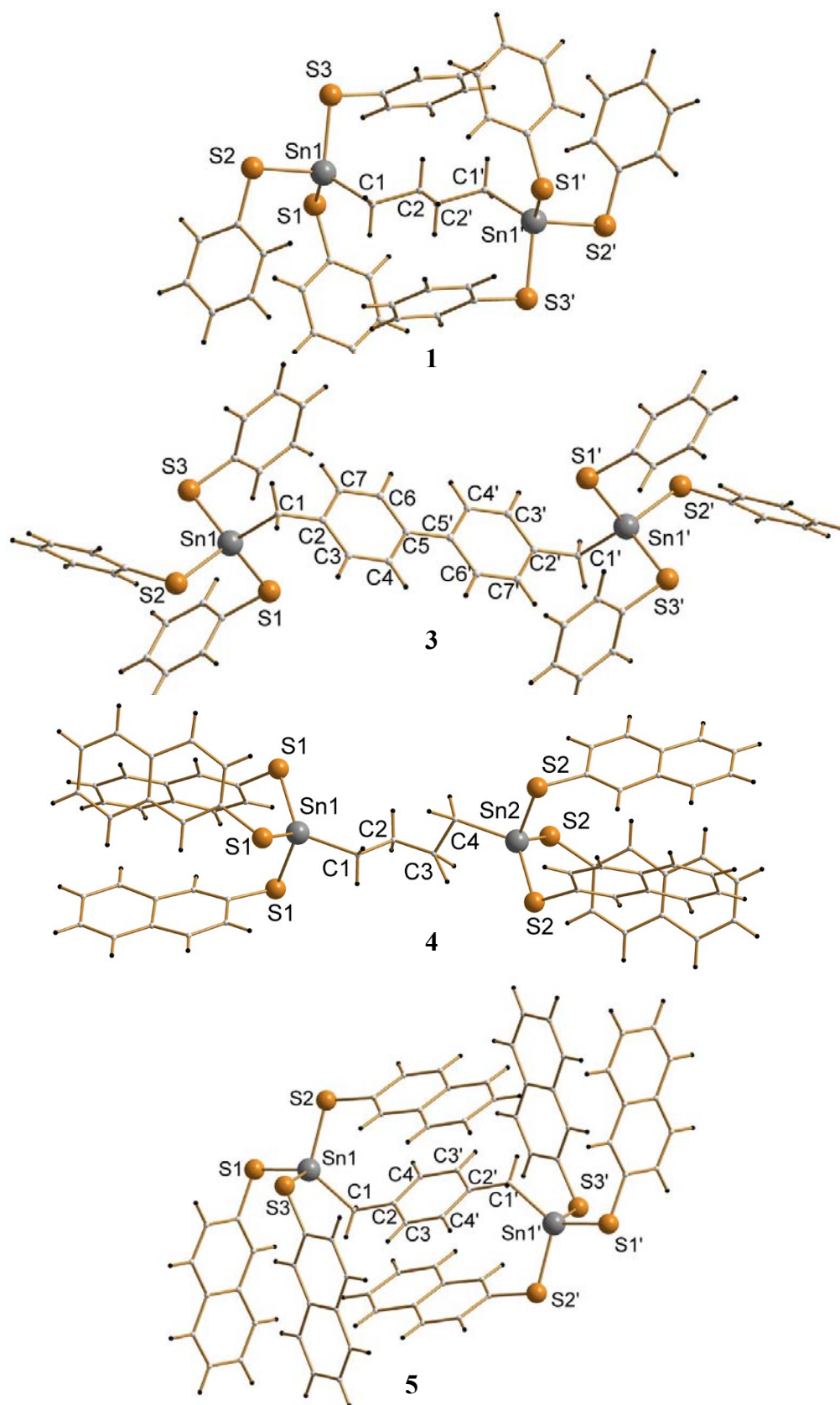
Figure 3.5 Molecular structures of compounds **1** and **3-5**

A common feature of the **1**, **3** and **5** is their intramolecular inversion symmetry or near inversion symmetry which is only frustrated to be ideal by the conformation of the butyl group in **4**. The crystallographic C_3 symmetry of the molecule of **4** is achieved by rotational disorder of the C and H atoms of the butyl bridge (not shown in figure 3.5). Compounds **1** and **3** contain two (SPh)$_3$Sn units connected by butyl (**1**) or 4,4'-dimethylbiphenyl (**3**) residue. In **4** and **5**, butyl or 1,4-dimethylbenzene residue connect two (SNp)$_3$Sn units respectively. Two crystallography equivalent tin atoms (Sn1, Sn1') are connected by a butyl or 4,4'-dimethylbiphenyl or 1,4-dimethylbenzene residue in all compounds except **4**, where the asymmetric unit contains two crystallographically independent tin atoms (Sn1 and Sn2). Each tin atom shows a distorted tetrahedral geometry formed by three sulfur donor atoms of the three thiophenolate (**1**, **3**) or 2-thionaphthylate (**4**, **5**) ligands and one carbon atom of the bridging organyl. Table 3.1 provides the selected distances and angles of the compound **1** and **3-5**. Figure 3.6 and figure 3.7 show the packing of the molecules of **1**, **3** and **4, 5** within the crystal.

Table 3.1 Selected distances /pm and angles /° in compounds **1-5**

	1	**3**	**4**	**5**
Sn–C	215.0(3)	217.6(3)	217.0(12), 219.4(14)	216.8 (3)
Sn–S	240.5(9)- 241.7(8)	240.2(10)- 242.5(10)	234.5(4)- 246.6(5)	241.26(13)- 242.50(12)
C–S	178.4(3)- 178.5(3)	178.5(3)- 179.2(4)	179.0(17)- 179.5(12)	178.2(4)- 179.0 (3)
C–Sn–S	112.6(8)- 117.9(10)	107.4(10)- 113.8(11)	91.3(5)- 126.6(7)	108.52(10)- 115.72(10)
S–Sn–S	95.89(4)- 109.67(4)	105.2(4)- 110.5(3)	108.59(10)- 109.15(10)	99.42(3)- 109.84(4)
Sn–C–C	116.6(2)	108.8(2)	99.7(9)- 122.0(12)	113.4(2)

1

3
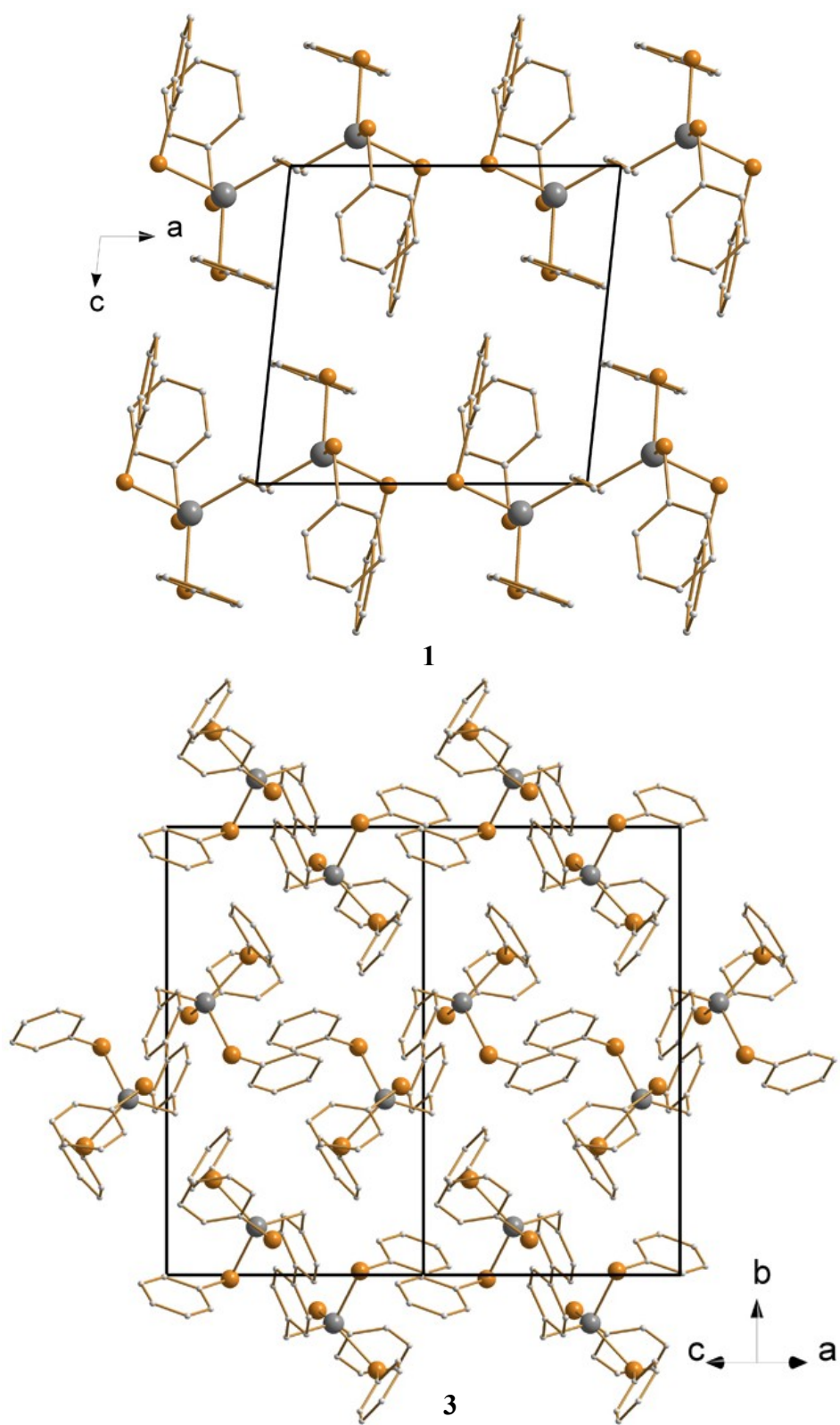
Figure 3.6 Packing of the molecules of compounds **1** (top) and **3** (bottom) within the

crystal

4

5
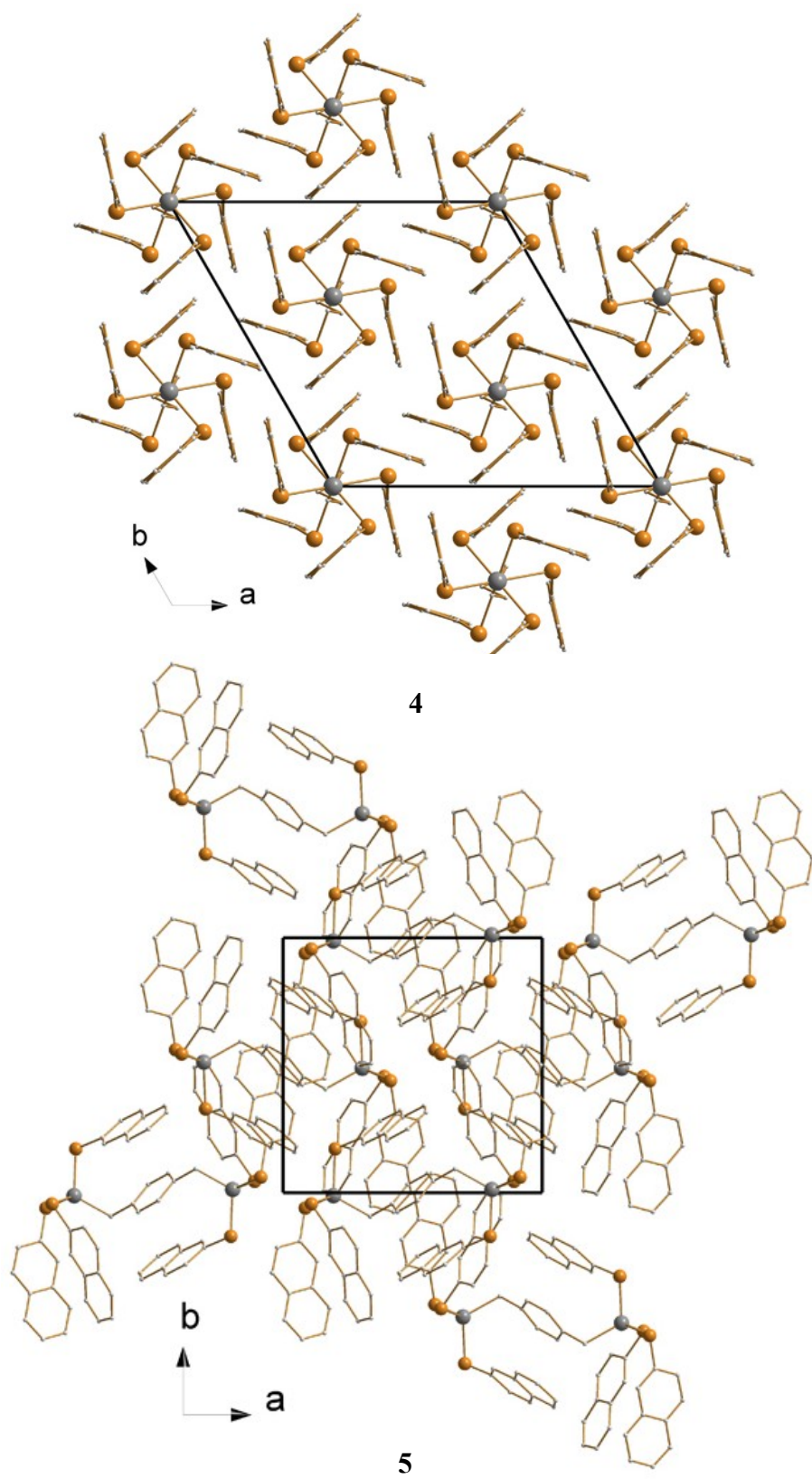
Figure 3.7 Packing of the molecules of compounds **4** (top) and **5** (bottom) within the crystal

However, the coordination geometry around tin atoms differs in **1**, **3** and **4**. The orientation of the three thiophenolate groups around the tin atoms with respect to the Sn–C bond, one can recognize a specific pattern, sketched in figure 3.8, named Type I, where all the carbon atoms of the phenyl rings of the thiophenolate ligands are oriented towards the bridging butyl group (**1**). This results in an all-*cis* conformation of the C1–Sn–S–C_{aryl} connections with dihedral angles of C1–Sn–S–C_{aryl} 28.72-64.26º. In **3**, there are two different type of orientations of the six thiophenolate ligands around the tin atoms. Two thiophenolate ligands, containing S1 and S2 (S1', S2') are oriented opposite to the bridging biphenyl residue with dihedral angles of C1–Sn–S–C_{Ph} 134.45 and 168.37º, while the other thiophenolate ligands, containing S3 (S3') are oriented toward the bridging biphenyl residue with a dihedral angle of 47.99º. This leads to a *cis-trans* mixed conformation of the C1–Sn–S–C_{Ph} connection, named Type II conformation. In **4**, all the 2-thionaphthylate groups are placed on the opposite side of the bridging butyl residue with dihedral angles of 129.81-167.96º for C1–Sn–S–C_{aryl} connection. This kind of orientation, an all-*trans* conformation called Type III, which is completely opposite to that of the Type I. But in **5**, six 2-thionaphthylate groups are oriented towards the bridging 1,4-dimethylbenzene residue forming a Type I situation with dihedral angles C1–Sn–S–C_{Np} of 11.43-68.67º.
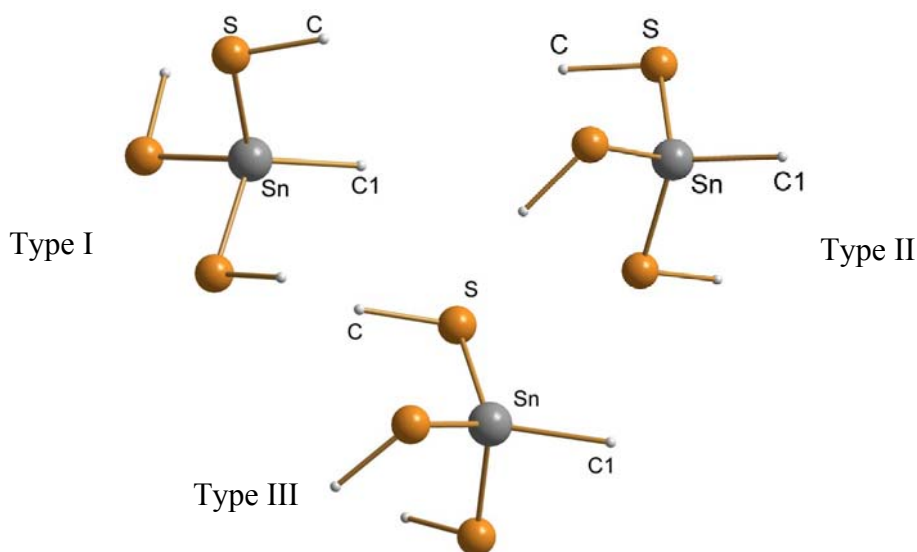
Figure 3.8 Orientation of thiophenolates around tin atoms, a *cis* (left hand side, top), *cis-trans* mixed (right hand side, top), *trans*-conformation (bottom)

N.B.: "cis" for << 90º C1–Sn–S–C_{aryl} dihedral angle (i.e. "cis" and "near cis gauche") and "trans" for >> 90º (i.e. "trans" and "near trans gauche")

3.1.3 Reactivity of Bis(trichlorostannyl)organyls toward Selenolates

A wide variety of selenophenolates of tin and organotin compounds have been reported with the general formulae $Sn(SeR)_4$ or $R'_nSn(SeR)_{4-n}$ (n = 1-3, R = aryl, R' = Me, n-Bu, n-heptane) [9]. They have been synthesized either by reduction of the diaryl diselenide by $NaBH_4$, or by reaction with benzene selenophenol in the presence of triethyl amine as a base [10, 11].

Here, $Cl_3Sn-R-SnCl_3$ was reacted with one or three equivalents of diaryl diselenide in ethanol in the presence of sodium boronhydride as reducing agent to produce $(PhSeCl_2)Sn-(CH_2)_4-Sn(Cl_2SePh)$ (6) or $(PhSe)_3Sn-(CH_2)_4-Sn(SePh)_3$ (7), $(NpSe)_3Sn-(CH_2)_4-Sn(SeNp)_3$ (8), $(PhSe)_3Sn-CH_2-C_4H_4-CH_2-Sn(SePh)_3$ (9), $(PhSe)_3Sn-Fc-Sn(SePh)_3$ (Fc = 1,1'-Ferrocenyl) (10) and $(NpSe)_3Sn-Fc-Sn(SeNp)_3$ (11) (Scheme 3.4).
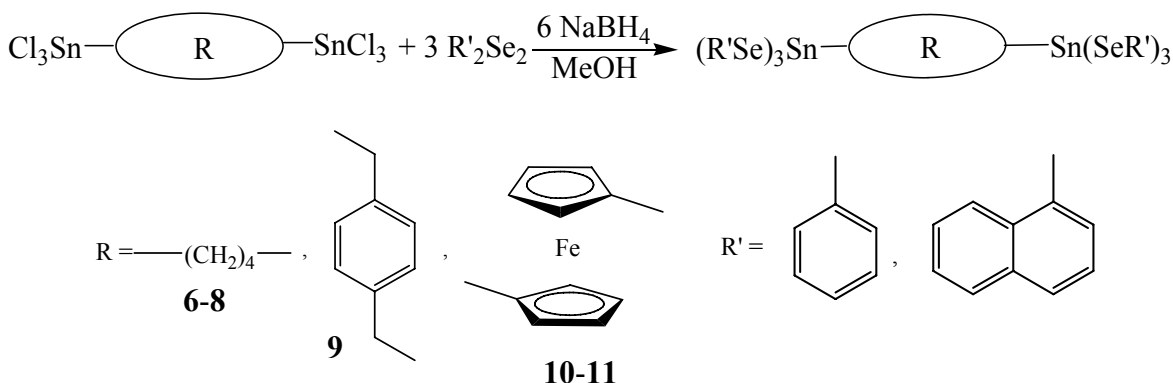
Scheme 3.4 Synthesis of $(R'Se)_3Sn-R-Sn(SeR')_3$

Pure compounds were isolated by recrystallization from a dichloromethane/n-hexane (1:1) mixture as light yellow (6-9) or orange solids (10 and 11). The compounds were characterized by means of ^1H NMR, ^{13}C NMR, ^{119}Sn NMR and single crystal X-ray diffraction.

3.1.3.1 Characterization of (PhSeCl₂)Sn–(CH₂)₄–Sn(Cl₂SePh) (6) and (R'Se)₃Sn–R–Sn(SeR')₃ R', R = Ph, 1,4-Bu (7), 1-Naphthyl, 1,4-Bu (8) Ph, 1,4-Dimethylbenzene (9), Ph, 1,1'-Ferrocenyl (10), 1-Naphthyl, 1,1'-Ferrocenyl (11)

Light yellow or yellow solids of **6-9** and orange solids of **10** and **11** are highly soluble in dichloromethane, chloroform and toluene. Compound **6** is also soluble in alcohol like methanol and ethanol. The X-ray structure analysis shows that light yellow blocks of **6** crystallize in the monoclinic space group $P\,2_1/c$ (No.14) with two formula units in the unit cell. Yellow blocks of **7** and **8** crystallize in the triclinic space group $P\bar{1}$ (No. 2) with one formula unit in the unit cell. Thus, compound **8** differs from the thiolate homologue **4**. Compound **9** crystallizes in the monoclinic space group $C2/c$ (No. 15) with four formula units in the unit cell and **10** crystallizes in the monoclinic space group $P\,2_1/n$ (No.14) with two formula units in the unit cell. The molecular structures of **6-10** are shown in figure 3.9. All compounds possess intramolecular inversion symmetry. In **6**, two crystallographically equivalent tin atoms possess pseudo tetrahedral coordination geometry by two chloride ligands, one selenophenolate ligand and one carbon atom of the bridging butyl residue. Selected bond lengths and angles are given in the table 3.2. The dihedral angle for the C1–Sn–Se–C_{Ph} connection is 187º, indicating the C1–Sn and Se–C_{Ph} bonds to be in *trans* position to each other.

Table 3.2 Selected distances and angles in compound **6**

Distances	[pm]	Angles	[º]
Sn–C	212.5(3)	C–Sn–Se	120.98(11)
Sn–Se	248.93(6)	Cl–Sn–Cl	102.31(4)
C–Se	193.9(4)	C–Sn–Cl	108.17(11)-110.71(11)

Compound **7** is isostructural and isotypic to compound **1**. Here, the dihedral angles of the Type I coordination around the tin atoms are 25.64-81.01º, thus larger for compound **1**.
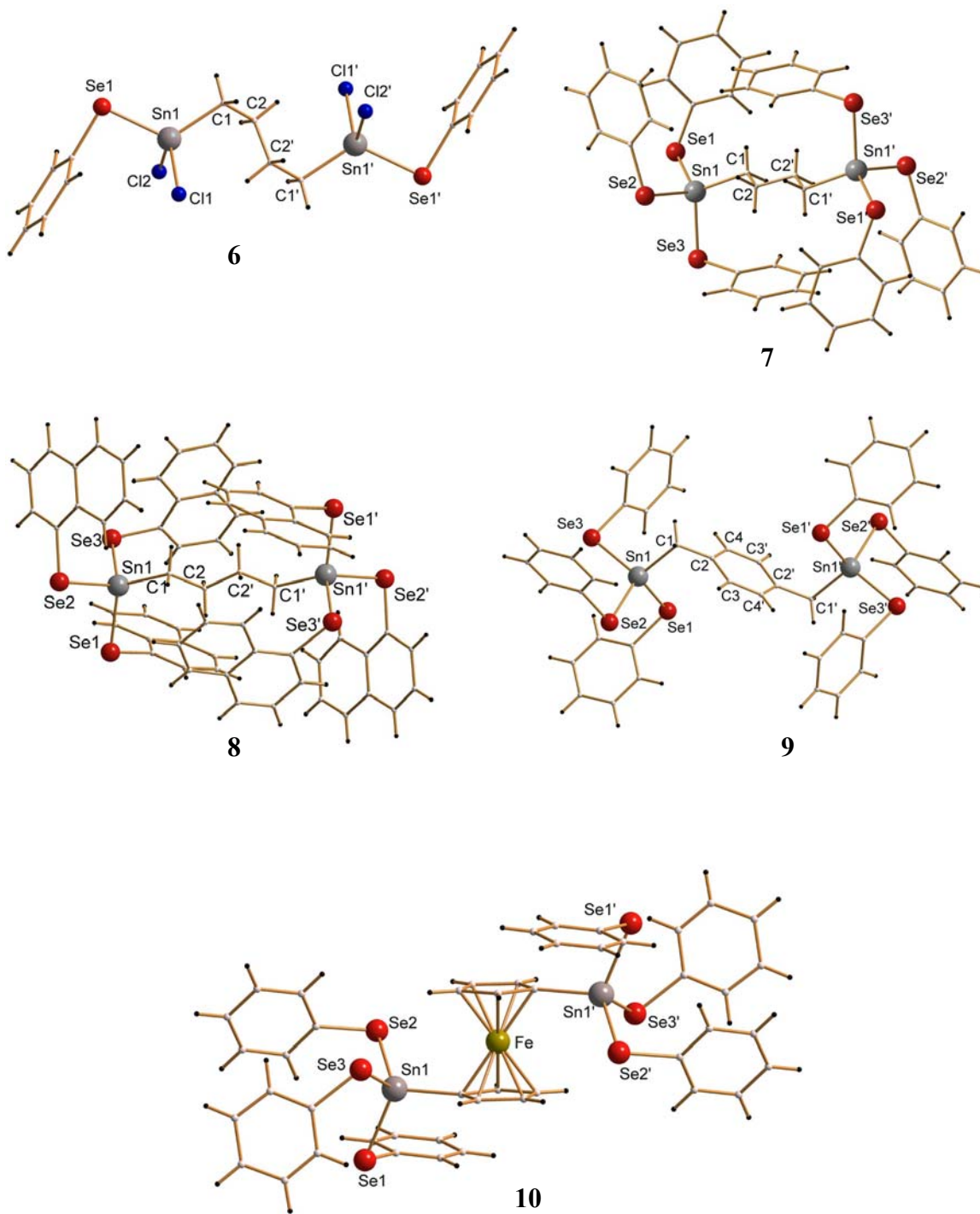
Figure 3.9 Molecular structures of compounds **6-10**

Two crystallographically equivalent tin atoms are connected by a butyl (**7**, **8**) or 1,4-dimethylbenzene (**9**) or 1,1'-ferrocenyl (**10**) residue. Each tin atom shows a distorted tetrahedral environment formed by the selenium donor atoms of the three selenonaphthylate (**8**) or selenophenolate (**9-10**) ligands and one carbon atom of the bridging organyl group. Selected bond lengths and angles are given in the table 3.3. In compound **8**, the selenonaphthylate groups are oriented around the tin atoms in a similar manner as in compound **1** with respect to the Sn–C bond. Therefore compound **8** can be considered as Type I conformation with dihedral angle C1–Sn–Se–C_{aryl} 25.80º-78.16º. In this context, it differs from thionaphthylate analogue compound **4**.

Table 3.3 Selected distances /pm and angles /º in compounds **7-10**

	7	8	9	10
Sn–C	214.9(3)	215.2(5)	217.3(6)	210.4(7)
Sn–Se	252.5(10)-254.1(9)	253.97(10)-254.93(8)	252.66(10)-254.02(8)	250.58(11)-254.13(11)
C–Se	192.6(4)-193.6(4)	181.1(11)-197.1(8)	192.0(7)-193.2(6)	191.5(8)-194.2(7)
C–Sn–Se	110.7(10)-112.2(11)	107.82(14)-116.21(14)	107.46(15)-117.17(18)	104.86(19)-113.2 (2)
Se–Sn–Se	108.00(4)-113.15(3)	98.32(3)-111.38(4)	103.26(3)-110.86(3)	106.47(3)-111.83(4)
Sn–C–C	114.7(2)	114.5(4)	109.0(4)	92.0(2)-96.082)

The Se homologue of **2**, compound **9** produced crystals suitable for single crystal X-ray diffraction. However, comparison of ^{119}Sn NMR spectra again confirms the identity of **2** with typical Δδ of 82.89 ppm upon the exchange of three thiophenolate to three selenophenolate.

-21.47
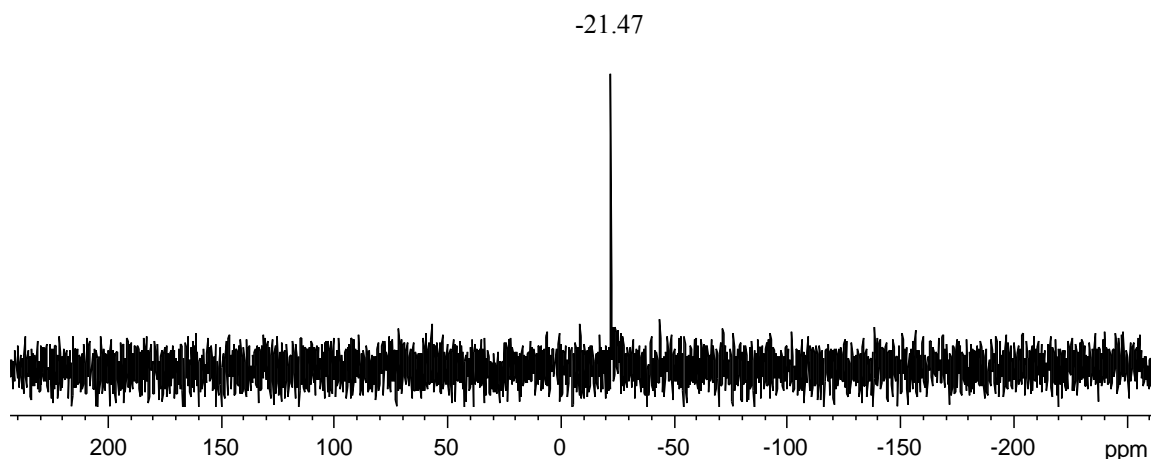
Figure 3.10 [119]Sn spectrum of compound **9**

On careful exploration of compound **9**, one can find two different types of orientations of the six selenophenolato ligands around the tin atoms. Dihedral angles of 157.70º for C1–Sn–Se–C_{Ph} or C1'–Sn–Se–C_{Ph} beside 40.73º and 74.20º for all other SePh groups indicates a Type II conformation in **9**. The bright orange solid of **10** is air stable although the starting material, 1,1'-bis(trichlorostannyl)ferrocene was highly air sensitive. In compound **10**, two [Sn(SePh)$_3$] units are connected to each other by a ferrocenyl bridge, being bonded to the two different cyclopentadienyl units of the ferrocene. The [CpSn(SePh)$_3$] units adopt a staggered conformation around the Fe atom, as observed for ferrocene Cp$_2$Fe in the solid state. This way they minimize the steric interactions within the molecules. The orientation of the selenophenolato ligands around tin atoms leads to a Type II situation with dihedral angles of 137.20º, 162.30º and 72.48º for C1–Sn–Se–C_{Ph} connections. Figure 3.11 shows the packing of the molecules of **6-10** within the crystal.

6

7
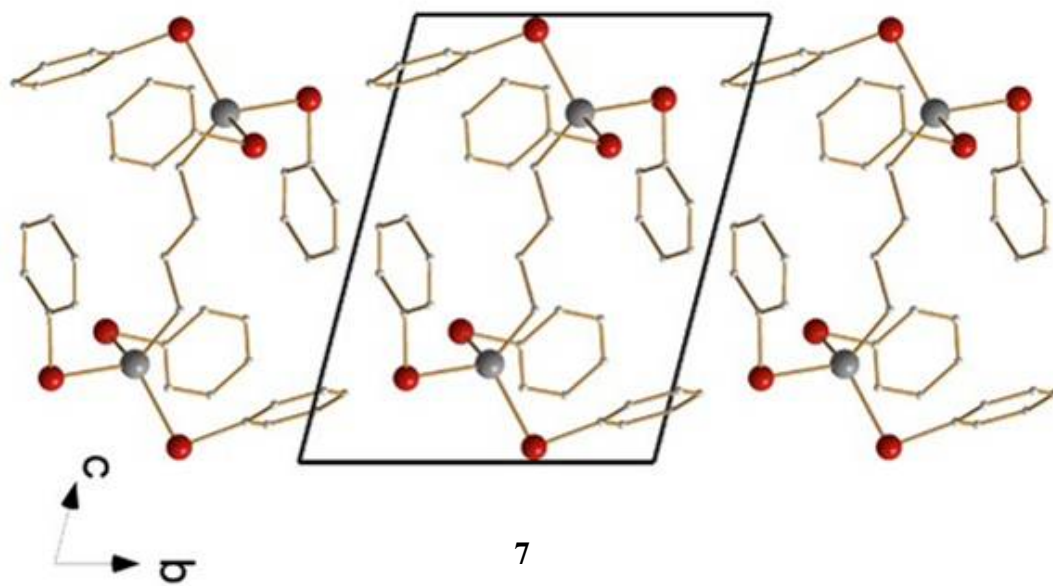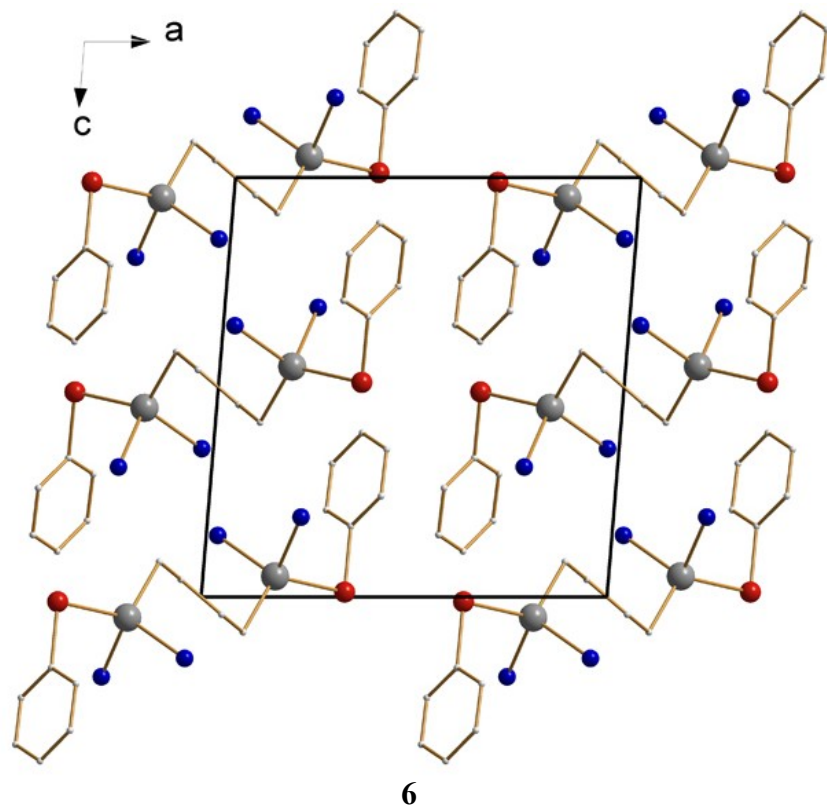
Figure 3.11 Packing of the molecules of compounds **6** and **7** within the crystal

8
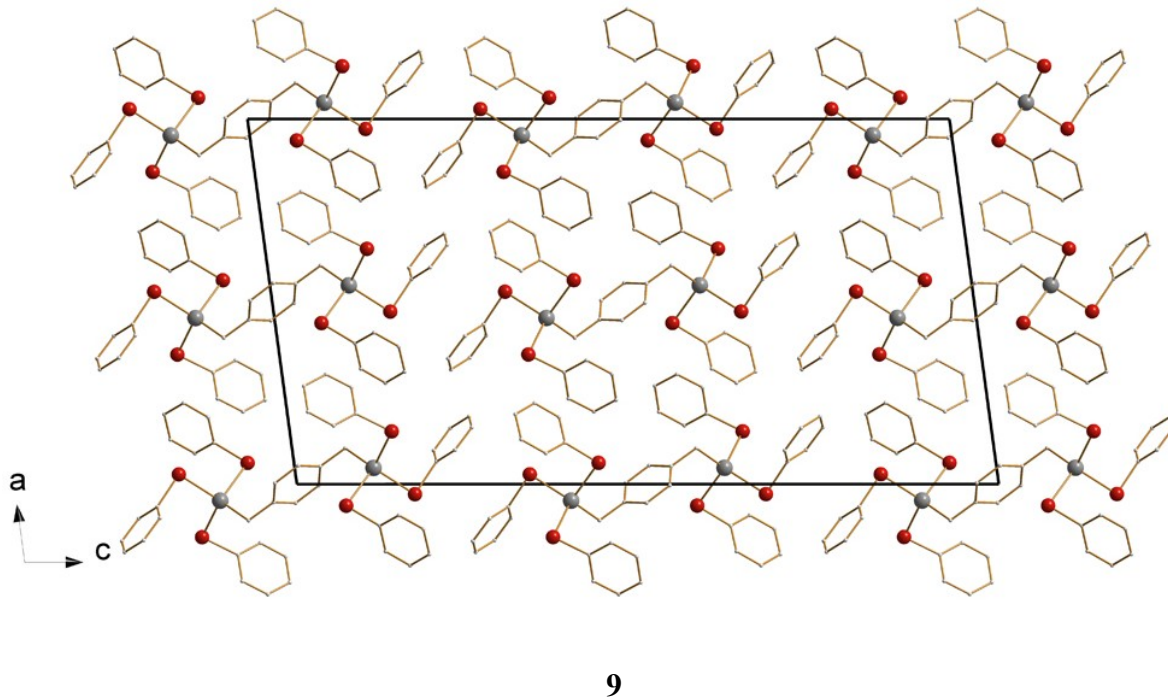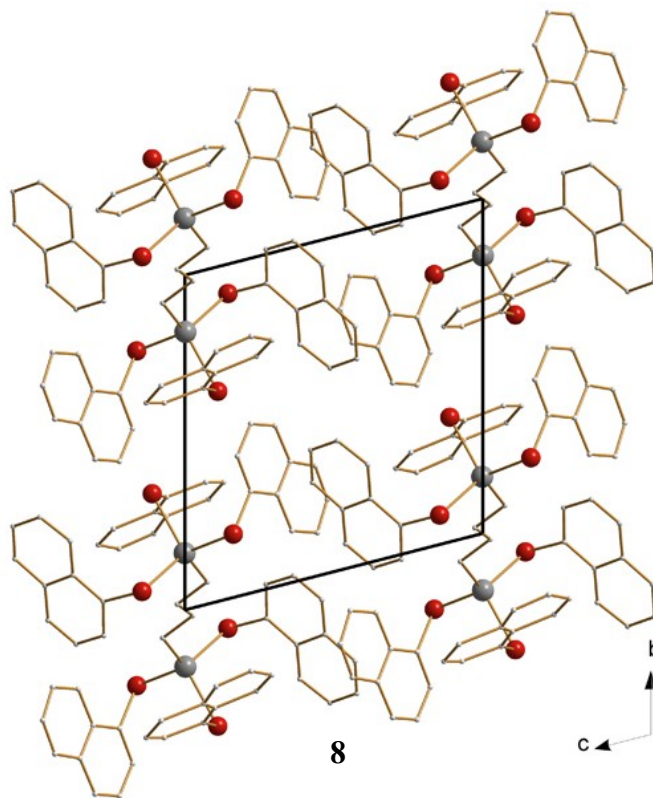
9

Figure 3.11 (continued) Packing of the molecules of compounds **8** and **9** within the

crystal
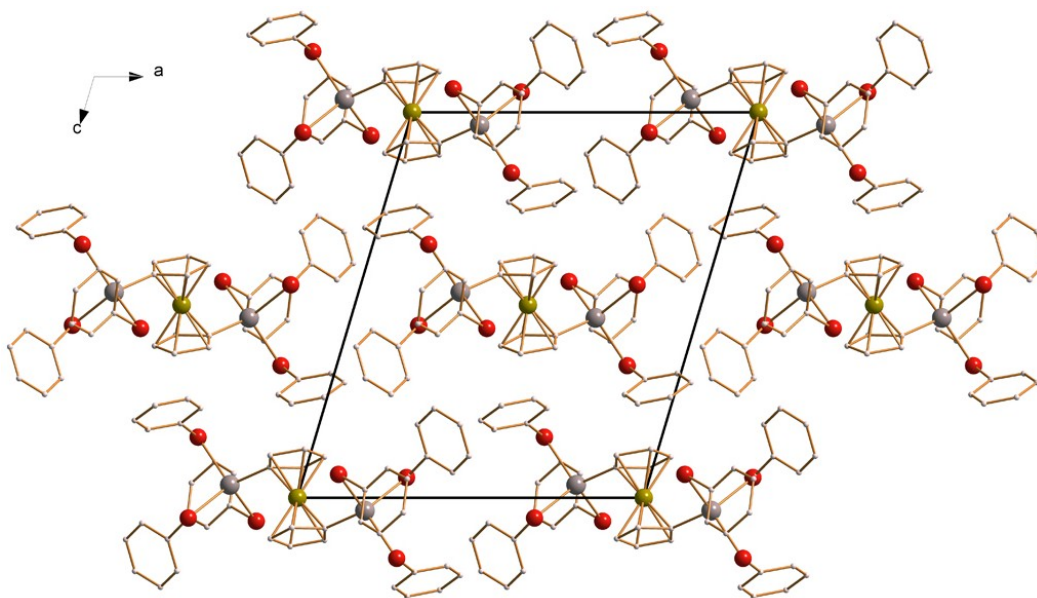
10

Figure 3.11 (continued) Packing of the molecules of compound **10** within the crystal

The crystal quality of compound **11** was not sufficient for X-ray diffraction. Therefore, compound **11** was characterized only by means of NMR spectroscopy (see experimental section). Figure 3.12 shows ^{119}Sn spectrum of compound **11**. The singlet at δ = –49.92 indicates that both the tin atoms are situated within the same chemical environment. A comparison to the spectrum of **9** (–21.47 ppm) or **10** (–49.27 ppm) shows the influence of the Fc bridge or the substitution of Np for Ph ligands respectively. This is discussed in more details in the following chapter.
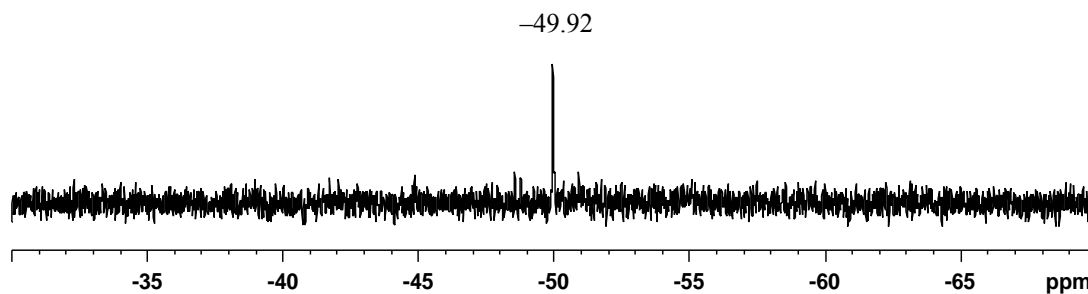
Figure 3.12 ^{119}Sn NMR spectrum of compound **11**

3.1.4 NMR spectroscopy

All compounds were characterized by means of NMR spectroscopy. In the ^{119}Sn NMR spectra, each of these compounds shows a single signal indicating that both tin atoms in every compound are situated within the indentical chemical environment in solution. Thiophenolato compounds **1**, **2**, **3** and 2-thionaphthylatocompounds **4**, **5** show signals at δ = 89.44, 61.42, 59.78, and δ = 85.49, δ = 55.44, respectively. The shift of the δ value toward higher field is put down to the change of the thiophenolate by the more electron rich thionaphthylate groups (**1** → **4**), and by replacing the bridging *n*-butyl group by the electron rich 4,4'-dimethylbiphenyl or 1,4-dimethylbenzene moieties (**4** → **3** or **5**). Selenolato compounds **7**, **8**, **9** and **10-11** produce signals at δ = –4.92, –6.2, –21.47 and –49.27, –49.92, respectively. Beside similar changes in δ upon variation of the organic groups (**7** → **8**, **8** → **9**) as observed for the thiolato compounds, the overall shift to again higher field is due to the substitution of less electronegative selenolate ligands for the thiolato groups, thus increasing the shielding of the tin atoms.

3.1.5 Quantum Chemical Study

In order to shed light on the observation of a certain preference for one conformer rather than the other density functional theory (DFT) [75] calculations were performed employing the program system TURBOMOLE [76-77]. As examples, both electronic and geometric structure of three molecules of the type (R'S)$_3$Sn–R–Sn(SR')$_3$ (R' = Ph, 1-naphthyl or 2-naphthyl and R = butyl, 1,4-dimethylbenzene) were optimized simultaneously, according to **1**, **4** and the R'S analogs of **7**, **8** and **9** in all three different conformations. Table 3.4 provides the resulting dihedral angles in comparison with the experimentally observed ones. Comparison of the structural parameters shows that intramolecular steric effects are well reproduced. Largest deviations are found in those cases, where calculations consider R'S ligands coordinated to the tin atoms whereas the experimentally obtained compounds are ligated by R'Se groups. Table 3.5 provides the relative energies of the resulting conformers. For E = S, all calculated species prefer the all-*cis* conformation Type I, which is indeed in agreement by most of the compounds in

the solid state. Although the stabilization is very small, this is a clear hint for a thermodynamic support of the observed conformation. For the calculated PhSe/1,4-dimethylbenzene combination, a slight preference for the *cis-trans* mixture was reproduced as it was also experimentally observed for respective compound **9**.

Table 3.4 Values of dihedral angles /° as resulting from DFT calculations of thiolato compounds (R'S)$_3$Sn–R–Sn(SR')$_3$ (R'/R = Ph/*n*Bu, 1-Np/*n*Bu, 2-Np/*n*Bu) and selenolato compound (PhSe)$_3$Sn–1,4-dimethylbenzene–Sn(SePh)$_3$, according to the three possible types of conformations explained before. Experimentally observed values for compounds exhibiting the respective R/R' combination (**7** and **8** containing selenolato groups R'Se instead of thiolato groups R'S) are given in parantheses

R'E/R	PhS/*n*Bu	1-NpS/*n*Bu	2-NpS/*n*Bu	PhSe/1,4-dimethylbenzene
Type I	38.2-46.5 (**1**: 28.72-64.26) (**7**, Se: 25.64-80.01)	37.3-46.2 (**8**, Se: 25.57-78.00)	28.7-50.1	2.8-82.8
Type II *cis*	17.2-84.2	21.6, 46.8	23.1, 40.5	37.0-45.3 (**9**: 40.73, 74.20)
trans	132.5-171.5	127.3-174.3	106.2-176.1	174.2, 179.9 (**9**: 157.73)
Type III	145.7-147.9	142.5-148.6	120.6-152.6 (**4**: 129.81-167.96)	144.6-149.7

The only case where the calculated structural preference does not agree with the experimental finding is the 2-NpS/*n*Bu combination as observed in **4**, the only compound obtained so far that features an all-*trans* configuration Type III: according to the calculations, Type III is disadvantaged by 2.5 kJ·mol^{-1} with respects to the mixed type II, and it is by 16.5 kJ·mol^{-1} less stable than the preferred all-*cis* conformation (Type I, Figure 3.13). Since the calculations represent gas phase conditions, I am only in the position to judge about the thermodynamic preferences of isolated molecules that might be overcompensated by intermolecular interactions in the crystal lattice. In **4**, the all-*trans* situation allows for a highly symmetric arrangement of the nearly linear molecules in the

crystal lattice, which would definitely be diminuated by different orientation of the 2-naphthyl groups.

Table 3.5 Relative energies ΔE /kJ·mol^{-1} of the three conformer types I, II and III, modelled for thiolato compounds (R'S)$_3$Sn–R–Sn(SR')$_3$ (R'/R = Ph/nBu, 1-Np/nBu, 2-Np/nBu) and selenolato compound (PhSe)$_3$Sn–1,4-dimethylbenzene–Sn(SePh)$_3$ using DFT methods. Most stable conformers are highlighted by grey background; experimental conformers are indicated by an asterisk

R'E/R	PhS/nBu		1-NpS/nBu		2-NpS/nBu		PhSe/p-1,4-dimethylbenzene	
Type I	−11.4	*	−24.0	*	−16.5		−1.5	
Type II	−5.4		−20.3		−2.5		−15.0	*
Type III	0.0		0.0		0.0	*	0.0	

This is not the case for the two further compounds with naphtyl substituents: **8** carries 1-naphtyl ligands that can not be arranged in a straight parallel manner and **5** is forced into an at least more bent conformation of the Sn–R–Sn backbone due to the rigid 1,4-dimethylbenzene bridge.
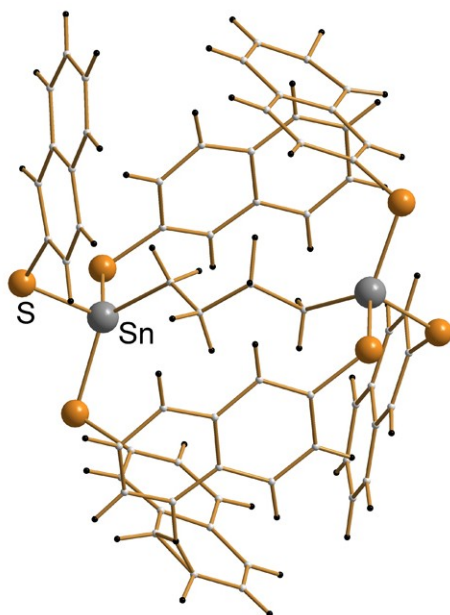
Figure 3.13 Calculated molecular structure of compound **4,** an all *cis* conformation

3.2 Stability and Reactivity of Bis[tris(arylchalcogenolato)-stannyl]organyls

3.2.1 Thermolysis of Bis[tris(arylchalcogenolato)stannyl]organyls

As discussed before, arylchalcogenolatomonotin compounds or organotin compounds have been used to synthesize tin chalcogenide materials by thermolysis. Similar efforts were undertaken to investigate the thermal behavior of the newly synthesized bis[tris(arylchalcogenolato)stannyl]organyl compounds. TGA analyses of $(PhS)_3Sn-(CH_2)_4-Sn(SPh)_3$ (**1**) and $(PhSe)_3Sn-(CH_2)_4-Sn(SePh)_3$ (**6**) were carried out at atmospheric pressure under a N_2 flow. The thermogravimetric analysis of **1** (Figure 3.14) shows a sharp weight loss at 375 ºC, leading to the formation of SnS_2 (observed mass loss: 62.2%; calculated: 61.45%). TGA of **7** (Figure 3.15) shows the formation of $SnSe_2$ at 335 ºC (observed mass loss: 56.0%; calculated: 55.0%). The quoted compositions were confirmed by EDX analyses. A slightly larger weight loss than calculated might be due to absorbed moisture during handling of the compound during the measurement. The study of the thermal behavior of the bis[tris(arylchalcogenolato)stannyl]organyl compounds soptlight them as valuable precursors for the synthesis of tin chalcogenide materials.
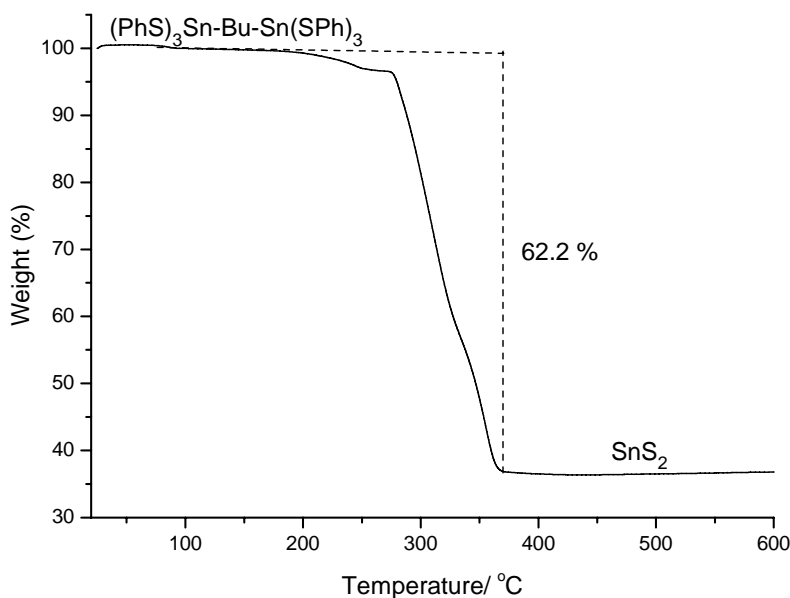
Figure 3.14 Thermogravimetric analysis plot of compound **1**
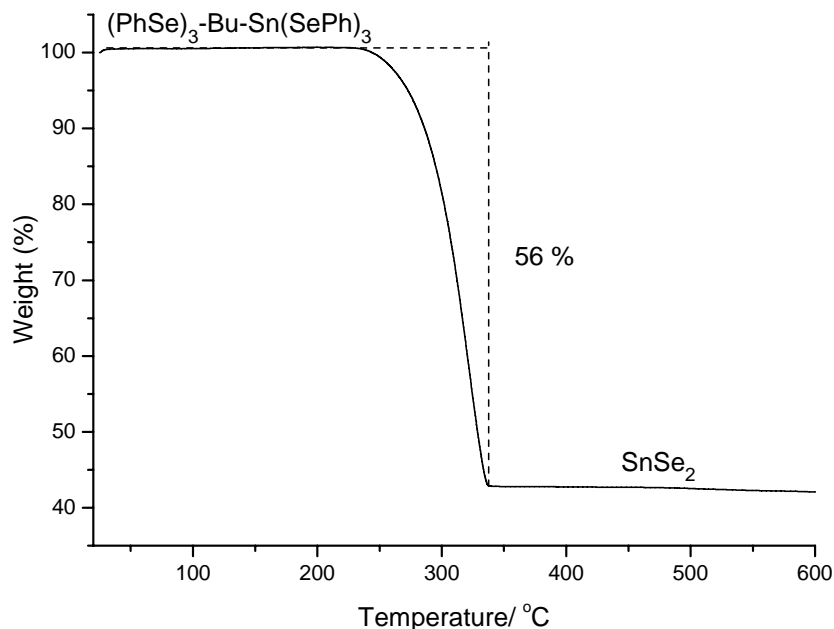
Figure 3.15 Thermogravimetric analysis plot of compound **7**

3.2.2 Reactivity of Bis[tris(arylchalcogenolate)stannyl]organyls

The syntheses and characterizations of various bis[tris(arylchalcogenolato)stannyl]organ-

yl compounds have been discussed in the previous section. They were sub-divided into three families depending on the orientation of the three arylchalcogenolate groups around the tin atoms, Type I, Type II and Type III. The structural and chemical characteristics suggest that these compounds can be used as a synthon for the synthesis of metal chalcogenide clusters or complexes; especially, Type I is promising candidate because of the available "free" electron density at the E ligands as shown in the figure 3.8. Furthermore they might served as arylchalcogenolate source. For instance, $Sn(SPh)_4$ has been reported to be an efficient starting material for the synthesis of ternary Sn/Cu/S clusters as $[(Ph_3P)Cu]_2Sn(SPh)_6$. Organotin chalchogenolate compounds like R_3SnER' (R = Me; R' = Bu, Ph; E = S, Se, Te) have been used as arylchalcogenolate sources for the synthesis of various arylchalcogenolate groups containing organic compound via the formation of a palladium arylchalcogenolate intermediate complex.

Thus I intended to study the nature of bis [tris(arylchalcogenolato)stannyl]organyl compounds. The most likely reactions are (a) the formation of complexes with transition

metals, (b) the transfer of arylchalcogenolate groups to transition metal ions to form metal chalcogenolate complexes or (c) an arylchalcogenolate transfer to reactants to result in the formation of chalcogenolate functionalized organic compounds (Scheme 3.5).
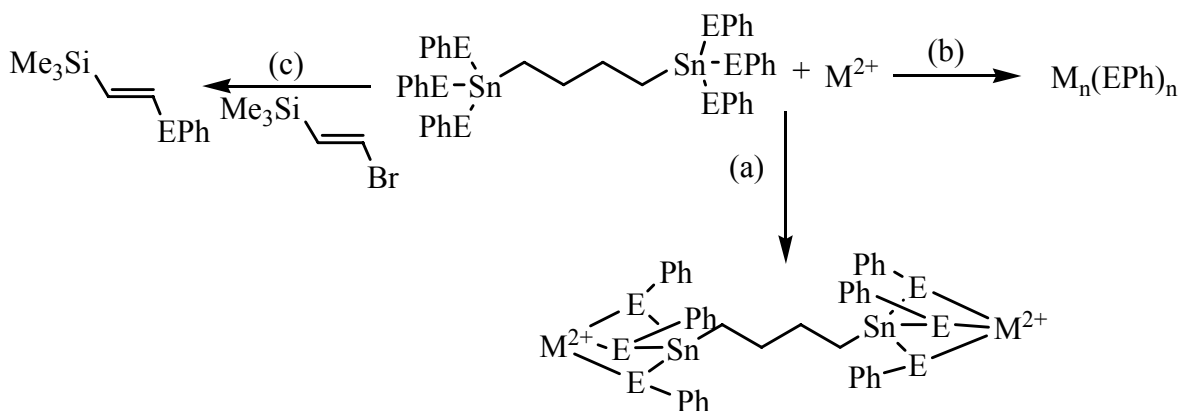
Scheme 3.5 Possible reactivities of bis[tris(arylchalcogenolato)stannyl]organyls toward transition metal ions

Some of the bis[tris(arylchalcogenolato)stannyl]organnyl compounds discussed above were subjected to reactions with different transition metal complexes. However, because of the multidentate nature, insoluble solids were obtained in all cases with various binary metal chalcogenide complexes in very low yields. For example $(PhSe)_3Sn-(CH_2)_4-Sn(SePh)_3$ reacts with transition metal complex, palladium acetate, to serve as selenophenolate ligand donor to form binary metal chalcogenide cluster in low yield with insoluble unknown solid..

3.2.2.1 Synthesis and Characterization of $[Pd(SePh)(OAc)]_4$ (12)

Compound **12** was synthesized by reacting a dichloromethane (DCM) solution of palladium acetate and $(PhSe)_3Sn-(CH_2)_4-Sn(SePh)_3$ as a mild, SePh donating species at room temperature (Scheme 3.6). Red crystals of **12** were obtained upon layering of the reaction solution by *n*-hexane in low yield. Compound **12** was characterized by means of single-crystal X-ray diffraction, UV-visible and NMR spectroscopy.

$(PhSe)_3Sn–(CH_2)_4–Sn(SePh)_3 + 2\ Pd(OAc)_2$

DCM, stirring, filtration
layering by *n*-hexane

$[Pd(SePh)(OAc)]_4$ (30%)
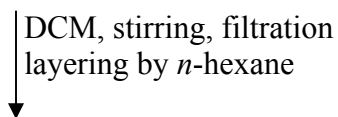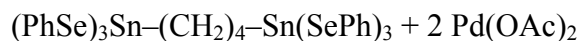
Scheme 3.6 Synthesis of compound **12**

Compound **12** is the first tetranucler palladium selenophenolate complex. Compound **12** crystallizes in the monoclinic space group $P2_1/n$ with two formula units in the unit cell. The molecule shows a paddle-wheel type geometry with each of the divalent palladium cations being surrounded by two oxygen atoms and two selenium atoms of the acetate and selenophenolate ligands in square planar geometry, as found for the SEt-bridged isostructural analogue $[Pd(SEt)(OAc)]_4$ [78]. Figure 3.16 shows the molecular structure of this compound.
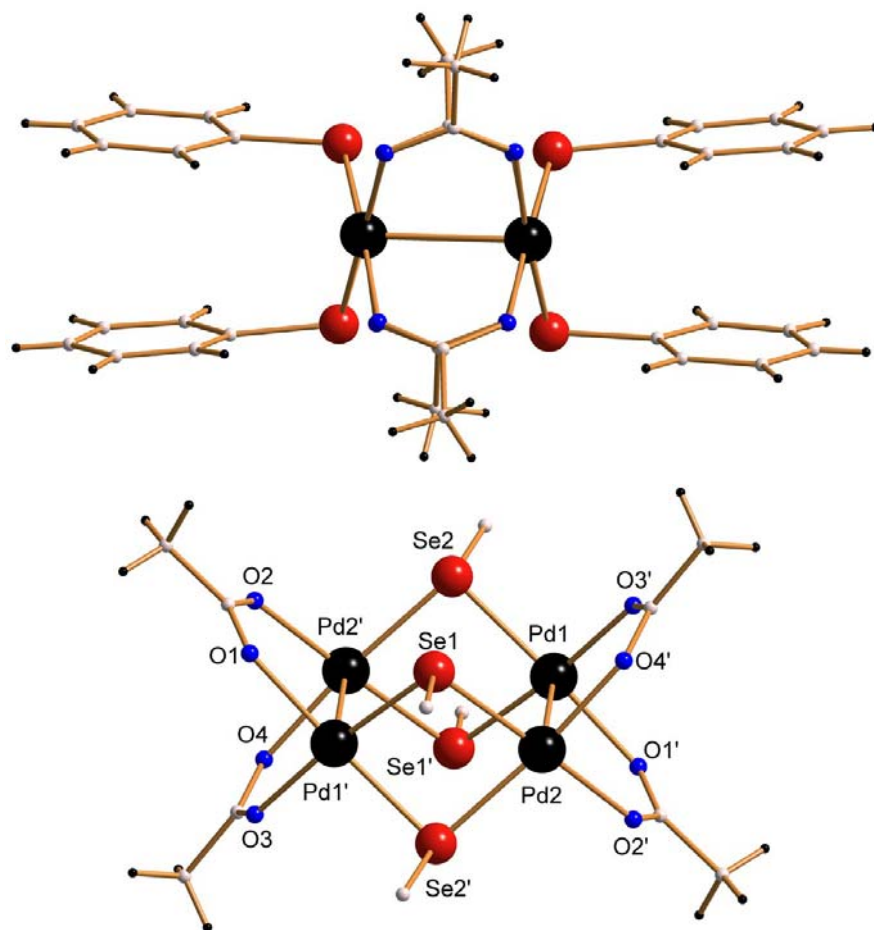
Figure 3.16 Molecular structure of **12** in two different views (bottom: Ph omitted)

Owing to a heteroleptic bridging mode by two (OAc) or two (SePh)⁻ units, respectively, the four Pd atoms form a rectangle with two $[Pd_2(OAc)_2]^{2+}$ units. The Pd–Pd distance is 286.40(18) pm, which is within the range of known bonds in d^8 Pd^{2+} compounds. The two $[Pd_2(OAc)_2]^{2+}$ units are linked by four (SePh)⁻ groups at two longer, non-bonding Pd…Pd contacts, 349.6(2) pm. In this regard, the compound differs from known tetranuclear Pd complexes, of which only $[Pd(\mu\text{-}Cl)\{\mu\text{-}(\sigma\text{-}\kappa\text{-}PhSCHCH_2C_6F_5)\}]_4$ exhibits, however longer, Pd–Pd bonds 291.7(2) pm [79]. The phenyl groups are oriented parallel to each other within the molecules, but inclined with respect to adjacent molecules within the crystal. This indicates the absence of intermolecular pi-stacking for additional stabilization (Figure 3.17).
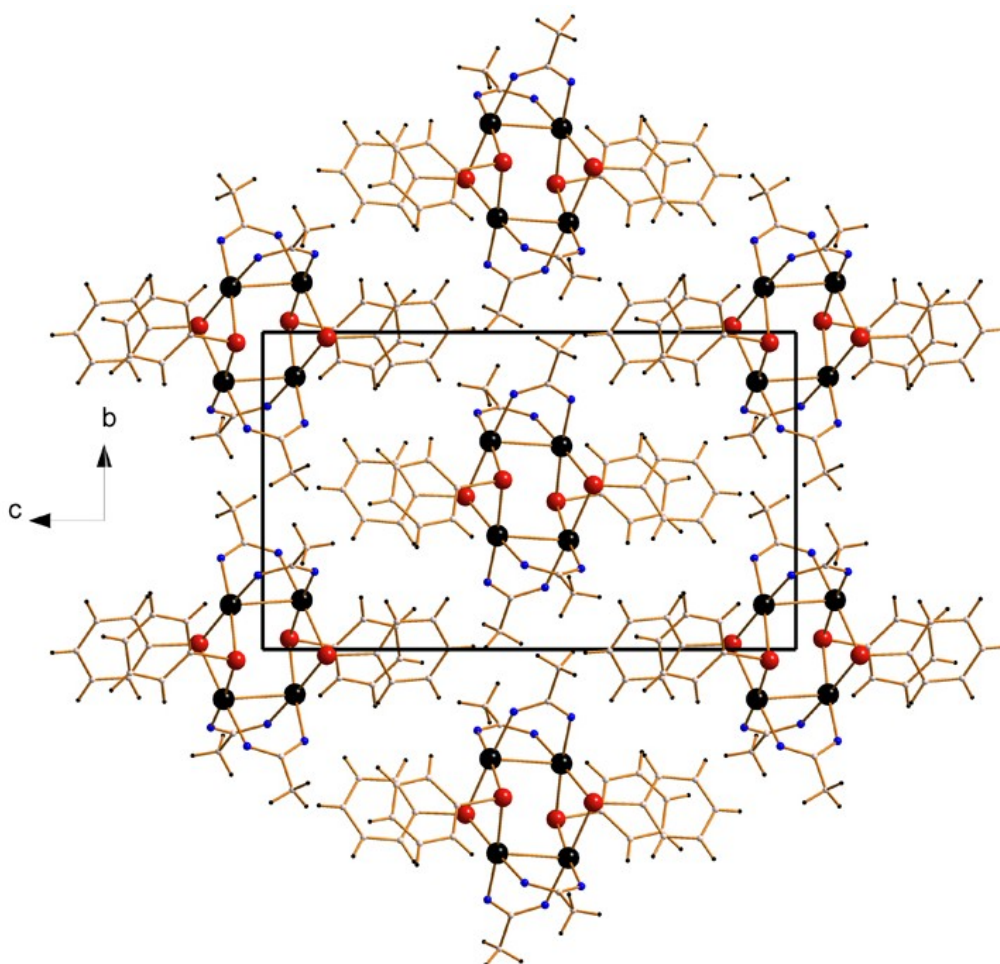
Figure 3.17 Packing of the molecules of compound **12** within the crystal, viewed along crystallographic *a* axis, color code: Pd, black (large spheres); Se, red; O, blue; C, grey; H, black (small spheres)

There is a possibility of all four acetate groups and and four selenophenolate groups to arrange themselves to give different isomers. But, only one isomer is obtained experimentally. The thermodynamic preferences of the obtained isomer is rationized by quantum chemical investigations in the following chapter.

The UV-visible spectrum of **12** (Figure 3.18) shows a sharp absorption at 2.01 eV (617 nm), in accordance with the visible color of the single crystals. Since d-d transitions do not occur at square planar d^8 complexes (non-degenerate ground state), the shown excitation is exclusively due to Se $\rightarrow$ Pd charge transfer (LMCT). Similar CT energies have been previously observed for further Pd/Se compounds [80-82].
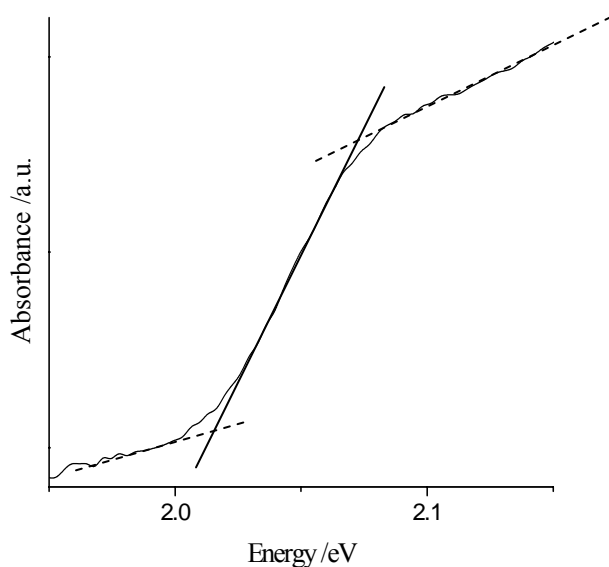
Figure 3.18 UV-visible spectrum of compound **12**, recorded as suspension of pulverized single crystals in nujol oil.

Thermogravimetric analysis of **12** (Figure 3.19) reveals that the compound decomposes between 200 and 300 °C, with a first, inconspicuous step ending up with 54% of the original mass. This would accord to the formation of the known phase $Pd_{17}Se_{15}$ [83-85] (calculated weight loss: 54.77%). However, a further weight loss to a final of about 50% of the original is observed while the sample mass reaches a minimum at 440 °C.
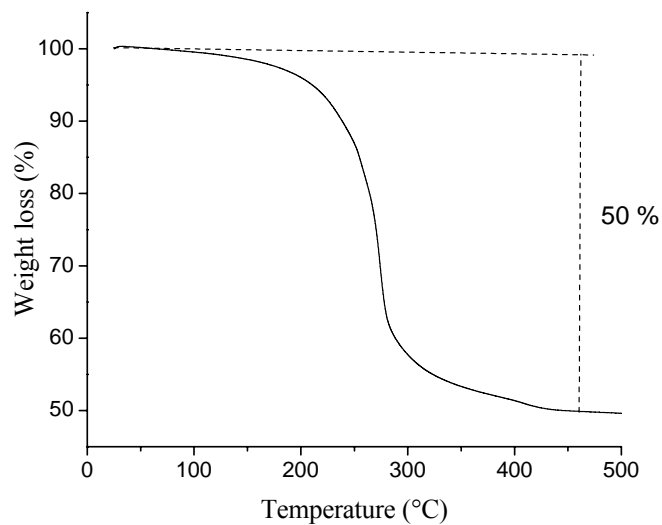
Figure 3.19 Thermogravimetric analysis plot of compound **12**

According to semi-quantitative analysis (EDX), the remaining phase exhibits a Pd:Se atomic ratio of 1.0:0.7, in agreement with the findings (calculated weight loss: 50.29%). The resulting, nominal composition $Pd_{10}Se_7$ was hitherto unknown. I put this observation down on the presence of Pd–Pd interactions in **12** and the yet unprecedented; heteroleptic bridging of these that might enable different decomposition pathways.
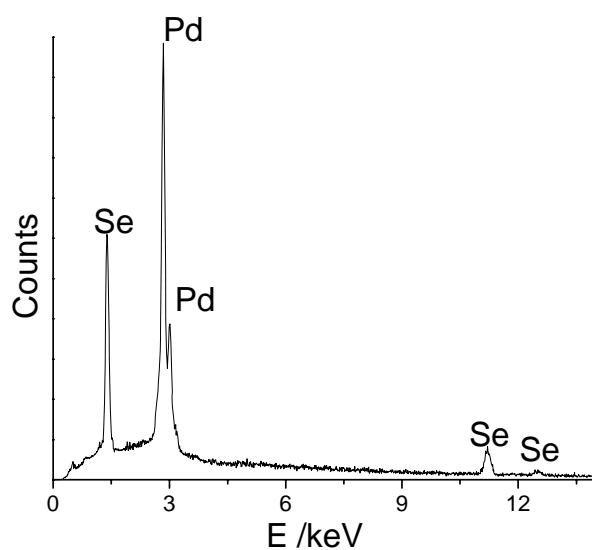
Figure 3.20 EDX spectrum of compound **12**

3.2.2.2 Quantum Chemical Study of Compound 12

In order to shed light on the observed arrangement of acetate and selenophenolate ligands, density functional theory (DFT) calculations were performed. Geometric and electronic structures of **12** were optimized simultaneously for nine different isomers (I-**1** to I-**9**), that differ in the arrangement of the eight ligand groups around the Pd_4 rectangle (Figure 3.21).
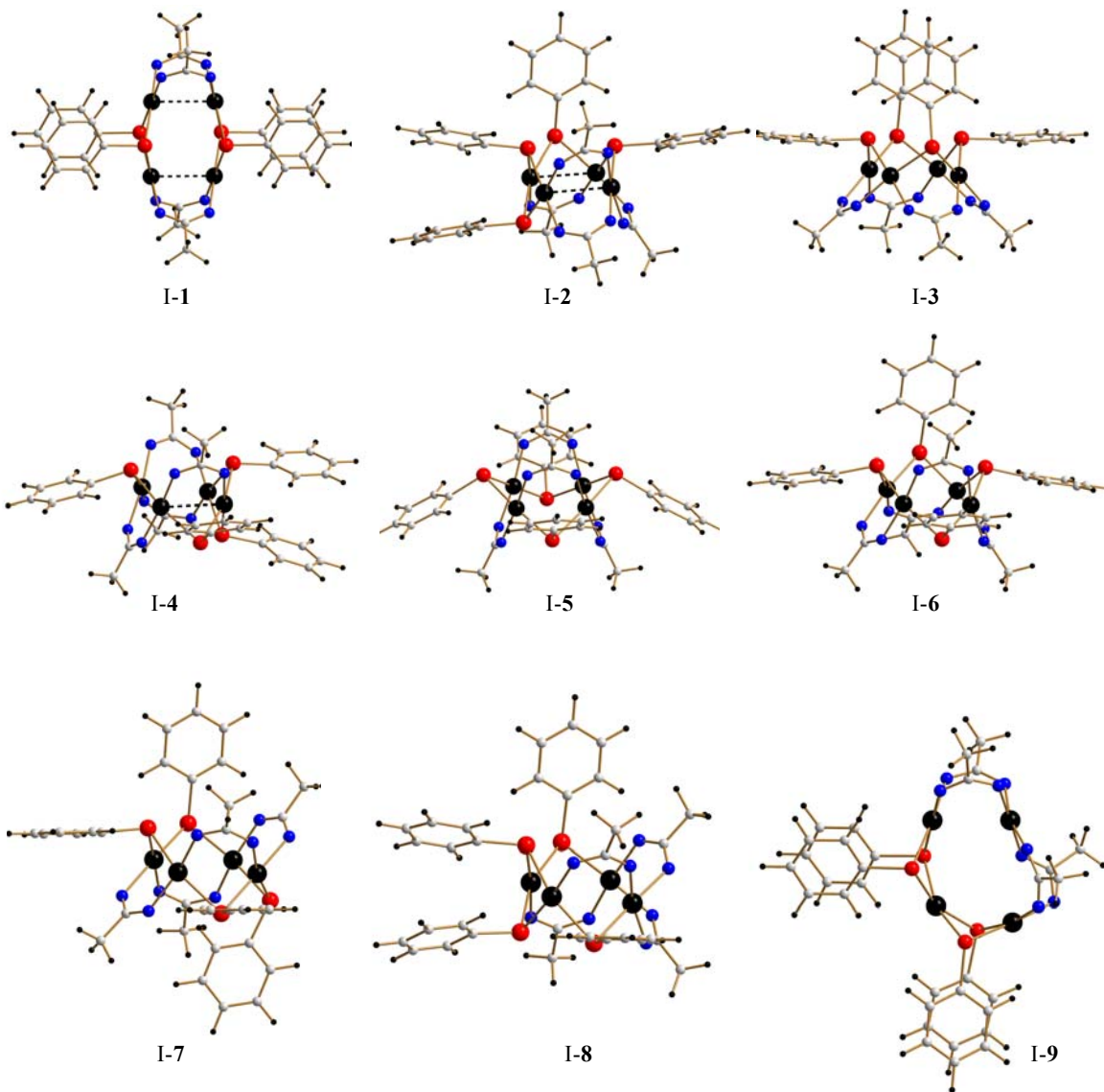
Figure 3.21 Molecular structures of different isomers of compound **1**, I-**1** to I-**9**, as calculated using DFT methods, color code: Pd, black (large spheres); Se, red; O, blue; C, grey; H, black (small spheres). Pd–Pd distances below 300 pm are given as dashed lines.

The structural parameters of isomer I-**1**, representing the geometry found in the crystal structure, are in excellent agreement with the experimentally observed ones. The maximum deviations of distances and angles are 8.0 pm and 3.0° (Table 3.6).

Table 3.6 Distances /pm and angles /° of the most stable isomer I-**1** in comparison to those of experimentally observed for **12**

	Experimental **12**	Calculated I-**1**
Pd–Se	237.0(3)-242.3(3)	244.0
Pd–O	205.5(15)-208.2(14)	212.0
Pd–Pd	286.40(18), 349.6(2)	293.0, 354.0
Pd–Se–Pd	93.22(9)-94.67(9)	93.0-93.0
Se–Pd–Pd	97.72(7)-101.79(7)	100.1-100.6
Se–Pd–Se	82.54(9)-83.00(9)	83.3-83.3
C–Se–Pd	102.3(7)-105.9(7)	103.4-106.3
C–O–Pd	125.1(11)-128.2(13)	125.1-125.2
O–Pd–Pd	80.6(3)-82.5(3)	81.1
O–Pd–Se	91.8(4)-174.7(4)	93.1-176.4
O–Pd–O	90.6(6)-92.8(6)	90.8-91.0

The structure of I-**1** is the thermodynamically most favored one in agreement with the experimental observation. A comparison of the relative energies of all calculated isomers, with respect to that of I-**1** together with the ligand arrangement characteristics are given in table 3.7. The energy differences indicate to which extent the isomers (a) meet the requirements of an optimizated coordination situation at the Pd atoms, (b) whether or not Pd…Pd interactions are maintained and, as a minor point, (c) whether or not intramolecular pi-stacking is possible.

Table 3.7 Relative energies ΔE /kJ·mol−1, donor atom arrangement (L = Se, O), maximum deviation from planar coordination/°, and Pd…Pd distances /pm as calculated for different isomers I-**1** to I-**9** using DFT methods

	ΔE	No. of L–Pd–L diagonals (L–Pd distances/pm)			$\Delta<_{max}$	Pd...Pd
		Se–Pd–O	Se–Pd–Se	O–Pd–O		
I-**1**	0.0	8 (244/212)	–	–	0.6	293, 354
I-**2**	34.3	6 (240-246/209-213)	1 (250-251)	1 (205-207)	14.2	298-369
I-**3**	35.5	8 (240-243/210-213)	–	–	3.8	322, 350
I-**4**	41.1	4 (242-244/211-212)	2 (246-254)	2 (205-207)	12.3	295-364
I-**5**	48.5	–	4 (248-249)	4 (205-206)	5.3	328, 329
I-**6**	56.7	4 (241-244/210-212)	2 (247-251)	2 (206)	12.4	310-353
I-**7**	68.8	4 (241-243/210-212)	2 (249-252)	2 (207)	14.8	325-343
I-**8**	82.6	4 (243-245/211-212)	2 (247-250)	2 (204-207)	17.3	320-359
I-**9**	119.7	4 (244/211-213)	2 (249-251)	2 (204-207)	14.7	304-407

[a] defined as the maximum angle of an L3–Pd bond with the plane defined by L1, L2, L3, for all L1-L3 combinations at each Pd atom in the given isomer.
atom in the given isomer.

Both electronic and sterical effects lead to modification of the Pd–Se and Pd-O bond lengths and deviations from linearity of the L–Pd–L diagonals (E = O, Se). The larger *trans*-effect [86] of (PhSe)⁻ when compared to (MeCOO⁻) leads to elongation of the bonds opposite of Pd–Se and a shortening opposite of Pd–O. This means weakening of the Pd–Se bonds in an Se–Pd–Se arrangement (elongation by 4-10 pm), which is obviously not overcompensated by the (smaller) shortening of the Pd–O bonds (by 0.03-0.07 pm) in the complementary O–Pd–O arrangment. Thus, in the most stable isomer, I-**1**, only Se–Pd–O diagonals are present that allow for a well balanced geometry and thus binding energy. Two Pd–Pd interactions and two parallel Ph rings further stabilize this isomer. Figure 3.22 shows the MOs that account for the Pd-Pd interaction. Coordination is performed mainly or exclusively by Se–Pd–O diagonals in I-**2** and I-**3**, as well; in I-**2**, a distinct deviation from planarity is overcompensated by two Pd–Pd bonds. A similar energy is achieved in I-**3** by an inverse situation: all Pd…Pd edges are bridged by a pair of different ligands, causing only deviation from planarity (3.8° maxium); however, the Pd…Pd distances are forced to become similar (Pd…Pd 322, 350 pm) at the expense of the Pd–Pd interactions, which destabilizes the isomer in turn.
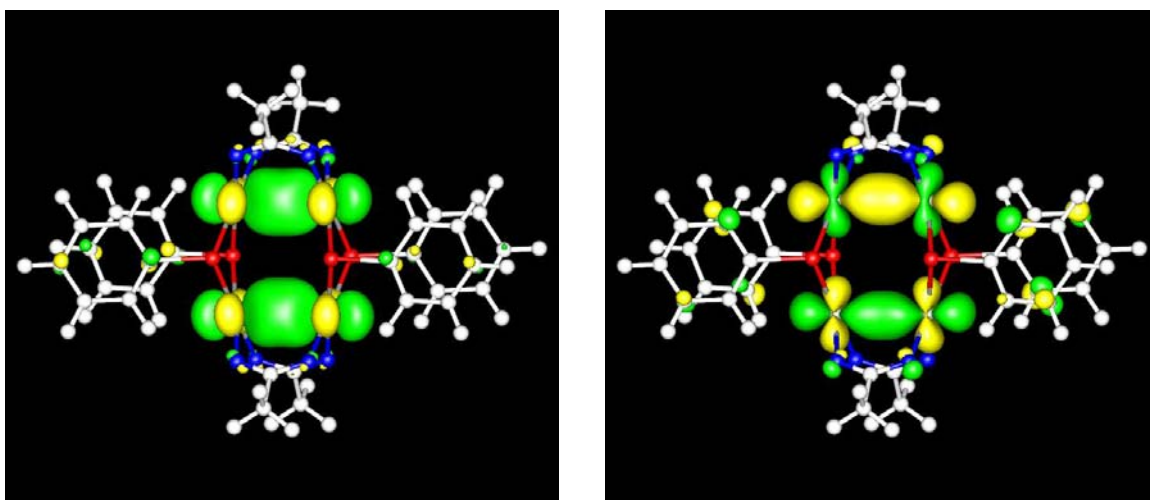
Figure 3.22 Pd1–Pd2 bonding molecular orbitals of compound I-**1**: HOMO–23 (left hand side) at 1.95 eV below ε(HOMO) and HOMO–24 (right hand side) at 1.96 eV below ε(HOMO)). Electron densities are drawn to 0.2 e⁻·Å⁻³.

I-**4** and I-**5** form another pair of this type, however, with a more distinct energy difference: in I-**5** the strictly alternating position of the ligands above and below the Pd$_4$ unit cause relatively small deviation from planarity (5.3° maximum) and four equivalent, non-bonding Pd–Pd edges (Pd…Pd 328, 329 pm), similar to I-**3**, but additionally cause non-existence of both Se–Pd–O diagonals and intramolecular pi-stacking. Variation of these effects by different ligand arrangements give rise for the energy differences in the calculated isomers – with highest significance of the bond distances around Pd and within the Pd…Pd edges, followed by the planarity and stabilization by parallel Ph groups. Consequently, the least stable isomer I-**9** shows large deviation from planarity (14.7° maximum) and extreme elongation of the Pd…Pd edges 304-407 that cannot be compensated by pi-pi interactions. This explain the preferences of I-**1** than others.

The above reaction shows that bis[tris(selenophenolato)stannyl]butane acts as mild selenophenolate donor towards transition metal to form arychalcogenolate complex of transition metal where straight foreward reactions fail, like the raction of palladium acetate with PhSeSiMe$_3$ or NaSePh in DCM or THF, respectively.

3.3 Reactivity of Bis(trichlorostannyl)organyls toward PhSeSiMe$_3$ and Coinage Metal Complexes

In section 3.1, 3.2, the synthesis of various bis[tris(arylchalcogenolato)stannyl]organyls compounds, their potential application for the synthesis of tin chalcogenide materials (SnS$_2$, SnSe$_2$) and their employment for the synthesis of a transition metal chalcogenide complex ([Pd(SePh)(OAc)]$_4$, **12**) have been discussed. While bis[tris(arylchalcogenolato)stannyl]organyls seem to serve as mild arylchalcogenolato donors to result in binary metal chalgenide complexes, they do not form any organoclad or organobridged ternary clusters. However, a wide variety of chalcogenide clusters of transition metals have been reported. Coinage metal chalcogenide complexes are also well established because of their widespread interest due to bonding diversity or tuneable band gaps, for example [87-90]. To understand the reactivity of this kind of compounds in the presence of organotin compounds, an effort was taken to synthesize coinage metal selenide clusters in the presence of organo ditin or monotin compounds.

Here, bis(trichlorostannyl)organyls and mono organotin compounds were reacted with coinage metal complexes in the presence of PhESiMe$_3$ (E = S, Se; as source of both E^{2-} and PhE$^-$) to study their nature in one step reaction.

3.3.1 Synthesis and Characterization of [(Ph$_3$P)$_3$(SePh)$_2$Cu$_2$]·1.5THF (13)

Compound **13** was synthesized by the raection of [(PPh$_3$)$_3$CuCl] with PhSeSiMe$_3$ in the presence of 1,4-bis(trichlorostannyl)butane in THF. Yellow crystals of compound **13** were isolated from a THF/*n*-hexane mixed solution in 80% yield.

$$Cl_3Sn-Bu-SnCl_3 \ + \ 6 \ (PPh_3)_3CuCl \ \xrightarrow[\text{THF}]{\text{PhSeMe}_3} \ [(Ph_3P)_3(SePh)_2Cu_2]\textbf{.}1.5 \ THF$$
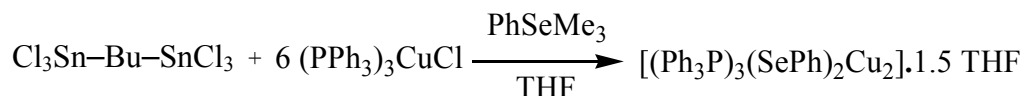
Scheme 3.7 Synthesis of compound **13**

The compound was structurally characterized by means of single crystal X-ray diffraction. It crystallizes in the monoclinic space group *C2/c* with eight formula units per unit cell. Figure 3.23 shows the molecular structure of this compound. The packing of the molecules within the crystal is shown in figure 3.24.
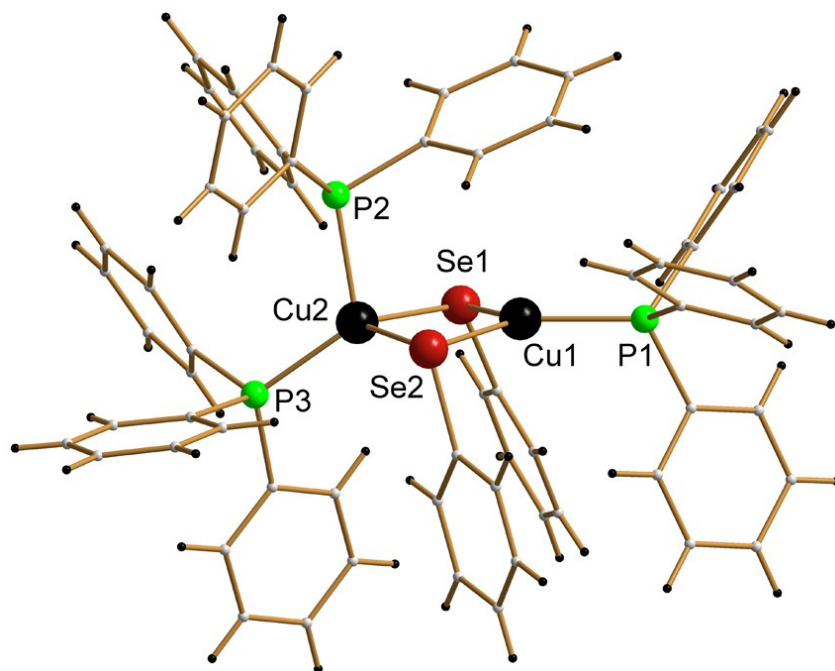
Figure 3.23 Molecular structure of compound **13**

The structure consists of a benzeneselenolate-bridged dimer containing both three- and four-coordinated copper atoms. The geometry around CuI is *pseudo*trigonal whereas it is *pseudo*tetrahedral around Cu2. The Se atoms are three-coordinate and serve as bridges between the copper atoms. The four-membered Cu_2Se_2 structural unit is nearly planar. Table 3.8 and table 3.9 provide selected bond lengths and angles of the compound. Both Ph groups are located one side of the Cu_2Se_2 ring, directing slightly toward the three-coordinate Cu atom.
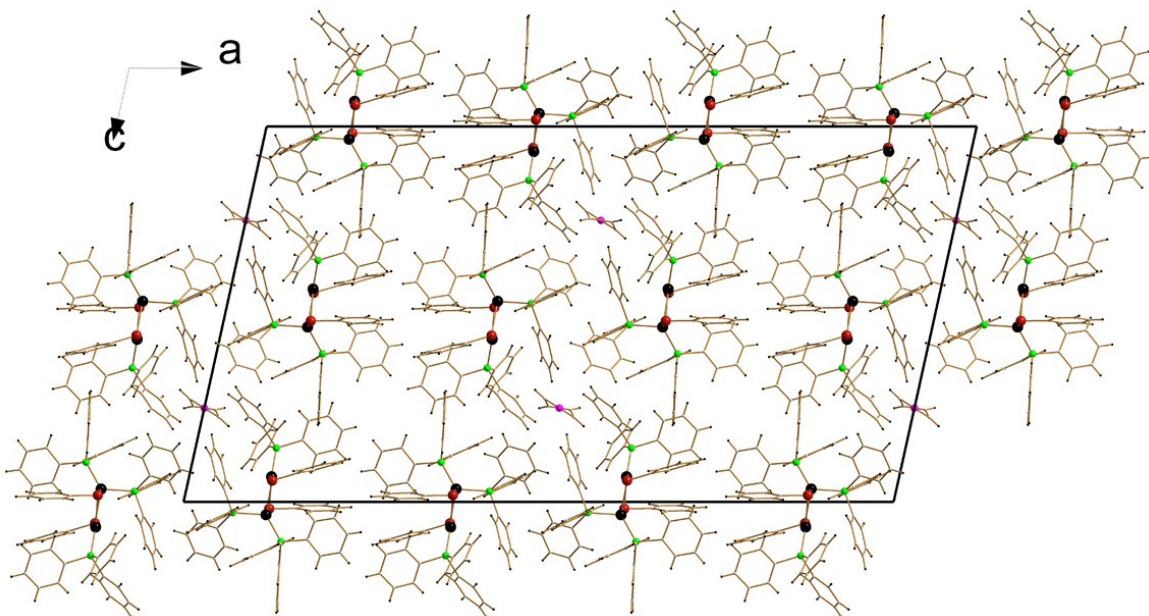
Figure 3.24 Packing of the molecules of compound **13** within the unit cell viewed along crystallographic *b* axis

The Sel–C$_{Ph}$ and Se2–C$_{Ph}$ vectors include angles of 113.1(8) and 97.78(5)° with the Cu$_2$Se$_2$ plane, respectively, which are larger than in the corresponding known compound [(Ph$_3$P)$_3$(SePh)$_2$Cu$_2$]·CH$_3$CN [91], prepared by electro-oxidation of a copper anode into a toluene/acetonitrile solution of diphenyl diselenide and triphenylphosphine. There are, however, substantial distortions in the molecule which appear to result from the sterically overloaded metal centers and come along with the different coordination mode of the two copper centers. The Cul–Se–C angles of 103.4(4) and 91.6(3)° are much smaller than the Cu2–Se–C angles of 119.9(3) and 107.3(3)°. The Cul-Cu2 distance of 290.54(16) pm which is only slightly longer than the sum of the Van der Waals radii of Cu (280.0 pm) [92], is much shorter than reported for (PPh$_3$)$_3$Cu$_2$Cl$_2$·C$_6$H$_6$ (314.0 pm) [93] or reported for (Ph$_3$P) Cu(μ-SPh)$_2$Cu(PPh$_3$)$_2$ (366.2 pm) [94] but larger than in [(Ph$_3$P)$_3$(SePh)$_2$Cu$_2$]·CH$_3$CN (273.8(1) pm). The large P2-Cu2-P3 angle of 115.76(10)° at pseudotetrahedrally coordinated Cu2 is a result of the steric repulsions of the adjacent triphenylphosphine groups. Further, the bridging selenolate ligands are not symmetric with respect to the Cu atoms.

Table 3.8 Selected bond lengths of compound **13**

Bond	Distance[pm]	Bond	Distance[pm]
Cu1–Cu2	290.54(16)	Cu1–P1	221.7(3)
Cu1–Se1	239.20(16)	Cu2–P2	228.8(3)
Cu1–Se2	243.33(15)	Cu2–P3	227.1(3)
Cu2–Se1	257.45(14)	Se1–C1(11)	191.8(10)
Cu2–Se2	248.32(16)	Se2–C221	193.7(9)

Table 3.9 Selected interatomic angles of compound **13**

Angels	/°	Angels	/°
Cu1–Se1–Cu2	71.50(5)	P2–Cu2–Se1	92.39(7)
Cu1–Se2–Cu2	72.44(5)	Se2–Cu2–Se1	104.06(5)
C111–Se1–Cu1	103.4(4)	P3–Cu2–Cu1	146.24(8)
C111–Se1–Cu2	119.9(3)	P2–Cu2–Cu1	97.60(7)
C221–Se2–Cu1	91.6(3)	Se2–Cu2–Cu1	52.99(4)
C221–Se2–Cu2	107.3(3)	Se1–Cu2–Cu1	51.33(4)
Cu1–Se2–Cu2	72.44(5)	P1–Cu1–Se1	123.50(9)
P3–Cu2–P2	115.76(10)	P1–Cu1–Se2	124.58(9)
P3–Cu2–Se2	119.55(8)	Se1–Cu1–Se2	111.46(5)
P2–Cu2–Se2	102.32(8)	P1–Cu1–Cu2	178.48(9)
P3–Cu2–Se1	118.42(8)	Se1–Cu1–Cu2	57.17(4)

The Cu1–Se distances of 239.20(16) and 243.33(15) pm are in close agreement, but there is a significant discrepancy for the Cu2–Se bond lengths (Cu2–Se1, 257.45(14) pm**;** Cu2–Se2, 248.32(16) pm). Thus, Cu–Se bond lengths in **13** range from 239.20(16) to 257.45(14) pm and are significantly longer than the average Cu–Se bond lengths of 237.0 pm in $[Ph_4P]_2[Cu_4(Se_4)_{2.4}(Se_5)_{0.6}]$ and 232.5 pm in $[Ph_4P]_4[Cu_2Se_{14}]$ [95-96]. The increased length may also result from the steric interactions present in the molecule. The Cu2–P distances of 228.8(3) and 227.1(3) pm are slightly longer than the Cu1-P1 distance of 221.7(3) pm, reflecting four-coordinate Cu2 versus three-coordinate Cu1. Another

factor may be π bonding involving the PPh$_3$ group and the remaining orbital at the three-coordinate copper atom. The same trend has been reported for dichlorotris(triphenylphosphine)dicopper(I)benzene [92]. The crystal lattice contains 1.5 THF solvent molecules, which do not form significant interactions with the copper complex; but they participate and thus influence the packing of the dimeric units within the crystal.

Single crystals of **13** have been investigated by means of optical absorption spectroscopy (Figure 3.25). Since copper atoms possess a complete d^{10} shell (formal Cu^I), only Se(p) $\rightarrow$ M(s,p) charge transfer processes are expected. The according onset of absorption is observed at 475 nm (2.61 eV), which is in accordance with the yellow color of the compound. A maximum in the UV region at 260 nm (4.76 eV) [97] is due to intraligand excitation of the PPh$_3$ ligand.
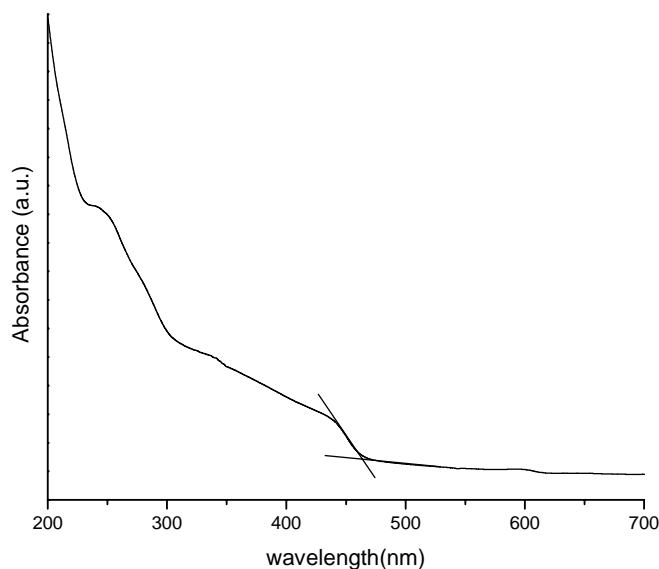
Figure 3.25 UV-vis spectrum of compound **13**

3.3.2 Synthesis and Characterization of [(Ph₃PAg)₈Ag₆(μ₆–Se)₁₋ₓ/₂(SePh)₁₂][R₃SnCl₂] (x = 0 (14), 1; R = Ph (15), Cy (16))

The cluster compound, $[(Ph_3PAg)_8(SePh)_{12}(\mu_6\text{-}Se)Ag_6]\cdot 6THF$ (**14**) was synthesized by the reaction of $(PPh_3)_3AgNO_3$ with $PhSeSiMe_3$ in presence of 1,4-bis(trichlorostannyl)butane in THF. Pure greenish-yellow crystals of **14** were obtained from a THF/*n*-hexane mixture at +6 ºC. 1,4-bis(trichlorostannyl)butane was not incorporated in the molecular structure of the product. However, since any effort to synthesize **14** in the absence of 1,4-bis(trichlorostannyl)butane was not successful, its role could not be rationilized so far. In order to explore the necessity of 1,4-bis(trichlorostannyl)butane for the formation and/or crystallization of **14** , similar reactions were carried out using R_3SnCl (R = Ph, Cy) instead of 1,4-bis(trichlorostannyl)butane in under identical conditions. This results in the formation of compounds **15**, $[(Ph_3PAg)_8(SePh)_{12}(\mu_6\text{-}Se)_{0.5}Ag_6][Ph_3SnCl_2]\cdot 6THF$ and **16**, $[(Ph_3PAg)_8(SePh)_{12}(\mu_6\text{-}Se)_{0.5}Ag_6][Cy_3SnCl_2]$. All three compounds were characterized by means of single crystal X-ray diffraction and EDX analyses. According to these investigations, the neutral compound **14** is based on an $Ag_{14}Se_{13}$ cluster core, which differs from the average composition of the cationic cluster core in **15** and **16**, $Ag_{14}Se_{12.5}$. The charge of the cluster cations in **15** and **16** is compensated by triorganotin dichloride anions R_3SnCl_2 (R = Ph, Cy).

Compound **14** crystallizes in the monoclinic space group $P2_1/c$ with four formula units in the unit cell. Compounds **15** and **16** crystallize in the monoclinic space group $I2/a$ with four formula units in the unit cell or in the trigonal space group R–3 with six formula units in the unit cell, respectively. Figure 3.26 shows the molecular structures of **14**, **15** and **16**, emphasizing the (*pseudo*)-D_{3d} symmetry, which is at least approximated by crystallographic C_3-symmetry in **16**. The $[Ag_{14}Se_{13-x}]^{2x+}$ cluster cores of compounds **14** (x = 0, Figure 3.27 top, left hand side), **15** and **16** (x = 0.5, Figure 3.27 top, right hand side) can all be described as a highly distorted fragment of the halite topology. The latter is encapsulated by an organic shell of eight PR_3 and twelve Ph groups. As in the halite topology itself, one might explain the cluster structures as consisting of four distorted polyhedra in onion-type arrangement (Figure 3.27 bottom): around a central μ_6-Se atom, one observes an Ag_6 octahedron within an Ag_8 cube (*i.e.* the face-centered cube).

14   **15**

16
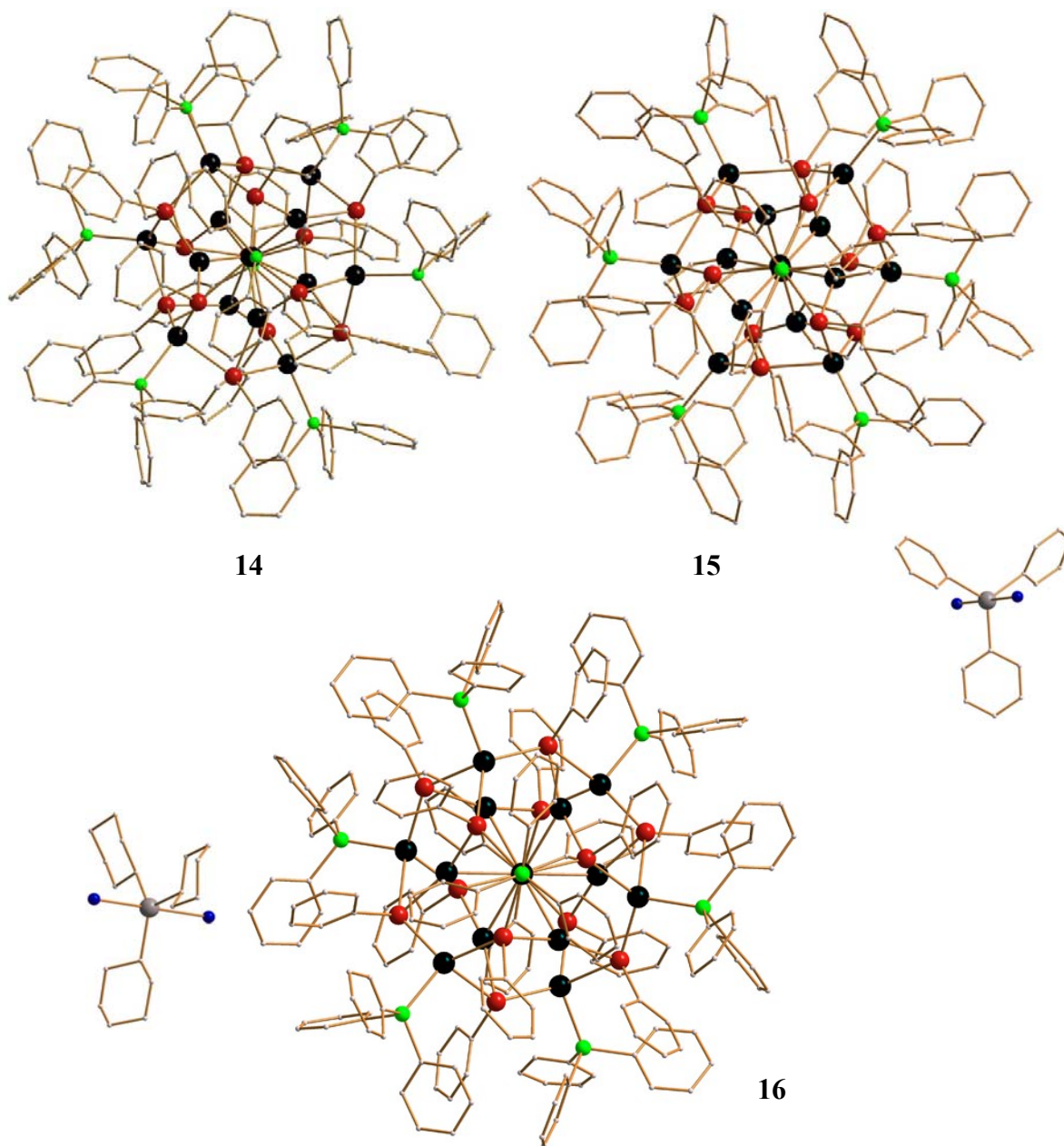
Figure 3.26 Molecular structures of the clusters in **14**, **15** and **16** as well as those of the anions in **15** and **16**, color code: Ag, black; Se, red; P, green; Sn, gray; Cl, blue; C, light gray. H atoms and disorder are not shown.

The latter is intertwining with an Se_{12} polyhedron that represents a mixture ("centauer-polyhedron") of an icosahedron (red part in figure 3.27 bottom, right) and a cubo-octahedron (blue part in figure 3.27 bottom, right). The whole is finally encapsulated by a

P_8 cube. Table 3.10 gives ranges of the bond lengths in the clusters in **14** and the cluster cations in **15** and **16**. Figures 3.28 shows the packing of the cluster cores of **14-16** within the crystal.
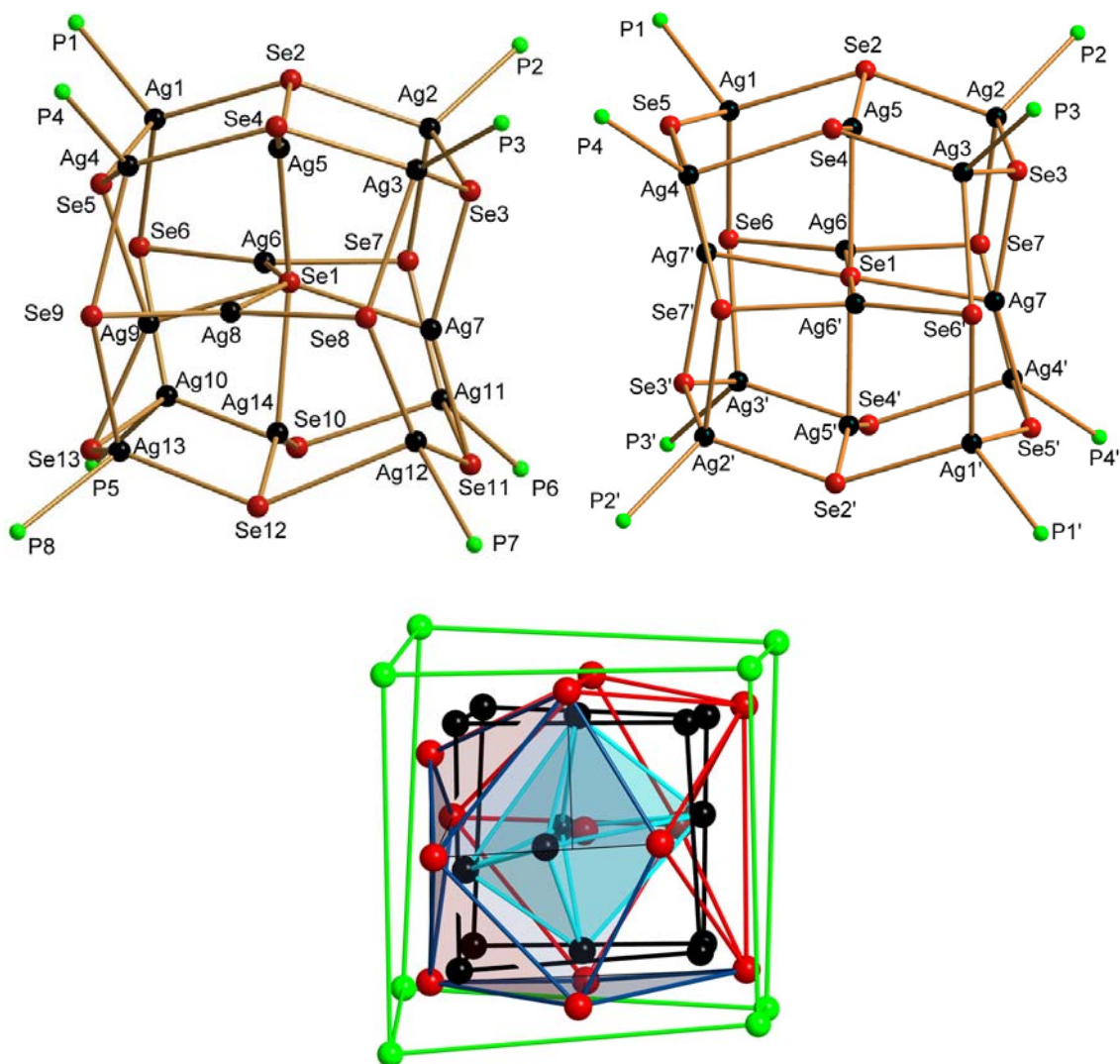
Figure 3.27 Top: Cluster cores of compound **14** (left hand side) and **15** (as a representative for **15** and **16**, right hand side) with the labeling scheme. Bottom: Representation of the intertwining, non-bonding polyhedra in **14** as an example for all three clusters. Note that the central μ_6-Se atom is only present to 50% on average in **15** and **16**, *i.e.* it is statistically missing in every second cluster.

Table 3.10 Ranges of interatomic distances in **14**, **15** and **16** regarding the geometric average of split portions. Ag$_{cube}$ and Ag$_{oct}$ denote Ag positions at the eight vertices of the distorted cubic arrangement or the six faces, respectively

	14	**15**	**16**
Ag$_{oct}$–μ_6-Se	264.1(2)-272.2(2)	280.88(5)-282.21(6)	279.29(10)-289.49(14)
Ag$_{oct}$–μ-Se	252.3(3)-267.3(19)	251.8(2)-256.0(13)	251.4(3)-255.0(3)
Ag$_{cube}$–μ-Se	255.61(2)-306.7(2)	266.03(7)-285.18(8)	252.0(2)- 290.0(2)
Ag–P	244.7(5)-255.8(4)	244.85(17)-251.09(16)	243.2(7)-248.0(6)

The six Ag atoms of the Ag$_6$ octahedron bind to the μ_6-Se atom and to two further Se neighbors in a slightly distorted linear manner (μ-Se–Ag–μ-Se: **14**: 137.60(7)-148.20(7)°, **15**: 148.7(3)-156.31(5)°, **16**: 153.23(10)-161.16(6)° to obtain a T-shaped coordination in the sum. The Ag atoms of the Ag$_8$ cube are located slightly above the centers of the eight triangular faces of the Se$_{12}$ polyhedron and adopt a near tetrahedral coordination by one P and three Se atoms (Se–Ag–Se: **14**: 86.07(6)-126.78(7)°, **15**: 93.5(2)-120.51(3)°, **16**: 86.14(5)-123.9(6)°; P–Ag–Se: **14**: 95.30(10)-132.09(11)°, **15**: 105.7(2)-127.3(2)°, **16**: 102.49(9)-123.65(10)°). The selenolate Se atoms, in turn, act as μ_3-bridges to two Ag atoms of the Ag$_8$ cube and one Ag atom of the Ag$_6$ octahedron. The Ag/S/P cluster cores of **14** on the one hand and **15** or **16** on the other hand are topologically identical to the cation in [Ag$_{14}$(μ_6–S)(Tab)$_{12}$(PPh$_3$)$_8$](PF$_6$)$_{12}$ (Tab = 4-(trimethylammonio)-benzenethiolate) [98], the charge of which is, however, caused by zwitterionic ammonium-thiolate ligands. However, in the cited compounds, the centers of the [Ag$_{14}$S$_{12}$] face-centered cubes are always fully occupied, as in **14**, whereas a defect situation as observed in **15** or **16** was so far not reported.

The different bond lengths in **14** on the one hand and **15**-**16** on the other hand correspond to the different charge in both cluster types: in **15** and **16**, the Ag$_{oct}$–μ_6-Se bonds are significantly elongated. This latter is in accordance with the observation that best refinement of the crystal structures with equally-sized thermal ellipsoids was achieved for s.o.f. = 0.5 at the central μ_6-bridging Se position to account for the overall +1 charge.

14

15

16
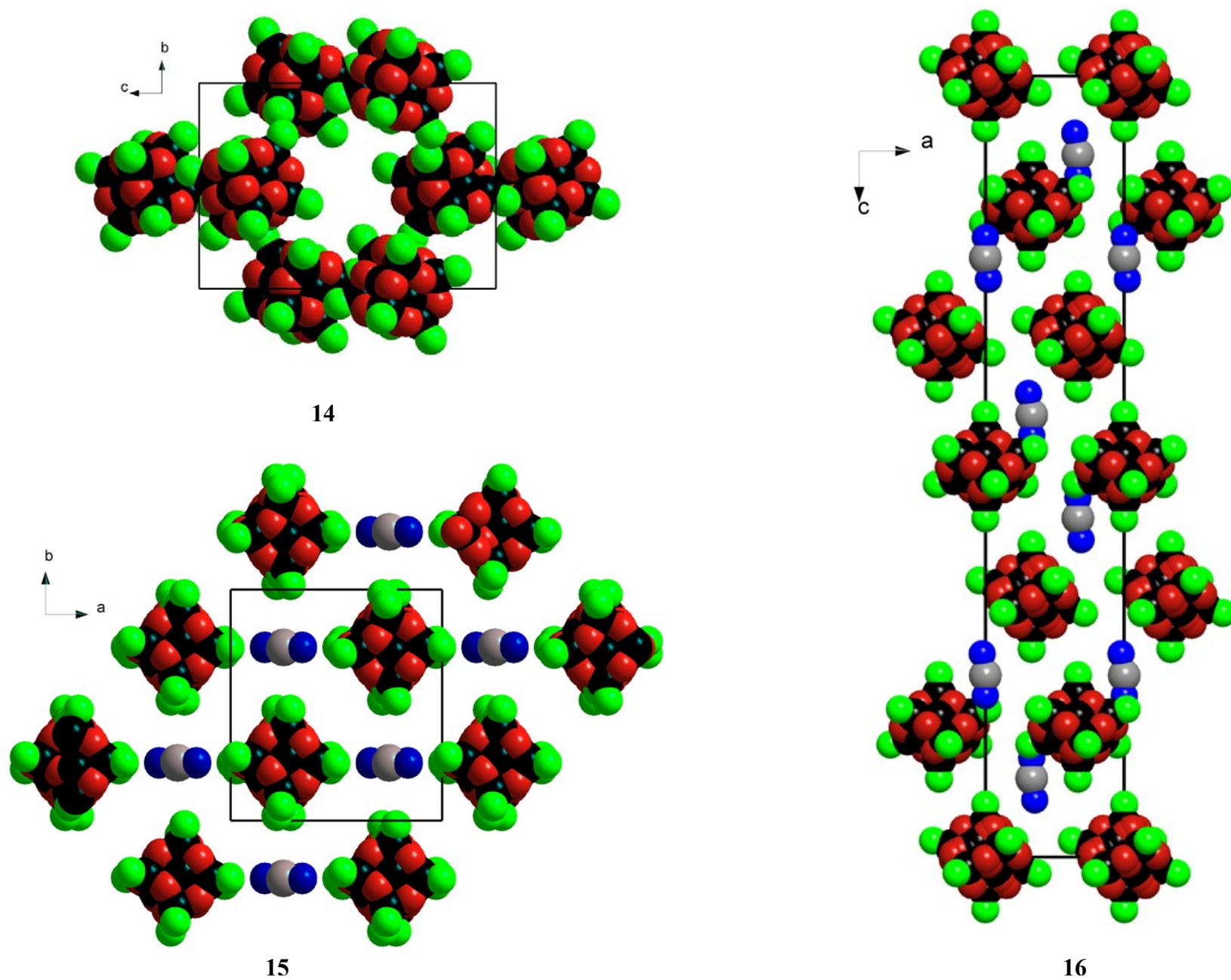
Figure 3.28 Packing of the cluster cores of **14**, **15** and **16** (bottom) within the unit cell, viewed along crystallographic *a* axis (**14**), *c* (**15**) or *b* (**16**) axis, Color code: Ag, black; Se, red; P, green (C, H, O omitted)

Thus, half of the clusters in **15, 16** contain a central Se ligand, whereas the other half exhibits an empty cluster center. The structures of the statistically distributed neutral and +2 charged clusters in **15, 16** are averaged over the crystal, leading to elongated thermal ellipsoids at the Ag positions that are sorted out by assignment of appropriate split positions to describe the disorder. On average, however, the 50% lack of a central ligand results in the observed bond elongations. The charge of the clusters in **15** and **16** is compensated for by one $[R_3SnCl_2]^-$ anion per formula unit (R = Ph or Cy). In both, the tin atom is bonded to three R groups and two chloride ligands, resulting a distorted trigonal bipyramidal geometry.

The clusters in **15** and **16** are connected by $Cl\cdots H–C_{Ph}$ hydrogen bonding interaction. In **15**, these interactions align the clusters into one-dimensional chains running approximately along the crystallographic [101] direction ($Cl\cdots H$ 272.00(5) pm, $Cl\cdots H–$ Ph 138.61(8)°, Figure 3.29), whereas in **16**, one $[Cy_3SnCl_2]^-$ anion connects ever six clusters by $Cl\cdots H–C_{Ph}$ hydrogen bonds from Cl1 or Cl2 to three adjacent clusters each around the crystallographic *c* axis ($Cl\cdots H$ 277.3(3)-323.0(5) pm, $Cl\cdots H–$Ph 136.35(10)-158.38(2)°) (Figure 3.30).
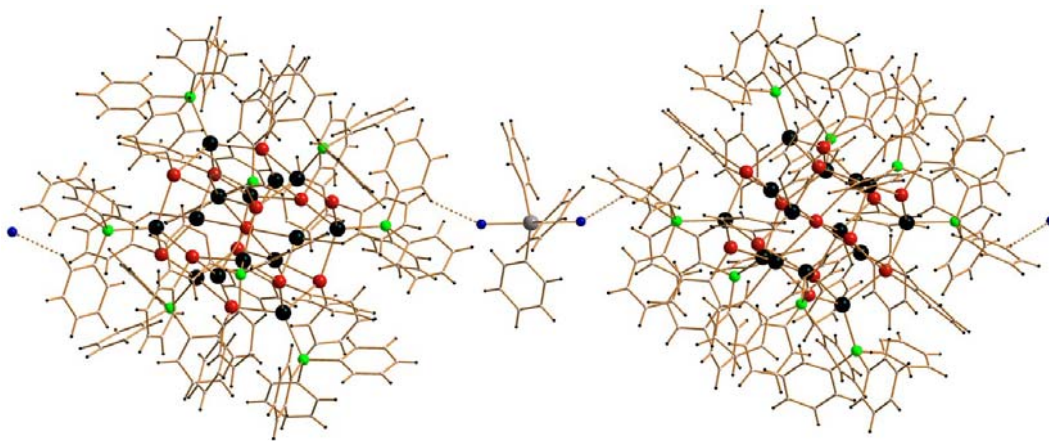
Figure 3.29 H…Cl hydrogen bonding in **15**, color code: Ag, black; Se, red; P, green; Sn, gray; Cl, blue; C, light gray; H, black; small spheres
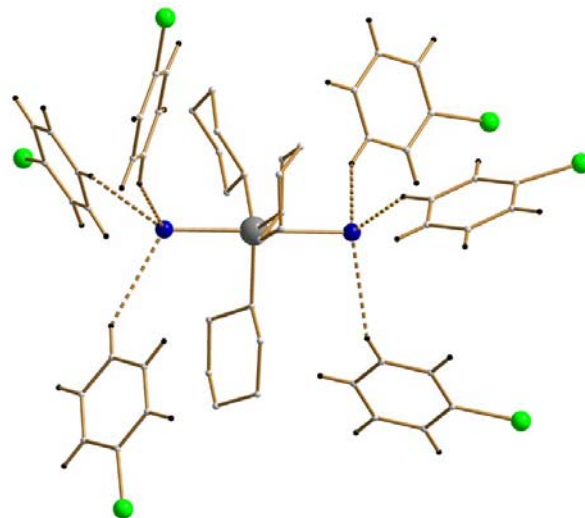
Figure 3.30 Fragment of the framework of clusters of **16** showing H…Cl hydrogen bonding in **16** (six P−Ph groups are from six clusters), color code: P, green; Sn, gray; Cl, blue; C, light gray; H, black; small spheres

Single crystals of **14**, **15** and **16** have been investigated by means of solid state optical absorption spectroscopy. Figure 3.31 shows the solid state UV-vis spectra of the compounds.
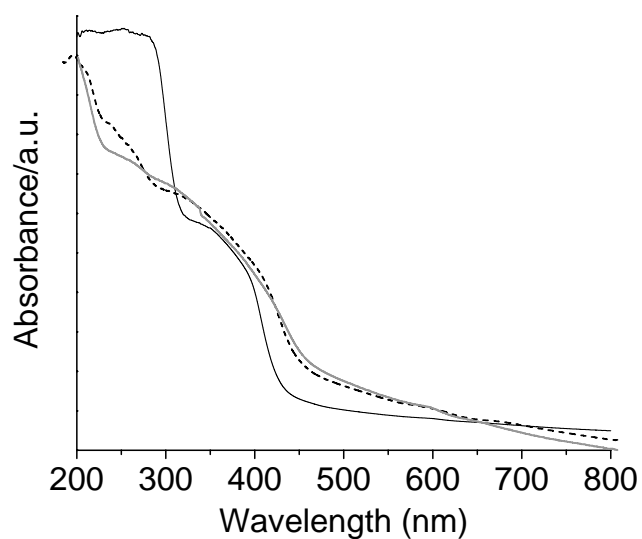
Figure 3.31 Solid state UV-visible spectra of **14** (black solid line), **15** (grey solid line) and **16** (dashed line), recorded as suspensions of single crystals in nujol oil

Since both the silver and tin atoms possess a complete d^{10} shell (formal Ag^I, Sn^{IV}), only Se(p) $\rightarrow$ M(s,p), charge transfer processes are expected. One observes an onsets of absorption, *i.e.* the lowest electronic excitation energy, at 433 nm (2.86 eV, **14**), 461 nm (2.68 eV, **15**) and 458 nm (2.70 eV, **16**) which are in agreement with the observed color of the compounds.

3.3.3 Quantum Chemical Study of Compound 14-16

DFT investigations were performed for model compounds with PH_3 instead of PR_3 groups in order to rationalize the unusual structural and electronic features. A neutral cluster (**14^c**) and two charged ones with (+1 charge, **15^{1+c}**) or without central Se ligand (+2 charge, **15^{2+c}**) were calculated to exclude the oxidation of the cluster with unchanged composition (**15^{1+c}**). The molecular structure of **14** is well reproduced by the calculations, *i.e.* the calculated parameters are in good agreement with experimental with maximum Δd = 15.6 pm at Ag–Se bonds. For **15, 16**, neither the structural parameters of the singly charged hypothetical species **15^{1+c}** nor those of the cluster with +2 charged showed satisfying agreement with the observed structures. As expected, best agreement with the average bond lengths in **15** were achieved by averaging the structural parameters of **14^c** and **15^{2+c}**, with maximum Δd = 14.26 pm (vs. **15**) or 9.37 pm (vs. **16**) at Ag–Se bonds. Table 3.11 and table 3.12 provide the calculated distances of compound **14** and **15**. The calculations show the identical trends on going from **14** to **15** [259.1-291.1 pm (**14**) to 256.9-288.2 pm (average distances of **15^{1+c}** and **15^{2+c}**)] for the Ag–Se and [246.9-260.6 pm (**14**) to 241.4-250.5 pm (average distances of **15^{1+c}** and **15^{2+c}**)] for Ag–P distances as experimental findings.

Although the role of bis(trichlorostannyl)butane for the synthesis of **14** is not obvious, its synthesis was (a) not possible without and (b) reactions with related mono-tin compounds led to different products (**15** and **16**) under the given reaction conditions. It is assumed either a catalytic activity or suppression of competitive reaction as most probable explanations for the necessity of the presence of the compound.

Table 3.11 Experimental and calculated distances for **14ᶜ or 15¹⁺ᶜ**

Compound	14	14ᶜ
Distances	experimental	calculated
Ag_{oct}–μ₆-Se		
Ag5-Se1	2.6446(19)	2.7022
Ag6-Se1	2.641(2)	2.6989
Ag7-Se1	2.6811(19)	2.7313
Ag8-Se1	2.705(2)	2.7326
Ag9-Se1	2.6481(19)	2.7046
Ag14-Se1	2.722(2)	2.7329
Ag_{oct}–μ-Se		
Ag5-Se2	2.629(2)	2.6922
Ag5-Se4	2.543(2)	2.5912
Ag6-Se6	2.523(3)	2.5898
Ag6-Se7	2.615(3)	2.6817
Ag7-Se3	2.601(2)	2.6795
Ag7-Se11	2.544(2)	2.5917
Ag8-Se8	2.6184(19)	2.6921
Ag8-Se9	2.558(2)	2.6190
Ag9-Se5	2.6737(19)	2.6953
Ag9-Se13	2.5561(19)	2.6179
Ag14-Se10	2.630(2)	2.6933
Ag14-Se12	2.549(2)	2.6176
Ag_{cube}–μ-Se		
Ag1-Se2	2.6976(19)	2.7349
Ag1-Se5	2.729(2)	2.7780
Ag1-Se6	2.770(2)	2.8556
Ag2-Se2	2.706(2)	2.7430
Ag2-Se3	2.709(2)	2.7466
Ag2-Se7	2.693(2)	2.7299
Ag3-Se3	2.645(2)	2.6934
Ag3-Se4	2.708(2)	2.7464
Ag3-Se8	2.843(2)	2.8704
Ag4-Se4	2.883(2)	2.9011
Ag4-Se5	2.6901(19)	2.7288
Ag4-Se9	2.787(2)	2.8601
Ag10-Se6	2.755(2)	2.8191
Ag10-Se10	2.656(2)	2.6944
Ag10-Se13	2.907(2)	2.9046
Ag11-Se7	2.721(8)	2.7523
Ag11-Se10	2.742(2)	2.7857
Ag11-Se11	2.748(2)	2.8099
Ag12-Se8	2.6001(19)	2.6761
Ag12-Se11	2.719(2)	2.7471
Ag12-Se12	3.067(2)	2.9107
Ag13-Se9	2.7425(19)	2.8082
Ag13-Se12	2.7251(19)	2.7529
Ag13-Se13	2.742(2)	2.7843
Ag–P		
Ag1-P1	2.496(4)	2.5043
Ag2-P2	2.447(5)	2.4690
Ag3-P3	2.463(4)	2.5050
Ag4-P4	2.518(4)	2.5587

Ag10-P5	2.480(4)	2.5575
Ag11-P6	2.459(4)	2.5051
Ag12-P7	2.478(4)	2.5585
Ag13-P8	2.558(4)	2.6063

Table 3.12 Experimental and calculated distances for 15^{1+c} and 15^{2+c}

Compound	**15**	15^{1+c}	15^{2+c}	**average 14 & 15^{2+c}**
Distances	Experimental	Calculated		
Ag$_{oct}$–μ_6-Se				
Ag5–Se1	2.8144(9)	2.8211		
Ag6–Se1	2.8221(6)	2.8055		
Ag7–Se1	2.8088(5)	2.8125		
Ag$_{oct}$–μ-Se				
Ag5–Se2	2.543(2)	2.6065	2.5139	2.60305
Ag5–Se4	2.518(2)	2.5754	2.5064	2.5488
Ag6–Se6	2.560(13)	2.6317	2.5203	2.55505
Ag6–Se7	2.5411(10)	2.5805	2.5126	2.59715
Ag7–Se3	2.557(13)	2.6070	2.5154	2.59745
Ag7–Se5'	2.5161(10)	2.5691	2.5064	2.54905
Ag$_{cube}$–μ-Se				
Ag1–Se2	2.6874(8)	2.7323	2.7033	2.7191
Ag1–Se5	2.7646(8)	2.8767	2.9276	2.8528
Ag1–Se6	2.762(8)	2.8703	2.9000	2.8778
Ag2–Se2	2.7235(8)	2.7532	2.7666	2.7548
Ag2–Se3	2.6985(8)	2.7348	2.7216	2.7341
Ag2–Se7	2.756(8)	2.7752	2.7810	2.75545
Ag3–Se3	2.7210(8)	2.7483	2.7527	2.72305
Ag3–Se4	2.7168(7)	2.7351	2.7522	2.7493
Ag3–Se6'	2.7444(7)	2.7381	2.7541	2.81225
Ag4–Se4	2.8518(8)	2.8822	2.9353	2.9182
Ag4–Se5	2.7169(8)	2.7055	2.7026	2.7157
Ag4–Se7	2.6603(7)	2.7351	2.7457	2.8029
Ag–P				
Ag1–P1	2.4754(14)	2.4991	2.4944	2.49935
Ag2–P2	2.4485(17)	2.4148	2.4135	2.44125
Ag3–P3	2.5109(16)	2.5053	2.4970	2.501
Ag4–P4	2.4728(14)	2.4981	2.4918	2.52525

3.4 Reactivity of Bis(trichlorostannyl)organyls under Solvothermal Conditions

The syntheses in this method are typically carried out under solvothermal conditions in polarizing solvents such as water (hydrothermal), alcohol (alcoholothermal) or organic amines (aminothermal) at relatively low temperatures ($T \approx 100–200$ ºC). The use of amines as solvent in solvothermal reactions bears the advantage that the chelating amine is not only an excellent solvent, but takes over at least two further important roles:

(1) offering a chalcogenide source by reacting with chalcogen elements in a redox reaction (eq. 3.1).

$$Q + amine \longrightarrow Q^{2-} \text{ (or } Q_m{}^{2-}) + (Hamine)^+ + \text{oxidized byproduct} \tag{3.1}$$
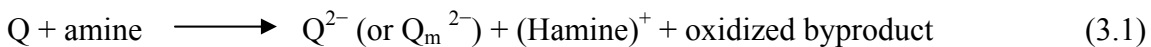
(2) formation of bulky $[M(amine)x]^{n+}$ cations upon chelating of the metal ions (eq. 3.2).

$$M^{n+} + amine \longrightarrow [M(amine)_x]^{n+} \tag{3.2}$$

Both processes can also occur at once (eq. 3.3)

$$Q + M + amine \longrightarrow [M(amine)_x]^{n+} + Q^{2-} \text{ (or } M_yQ_z{}^{m-}) \tag{3.3}$$
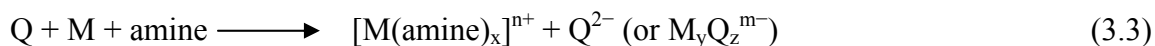
In solvothermal reactions using water or alcohol as solvents, these do not only act as solvent but also play a structure directing role by coordination to the product or crystallizing free solvent molecules [99].

Here, the reactivity of bis(trichlorostannyl)organyls in the presence of chalcogen, chalcogenide or/and transition metals was investigated under solvothermal conditions using *en* or in methanol as solvents.

3.4.1 Synthesis and Characterization of $_{\infty}^{1}$ [SnS$_2$·*en*] (17)

Compound **17** was synthesized by reaction of 1,4-bis(trichlorostannyl)butane with elemental sulfur under mild solvothermal condition using ethylenediamine as solvent at 180 ºC for five days. The compound crystallizes as colorless blocks. Details of the synthesis procedure are provided in the experimental section. Sn–C bond cleavage was occurred under the reaction condition. A possible reaction is given in equation 3.4.

$$0.5 \; Cl_3Sn\text{–}Bu\text{–}SnCl_3 + 2 \; S + en \xrightarrow{\; en, \; 180 \, ^{\circ}C \;} {_{\infty}^{1}}[SnS_2 \cdot en] + byproduct \qquad (3.4)$$
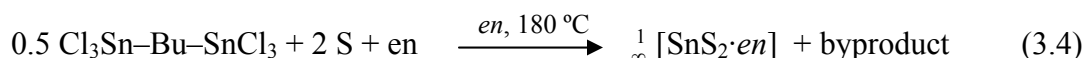
Compound **17** was structurally characterized by means of single-crystal X-ray diffraction. **17** crystallizes in the monoclinic space group *C2/c* with six asymmetric units, *i.e.* twelve formulae in the unit cell. According to the single crystal X-ray measurement **17** possesses a polymeric chain structure. The structure contains neutral tin sulfide chains running along the [101] direction. Figure 3.32 shows a fragment of the one-dimensional chain in compound **17**. Table 3.13 provides selected interatomic distances and angles. Figure 3.33 shows the packing of the strands in compound **17** within the crystal lattice, viewed along crystallographic *a* and *c* axes.
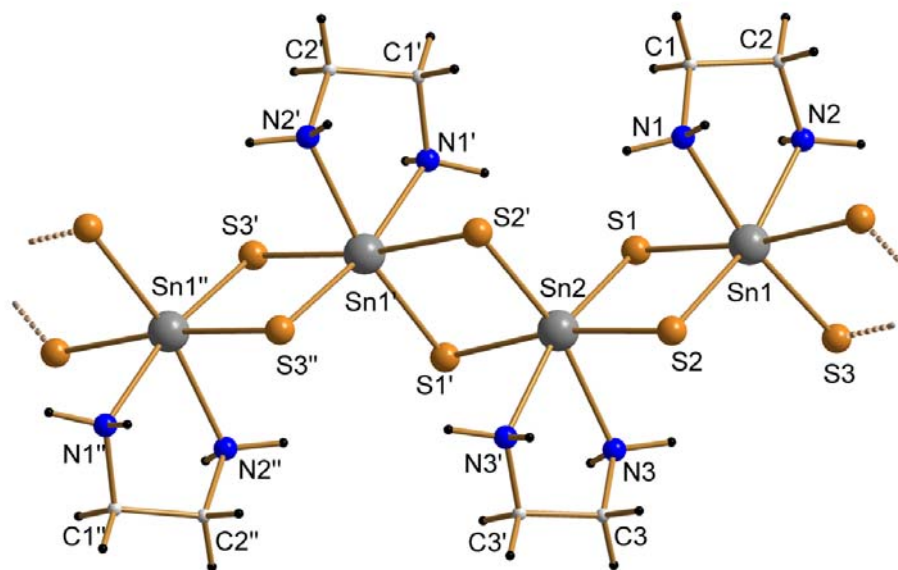
Figure 3.32 Fragment of the one dimensional chain in compound **17**

Table 3.13 Selected distances and angles of compound **17**

Distances	[pm]	Angles	[°]
Sn–S	244.3(4)-250.9(14)	Sn–S–Sn	88.74(11)-89.62(11)
Sn–N	232.3(11)-228.9(14)	S–Sn–S	90.38(11)-104.42(13)
C–N	143.0(2)-153.0(2)	N–Sn–S	84.8(3)-167.4(3)

Different to the compound $^1_\infty[2SnSe_2 \cdot en]$ [100], both of the two crystallographic independent Sn atoms are surrounded by four sulfur ligands and two nitrogen atoms of one *en* molecule each in a distorted octahedral manner with Sn–S and Sn–N distances of 244.3(4)-250.9(14) pm and 232.3(11)-228.9(14) pm.
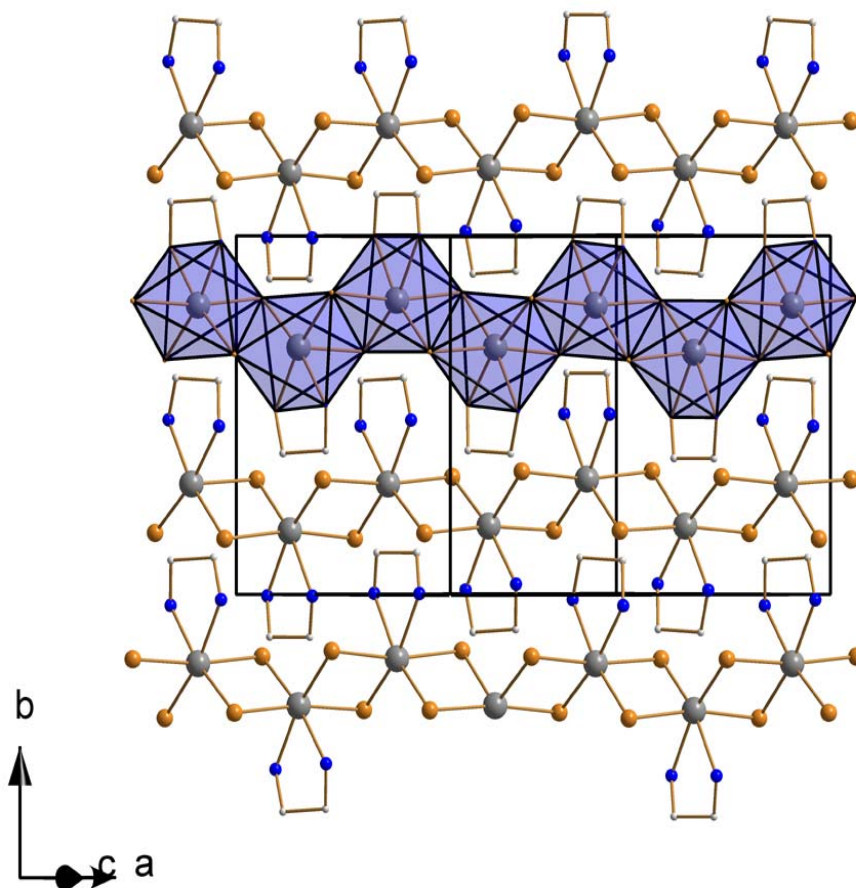
Figure 3.33 Arrangement of the one-dimensional chains in **17** within the crystal

Each octahedral unit shares two S…S edges with two neighboring octahedra (Sn…Sn 347.3(14) pm). The orientation of the coordinating *en* molecule at a given Sn atom is *trans* with regard to the adjacent Sn atoms. This leads to a syndiotactic arrangement of these extra ligands along the polymer chain. One might view the structure of **17** as a solvated variant of the SiS$_2$-type modification of SnS$_2$.

Several attempts were taken to synthesize compound **17** from common starting material, like, (a) reaction of elemental tin and sulfur with *en* or (b) reaction of tin tetrachloride and sulfur or sodium sulfide with *en* under identical reaction conditions. None of these reactions resulted in the formation of **17**. But the reaction of elemental tin and sulfur in *en* ended up with the formation of another compound [*en*H]$_4$[Sn$_2$S$_6$]·*en* (**18**), indicating the sensitivity of the product spectrum of solvothermal reactions to the reactant.

3.4.2 Synthesis and Characterization of [enH]$_4$[Sn$_2$S$_6$]·*en* (18)

Compound **18** was prepared by reacting metallic tin with elemental sulfer under solvothermal conditions at 180 ºC using ethylenediamine as solvent (eq. 3.5). Pure crystals of **18** were isolated as colorless blocks.

$$2\ Sn + 6\ S + 5\ en \xrightarrow{\ en,\ 180\ ^\circ C\ } [enH]_4[Sn_2S_6]\cdot en \qquad (3.5)$$

Compound **18** was characterized by means of single crystal X-ray diffraction. It crystallizes in the triclinic space group $P\bar{1}$ with two formula units in the unit cell. **18** is based on the prominent [Sn$_2$S$_6$]$^{4-}$ dimeric anionic unit, and is isostructural to two known homologues, [*en*H]$_4$[Sn$_2$Se$_6$]·*en* and [*en*H]$_4$[Sn$_2$Te$_6$]·*en* [101]. Figure 3.34 shows the coordination sphere of adjacent cations around one anion, and a fragment of the packing of ions and solvent molecules within the crystal lattice. Table 3.14 provides selected interatomic distances and angles of **18**. The anionic unit [Sn$_2$S$_6$]$^{4-}$ contains a Sn$_2$S$_2$ four-membered ring. Each tin atom additionally possesses two terminal sulfur ligands.
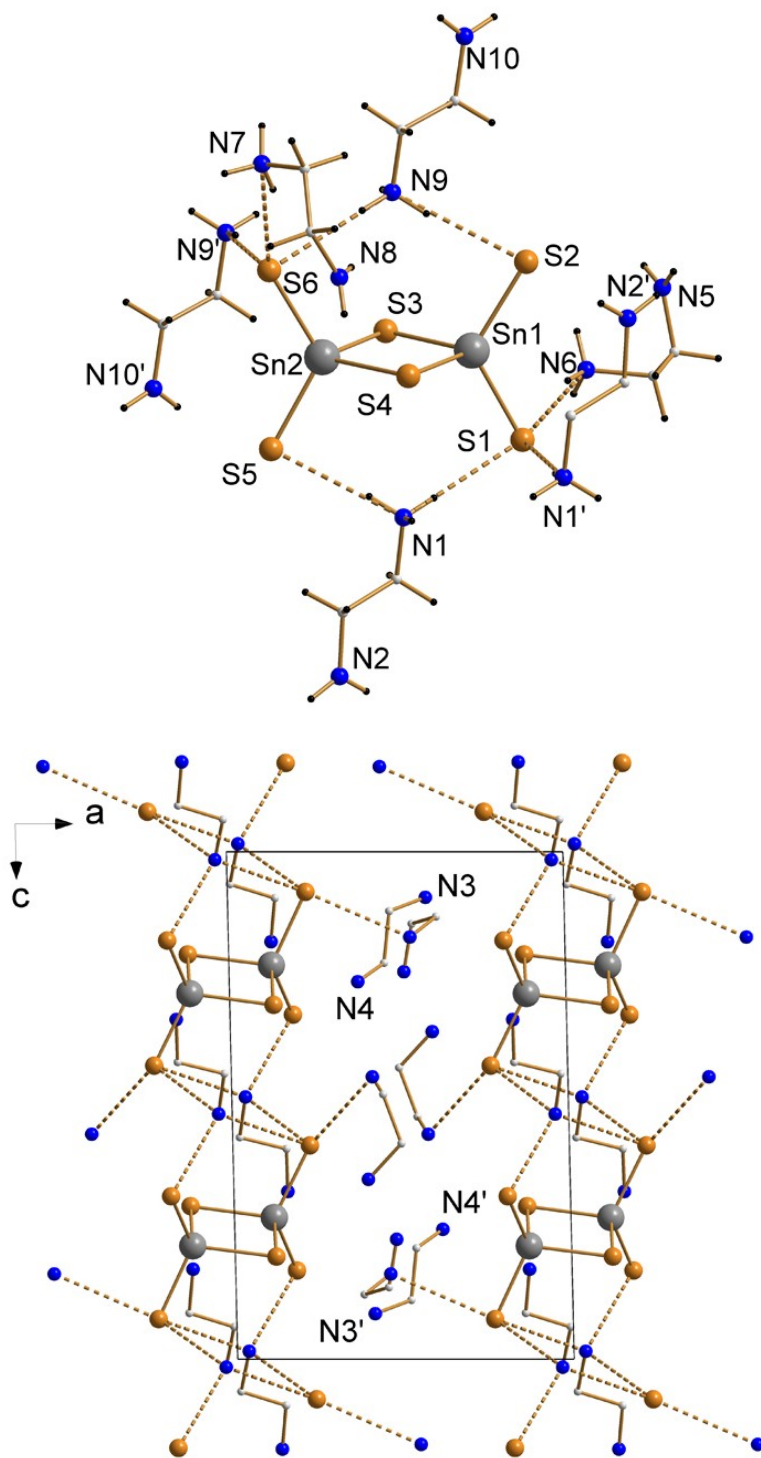
Figure 3.34 The $[Sn_2S_6]^{4-}$ anion in **18** within its cationic coordination environment (top) and packing of the ions and neutral solvent molecules (containing N3, N4) within the crystal, viewed along crystallographic *b* axis (bottom). Dashed lines indicate closest N(H)…S distances (328.6-342.8 Å)

This leads to a distorted tetrahedral geometry around the tin atoms, with Sn–S distances of 232.34(7)-244.78(7) pm and a non-bonding Sn….Sn distance of 332.12(3) pm.

Table 3.14 Selected distances and angels of compound **18**

Distances	[pm]	Angles	[°]
Sn–S	232.36(7)-244.90(7)	Sn–S–Sn	85.36(2)-85.41(2)
C–N	145.8(3)-148.9(4)	S–Sn–S	94.55(2)-120.58(2)

It was not possible to localize all the hydrogen atoms from the Fourier map. Thus it was not possible to distinguish between NH_2 and NH_3^+ groups by means of crystallography. However, the different groups can be assigned by an according analysis of N...S distances or N–H...S angles. Four nitrogen atoms (N1, N6, N7, N9) show smallest distances to neighboring sulfur atoms (328.6(4)-342.8(1) pm) with N–H...S angles of 161.87(3)-173.93(4)° and corresponding C–N...S angles of 98.52(3)-106.82(3)°. These N atoms are supposed to belong to the NH_3^+ groups of the cations, whereas larger N…S distances (347.5(2)-375.5(5) pm) are more appropriately assigned to the less interacting amine groups. From five independent *en*/[*en*H]$^+$ molecules, three exhibit *trans* conformation with N–C–C–N torsion angles of 164.66(3)-171.93(3)°, and two adopt *cis* conformation (N–C–C–N 60.28(2)-67.55(1)°). An additional, neutral *en* molecule – the one containing N3 and N4 – is situated within the crystal as free solvent molecule, while all [*en*H]$^+$ units are placed between neighboring anions to result in a three-dimensional coordination network.

3.4.3 Optical Absorption Behavior of compounds 17 and 18

Compounds **17** and **18** show an onset of absorption around 4.25 eV due to an S to Sn ligand-to-metal charge transfer (LMCT) process. In **17**, the polymerization of smaller Sn/S units, such as the dimeric sulfidostannte units observed in **18**, increases the electronic density of states to result in a band structure. This should cause a red-shift of the electronic excitation energy in **17** with respect to the HOMO-LUMO transition of **18** containing molecular anions. However, an increase of the coordination number of the Sn atoms from 4 in **18** to 6 in **17**, due to additional coordination by *en* ligands, comes along with a blue-shift in turn, finally leading to equal optical absorption energies of both compounds.
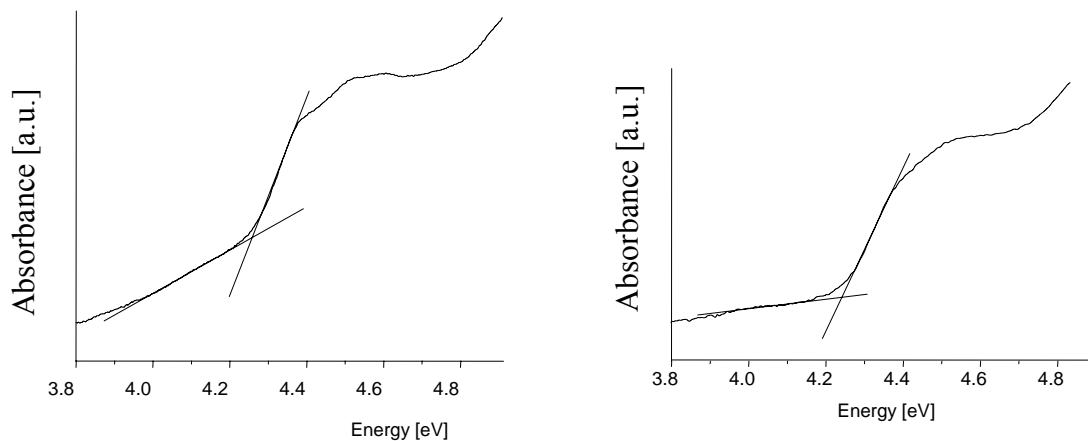
Figure 3.35 UV-vis spectra of compounds **17** (left hand side) and **18** (right hand side), recorded from suspensions of single crystals in Nujol oil

3.4.4 Synthesis and Characterization of [(Ph$_3$PCu)$_6${$cyclo$-(CH$_2$)$_4$SnS$_2$}$_6$Cu$_4$Sn] (19)

[(Ph$_3$PCu)$_6${$cyclo$-(CH$_2$)$_4$SnS$_2$}$_6$Cu$_4$Sn] was synthesized by reaction of Cl$_3$Sn–(CH$_2$)$_4$–SnCl$_3$ with [CuCl(Ph$_3$P)$_3$] and Na$_2$S·9H$_2$O under solvothermal conditions in MeOH at 110 ºC. The organotin(IV) compound was partially reduced by S^{2-} ions as indicated by the formation of elemental sulfur; additionally an unprecedented cyclization of a butyl rest occurred at the Sn atom upon Sn–C bond cleavage. A possible reaction scheme for the formation of **19** is given below.

$$10\,[Cu^ICl(PPh_3)_3] + 18\,Na_2S·9H_2O + 6\,Cl_3Sn^{IV}–C_4H_8–Sn^{IV}Cl_3$$

$$\downarrow \quad \begin{array}{l} MeOH \\ 110\,°C\ (4\ d) \end{array}$$

$$[(Ph_3PCu^I)_6\{(CH_2)_4Sn^{IV}S_2\}_6Cu^I_4Sn^{II}]\ (\mathbf{19},\ 23.3\%)$$
$$+\ ^6/_8\,S_8{}^0 + 5\,Sn^{II}Cl_2 + 36\,NaCl + 24\,PPh_3 + 162\,H_2O$$
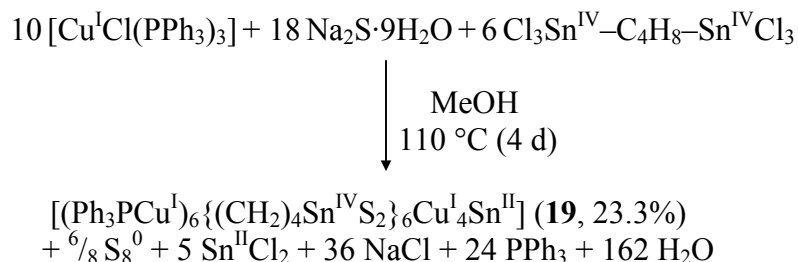
Scheme 3.8 Synthesis of compound **19**

Compound **19** crystallizes as light orange-yellow crystals in the monoclinic space group $P2_1/n$. Figure 3.36 shows the molecular structure of the C_i symmetric molecule, possessing a *pseudo* C_3 axis. The core of the heterometallic sulfide cluster comprises an unprecedented arrangement of four Cu atoms and one Sn atom in a distorted trigonal-bipyramidal way (Figure 3.37, right hand side). This fragment has accords to the inversion symmetry upon considering a disorder of the atoms Sn4 and Cu7 that are located 50% on the shown atomic sites, and to 50% on inverse position. An additionally observed rotational disorder of three of the four Cu atoms (Cu4,5,6) around the Sn4...Cu7 axis with 8.8(1)% occupation further indicates a large flexibility of this heterometallic core unit. For clarity, the disorder will be disregarded during the further discussion of the structure. The Cu$_4$Sn core is linked to the surface of the cluster via S atoms that belong to the six BuSnS$_2$ units (Cu(4-6)–S 243.5(2)-257.7(2) pm, Cu7–S 218.1(2)-223.8(2) pm, Sn4–S 251.9(1)-255.2(2) pm). Being three-coordinate (S1, S4, S6) or four-coordinate (S1', S6', S4', S2, S3, S5), the S atoms bridge to one further Sn atom and one CuPPh$_3$ unit, or to one Sn atom and two further CuPPh$_3$ units (Sn(1-3)–S 237.3(2)-243.8(1) pm, Cu(1-3)–S 237.7(1)-242.7(2) pm). This way, all inner Cu atoms show distorted trigonal planar (Cu7) or trigonal pyramidal (Cu4-Cu6, Sn1) coordination by S atoms besides three
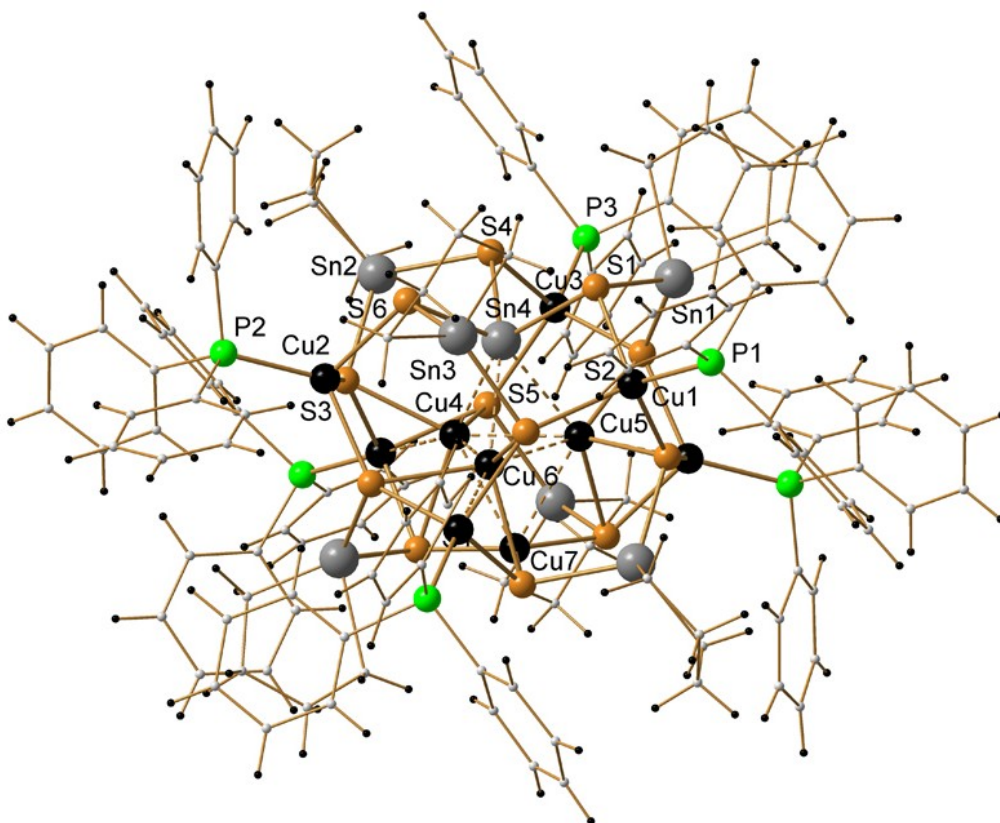
Figure 3.36 Molecular structure of **19**, disregarding the disorder of the central Cu_4Sn^{II} fragment, color code: C, grey (small spheres); H, black
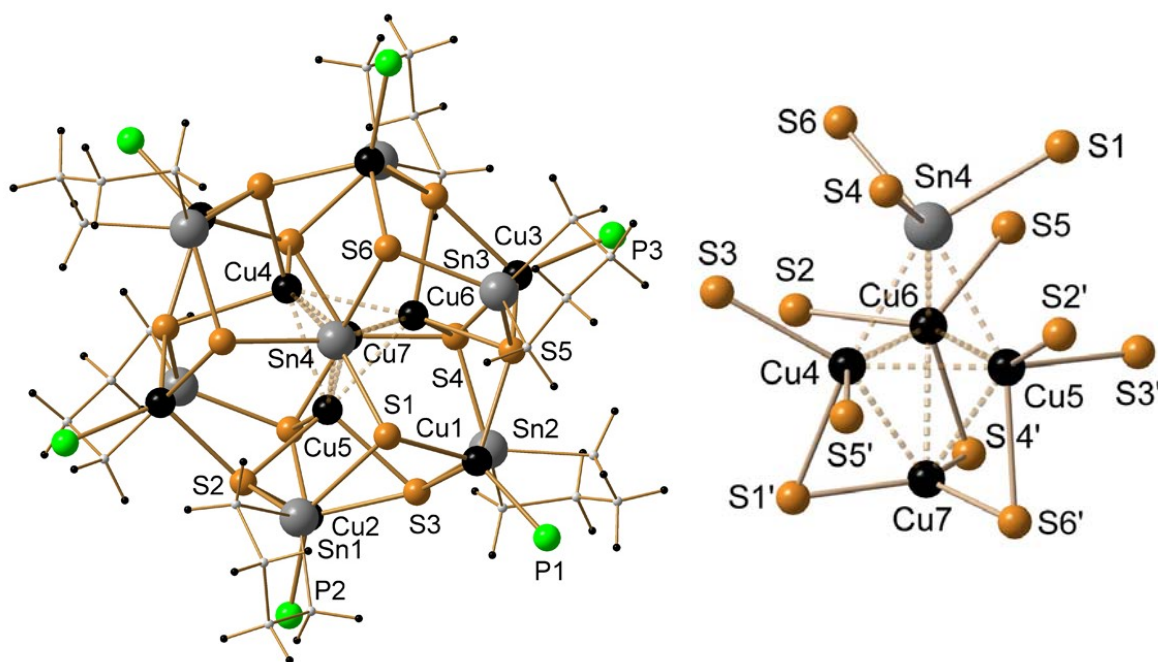
Figure 3.37 $[(PCu)_6\{cyclo\text{-}(CH_2)_4Sn)_6Cu_4Sn]$ framework viewed down the pseudo C_3 axis (left) and inner Cu_4Sn fragment within its coordination environment (right)

(Cu7, Sn1) or four (Cu4-Cu6) metal-metal contacts (Cu–Cu 257.5(2)-262.7(2) pm, Cu–Sn 262.6(1)-263.7(1) pm). In addition, Cu4-Cu6 that form the equatorial plane of the Cu_4Sn trigonal pyramid are each involved in one further, unusually short Cu–Cu contact (232.9(1)-238.8(1) pm) in the more dominant rotational disorder positions. At the $Cu_6(SnS_2)_6$ metalchalcogenide surface embedding the inner Cu_4Sn unit, the cluster is decorated by a ligand shell of six Ph_3P groups at the Cu atoms and six nBu groups at the Sn atoms, that are part of the six $[\{cyclo\text{-}(CH_2)_4Sn\}S_2]^{2-}$ ligands. The formation of the latter was obviously advantaged over growing two separate clusters at both ends of the originally reacted Cl_3Sn–$(CH_2)_4$–$SnCl_3$ unit. As rationalized by density functional theory (DFT) calculations employing the RIDFT approximation of the program system TURBOMOLE, the uncommon cyclization of Cl_3Sn–$(CH_2)_4$–$SnCl_3$ preliminarily producing $SnCl_4$ and $\{cyclo\text{-}(CH_2)_4Sn\}Cl_2$ is *not* enthalpically favored (Scheme 3.9).
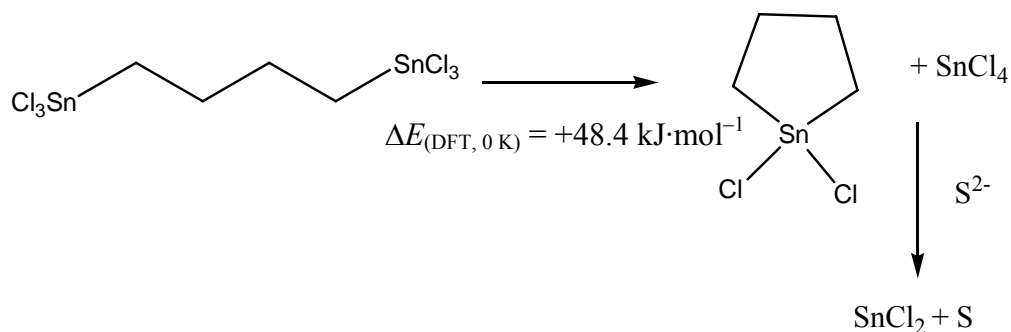
Scheme 3.9 Postulated and calculated cyclilization of 1,4-bis(trichlorostannyl)butane (DFT methods)

Therefore, it was rather driven by the reductive sulfidic conditions that led to the observed formation of elemental sulfur and reduction of $Sn^{IV}Cl_4$ to $Sn^{II}Cl_2$. Consequently, this might enable further reactivity of **19** involving the $\{cyclo\text{-}(CH_2)_4Sn\}$ unit. The Sn–C bond cleavage might have been induced thermally or catalytically by Cu^+ ions.

The most peculiar feature of **19** is the inner Cu_4Sn unit, containing direct M–M contacts, some of which are not even clamped by bridging ligands (Sn–Cu2,3,4).The Sn atom in **19** which is involved in the central cluster unit formally possesses oxidation state +II.

Single crystals of **19** have been investigated by means of optical absorption spectroscopy (Figure 3.38 top). Since all involved metal atoms possess a complete d^{10} shell (formal Cu^I, Sn^{II}, Sn^{IV}), only S(p) → M(s,p) charge transfer processes are expected. One observes a relatively weak, broad absorption with a smooth onset at 750 nm (1.65 eV), an inconspicuous shoulder around 446 nm (2.78 eV) and a maximum at 376 nm (3.30 eV), in accordance to the orange-yellow color of the crystals. A more significant maximum due to intraligand π→π* excitation at the phenyl groups is observed in the UV region at 263 nm (4.71 eV) [97].
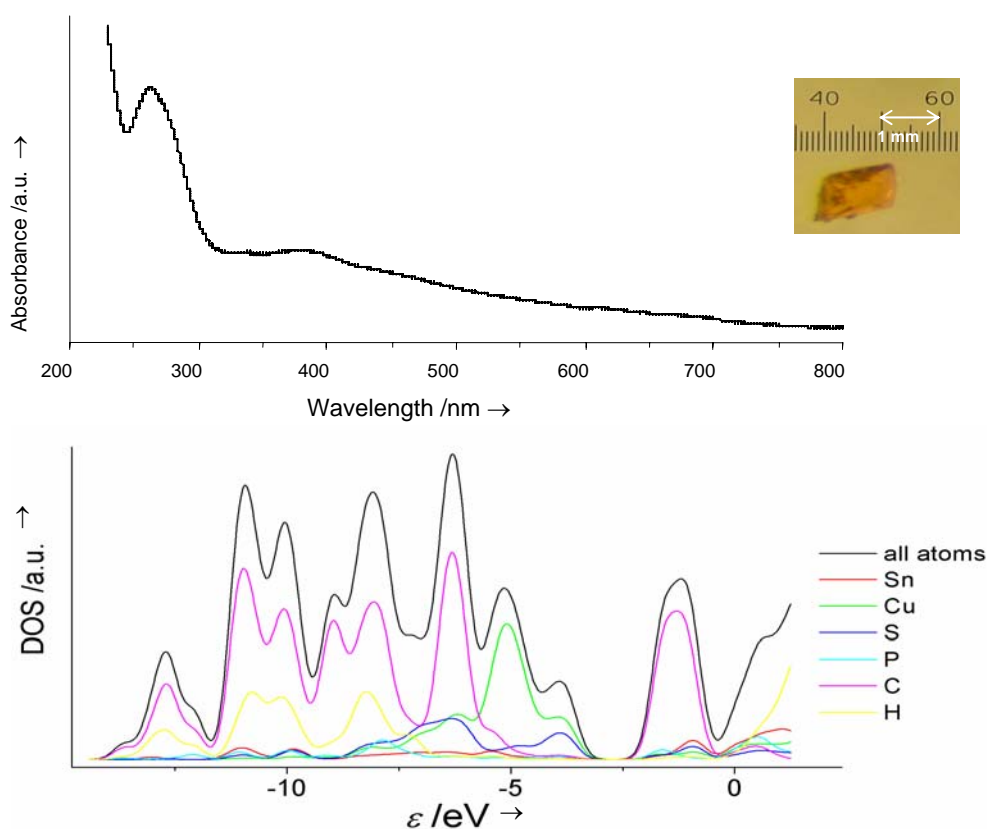
Figure 3.38 Solid state UV-visible spectrum recorded as suspension of single crystals in nujol oil, and picture of a single crystal of **19** (top); calculated density of states (DOS) indicating atomic orbital (AO) contributions of the different atoms to the frontier orbitals (bottom, see chapter 3.4.5).

3.4.5 Quantum Chemical Investigation of Compound 19

The molecular structure of **19** is well reproduced by the DFT calculations: Δd 0.8 − 11.9 pm for all bonds except three Cu–Cu distances involving atomic positions that show rotational disorder; for the latter, Δd is also acceptable (16.5 − 21.3 pm) taking into account that the experimental positions of the respective atoms may vary in a range estimated to 16 pm owing to the observed disorder. Table 3.15 summarizes experiemtally found (X-ray) and calculated (DFT) structural parameters. Based on the reasonable calculated structure, population analyses (Mulliken for density of states, NPA for natural charges) were carried out to rationalize both the optical absorption behavior and the mixed valence situation. Tables 3.16 and 3.17 provide the results of the analysis. As shown in figure 3.38 (bottom), the population of the highest occupied orbitals (*ca.* −7 eV to HOMO at −3.611 eV) is dominated by contribution of C(p) atomic orbitals, followed by contributions of Cu(d) and S(p) atomic orbitals. The first lowest unoccupied orbitals show essentially C(p) contribution. Therefore, the above mentioned intraligand $\pi\rightarrow\pi^*$ transition is certainly predominant. Further charge transfer processes between metal and chalcogenide atoms (MLCT and LMCT) are secondary, which is in good agreement with the experimental findings. Therefore, both maximum absorbance (high/low) and band widths (narrow/broad) of the UV-visible signals accord well with the calculated values of the DOS, *i.e.* the number of orbitals at a specific energy value, and the energy range of the DOS concerning the same involved atom, *i.e.* the range of possible (non-resolved) excitation energies, respectively. Analyzing the natural charges, the Sn atoms at the periphery indeed show approximately twice the value (+1.50±0.02) of the core Sn atom (+0.72) exhibiting a similar charge as observed for the Cu atoms (+0.69±0.07; *note* that these charges do not represent formal oxidation states). According to these results, Cu atoms are not involved in the mixed valency, whereas one formal Sn^{II} center is present in the heterometallic Cu_4Sn core besides six formal Sn^{IV} centers at the cluster surface.

Table 3.15 Selected interatomic distances /pm and angles /° observed in compound **19**

cluster core:	experimental (X-ray)	calculated (DFT)
Sn4–S	251.9(1) – 255.2(2)	256.1 – 258.0
Cu(4-6)–S	243.5(2) – 257.7(2)	244.3 – 253.7
Cu7–S	218.1(2) – 223.8(2)	230.0 – 231.4
Sn4…Cu(4,5,6)	262.6(1) – 263.7(1)	267.4 – 269.3
Cu(4-6)…Cu(4-6)	257.5(2) – 260.9(2)	263.7 – 265.8
Cu(4-6)…Cu7	259.2(1) – 262.7(2)	260.0 – 261.5
Cu(4-6)…Cu$_{periphery}$	232.9(1) – 238.8(1)	254.2 – 255.3
S–Sn4–S	97.42(5) – 98.33(5)	96.1 – 97.0
S–Cu(4,5,6)–S	93.45(6) – 98.42(6)	94.1 – 97.0
S- Cu7-S	116.25(7) – 121.14(7)	118.6 – 120.5

cluster periphery:	experimental (X-ray)	calculated (DFT)
Sn–S	237.3(2) – 243.8(1)	243.0 – 246.9
Cu–S	237.7(1) – 242.7(2)	244.3 – 253.7
Cu–P	220.7(2) – 222.1(2)	224.4 – 229.6
P–C	180.6(6) – 183.7(5)	183.9 – 184.8
Sn–C	213.8(6) – 218.0(7)	218.8 – 220.3
Sn…Cu	368.9(1) – 403.7(2)	352.5 – 417.0
Cu…Cu	449.2(1) – 453.7(1)	365.7 – 473.5
S–Sn–S	107.59(4) – 108.52(4)	105.8 – 109.0
S–Sn–C	106.6(2) – 121.4(2)	
C–Sn–C	87.2(2) – 88.3(2)	
S–Cu–S	98.82(5) – 102.67(5)	95.5 – 108.0
S–Cu–P	112.27(6) – 122.53(5)	112.9 – 124.2
Cu–S–Cu	140.75(5) – 142.25(6)	
Cu–S–Sn	102.40(5) – 113.49(7)	

Table 3.16 Summary of the natural population analysis (NPA) performed on calculated compound **19**. For C and H atoms, only ranges of the natural charges are given

atom no	atom type	natural charge	natural population			
			core	valence	Rydberg	total
1	Sn	1.51702	17.98552	2.45259	0.04487	20.48298
2	Sn	1.50223	17.98650	2.46484	0.04643	20.49777
3	Sn	1.48031	17.98539	2.49272	0.04158	20.51969
4	Sn	1.50256	17.98570	2.46710	0.04464	20.49744
5	Sn	1.48330	17.98659	2.48621	0.04390	20.51670
6	Sn	1.50429	17.98662	2.46167	0.04743	20.49571
7	Sn	0.71940	17.99332	3.16792	0.11937	21.28060
8	Cu	0.76009	17.99640	10.20217	0.04134	28.23991
9	Cu	0.69923	17.99568	10.25744	0.04765	28.30077
10	Cu	0.71216	17.99574	10.24928	0.04283	28.28784
11	Cu	0.62043	17.99322	10.32578	0.06057	28.37957
12	Cu	0.76040	17.99638	10.20180	0.04142	28.23960
13	Cu	0.61909	17.99321	10.32488	0.06281	28.38091
14	Cu	0.61953	17.99315	10.32551	0.06181	28.38047
15	Cu	0.70294	17.99664	10.24844	0.05199	28.29706
16	Cu	0.74078	17.99611	10.21357	0.04953	28.25922
17	Cu	0.71229	17.99572	10.24951	0.04247	28.28771
18	P	0.79146	9.99786	4.12075	0.08992	14.20854
19	P	0.78779	9.99785	4.12303	0.09133	14.21221
20	P	0.78929	9.99785	4.12483	0.08804	14.21071
21	P	0.79450	9.99787	4.11526	0.09237	14.20550
22	P	0.78886	9.99786	4.12216	0.09113	14.21114
23	P	0.79056	9.99785	4.12396	0.08763	14.20944
24	S	−0.91310	9.99943	6.87741	0.03625	16.91310
25	S	−1.06250	9.99946	7.02436	0.03868	17.06250
26	S	−1.08187	9.99946	7.04571	0.03670	17.08187
27	S	−1.04400	9.99953	7.00264	0.04183	17.04400
28	S	−1.06040	9.99949	7.02558	0.03533	17.06040
29	S	−0.86904	9.99943	6.82956	0.04005	16.86904
30	S	−0.90588	9.99943	6.86971	0.03673	16.90588
31	S	−1.01094	9.99952	6.96768	0.04374	17.01094
32	S	−1.08945	9.99949	7.05679	0.03317	17.08945
33	S	−1.04408	9.99953	7.00309	0.04146	17.04408
34	S	−1.04796	9.99948	7.00981	0.03868	17.04796
35	S	−1.07994	9.99946	7.04328	0.03720	17.07994
36-167	C	−0.19377 - −0.87198				
168-305	H	0.21088 - 0.25285				
total[a]		0.00000	749.6994	901.8340	4.46662	1656.000

[a] Statistic for all atoms:
Core 749.69937(99.9599% of 750)
Valence 901.83401(99.5402% of 906)
Natural Minimal Basis 1651.53338(99.7303% of 1656)
Natural Rydberg Basis 4.46662(0.2697% of 1656)

Table 3.17 Atomic populations from total density. For C and H atoms, only ranges of the natural charges are given

atom number	atom type	charge	n(s)	n(p)	n(d)
1	Sn	1.51702	3.10555	7.37153	10.00133
2	Sn	1.50223	3.10349	7.38812	10.00155
3	Sn	1.48031	3.10199	7.41242	10.00073
4	Sn	1.50256	3.10280	7.38925	10.00090
5	Sn	1.48330	3.10275	7.40805	10.00131
6	Sn	1.50429	3.10571	7.38353	10.00188
7	Sn	0.71940	3.50655	7.75544	10.01510
8	Cu	0.76009	6.35211	12.01366	9.87412
9	Cu	0.69923	6.39803	12.01446	9.88826
10	Cu	0.71216	6.38690	12.01449	9.88643
11	Cu	0.62043	6.43318	12.03287	9.91350
12	Cu	0.76040	6.34959	12.01370	9.87629
13	Cu	0.61909	6.43642	12.03357	9.91090
14	Cu	0.61953	6.43290	12.03307	9.91448
15	Cu	0.70294	6.39594	12.02953	9.87157
16	Cu	0.74078	6.36548	12.01392	9.87980
17	Cu	0.71229	6.38742	12.01431	9.88597
18	P	0.79146	5.29103	8.87184	0.04429
19	P	0.78779	5.27636	8.88839	0.04599
20	P	0.78929	5.29288	8.87251	0.04396
21	P	0.79450	5.27551	8.88221	0.04628
22	P	0.78886	5.27758	8.88641	0.04569
23	P	0.79056	5.29228	8.87199	0.04382
24	S	−0.91310	5.78845	11.09644	0.02770
25	S	−1.06250	5.81236	11.22633	0.02336
26	S	−1.08187	5.81833	11.24136	0.02172
27	S	−1.04400	5.81795	11.19567	0.02997
28	S	−1.06040	5.81682	11.22167	0.02150
29	S	−0.86904	5.79055	11.04705	0.03095
30	S	−0.90588	5.78981	11.08695	0.02865
31	S	−1.01094	5.81969	11.15969	0.03113
32	S	−1.08945	5.81874	11.25010	0.02017
33	S	−1.04408	5.81662	11.19759	0.02944
34	S	−1.04796	5.81334	11.21047	0.02373
35	S	−1.07994	5.81541	11.24115	0.02290
36-167	C	−0.19377 - −0.87198			
168-305	H	0.21088 - 0.25285			

Chapter 4

Experimental Section

4.1 General Aspects

4.1.1 Working Techniques

Most of the compounds were air sensitive. They either decomposed in contact with air or transformed into some other kinds of compounds. Therefore, all synthetic manipulations were performed under argon atmosphere, using a high vacuum (10^{-3} Torr) double manifold Schlenk line, or in a glove box. Only some reactions were also performed under air.

4.1.2 Solvents

All organic solvents were refluxed for 3 hours with appropriate drying agent: methanol over magnesium, *n*-pentane, *n*-hexane over lithium aluminium hydride, toluene over sodium, THF over sodium and benzophenone, dichloromethane over calcium chloride, diethylether over calcium hydride, acetonitrile and chloroform over phosphorous pentoxide. The dried solvents were distilled and then collected under argon. Absolute ethanol was degassed in high vacuum for 1 hour and then saturated with argon. For NMR analyses, C_6D_6, $CDCl_3$ and DMSO-D6 were used as solvents. C_6D_6 was refluxed for 2 hours over sodium and then distilled under argon. $CDCl_3$ was distilled under argon. DMSO-D6, obtained from commercial source was transferred carefully and stored under argon.

During the synthesis of the starting materials, saturated NH_4Cl solution in water, brine and isopropanol were used as solvents to decompose the side products. The distilled water was evacuated for 2 hours at high vacuum to remove dissolved oxygen and carbon dioxide, and then stirred for 10 minutes under slow flow of argon.

4.1.3 Spectroscopic Studies

All compounds were characterized spectroscopically. Infrared spectra were measured on a Bruker IFS 88 spectrometer using a KBr pellet and are reported in cm^{-1} with indicated relative intensities: s (strong, 67-100%), m (medium, 34-66%), and w (weak, 0-33%). NMR spectra were measured on Brucker Avance 300 MHz and 400 MHz using TMS (^{1}H, ^{13}C) or Me$_4$Sn (^{119}Sn) as standards. NMR spectra of air sensitive compounds were measured using sealed NMR tubes; multiplicities are indicated by s (singlet), d (doublet), t (triplet), m (multiplet). UV-Visible spectra were recorded on a Varian Cary 5000 UV/Vis/NIR spectrometer in the range of 800–200 nm, employing double beam technique. The samples were measured as suspensions in nujol oil. The mixture was given between two quartz plates and rapidly brought into the UV-Visible beam. Energy dispersive X-Ray spectroscopy analyses (EDX) were performed using an EDX device Voyager 4.0 of Noran Instruments, coupled with an electron microscope CamScan CS 4DV. Data acquisition was performed with an acceleration voltage of 20 kV and 100 s accumulation time. Thermogravimetric analyses (TGA) were carried out by means of a Mettler Toledo TMA/SDTA 851 under a flowing nitrogen atmosphere with a flow rate of 50 ml·min^{-1}.

4.1.4 Quantum Chemical Investigation

The density functional theoretical (DFT) investigations were undertaken by means of the program system TURBOMOLE using the RIDFT [102] program with the Becke-Perdew 86 (B-P86) functional [103] and the gridsize m3. Basis sets were of def2-TZVPP quality (TZVPP = triple zeta valence plus double polarization) [104] for the calculation on the intramolecular cyclization of Cl$_3$Sn–(CH$_2$)$_4$–SnCl$_3$ producing SnCl$_4$ and {*cyclo*-(CH$_2$)$_4$Sn}Cl$_2$. def2-TZVP basis sets (TZVP = triple zeta valence plus polarization) were used for Cu, Sn, S and P atoms and def2-SV(P) basis sets (SV(P) = split valence plus polarization for non-H atoms) were assigned to C and H atoms [104] . For Sn, Pd atoms, an effective core potential (ECP-28) [105] was used for consideration of relativistic corrections and to reduce the computational effort. The simultaneous optimizations of geometric and electronic structures were performed without symmetry restrictions, *i.e.* in C_1 symmetry, also allowing for convergence into local minima at higher symmetry.

Population analyses (natural population analyses, NPA) [106] of the electron density were performed using the routine implemented in the TURBOMOLE software. Density of states results from according Mulliken population analyses [107]. Electron density plots were realized by using gOpenMol v3.0.

4.2 Synthesis of Starting Materials

4.2.1 Chemicals Used

Mg, 1,4-dibromobutane, 1,4-bis(chloromethyl)benzene , 4,4′-bis(chloromethyl)biphenyl, $SnCl_4$, NH_4Cl, NaCl, KF, CuCl, $AgNO_3$, $Na_2S \cdot 9H_2O$, S, Se, $PhSeSiMe_3$, Ph_3SnCl, Cy_3SnCl, Me_3SnCl, Me_2SnCl_2, ferrocene were available from local sources or have been purchased from Aldrich and Acros organics and used as received.

4.2.2 Synthesis of 1, 4-Bis(triphenylstannyl)butane [108]
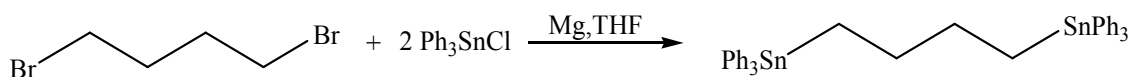
Mg turnings (6.3116 g, 259.42 mmol) were given in a 100 mL round bottle flask that was previously oven dried. It was fitted with a dry dropping funnel in argon atmosphere. The Mg turnings were heated by a heat gun for 45 minutes. During this time, the full system was evacuated and filled up by argon periodically. After 45 minutes, a small crystal of iodine was introduced in the dropping funnel and 10 mL of dry THF was added. This mixture was slowly added to the Mg. Then 70 mL of THF containing 3.1 mL (25.94 mmol) of 1,4-dibromobutane were added within 3 hours with constant stirring at 25 ºC. The mixture was stirred for 15 hours at the same temperature. The resulting Grignard solution was decanted into a dry dropping funnel and added to a solution of triphenyltin chloride (20 g, 51.88 mmol) in 50 mL of THF at 0 ºC during 4 hours. Then the mixture was allowed to stir at 25 ºC for 15 hours and then heated to reflux for 2 hours. The mixture was cooled to 0 ºC and hydrolyzed with 50 mL of saturated NH_4Cl solution. The organic layer was separated and washed by 30 mL of a saturated KF solution and 30 mL of a saturated NaCl solution. The organic layer was dried over $MgSO_4$ and vacuum dried. The product was recrystallized from dichloromethane/*n*-hexane for purification.

Molar Mass: 756.149 g/mol   **Yield:** 10 g, 13.22 mmol, 51%

¹H NMR: (300 MHz, CDCl₃) δ/ppm = 1.30-1.60 (4 H, m, CH₂), 1.65-1.90 (4 H, m, CH₂), 7.10-7.53 (30 H, m, Ph)

¹³C NMR: (75 MHz, CDCl₃) δ/ppm = 10.6, 31.3, (CH₂) 128.24, 128.7, 137.0, 138.9 (Ph)

¹¹⁹Sn NMR: (CDCl₃) δ/ppm = −98.80

4.2.3 Synthesis of 1,4-Bis(trichlorostannyl)butane [56]

To 3.462 g (4.58 mmol) of 1,4-bis(triphenylstannyl)butane in a dry 25 mL dry round bottle flask, 3.76 mL (32.04 mmol) of SnCl₄ was added dropwise, and the mixture was heated to 120-130° C for 2 hours. All the volatile products were removed under vacuum. The resulting mixture was distilled. The desired product was obtained at 130-150° C and collected as colorless solid at the cooling part of the distillation unit.

Molar Mass: 506.24 g/mol   **Yield:** 1.76 g, 3.48 mmol, 76%.

¹H NMR: (300 MHz, CDCl₃) δ/ppm: 2.02 (4 H, m, CH₂), 2.25 (4 H, m, CH₂)

¹³C NMR: (75 MHz, CDCl₃) δ/ppm: 27.19, 30.36

¹¹⁹Sn NMR: (CDCl₃) δ/ppm: 6.21

^{1}H NMR: (300 MHz, CDCl$_3$) δ/ppm = 1.30-1.60 (4 H, m, CH$_2$), 1.65-1.90 (4 H, m, CH$_2$), 7.10-7.53 (30 H, m, Ph)

^{13}C NMR: (75 MHz, CDCl$_3$) δ/ppm = 10.6, 31.3, (CH$_2$) 128.24, 128.7, 137.0, 138.9 (Ph)

^{119}Sn NMR: (CDCl$_3$) δ/ppm = −98.80

4.2.3 Synthesis of 1,4-Bis(trichlorostannyl)butane [56]

To 3.462 g (4.58 mmol) of 1,4-bis(triphenylstannyl)butane in a dry 25 mL dry round bottle flask, 3.76 mL (32.04 mmol) of SnCl$_4$ was added dropwise, and the mixture was heated to 120-130°C for 2 hours. All the volatile products were removed under vacuum. The resulting mixture was distilled. The desired product was obtained at 130-150°C and collected as colorless solid at the cooling part of the distillation unit.

Molar Mass: 506.24 g/mol   **Yield:** 1.76 g, 3.48 mmol, 76%.

^{1}H NMR: (300 MHz, CDCl$_3$) δ/ppm: 2.02 (4 H, m, CH$_2$), 2.25 (4 H, m, CH$_2$)

^{13}C NMR: (75 MHz, CDCl$_3$) δ/ppm: 27.19, 30.36

^{119}Sn NMR: (CDCl$_3$) δ/ppm: 6.21

4.2.4 Synthesis of 1,4-Bis(tricyclohexylstannylmethyl)benzene [57]
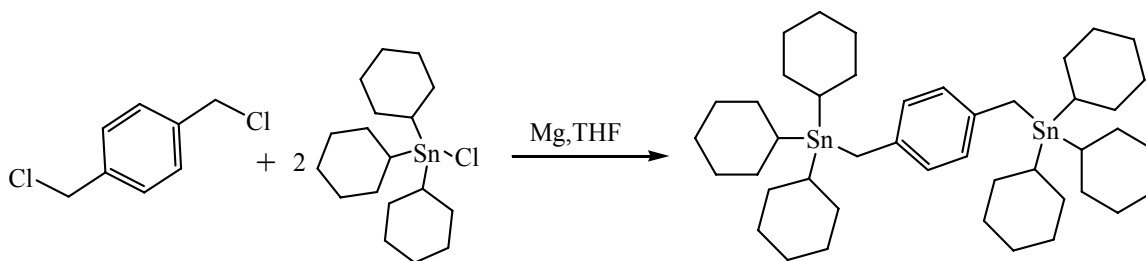
A solution of 4.83 g (27.0 mmol) of 1,4-bis(chloromethyl)benzene and 22.2 g (49.5 mmol) of tricyclohexyltinchloride in 90 mL of dry THF was slowly added to a suspension of 2.60 g (107 mmol) of magnesium in 125 mL of THF at room temperature. The light grey mixture was then refluxed for 1 hour. After hydrolysis with 50 mL of a saturated solution of ammonium chloride, the suspension was filtered and the solid was washed with 25 mL of THF. 50 mL of n-pentane was added to the filtrate, and after extraction, the organic layer was dried by adding Na_2SO_4. After evaporation of the solvent and drying in high vacuum, 17.7 g (21.1 mmol, 78%) of 1,4-bis(tricyclohexylstannylmethyl)benzene were obtained as a white solid.

Molar Mass: 840.48 g/mol   **Yield:** 17.7 g, 21.06 mmol, 78%

^{1}H NMR: (300 MHz, CDCl$_3$) δ/ppm: 1−2 (m, 66H, Cy), 2.17 (s, 4H, CH$_2$), 6.81 (s, 4H, Ar)

^{13}C NMR: (75 MHz, CDCl$_3$) δ/ppm: 15.0, 26.9, 27.4, 29.4, 32.3, 127.5, 136.1, 142.9

^{119}Sn NMR: (CDCl$_3$) δ/ppm: −76.2

4.2.5 Synthesis of 1,4-Bis(trichlorostannylmethyl)benzene [57]
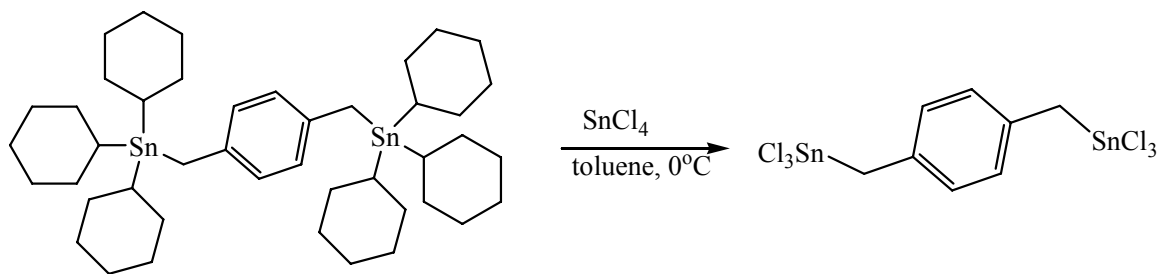
2.78 mL (23.8 mmol) of SnCl4 was slowly added to a solution of 7.73 g (9.20 mmol) of 1,4-bis(tricyclohexyltinmethyl)benzene in 100 mL of toluene at −30 °C. The white suspension was stirred at 70 °C for 15 h. Toluene and excess of SnCl$_4$ were evaporated. The white residue was dissolved in 150 mL of acetonitrile and by-products were removed by extracting five times with 50 mL of *n*-pentane. Evaporation of the acetonitrile layer ended up with a white solid, which was dissolved in 100 mL of THF to replace the coordinating acetonitrile. A white solid was also obtained after evaporation of THF. The compound was recrystallized from THF/CH$_2$Cl$_2$.

Molar Mass: 554.28 g/mol   **Yield:** 3.8 g, 6.85 mmol, 74.5%.

^{1}H NMR: (300 MHz, CDCl$_3$) δ/ppm: 3.73 (s, 4H, CH$_2$), 7.37 (s, 4H, ArH)

^{13}C NMR: (75 MHz, CDCl$_3$) δ/ppm: 44.0 (CH$_2$), 117.2 (Ar), 130.2 (Ar)

^{119}Sn NMR: (CDCl$_3$) δ/ppm: −33.5

4.2.6 Synthesis of 4,4'-Bis(tricyclohexylstannylmethyl)biphenyl [58]
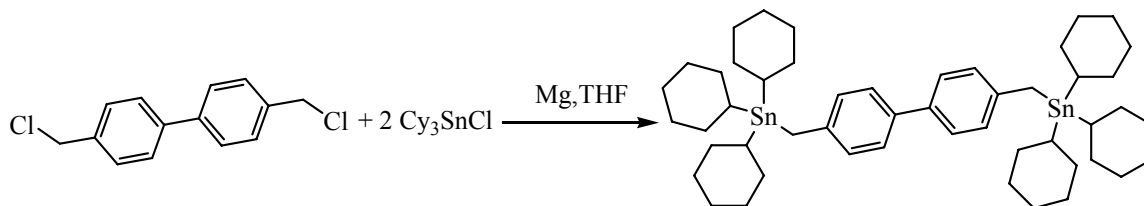
A solution of 3.89 g (15.5 mmol) of 4,4′-bis(chloromethyl)biphenyl and 12.5 g (31.0 mmol) of tricyclohexyltinchloride in 50 mL of THF was slowly added to a suspension of 2.51 g (103 mmol) of Mg in 25 mL of THF at room temperature. The light grey mixture was then refluxed for 2 h. After hydrolysis by 25 mL of a saturated solution of NH_4Cl, the suspension was filtered and the solid was washed with 35 mL of THF. 25 mL of n-pentane was added to the filtrate and after extraction the organic layer was dried with Na_2SO_4. After evaporation of the solvent and drying in high vacuum, 4,4′-bis(tricyclohexyltinmethyl)biphenyl was obtained as a white solid.

Molar Mass: 916.57 g/mol   **Yield:** 10.7 g, 11.7 mmol, 76%.

^{1}H NMR: (300 MHz, $CDCl_3$) δ/ppm: 1–2 (m, 66H, Cy), 2.27 (s, 4H, Ar*CH₂*), 7.00 (d, 4H, ArH), 7.31 (d, 4H, ArH)

^{13}C NMR: (75 MHz, $CDCl_3$) δ/ppm: 15.6, 27.2, 27.3, 29.4 (Cy), 32.3 (Ar*CH₂*), 126.5 (Ar), 127.9 (Ar), 136.1 (Ar), 142.9 (Ar)

^{119}Sn NMR: ($CDCl_3$) δ/ppm: −74.2

4.2.7 Synthesis of 4,4'-Bis(trichlorotinmethyl)biphenyl [58]
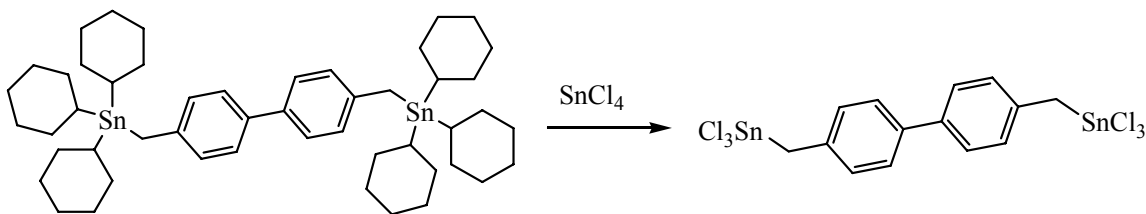
3.56 mL (30.5 mmol) of $SnCl_4$ was slowly added to a white suspension of 10.5 g (11.5 mmol) of 4,4′-bis(tricyclohexyltinmethyl)biphenyl in 135 mL of toluene. The yellow suspension was stirred at room temperature for 15 h. Toluene and excess $SnCl_4$ were evaporated. The yellow residue was dissolved in 150 mL of acetonitrile and extracted five times by 35 mL of n-pentane. Evaporation of the acetonitrile layer ended up with a

green oil, which was dissolved in 200 mL of THF. Evaporation of the THF leads to the generation of light yellow-green solid of the desired product.

Molar Mass: 630.38 g/mol   **Yield:** 2.5 g, 3.96 mmol, 38%

^{1}HNMR: (300 MHz, DMSO-d6) δ/ppm: 2.98 (s, 4H, CH$_2$), 7.24 (d, 4H, ArH), 7.54 (d, 4H, ArH)

^{13}CNMR: (75 MHz, DMSO-d6) δ/ppm: 39.3 (CH$_2$), 125.3 (Ar), 129.6 (Ar), 136.4 (Ar), 138.4 (Ar)

4.2.8 Synthesis of 1, 1'-Dilithioferrocene·TMEDA [109]
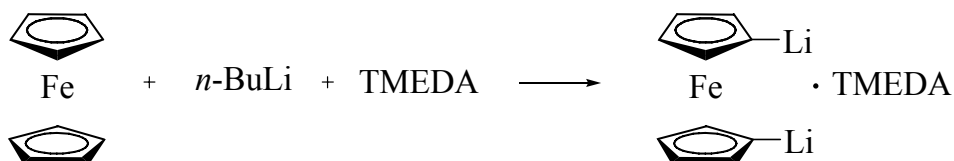
A mixture of ferrocene (20 g, 108 mmol), *n*-butyl-lithium (99 mL, 2.5 M), *n*-hexane (135 mL) and tetramethylethylenediamine (TMEDA, 20 mL) was stirred at 0 ºC for 16 hours. The resulting yellow solid was isolated by filtration and washed several times with anhydrous *n*-hexane. The product was dried under vacuum.

Molar Mass: 314.10 g/mol   **Yield:** 30 g, 95.5 mmol, 87%.

4.2.9 Synthesis of 1,1'-Bis(trimethylstannyl)ferrocene [110]
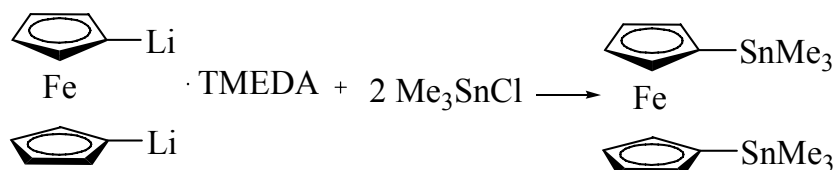
To a stirred suspension of Fe(C$_5$H$_4$Li)$_2$·TMEDA (6.3 g, 20 mmol) in *n*-hexane (50 mL), a solution of Me$_3$SnCl (8.95 g, 45 mmol) in *n*-hexane (30 mL) was added within two hours at room temperature. The mixture was stirred for 14 hours. LiCl, insoluble by-products, and the solvents were removed by filtration or evaporation, respectively. Ferrocene, TMEDA and unreacted Me$_3$SnCl were removed in vacuum at 40 ºC at 1×10^{-3} mbar. Distillation of the remaining red oil at 1×10^{-3} mbar afforded the compound as red oil.

Molar Mass: 511.64 g/mol   **Yield:** 5.4 g, 10.5 mmol, 53%

EI MS: m/z (%): 512 (100)

^{1}H NMR: (300 MHz, CDCl$_3$) δ/ppm: 0.34 (s, 18H, CH$_3$), 4.10 (s, 4H, ArH), 4.34
     (s, 4H, ArH)

^{13}C NMR: (75 MHz, CDCl$_3$) δ/ppm: -8.5 (CH$_3$), 68.3, 70.8, 74.3 (Ar)

^{119}Sn NMR: (CDCl$_3$) δ/ppm: −4.0

4.2.10 Synthesis of 1,1'-Bis(chlorodimethylstannyl)ferrocene [59]
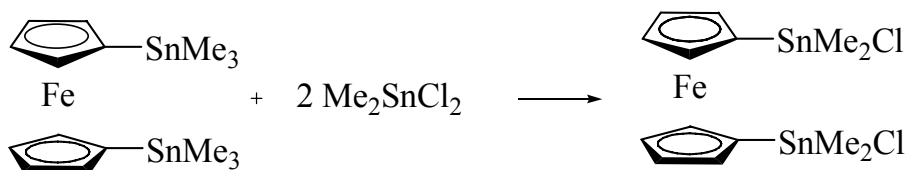
A round bottom Schlenk flask was fitted with Fe(C$_5$H$_4$SnMe$_3$)$_2$ (1.14 g, 2.8 mmol). Then Me$_2$SnCl$_2$ (1.23 g, 5.6 mmol) was added at 0 ºC. The mixture was heated at 140 ºC for 3 hours. There upon, it was cooled to room temperature and Me$_3$SnCl and Me$_2$SnCl$_2$ were removed in vacuum. A viscous dark orange oil was remained which crystallized upon cooling in *n*-hexane as an orange solid.

Molar Mass: 552.48 g/mol   **Yield:** 1 g, 1.81 mmol, 81.3%.

4.2.11 Synthesis of 1,1'-Bis(trichlorostannyl)ferrocene [59]
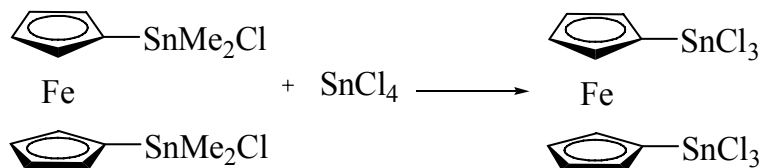
SnCl$_4$ (0.9 mL, 7.54 mmol) was added to a solution of Fe(C$_5$H$_4$SnMe$_2$Cl)$_2$ (1.60 g, 2.90 mmol) in DCM (5 mL) and *n*-hexane (15 mL) at 0 ºC. The color of the reaction mixture turned rapidly from yellow to green. The mixture was stirred for 2 hours at 30 ºC. Then all the volatile compounds were removed in vacuum and DCM/*n*-hexane (1:10, 20 mL) was used to extract the product. After filtration and removal of the solvents, the product was obtained as yellow solid.

Molar Mass: 634.15 g/mol   **Yield:** 1.4 g, 2.20 mmol, 76.2%.

4.2.12 Synthesis of Tris(triphenylphosphine)copper(I)chloride [111]

$$CuCl + 3\ PPh_3 \xrightarrow{\text{CHCl}_3/\text{EtOH}} (Ph_3P)_3CuCl$$
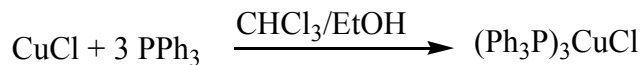
CuCl (1.23 g, 14.04 mmol) and PPh$_3$ (13.2 g, 50.38 mmol) were dissolved in 100 mL of dry CHCl$_3$. The mixture was stirred for 30 minutes at room temperature. Then 400 mL of absolute ethanol was added. The colorless, large crystals of (PPh$_3$)$_3$CuCl were collected by filtration, washed with ethanol, *n*-hexane and vacuum-dried.

Molar Mass: 885.87 g/mol   **Yield:** 6 g, 6.773 mmol, 55%.

4.2.13 Synthesis of Tris(triphenylphosphine)silver(I)nitrate [112]

$$AgNO_3 + 3\ PPh_3 \xrightarrow{\ CH_3CN/EtOH\ } (Ph_3P)_3AgNO_3$$
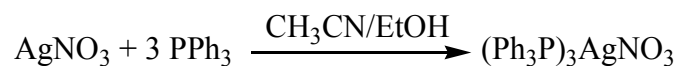
$AgNO_3$ (4.25 g, 0.025 mmol) was dissolved in 25 mL of hot acetonitrile and added to a warm solution of PPh_3 (19.65 g, 0.075 mmol) in 600 mL of absolute ethanol. The warm, clear solution was allowed to cool down slowly in the dark to give well formed crystals of desired the product. The crystals were separated from the solution and vacuum dried.

Molar Mass: 956.69 g/mol   **Yield:** 18 g, 18.81 mmol, 75%.

4.3 Synthesis of Novel Compounds

4.3.1 Synthesis of Polymeric Solid

1,4-Bis (trichlorostannyl)butane (0.1 g, 0.1975 mmol) was dissolved in 10 mL of dry THF. The solution was cooled to −40 ℃. S(SiMe₃)₂ (0.13 mL, 0.6163 mmol) was added drop wise to it. The mixture was allowed to warm up to room temperature slowly. The white solid was collected by filtration, washed with hexane and then dried in vacuum.

Elemental analysis: Found: C, 14.91 %; H, 2.70 %

EDX analysis: Sn:S; 1:1.25

4.3.2 Synthesis of 1, 4-Bis[tris(thiophenolato)stannyl]butane (1)

1
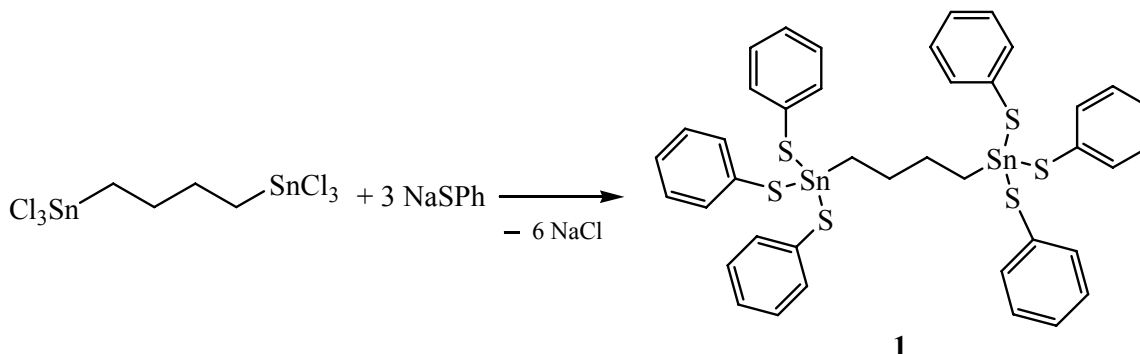
To a solution of NaSPh (0.156 g, 1.185 mmol) in 5 mL of dry methanol, a solution of 1,4 -bis(trichlorostannyl)butane (0.10 g, 0.1975 mmol) in 5 mL of dry methanol was added slowly at 0 ℃. A white precipitate formed immediately, the mixture was stirred for 24 hours. The solid was collected by filtration, washed with methanol and then dried in vacuum. The compound was recrystallized from dichloromethane/n-hexane (1:1).

Molar Mass: 948.44 g/mol   **Yield:** 0.112 g, 0.118 mmol, 64 %

[1]**H NMR:**   (400 MHz, CDCl₃, 25°C) δ/ppm: 0.94-1.11 (m, 8H, CH₂), 7.19-7. 23 (m, 18H, ArH), 7.34-7.39 (m, 12H, ArH),

¹³C NMR: (100 MHz, CHCl₃, 25°C) δ/ppm: 21.18 (CH₂), 28.60 (CH₂), 127.40,

129.10, 130.40, 135.40, (Ar),

¹¹⁹Sn NMR: (CDCl₃) δ/ppm: 89.44 (s)

4.3.3 Synthesis of 1,4-Bis[tris(thiophenolato)stannylmethyl]benzene (2)
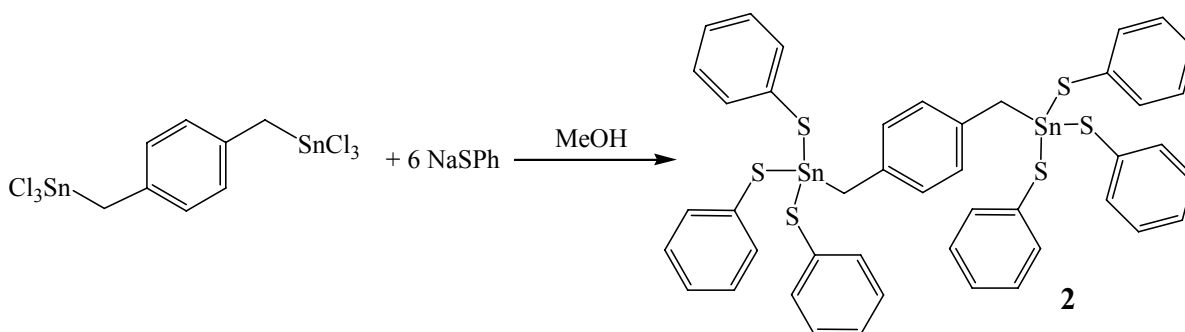
A solution of 1,4-bis(trichlorostannylmethyl)benzene (0.2 g, 0.36 mmol) in 5 mL of dry methanol was added to a solution of NaSPh (0.286 g, 2.165 mmol) in 5 mL of dry methanol, whereupon a white solid precipitated immediately. The reaction mixture was stirred for 24 hours. The solid was collected by filtration, washed with methanol, hexane and dried in vacuum.

Molar Mass: 996.58 g/mol   **Yield:** 0.2 g, 0.2 mmol, 57%

¹H NMR: (400 MHz, CDCl₃, 25°C) δ/ppm: 2.58 (s, 4H, CH₂), 6.49 (s, 4H, ArH), 7.12-

7.50 (m, 30H, ArH),

¹³C NMR: (100 MHz, CHCl₃, 25°C) δ/ppm: 30.91 (CH₂), 127.33, 127.38, 128.79,

129.09, 130.14, 135.50 (Ar),

¹¹⁹Sn NMR: (CDCl₃) δ/ppm: 61.42 (s)

4.3.4 Synthesis of 4,4'-Bis[tris(thiophenolato)tinmethyl]biphenyl (3)
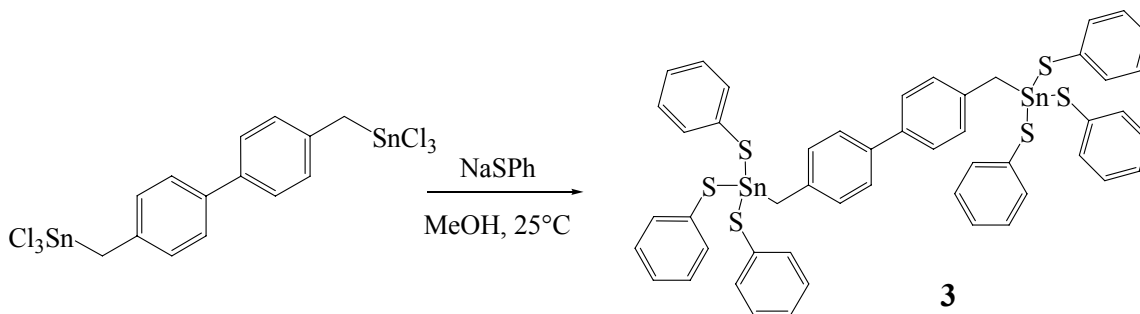
To a colorless solution of 0.252 g (1.90 mmol) of sodium thiophenolate in 5 mL of methanol was slowly added a solution of 0.2 g (0.317 mmol) of 4,4′-bis(trichlorostannylmethyl)biphenyl in 5 mL of methanol. After stirring for 12 hours, the yellow suspension was filtered and the yellow solid was washed with 10 mL of methanol, 10 mL of *n*-hexane and vacuum dried. The compound was crystallized by slow evaporation of dichloromethane/*n*-hexane (1:1) solution.

Molar Mass: 1072.58 g/mol   **Yield:** 0.238 g, 0.222 mmol, 70 %

^{1}H NMR: (300 MHz, CDCl$_3$, 25°C) δ/ppm: 2.62 (s, 4H, CH$_2$), 6.62-6.74 (m, 8H, ArH), 7.1-7.3 (m, 30H, ArH)

^{13}C NMR: (75.5 MHz, CHCl$_3$, 25°C) δ/ppm: 27.9 (CH$_2$), 126.0, 126.4, 127. 9,128.0, 129.2, 133.8, 134.4, 136.9 (Ar)

^{119}Sn NMR: (CDCl$_3$) δ/ppm: 59.78 (s)

4.3.5 Synthesis of 1,4-Bis[tris(thionaphthylato)stannyl]butane (4)

4
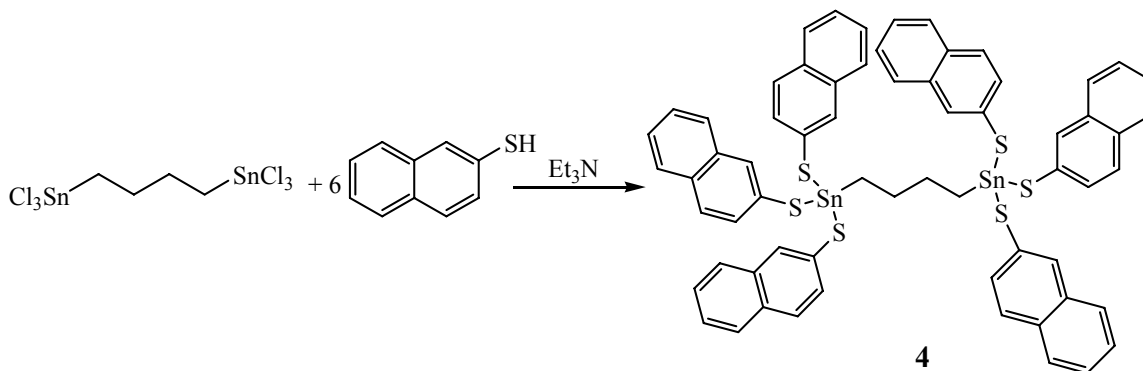
A solution of 1,4-bis(trichlorostannyl)butane (0.107 g, 0.21 mmol) in 5 mL of toluene was added to a solution of 2-thionaphthol (0.203g, 1.27 mmol) and Et$_3$N (0.18 mL, 1.27 mmol) in 5 mL of toluene. The reaction mixture was stirred for 12 hours. Then toluene was removed under reduced pressure, and 10 mL of methanol were added to the obtained solid. The mixture was filtered to remove Et$_3$NHCl, and the solid was washed with methanol, *n*-hexane and dried in vacuum. The compound was recrystallized by layering a dichloromethane solution of the compound with *n*-hexane.

Molar Mass: 1248.78 g/mol   **Yield:** 0.145 g, 0.12 mmol, 55 %.

^{1}H NMR: (400 MHz, CDCl$_3$, 25°C) δ: 0.813 (m, 4H, CH$_2$), 0.946 (m, 4H, CH$_2$), 7.24-
7.73 (m,42H, ArH),

^{13}C NMR: (100 MHz, CHCl$_3$, 25°C) δ: 21.80 (CH$_2$), 28.80 (CH$_2$), 125.56, 126.32,
126.59, 127.26, 127.67, 128.43, 132.27, 132.52, 133.60, 134.36 (Ar),

^{119}Sn NMR: (CDCl$_3$) δ: 85.49 (s)

4.3.6 Synthesis of 1,4-Bis[tris(thionaphthylato)stannylmethyl]benzene (5)

5
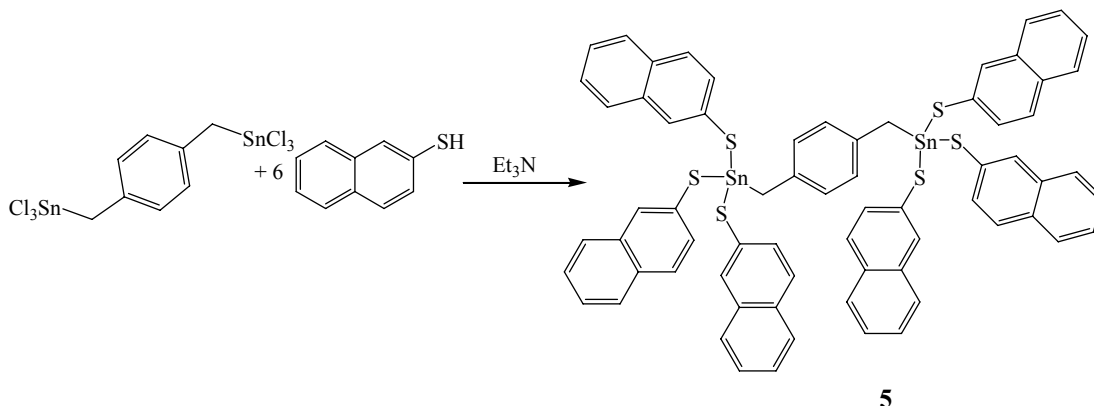
2-Thionaphthol (0.173 g, 1.08 mmol) was dissolved in 5 mL of toluene, and Et₃N (0.15 mL, 1.08 mmol) was added to it. The mixture was stirred for 10 minutes. A solution of 1,4-bis(trichlorostannylmethyl)benzene (0.1 g, 0.18 mmol) in 5 mL of toluene was added to the mixture. The mixture was stirred for 12 hours, toluene was removed under reduced pressure, and 10 mL of methanol were added to the obtained solid. The mixture was filtered and the solid was washed with methanol, hexane and dried in vacuum. The compound was recrystallized from a dichloromethane/ *n*-hexane mixture within one week.

Molar Mass: 1296.82 g/mol   **Yield:** 0.157 g, 0.12 mmol, 67 %

^{1}H NMR: (400 MHz, CDCl₃, 25°C) δ/ppm: 2.30 (s, 4H, CH₂), 7.11 (s, 4H, ArH), 7.29-7.73 (m, 42H, ArH)

^{13}C NMR: (100 MHz, CHCl₃, 25°C) δ/ppm: 31.0 (CH₂), 125.54, 126.687, 126.754, 127.20, 127.75, 127.86, 128.17, 128.66, 131.6, 133.6 (Ar)

^{119}Sn NMR: (CDCl₃) δ/ppm: 55.44 (s)

4.3.7 Synthesis of 1,4-Bis[dichloro(selenophenolato)stannyl]butane (6)
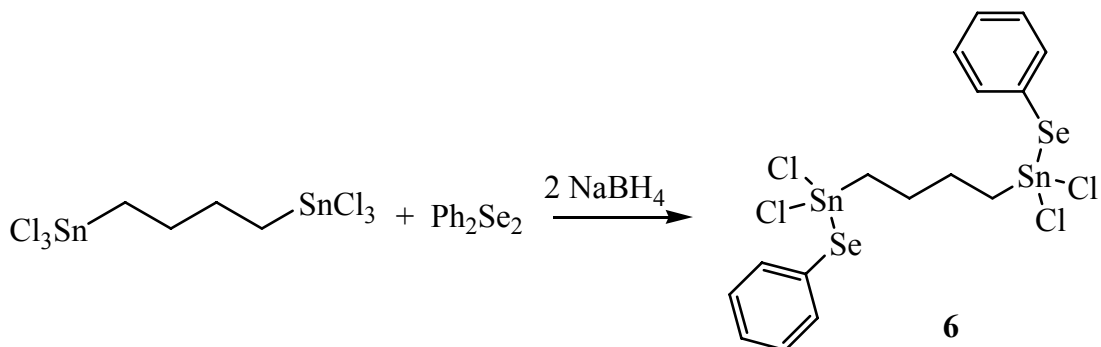
Ph$_2$Se$_2$ (0.136 g, 0.44 mmol) was dissolved in 5 mL of degassed, absolute ethanol. NaBH$_4$ (0.033 g, 0.87 mmol) was added to this solution in small portions until the solution has became completely colourless. 1,4-bis(trichlorostannyl)butane (0.22 g, 0.4345 mmol) was dissolved in 5 mL of ethanol and then added to the previously prepared NaSePh solution slowly. The mixture was stirred for 24 hours, filtered and washed with ethanol. The filtrate was evaporated to end up with a white solid. 10 mL of methanol was added to the solid. After filtration, the product was isolated by evaporating the solvent. Light yellow crystals were obtained by slow evaporation of a dichloromethane/*n*-hexane solution.

Molar Mass: 818.37 g/mol   **Yield:** 0.165 g, 0.20 mmol, 46%

^{1}H NMR: (400 MHz, CDCl$_3$, 25°C) δ/ppm: 0.99-1.04 (m, 8H, CH$_2$), 7.16-7.42 (m, 10H, ArH)

^{13}C NMR: (100 MHz, CHCl$_3$, 25°C) δ/ppm: 22.19 (CH$_2$), 29.32(CH$_2$), 124.22, 127.63,130.89, 137.00 (Ar)

^{119}Sn NMR: (CDCl$_3$) δ/ppm: −4.13 (s)

4.3.8 Synthesis of 1,4-Bis[tris(selenophenolato)stannyl]butane (7)
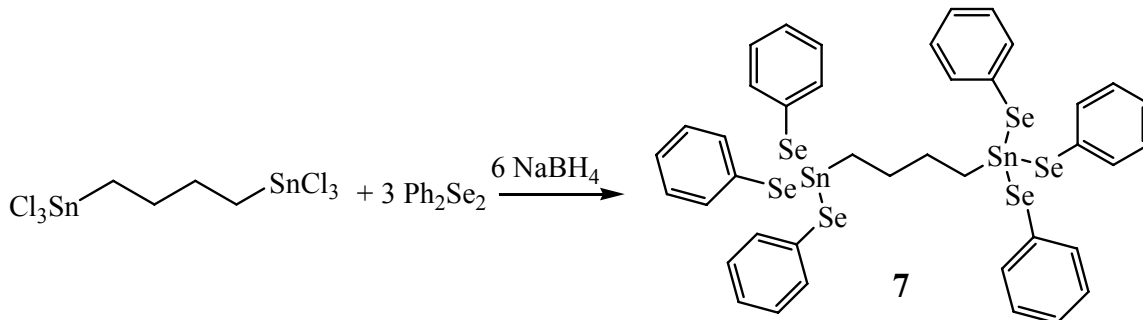
Ph$_2$Se$_2$ (0.185 g, 0.59 mmol) was dissolved in 5 mL of degassed absolute ethanol. 0.06 g (1.586 mmol) of NaBH$_4$ was added to this solution in small portions until the solution has become completely colorless. 1,4-Bis (trichlorostannyl)butane (0.1 g, 0.1975 mmol) was dissolved in 5 mL of ethanol and then added to the previously prepared NaSePh solution slowly at 0 ºC. The mixture was stirred for 24 hours, filtered, washed with ethanol and dried in vacuum. Then the solid was dissolved in 5 mL of dry dichloromethane, layered by 10 mL of *n*-hexane and stored at 6 ºC. After six days, light yellow crystals were obtained.

Molar Mass: 1229.84 g/mol   **Yield:** 0.145 g, 0.1185 mmol, 60%

^{1}H NMR: (400 MHz, CDCl$_3$, 25°C) δ/ppm: 0.95-1.03 (m, 8H, CH$_2$), 7.01-7.18 (m, 16H ArH), 7.366-7.44 (m, 14H, ArH)

^{13}C NMR: (100 MHz, CHCl$_3$, 25°C) δ/ppm: 21.00(CH$_2$), 28.10(CH$_2$), 123.30, 126.60, 128.40, 135.80, (Ar),

^{119}Sn NMR: (CDCl$_3$) δ/ppm: −4.92 (s)

4.3.9 Synthesis of 1,4-Bis[tris(1-selenonaphthylato)stannyl]butane (8)
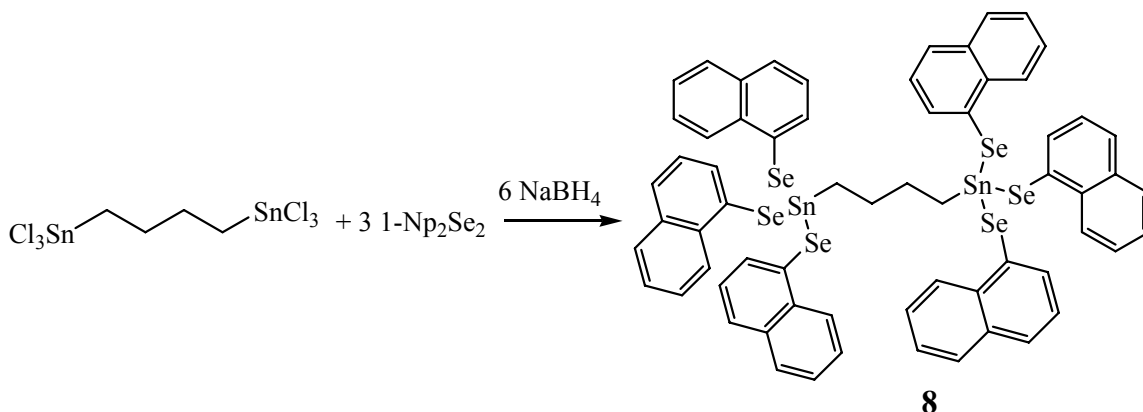
8

1,4-Bis (trichlorostannyl)butane (0.1 g, 0.1975 mmol) was dissolved in 5 mL of degassed absolute ethanol and added to a solution of sodium 1-selenonaphthylate prepared from Np_2Se_2 (0.244 g, 0.592 mmol) and $NaBH_4$ (0.045 g, 1.184 mmol) in 5 mL of ethanol. The mixture was stirred for 12 hours, whereupon the solid was collected by filtration and dried in vacuum. The product was recrystallized from a dichloromethane/*n*-hexane (1:1) mixture.

Molar Mass: 1530.18 g/mol   **Yield:** 0.175 g, 0.115 mmol, 58%

¹H NMR: (400 MHz, $CDCl_3$, 25°C) δ/ppm: 0.92 (m, 4H, CH_2), 1.03 (m, 4H, CH_2), 7.14-8.33 (m, 42H, ArH)

¹³C NMR: (100 MHz, $CHCl_3$, 25°C) δ/ppm: 22.50 (CH_2), 28.80 (CH_2), 125.66, 126.30, 126.77, 127.98, 128.55, 128.98, 129.41, 129.83, 134.10, 136.90 (Ar)

¹¹⁹Sn NMR: ($CDCl_3$) δ/ppm: −6.2 (s)

4.3.10 Synthesis of 1,4-Bis[tris(selenophenolato)stannylmethyl]benzene (9)
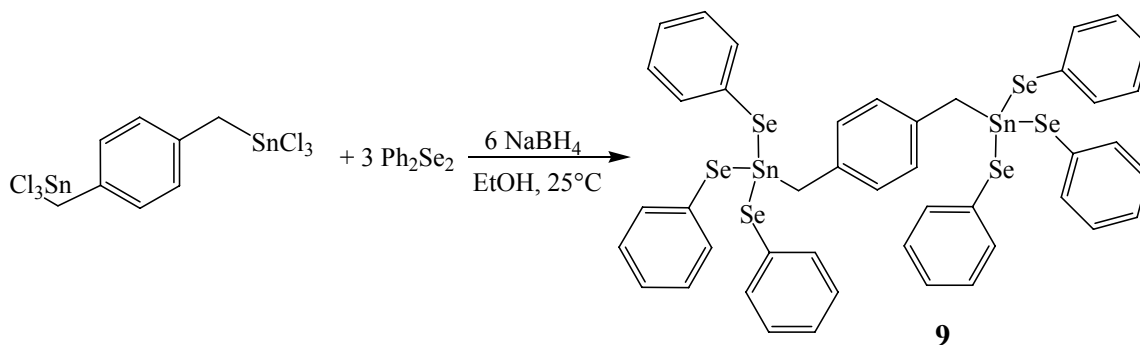
A solution of NaSePh was prepared from Ph_2Se_2 (0.206 g, 0.66 mmol) and $NaBH_4$ (0.50 g, 1.32 mmol) in 5 mL of degassed absolute ethanol. To this solution a solution of 1,4-bis(trichlorostannylmethyl)benzene 0.122 g, 0.22 mmol) in 5 mL of ethanol was added. The mixture was stirred for 12 hours. The solid was isolated by filtration, washed with ethanol, *n*-hexane, and dried in vacuum. Crystals were obtained by layering a dichloromethane solution of the compound by *n*-hexane.

Molar Mass: 1277.88 g/mol   **Yield:** 0.205 g, 0.16 mmol, 73 %.

^{1}H NMR: (400 MHz, $CDCl_3$, 25°C) δ/ppm: 2.67 (s, 4H, CH_2), 7.16-7.42 (m, 34H, ArH)

^{13}C NMR: (100 MHz, $CHCl_3$, 25°C) δ/ppm: 29.46 (CH_2), 124.10, 127.6, 129.10, 131.4, 134.1, 137.2 (Ar)

^{119}Sn NMR: ($CDCl_3$) δ/ppm: −21.47 (s)

4.3.11 Synthesis of 1,1'-Bis[tris(selenophenolato)stannyl]ferrocene (10)
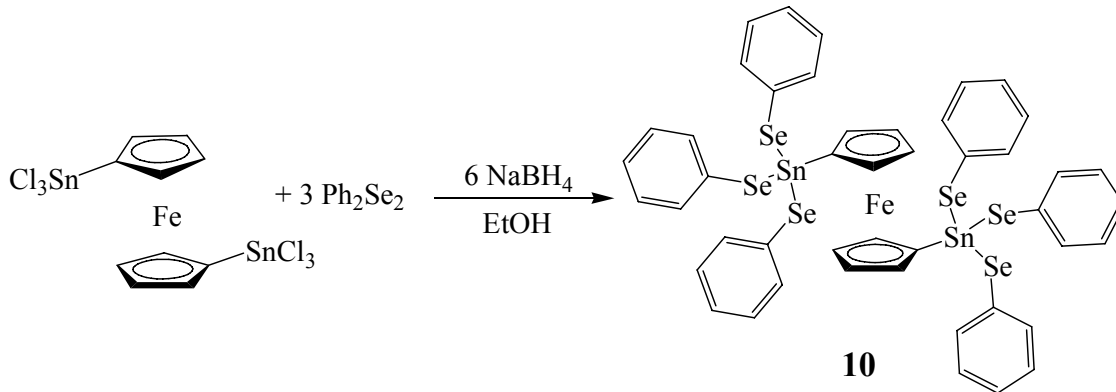
1,1'-Bis(trichlorostannyl)ferrocene (0.1 g, 0.16 mmol) was dissolved in 5 mL of degassed absolute ethanol and added to 5 mL of an ethanolic solution of NaSePh prepared from Ph_2Se_2 (0.147 g, 0.47 mmol) and $Na[BH_4]$ (0.04 g, 1.06 mmol) *in situ*. The mixture was stirred for 24 hours. The orange solid was isolated by filtration, washed with ethanol and *n*-hexane, and dried in vacuum. Crystals were obtained by slow evaporation of a dichloromethane/ *n*-hexane (1:1) mixture.

Molar Mass: 1357.82 g/mol   **Yield:** 0.085 g, 0.063 mmol, 40%.

^{1}H NMR: (400 MHz, $CDCl_3$) δ/ppm: 3.75 (s, 4H, ArH), 4.28 (s, 4H, ArH), 7.14-7.50 (m, 30H, ArH)

^{13}C NMR: (100 MHz, $CDCl_3$) δ/ppm: 70.30, 72.47, 74.16, (Cp) 124.23, 129.00, 131.53, 137.08 (Ar)

^{119}Sn NMR: ($CDCl_3$) δ/ppm: −49.27 (s)

4.3.12 Synthesis of 1,1'-Bis[tris(selenonaphthylato)stannyl]ferrocene (11)
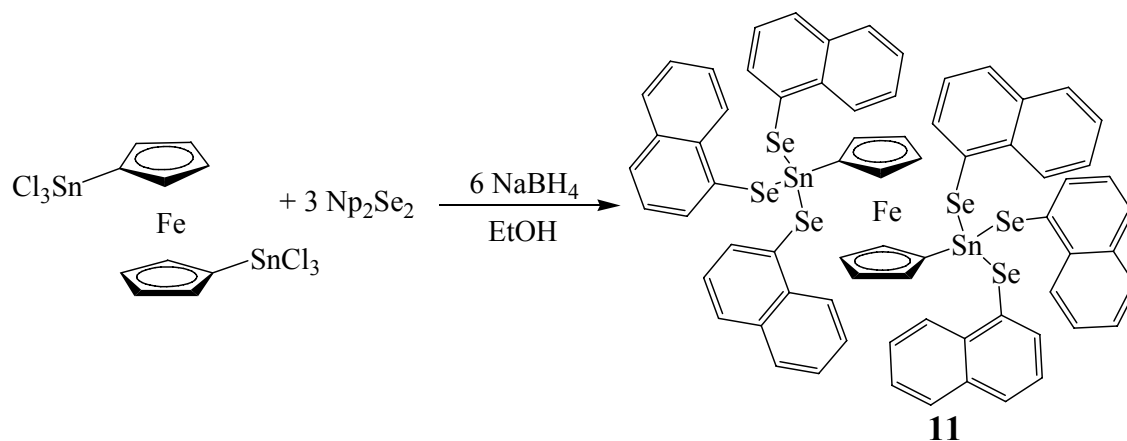
A solution of 1,1'-bis(trichlorostannyl)ferrocene (0.207 g, 0.33 mmol) in 5 mL of degassed ethanol was added to a solution of NaSeNp prepared from Np$_2$Se$_2$ (0.405 g, mmol) and NaBH$_4$ (0.1 g, 2.6 mmol) in 5 mL of ethanol. The mixture was stirred for 24 hours. The orange solid was isolated by filtration, washed with ethanol and *n*-hexane, and dried in vacuum.

Molar Mass: 1658.17 g/mol   **Yield:** 0.175 g, 0.1055 mmol, 32%

^{1}H NMR: (400 MHz, CDCl$_3$) δ/ppm: 3.23 (s, 4H, ArH), 3.83 (s, 4H, ArH), 7.1-7.76 (m, 42H, ArH).

^{13}C NMR: (100 MHz, CDCl$_3$) δ/ppm: 71.79, 73.57, 74.32, 124.78, 125.60, 126.19, 126.71, 128.50, 129.02, 129.39, 134.14, 136.15, 136.97(Ar).

^{119}Sn NMR: (CDCl$_3$) δ/ppm: −49.92 (s)

4.3.13 Synthesis of [Pd(SePh)(OOCCH₃)]₄ (12)

$(PhSe)_3–Bu–Sn(SePh)_3 + 2\ Pd(OAc)_2 \xrightarrow{\text{DCM}}$

12
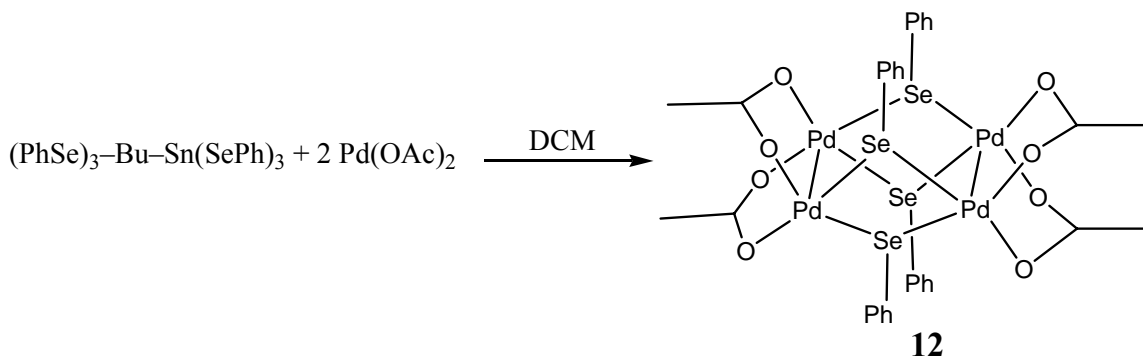
Pd(OAC)₂ (0.036g, 0.160 mmol) and bis[tris(selenophenolate)stannyl]butane (0.1g, 0.081 mmol) were dissolved separately in 5 mL of dry dichloromethane each. The Pd(OAC)₂ solution was slowly added to the bis[tris(selenophenolate)stannyl]butane solution, resulting in a red suspension. After two hours stirring, an insoluble solid was filtered off and the red solution was layered by *n*-hexane. Red crystals were obtained after one month.

Molar Mass: 1286.02 g/mol   **Yield:** 0.015 g, 0.011 mmol, 30%

¹H NMR: (400 MHz, CDCl₃, 25°C) δ/ppm: 2.16 (s, 12H, CH₃), 6.95-7.64 (m, 20H, Ph)

¹³C NMR: (100 MHz, CDCl₃, 25°C) δ/ppm: 31.32 (CH₃), 128.1, 129.6, 132.1, 137.4 (Ph), 207.41 (COO)

⁷⁷Se NMR: (CDCl₃) δ/ppm: −1487.37 (s)

4.3.14 Synthesis of [(Ph₃P)₃(SePh)₂Cu₂]·1.5THF (13·1.5THF)

1,4-Bis(trichlorostannyl)butane (0.05 g, 0.098 mmol) and [(Ph₃P)₃CuCl] (0.524 g, 0.5915 mmol) were suspended in 20 mL of dry THF. The mixture was cooled to –40 ℃ and PhSeSiMe₃ (0.6 mL, 2.37 mmol) was added dropwise to it. It was then allowed to warm up to room temperature. After stirring at room temperature for one hour, the solution was reduced to 5 m, and 2 mL of dry *n*-hexane was added to it. The mixture was placed at 6℃, and crystals of **13** were obtained after three days. Semiquantitative elemental analysis (EDX): $Cu_1Se_{1.07}P_{1.34}$ (calc.: $Cu_1Se_1P_{1.5}$).

Molar Mass: 1334.17 g/mol   **Yield:** 0.247 g, 0.43 mmol, 62.5%
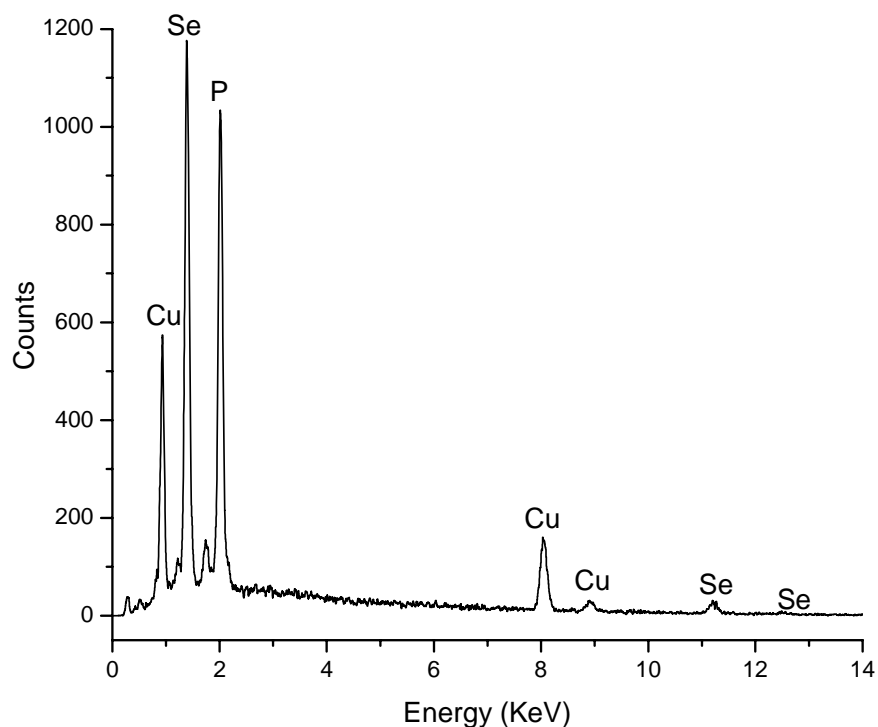
Figure 4.1 EDX spectrum of compound **13**·1.5THF

4.3.15 Synthesis of [(Ph₃PAg)₈(SePh)₁₂(μ₆-Se)Ag₆]·6THF (14·6THF)

1,4-Bis(trichlorostannyl)butane (0.05 g, 0.098 mmol) and [(Ph₃P)₃AgNO₃] (0.566 g, 0.5916 mmol) were suspended in 10 mL of dry THF. The mixture was cooled to –40 ºC and PhSeSiMe₃ (0.15 mL, 0.6322 mmol) was added dropwise to it. It was then allowed to warm up to room temperature slowly and stirred for two hours at room temperature. The clear yellow solution was stored at 6 ºC and crystals of **14** were obtained after two days. Semiquantitative elemental analysis (EDX): $Ag_{1.06}Se_{1.0}P_{0.66}$ (calc.: $Ag_{1.08}Se_{1.0}P_{0.61}$)

Molar Mass: 5992.64 g/mol   **Yield:** 0.165 g, 0.027 mmol, 65%
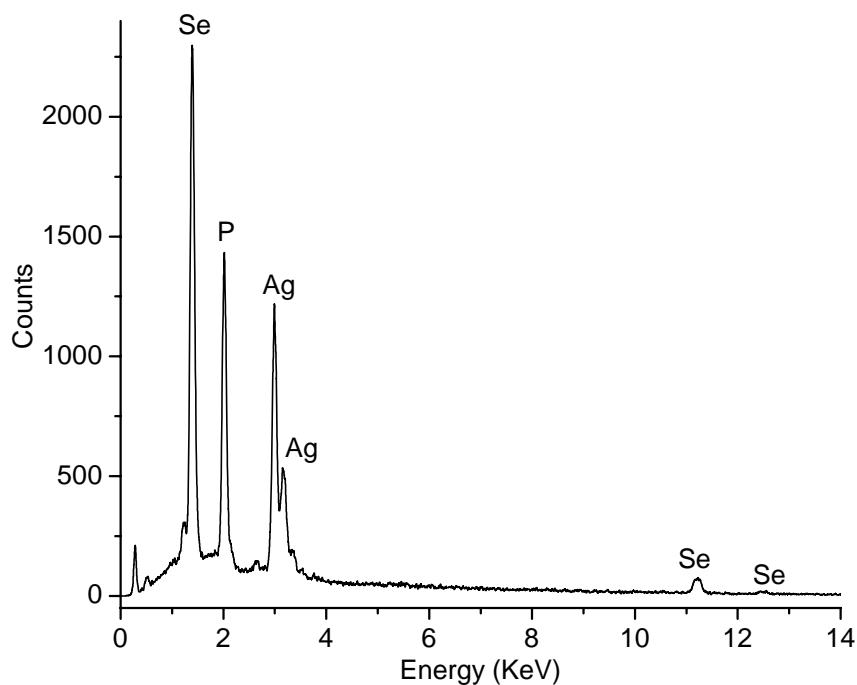
Figure 4.2 EDX spectrum of compound **14**·6THF

4.3.16 Synthesis of [(Ph₃PAg)₈(SePh)₁₂(μ₆-Se)₀.₅Ag₆][Ph₃SnCl₂]·6THF (15·6THF)

[(Ph₃P)₃AgNO₃] (0.248 g, 0.2529 mmol) and Ph₃SnCl (0.1 g, 0.2594 mmol) were suspended in 10 mL of dry THF. The solution was cooled to –40 ºC and PhSeSiMe₃ (0.06 mL, 0.2529 mmol) was added dropwise. The mixture was allowed to warm up to room temperature slowly. Crystals were obtained after one week upon layering 5 mL of the solution with 5 mL of *n*-hexane. Semiquantitative elemental analysis (EDX): $Ag_{14.02}Se_{12.73}P_{7.98}Sn_{1.0}Cl_{1.95}$ (calc.: $Ag_{14}Se_{12.5}P_8Sn_1Cl_2$).

Molar Mass: 6374.05 g/mol   **Yield:** 0.053 g, 0.008 mmol, 45%
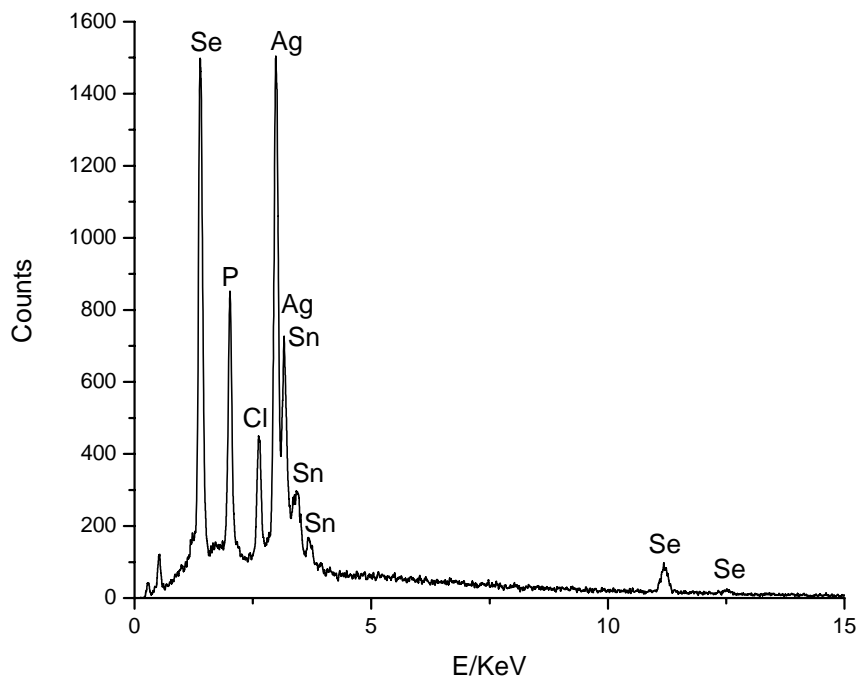
Figure 4.3 EDX spectrum of compound **15**·6THF

4.3.17 Synthesis of [(Ph₃PAg)₈(SePh)₁₂(μ₆-Se)₀.₅Ag₆][Cy₃SnCl₂] (16)

To a suspension of [(Ph$_3$P)$_3$AgNO$_3$] (0.252 g, 0.2634 mmol) and Cy$_3$SnCl (0.106 g, 0.2626 mmol) in 10 mL of dry THF, PhSeSiMe$_3$ (0.06 mL, 0.2529 mmol) was added dropwise at −70 ºC. The mixture was allowed to warm up to room temperature slowly. Crystals were obtained by layering 5 mL of THF solution by 5 mL of *n*-hexane. Semiquantitative elemental analysis (EDX): Ag$_{14.09}$Se$_{12.80}$P$_{8.63}$Sn$_{1.0}$Cl$_{1.80}$ (calc.: Ag$_{14}$Se$_{12.5}$P$_8$Sn$_1$Cl$_2$).

Molar Mass: 5941.43 g/mol   **Yield:** 0.04 g, 0.006 mmol, 35%
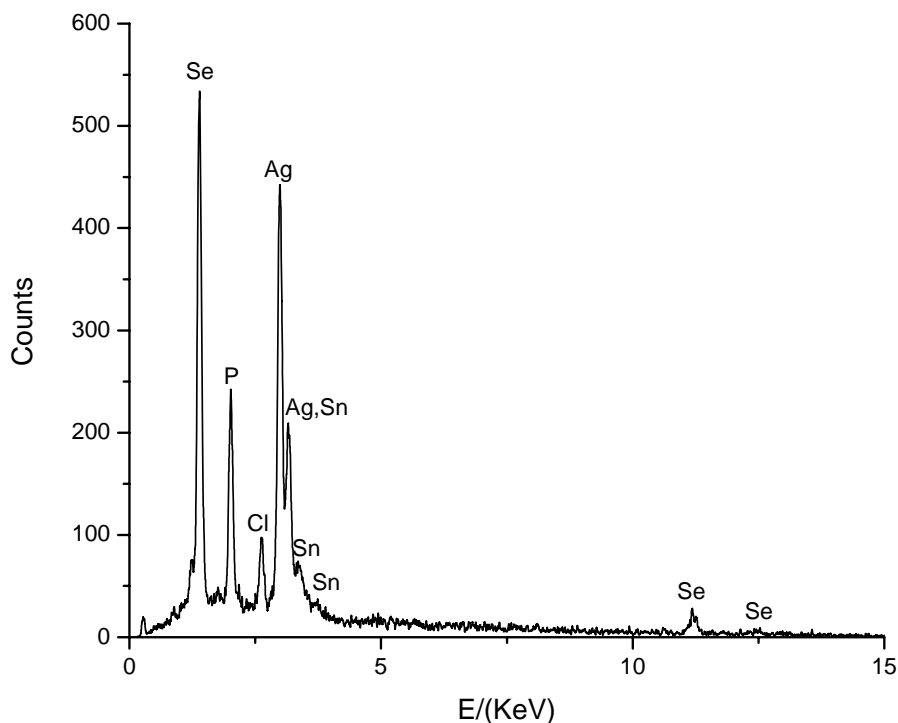
Figure 4.4 EDX spectrum of compound **16**

4.3.18 Synthesis of $_\infty^1$ [SnS$_2$·*en*] (17)

$$0.5 \text{ Cl}_3\text{Sn–Bu–SnCl}_3 + 2 \text{ S} + en \xrightarrow{\quad en,\ 180\ ^\circ\text{C}\quad} {}_\infty^1 [\text{SnS}_2\cdot en] + \text{byproduct}$$
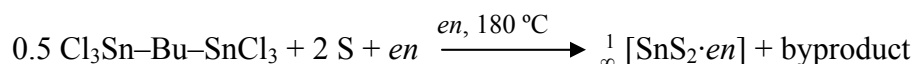
In a typical synthesis, a mixture of 1,4-bis(trichlorostannyl)butane (0.2 g, 0.395 mmol), S (0.038g, 1.187 mmol) and 10 mL of ethylenediamine (*en*) were sealed in a Teflon-lined steel autoclave and heated at 180 °C for 5 days. Colorless crystals of **17** were obtained. Semi quantitative elemental analysis (EDX): Sn$_1$S$_{1.88}$ (calc.: Sn$_1$S$_2$).

Molar Mass: 485.83 g/mol $\qquad\qquad$ **Yield:** 0.058 g, 0.12 mmol, 30%

Raman data/cm^{-1}: 3292.6 (vs), 3203.4 (vs), 3139.1 (s), 3092.5 (s), 2953.6 (m), 2932.6 (vs), 2898.5 (s), 2866.1 (s), 1573.7 (vs), 1450.7 (vs), 1317.9 (s), 1280.5 (m), 1065.6 (w), 1012.8 (m), 956.7 (w), 870.5 (vs), 637.5 (s), 515.3 (w), 431.5 (m), 336.5 (s), 305.6 (m), 249.3 (w), 212.5 (w), 159.0 (s), 127.5 (s), 111.5 (s).
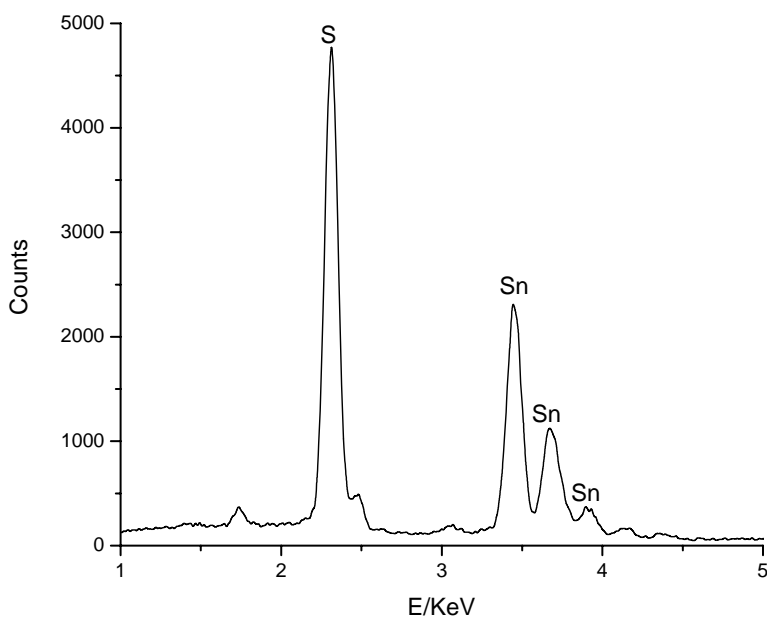
Figure 4.5 EDX spectrum of compound **17**

4.3.19 Synthesis of [enH]$_4$[Sn$_2$S$_6$]·*en* (18)

$$2 \text{ Sn} + 6 \text{ S} + 5 \text{ } en \xrightarrow{\text{ } en, \text{ } 180 \text{ }^\circ\text{C}} [en\text{H}]_4[\text{Sn}_2\text{S}_6]\cdot en + \text{byproduct}$$

In a typical synthesis for compound **2**, a mixture of Sn (0.4 g, 3.389 mmol), S (0.216g, 6.650 mmol) and 10 mL of ethylenediamine (*en*) were sealed in a Teflon-lined steel autoclave and heated at 180 °C for 5 days. Colorless crystals of **18** were obtained. Semiquantitative elemental analysis (EDX): Sn$_1$S$_{3.07}$ (calc.: Sn$_1$S$_3$).

Molar Mass: 734.29 g/mol   **Yield:** 0.80 g, 1.08 mmol, 65%

Raman data/cm^{-1}:   3337.0 (w), 3317.6 (w), 3276.5 (s), 3261.7 (s), 3160.2 (w), 2991.5 (w), 2949.3 (s), 2933.4 (s), 2920.8 (s), 2885.5 (m), 2867.2 (s), 2790.8 (w), 1625.7 (w), 1582.2 (m), 1541.1 (w), 1505.9 (w), 1449.1 (s), 1435.7 (m), 1407.0 (w), 1389.4 (w), 1357.5 (w), 1325.6 (m), 1272.9 (w), 1173.3 (m), 1137.2 (w), 1100.8 (m), 1082.9 (m), 1064.1 (s), 1021.7 (m), 970.4 (s), 924.8 (s), 833.2 (m), 779.7 (w), 680.1 (m), 644.1 (s), 367.4 (m), 339.7 (vs), 262.6 (m), 191.2 (w), 124.6 (w).
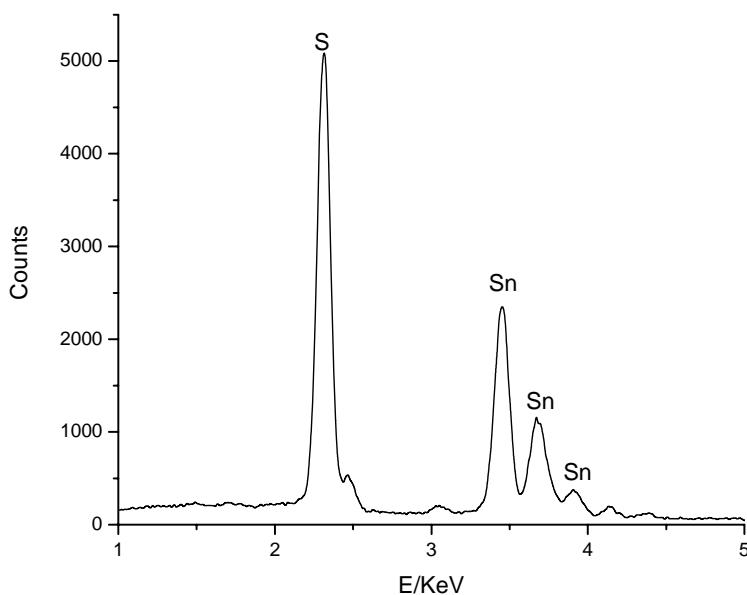
Figure 4.6 EDX spectrum of compound **18**

4.3.20 Synthesis of [(Ph$_3$PCu)$_6$\{*cyclo*-(CH$_2$)$_4$SnS$_2$\}$_6$Cu$_4$Sn] (19)

$$10\ [(Ph_3P)_3Cu^ICl] + 6\ Cl_3Sn^{IV}(CH_2)_4Sn^{IV}Cl_3 + 18\ Na_2S \cdot 9H_2O$$

MeOH

110 ºC

4 days

$$[(Ph_3PCu^I)_6\{(CH_2)Sn^{IV}S_2\}_6Cu^I_4Sn^{II}] + {}^6/_8\ S_8^0 + 5\ Sn^{II}Cl_2 + 36\ NaCl + 24\ PPh_3 + 162\ H_2O$$
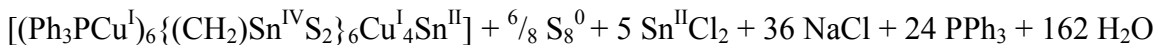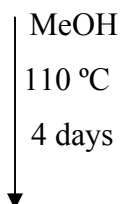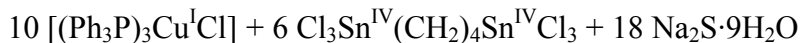
1,4-Bis(trichlorostannyl)butane (0.05 g, 0.098 mmol), [(PPh$_3$)$_3$CuCl] (0.524g, 0.5922 mmol) and Na$_2$S·9H$_2$O (0.142 g, 0.5922 mmol) were mixed in a glass ampoule (22 cm^3) under Ar. 1 mL of dry methanol was added and the tube was sealed. The mixture was heated to 110 ºC during 0.5 h, kept at 110°C for four days, and cooled down to room temperature during 1 hour. Orange-yellow crystals were obtained within a ring inside the glass wall at Δh = 6-9 mm from the bottom of the ampoule. Semi quantitative elemental analysis (EDX) of Cu:Sn:P:S: Cu$_{10.08}$Sn$_{7.51}$P$_{6.00}$S$_{12.42}$ (calc.: Cu$_{10}$Sn$_7$P$_{6.00}$S$_{12}$).

Molar Mass: 3761.56 g/mol   **Yield:** 0.014 mg, 0.0038 mmol, 23.3%
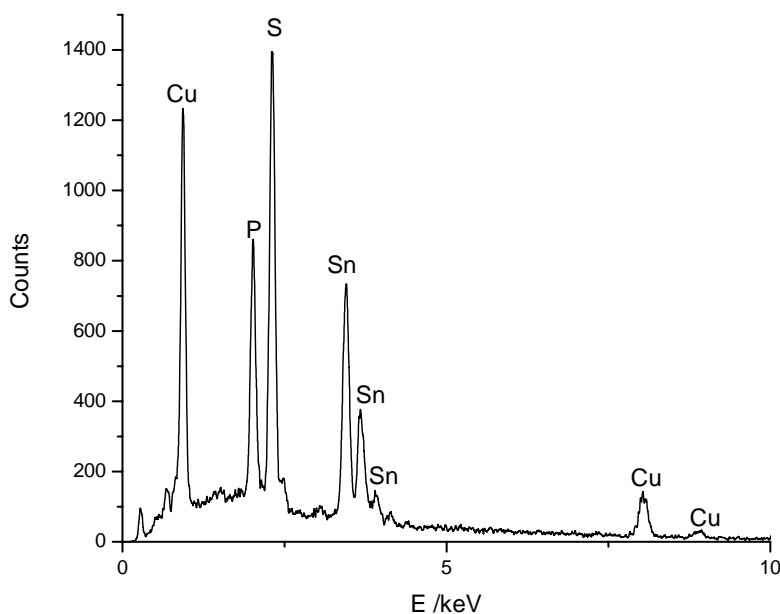
Figure 4.7 EDX spectrum of compound **19**

Chapter 5

Crystal data

5.1 Data collection and refinement

The crystal structure investigations were carried out via X-ray diffraction experiments at single crystals using an imaging plate detector system (IPDS 2 or 2T) of STOE. A sealed-tube anode with Mo-radiation and a graphite monochromator served as radiation source, so that the crystals were examined by Mo-Kα-radiation ($\lambda = 0.71073$ Å).

The crystal structure analysis was undertaken according to the following steps:

a) Determination of the cell constants of the compounds by using orientation-parameters up to 2000 reflexes which were collected several times with different angles Φ.

b) Determination of the reflex intensities by integration of the reflex profile.

c) Data-reduction: Scaling of the calculated F-value according to the corresponding reflexes; the reflex intensities were converted via application of Lorentz-factor and polarization correction.

d) Solution of the crystal structure by means of direct methods and ensuing difference Fourier syntheses using SHELXS-97 software [113].

e) Refinement of the crystal structures by optimization of the atomic parameters against F_o^2 (measurement) according to a full-matrix-least-squares method on F_o^2 by using the following function (equation 5.1):

$$\frac{1}{w} = \sigma^2 F_o^2 + (aP)^2 + bP \tag{5.1}$$

$$\text{where} \quad P = \frac{1}{3} Max\left(F_o^2, 0\right) + \frac{2}{3} F_c^2$$

The use of this combination of F_o^2 and F_c^2 was shown by Wilson (1976) to reduce statistical bias. The values for the parameters a and b were automatic determined and adjusted by application of the program SHELXL-97 [114].

The determined *R*-indices are defined as follows (equation 5.2):

$$R_1 = \frac{\sum \left\| F_o \right| - \left| F_c \right\|}{\sum \left\{ \left| F_o \right| \right\}} \qquad wR_2 = \sqrt{\frac{\sum \left[w \cdot \left(F_o^2 - F_c^2 \right)^2 \right]}{\sum \left[w \cdot \left(F_o^2 \right)^2 \right]}} \tag{5.2}$$

The *Goodness of Fit* is always based on F^2 (equation 5.3):

$$GooF = S = \sqrt{\frac{\sum \left[w(F_0^2 - F_c^2)^2 \right]}{(n - p)}} \tag{5.3}$$

where *n* is the number of reflections and *p* is the total number of parameters refined.

According to the theory formulated by Debye and Waller, the correction of the atomic form factor f_0 is performed by means of a temperature-dependent factor (equation 5.4):

$$f = f_0 \exp\left(-8\pi^2 U \frac{\sin \theta^2}{\lambda^2} \right) \tag{5.4}$$

The coefficient *U* of the temperature factor is calculated form the average displacement $\bar{u}$ of the atom, which is perpendicular to the layer according to the following equation:

$$U = \overline{u^2} \tag{5.5}$$

The isotropic displacement parameter *U* is multiplied by $8\pi^2$ to give the Debye-Waller-Faktor *B* (equation 6.6)

$$B = 8\pi^2 U \tag{5.6}$$

It is more realistic to allow the atoms in the crystal to perform anisotropic vibration. The anisotropic vibration of an atom is represented by an displacement ellipsoid. This is described by six components (U_{ij}) of a tensor in its spatial location. For B and the components U_{ij}, equation 5.7 is applicable.

$$T = -\ln \frac{f}{f_o} \qquad (5.7)$$

Using following connections:

$$T_{iso} = B \frac{\sin^2 \theta}{\lambda^2} \qquad (5.8)$$

$$T_{aniso} = 2\pi^2 (\sum_{i=1}^{3} \sum_{j=1}^{3} U_{ij} m_i m_j a_i^* a_j^*) \qquad (5.9)$$

The coefficient U_{eq} is determined from the coefficients U_{ij} according to equation 5.10:

$$U_{eq} = \frac{1}{3} (\sum_{i=1}^{3} \sum_{j=1}^{3} U_{ij} a_i^* a_j^* a_i a_j) \qquad (5.10)$$

with

m_i, m_j	Miller-Indices	$(m_1 = h, m_2 = k, m_3 = l)$
a_i, a_j	cell parameters	$(a_1 = a, a_2 = b, a_3 = c)$
a_i^*, a_j^*	reciprocal cell parameters	$(a_1^* = a^*, a_2^* = b^*, a_3^* = c^*)$

Atomic coordinates and the displacement parameters U_{eq} are given in the following tables. The H-atoms were kept riding on calculated positions with isotropic displacement parameters set to 1.2 U_{eq} of their bonding partners.

5.2 (PhS)$_3$Sn–(CH$_2$)$_4$–Sn(SPh)$_3$ (1)

Compound **1** crystallizes as colorless blocks from a DCM/*n*-hexane mixture.

Table 5.1 Crystal data and structure refinement for **1**

Empirical formula	C$_{40}$H$_{38}$S$_6$Sn$_2$
Formula weight /g·mol^{-1}	948.44
Crystal system	triclinic
Space group	$P\bar{1}$
a /Å	10.040(2)
b /Å	10.190(2)
c /Å	10.429(2)
α /°	111.47(3)
β /°	95.57(3)
γ /°	90.24(3)
V /Å^3	987.3(39
Z	1
ρ_{calc} /g·cm^{-3}	1.595
μ(Mo$_{K\alpha}$) /mm^{-1}	1.610
2Θ range /°	4-60
Reflections measured	12041
Independent reflections	5499
R(int)	0.0529
Indepedent reflections ($I > 2\sigma(I)$)	4627
Parameters	217
R_1 ($I > 2\sigma(I)$)	0.0255
wR_2 (all data)	0.0756
GooF (all data)	1.109
Max. peak/hole /e$^-$·10^{-6}pm^{-3}	1.114/-0.609

Table 5.2 Atomic coordinates and equivalent isotropic displacement parameters for **1**

Atom	x/a	y/b	z/c	$U_{eq/iso}$
Sn1	0.192063(16)	0.706004(19)	-0.09265(2)	0.02660(6)
S1	0.39919(7)	0.64672(9)	0.00536(8)	0.03628(16)
S2	0.22079(7)	0.93101(8)	-0.11715(8)	0.03539(15)
S3	0.18083(9)	0.56556(9)	-0.33610(8)	0.04260(17)
C1	0.0216(3)	0.6967(3)	0.0142(3)	0.0364(6)
C2	-0.0446(2)	0.5506(3)	-0.0206(3)	0.0323(6)
C11	0.3736(2)	0.6979(3)	0.1838(3)	0.0296(5)
C12	0.3773(3)	0.8394(3)	0.2695(3)	0.0367(6)
C13	0.3636(3)	0.8764(4)	0.4094(4)	0.0465(7)
C14	0.3490(3)	0.7730(4)	0.4645(4)	0.0480(8)
C15	0.3468(3)	0.6321(4)	0.3787(3)	0.0432(7)
C16	0.3584(3)	0.5941(3)	0.2390(3)	0.0332(6)
C21	0.2548(3)	1.0479(3)	0.0589(3)	0.0325(6)
C22	0.3750(3)	1.1278(3)	0.1001(3)	0.0372(6)
C23	0.4035(4)	1.2218(3)	0.2345(4)	0.0473(8)
C24	0.3135(4)	1.2372(4)	0.3311(4)	0.0520(8)
C25	0.1926(4)	1.1584(4)	0.2900(4)	0.0514(8)
C26	0.1629(3)	1.0648(3)	0.1549(4)	0.0409(7)
C31	0.1567(3)	0.3932(3)	-0.3328(3)	0.0317(5)
C32	0.0309(3)	0.3248(3)	-0.3760(3)	0.0354(6)
C33	0.0124(3)	0.1891(3)	-0.3780(3)	0.0400(6)
C34	0.1174(3)	0.1217(3)	-0.3365(3)	0.0417(7)
C35	0.3153	0.2424(3)	0.1900(3)	-0.2930(3)
C36	0.2626(3)	0.3248(3)	-0.2924(3)	0.0372(6)

Table 5.3 Anisotropic displacement parameters for **1**

Atom	U_{11}	U_{22}	U_{33}	U_{23}	U_{13}	U_{12}
Sn1	0.02497(8)	0.03107(9)	0.03080(10)	0.01885(7)	0.00625(6)	0.00061(6)
S1	0.0289(3)	0.0517(4)	0.0382(4)	0.0267(3)	0.0100(3)	0.0105(3)
S2	0.0372(3)	0.0373(3)	0.0414(4)	0.0264(3)	0.0031(3)	-0.0025(3)
S3	0.0611(5)	0.0428(4)	0.0303(4)	0.0209(3)	0.0057(3)	-0.0022(3)
C1	0.0342(13)	0.0364(14)	0.0487(18)	0.0239(14)	0.0191(12)	0.0055(11)
C2	0.0252(11)	0.0397(14)	0.0408(16)	0.0236(13)	0.0095(10)	0.0014(10)
C11	0.0207(10)	0.0378(14)	0.0348(14)	0.0192(12)	0.0011(9)	0.0016(9)
C12	0.0296(12)	0.0377(14)	0.0465(18)	0.0205(14)	0.0014(11)	-0.0003(11)
C13	0.0384(15)	0.0467(18)	0.0449(19)	0.0069(15)	-0.0002(13)	0.0014(13)
C14	0.0390(15)	0.072(2)	0.0338(16)	0.0214(17)	0.0010(12)	0.0057(15)
C15	0.0399(15)	0.060(2)	0.0414(18)	0.0316(16)	0.0059(13)	0.0032(14)

C16	0.0295(11)	0.0383(14)	0.0384(15)	0.0213(13)	0.0055(11)	0.0021(10)
C21	0.0298(11)	0.0310(13)	0.0463(17)	0.0244(13)	0.0082(11)	0.0058(10)
C22	0.0360(13)	0.0325(13)	0.0479(18)	0.0186(13)	0.0122(12)	-0.0005(11)
C23	0.0516(17)	0.0382(16)	0.052(2)	0.0164(15)	0.0081(15)	-0.0073(14)
C24	0.072(2)	0.0377(16)	0.047(2)	0.0132(15)	0.0179(17)	0.0016(15)
C25	0.060(2)	0.0463(18)	0.056(2)	0.0225(17)	0.0313(17)	0.0126(15)
C26	0.0339(13)	0.0419(16)	0.056(2)	0.0265(16)	0.0164(13)	0.0067(12)
C31	0.0352(12)	0.0363(14)	0.0257(13)	0.0134(11)	0.0055(10)	0.0013(11)
C32	0.0317(12)	0.0465(16)	0.0295(14)	0.0159(13)	0.0027(10)	0.0035(11)
C33	0.0365(14)	0.0479(17)	0.0341(16)	0.0138(14)	0.0014(12)	-0.0070(12)
C34	0.0520(17)	0.0377(15)	0.0367(16)	0.0152(14)	0.0050(13)	-0.0017(13)
C35	0.0403(14)	0.0433(16)	0.0405(17)	0.0168(14)	0.0019(12)	0.0087(12)
C36	0.0292(12)	0.0441(16)	0.0374(16)	0.0142(13)	0.0037(11)	0.0006(11)

5.3 (PhS)$_3$Sn–CH$_2$–(C$_6$H$_4$)$_2$–CH$_2$–Sn(SPh)$_3$ (3)

Compound **3** crystallizes as colorless blocks from a DCM/*n*-hexane mixture.

Table 5.3 Crystal data and structure refinement for **3**

Empirical formula	C$_{50}$H$_{42}$S$_6$Sn$_2$
Formula weight /g·mol^{-1}	1072.58
Crystal system	monoclinic
Space group	$P2_1/c$
a /Å	12.038(2)
b /Å	16.771(3)
c /Å	11.896(2)
β /°	106.73(3)
V /Å^3	2299.9(8)
Z	2
ρ_{calc} /g·cm^{-3}	1.549
μ(Mo$_{K\alpha}$) /mm^{-1}	1.392
2Θ range /°	4-52
Reflections measured	16075
Independent reflections	4476
R(int)	0.0472
Independent reflections ($I > 2\sigma(I)$)	3479
Parameters	262
R_1 ($I > 2\sigma(I)$)	0.0322
wR_2 (all data)	0.0744
GooF (all data)	0.929
Max. peak/hole /e$^-$·10^{-6}pm^{-3}	0.702/−1.158

Table 5.4 Atomic coordinates and equivalent isotropic displacement parameters for **3**

Atom	x/a	y/b	z/c	Ueq/iso
Sn1	0.82144(2)	0.107560(13)	0.471292(19)	0.03351(8)
S1	0.69770(8)	-0.00883(5)	0.45118(8)	0.03760(19)
S2	1.01269(8)	0.07913(5)	0.60015(8)	0.0380(2)
S3	0.74714(9)	0.21267(6)	0.56637(8)	0.0447(2)
C1	0.8313(3)	0.1387(2)	0.2968(3)	0.0385(8)
C2	0.7343(3)	0.0982(2)	0.2082(3)	0.0369(7)
C3	0.7486(4)	0.0242(2)	0.1631(3)	0.0481(9)
C4	0.6579(3)	-0.0140(2)	0.0841(3)	0.0470(9)
C5	0.5480(3)	0.01995(19)	0.0438(3)	0.0320(7)
C6	0.5349(3)	0.0950(2)	0.0892(3)	0.0400(8)
C7	0.6253(3)	0.1324(2)	0.1701(3)	0.0404(8)
C11	0.7321(3)	-0.03075(19)	0.6043(3)	0.0344(7)
C12	0.8308(3)	-0.0755(2)	0.6591(3)	0.0385(8)
C13	0.8592(3)	-0.0912(2)	0.7784(3)	0.0433(9)
C14	0.7892(3)	-0.0631(2)	0.8441(3)	0.0454(9)
C15	0.6908(3)	-0.0196(2)	0.7899(3)	0.0418(8)
C16	0.6608(3)	-0.0040(2)	0.6700(3)	0.0374(8)
C21	1.0197(3)	0.1313(2)	0.7329(3)	0.0347(7)
C22	0.9417(3)	0.1182(2)	0.7973(3)	0.0396(8)
C23	0.9573(3)	0.1572(2)	0.9036(3)	0.0463(9)
C24	1.0497(4)	0.2080(2)	0.9465(3)	0.0501(10)
C25	1.1287(4)	0.2196(2)	0.8846(4)	0.0580(11)
C26	1.1128(4)	0.1821(2)	0.7773(3)	0.0508(10)
C31	0.6232(3)	0.2373(2)	0.4462(3)	0.0378(8)
C32	0.6257(3)	0.3046(2)	0.3784(3)	0.0447(8)
C33	0.5282(3)	0.3264(2)	0.2887(3)	0.0469(9)
C34	0.4284(3)	0.2815(2)	0.2658(4)	0.0462(9)
C35	0.4255(3)	0.2145(2)	0.3331(4)	0.0469(9)
C36	0.5220(3)	0.1932(2)	0.4236(3)	0.0433(9)

Table 5.5 Anisotropic displacement parameters for **3**

Atom	U_{11}	U_{22}	U_{33}	U_{23}	U_{13}	U_{12}
Sn1	0.03514(13)	0.03659(12)	0.02836(12)	0.00103(10)	0.00845(9)	0.00048(11)
S1	0.0363(5)	0.0403(4)	0.0357(4)	-0.0032(4)	0.0095(4)	-0.0026(4)
S2	0.0329(5)	0.0472(5)	0.0334(4)	0.0011(4)	0.0089(4)	0.0033(4)
S3	0.0483(6)	0.0439(5)	0.0373(5)	-0.0064(4)	0.0049(4)	0.0096(4)
C1	0.0395(19)	0.0479(19)	0.0264(16)	0.0052(15)	0.0067(15)	-0.0042(16)
C2	0.0397(19)	0.0431(19)	0.0267(15)	0.0038(14)	0.0077(14)	-0.0042(16)
C3	0.045(2)	0.057(2)	0.0351(19)	-0.0054(17)	-0.0008(17)	0.0150(18)
C4	0.050(2)	0.048(2)	0.0356(19)	-0.0066(16)	0.0012(18)	0.0118(18)
C5	0.0341(18)	0.0363(17)	0.0273(15)	0.0035(13)	0.0114(14)	-0.0011(14)
C6	0.0330(18)	0.0382(19)	0.050(2)	-0.0010(16)	0.0147(16)	-0.0013(15)
C7	0.043(2)	0.0352(17)	0.046(2)	-0.0024(15)	0.0176(17)	-0.0047(15)
C11	0.0352(19)	0.0313(16)	0.0390(18)	0.0000(14)	0.0144(16)	-0.0053(14)
C12	0.0355(19)	0.0389(17)	0.046(2)	0.0041(15)	0.0197(17)	0.0020(15)
C13	0.040(2)	0.043(2)	0.049(2)	0.0134(16)	0.0165(17)	0.0094(16)
C14	0.048(2)	0.048(2)	0.043(2)	0.0122(17)	0.0180(18)	0.0028(18)
C15	0.045(2)	0.0428(19)	0.044(2)	0.0060(16)	0.0227(18)	0.0025(16)
C16	0.0346(19)	0.0356(17)	0.0450(19)	0.0049(15)	0.0161(16)	0.0017(14)
C21	0.0338(18)	0.0353(17)	0.0328(17)	0.0051(13)	0.0062(15)	0.0024(14)
C22	0.0350(18)	0.0428(19)	0.0386(18)	-0.0029(15)	0.0070(15)	0.0026(15)
C23	0.044(2)	0.057(2)	0.0362(19)	-0.0017(17)	0.0097(17)	0.0153(18)
C24	0.063(3)	0.039(2)	0.0369(19)	-0.0028(16)	-0.0027(19)	0.0112(19)
C25	0.069(3)	0.045(2)	0.045(2)	0.0066(18)	-0.006(2)	-0.015(2)
C26	0.051(2)	0.052(2)	0.043(2)	0.0079(18)	0.0053(19)	-0.0129(19)
C31	0.039(2)	0.0364(17)	0.0364(18)	-0.0009(14)	0.0090(16)	0.0054(15)

5.4 (NpS)₃Sn–(CH₂)₄–Sn(SNp)₃ (4)

Compound **4** crystallizes as colorless blocks from a DCM/*n*-hexane mixture.

Table 5.6 Crystal data and structure refinement for **4**

Empirical formula	$C_{64}H_{50}S_6Sn_2$
Formula weight /g·mol^{-1}	1248.78
Crystal system	trigonal
Space group	$R3$
a /Å	13.5899 (19)
b /Å	13.5899 (19)
c /Å	24.876(5)
V /Å^3	3978.7(11)
Z	3
ρ_{calc} /g·cm^{-3}	1.564
$\mu(Mo_{K\alpha})$ /mm^{-1}	1.220
2Θ range /°	4-58
Reflections measured	12898
Independent reflections	4790
R(int)	0.0482
Ind. reflections ($I > 2\sigma(I)$)	2686
Parameters	230
R_1 ($I > 2\sigma(I)$)	0.0556
wR_2 (all data)	0.1604
GooF (all data)	1.011
Max. peak/hole /e$^-$·10^{-6}pm^{-3}	1.566/–2.023

It was refined as a partial racemic twin with a batch scale factor of 0.43(9). The structure shows disorder of carbon atoms of the bridging butyl residue.

Table 5.7 Atomic coordinates and equivalent isotropic displacement parameters for **4**

Atom	x/a	y/b	z/c	$U_{eq/iso}$
Sn1	0.0000	0.0000	0.81863(3)	0.0790(6)
Sn2	0.0000	0.0000	1.11519(3)	0.0794(6)
S3	-0.1496(4)	-0.1850(4)	0.78418(17)	0.0731(11)
S2	0.0340(4)	-0.1426(3)	1.14710(16)	0.0720(11)
C5	0.0074(9)	-0.1471(9)	1.2565(5)	0.042(2)
C7	-0.2825(10)	-0.1022(10)	0.6319(6)	0.047(3)
C8	-0.1983(9)	-0.1374(9)	0.6283(5)	0.044(3)
C9	-0.0587(9)	-0.1971(10)	1.3048(6)	0.047(3)
C10	-0.3091(10)	-0.0806(10)	0.6848(6)	0.058(3)
C12	-0.2642(12)	-0.1036(11)	0.7303(6)	0.058(3)
C13	-0.2388(13)	-0.3153(11)	1.3516(6)	0.061(3)
C14	-0.1736(11)	-0.2752(9)	1.3024(6)	0.044(3)
C15	-0.0085(13)	-0.1653(11)	1.3548(6)	0.060(4)
C16	-0.1955(14)	-0.1416(13)	0.7259(6)	0.072(4)
C17	-0.1817(12)	-0.2805(10)	1.3999(5)	0.054(3)
C18	-0.1598(11)	-0.1511(10)	0.5759(5)	0.048(3)
C19	-0.3251(9)	-0.0847(9)	0.5848(6)	0.043(3)
C20	-0.2263(8)	-0.3184(10)	1.2524(6)	0.046(3)
C21	-0.2883(11)	-0.0918(11)	0.5369(7)	0.061(3)
C22	-0.0453(7)	-0.1884(8)	1.2086(5)	0.037(2)
C23	-0.0697(12)	-0.2077(10)	1.4024(5)	0.057(3)
C24	-0.1686(9)	-0.2770(10)	1.2071(6)	0.049(3)
C25	-0.2005(12)	-0.1253(11)	0.5327(6)	0.058(3)
C26	-0.1644(9)	-0.1625(9)	0.6759(6)	0.052(3)
C101	0.0383(19)	0.049(3)	0.9024(5)	0.064(4)
C102	-0.0532(15)	0.008(2)	0.9446(6)	0.064(4)
C103	-0.005(2)	0.0432(17)	1.0023(5)	0.064(4)
C104	-0.006(3)	-0.056(2)	1.0319(5)	0.064(4)

Table 5.8 Anisotropic displacement parameters for **4**

Atom	U_{11}	U_{22}	U_{33}	U_{23}	U_{13}	U_{12}
Sn1	0.1044(9)	0.1044(9)	0.0280(9)	0.000	0.000	0.0522(5)
Sn2	0.1052(9)	0.1052(9)	0.0276(8)	0.000	0.000	0.0526(5)
S003	0.091(3)	0.073(2)	0.070(2)	0.0302(17)	0.0297(19)	0.051(2)
S2	0.096(3)	0.0567(18)	0.059(2)	0.0089(14)	0.0311(18)	0.0350(18)
C005	0.038(5)	0.029(4)	0.047(5)	-0.015(3)	0.004(4)	0.008(4)
C007	0.045(6)	0.034(5)	0.058(8)	0.003(5)	0.008(5)	0.017(5)
C008	0.030(5)	0.029(5)	0.055(7)	0.010(4)	-0.005(4)	0.002(4)
C009	0.036(5)	0.042(6)	0.060(8)	-0.017(5)	-0.027(5)	0.017(5)
C010	0.035(5)	0.054(6)	0.069(8)	-0.002(5)	0.024(5)	0.011(4)
C012	0.060(7)	0.037(6)	0.049(6)	0.000(4)	0.012(5)	0.005(5)
C013	0.076(8)	0.051(7)	0.064(8)	0.020(6)	0.015(6)	0.037(6)
C014	0.050(6)	0.021(4)	0.061(8)	0.001(4)	0.005(5)	0.019(4)
C015	0.066(8)	0.036(6)	0.070(9)	0.006(5)	-0.007(6)	0.020(6)
C016	0.095(10)	0.050(7)	0.050(8)	0.008(6)	0.011(7)	0.021(7)
C017	0.087(9)	0.046(6)	0.041(5)	0.002(4)	0.009(5)	0.043(6)
C018	0.060(7)	0.037(5)	0.050(6)	0.002(4)	0.020(5)	0.026(5)
C019	0.035(5)	0.028(4)	0.070(7)	0.003(4)	0.011(4)	0.019(4)
C020	0.020(4)	0.054(6)	0.073(7)	-0.002(5)	0.001(4)	0.025(4)
C021	0.061(7)	0.051(6)	0.076(8)	-0.026(5)	-0.026(6)	0.031(6)
C022	0.020(4)	0.028(4)	0.056(7)	-0.016(4)	0.001(4)	0.007(3)
C023	0.089(9)	0.039(6)	0.049(7)	-0.001(4)	-0.026(6)	0.037(6)
C024	0.032(5)	0.043(5)	0.058(7)	-0.024(4)	-0.008(4)	0.008(4)
C025	0.073(8)	0.051(6)	0.057(8)	0.008(5)	0.010(6)	0.037(6)
C026	0.040(5)	0.022(4)	0.082(8)	-0.001(4)	0.001(5)	0.007(4)
C101	0.084(10)	0.098(10)	0.024(4)	-0.013(4)	-0.028(6)	0.055(9)
C104	0.084(10)	0.098(10)	0.024(4)	-0.013(4)	-0.028(6)	0.055(9)
C102	0.084(10)	0.098(10)	0.024(4)	-0.013(4)	-0.028(6)	0.055(9)
C103	0.084(10)	0.098(10)	0.024(4)	-0.013(4)	-0.028(6)	0.055(9

5.5 (NpS)$_3$Sn–CH$_2$–(C$_6$H$_4$)–CH$_2$–Sn(SNp)$_3$ (5)

Compound **5** crystallizes as colorless blocks from a DCM/*n*-hexane mixture.

Table 5.9 Crystal data and structure refinement for **5**

Empirical formula	C$_{68}$H$_{50}$S$_6$Sn$_2$
Formula weight /g·mol^{-1}	1296.82
Crystal system	monoclinic
Space group	*P*2$_1$/*n*
a /Å	13.257(5)
b /Å	13.023(5)
c /Å	16.256(7)
β /°	91.02(3)
V /Å^3	2806.1(19)
Z	2
ρ$_{calc}$ /g·cm^{-3}	1.535
μ(Mo$_{K\alpha}$) /mm^{-1}	1.156
2Θ range /°	4-52
Reflections measured	38626
Independent reflections	5459
R(int)	0.1090
Indepedent reflections (I > 2σ(I))	4372
Parameters	343
R$_1$ (I > 2σ(I))	0.0340
wR$_2$ (all data)	0.0845
GooF (all data)	0.983
Max. peak/hole /e$^-$·10^{-6}pm^{-3}	0.841/–0.989

Table 5.10 Atomic coordinates and equivalent isotropic displacement parameters for **5**

Atom	x/a	y/b	z/c	$U_{eq/iso}$
Sn1	0.805730(15)	0.012167(15)	0.084379(13)	0.03677(8)
S1	0.91408(6)	0.06078(6)	0.19967(5)	0.03862(18)
S2	0.79887(7)	-0.17158(6)	0.10683(6)	0.0458(2)
S3	0.89072(7)	0.04422(7)	-0.04309(5)	0.0456(2)
C1	0.6636(2)	0.0932(3)	0.0945(2)	0.0437(8)
C2	0.5792(2)	0.0449(3)	0.0456(2)	0.0404(7)
C3	0.5587(2)	0.0755(2)	-0.0350(2)	0.0426(7)
C4	0.4806(2)	0.0313(3)	-0.0800(2)	0.0423(7)
C11	0.9343(2)	0.1912(2)	0.1685(2)	0.0372(7)
C12	1.0217(2)	0.2156(2)	0.1229(2)	0.0387(7)
C13	1.0416(2)	0.3151(2)	0.1028(2)	0.0403(7)
C14	0.9761(2)	0.3956(2)	0.1252(2)	0.0395(7)
C15	0.9936(3)	0.5001(2)	0.1034(2)	0.0474(8)
C16	0.9264(3)	0.5753(3)	0.1227(2)	0.0502(9)
C17	0.8400(3)	0.5513(3)	0.1665(2)	0.0504(9)
C18	0.8206(3)	0.4521(3)	0.1901(2)	0.0461(8)
C19	0.8881(2)	0.3719(2)	0.16914(19)	0.0385(7)
C20	0.8690(2)	0.2679(2)	0.1906(2)	0.0388(7)
C21	0.6968(3)	-0.2154(3)	0.0433(2)	0.0474(8)
C22	0.6244(3)	-0.2823(3)	0.0799(2)	0.0513(9)
C23	0.5469(3)	-0.3221(3)	0.0338(2)	0.0524(9)
C24	0.5379(3)	-0.2968(2)	-0.0501(2)	0.0448(8)
C25	0.4556(3)	-0.3404(3)	-0.1010(3)	0.0577(10)
C26	0.4485(3)	-0.3157(3)	-0.1824(3)	0.0560(10)
C27	0.5195(3)	-0.2495(3)	-0.2161(3)	0.0583(10)
C28	0.5978(3)	-0.2066(3)	-0.1702(2)	0.0561(10)
C29	0.6063(3)	-0.2312(3)	-0.0879(2)	0.0482(8)
C30	0.6891(3)	-0.1914(3)	-0.0365(2)	0.0496(9)
C31	0.8190(2)	0.1498(2)	-0.0836(2)	0.0395(7)
C32	0.7677(3)	0.1362(3)	-0.1596(2)	0.0427(7)
C33	0.7155(2)	0.2167(2)	-0.1948(2)	0.0413(7)
C34	0.7122(2)	0.3139(2)	-0.1561(2)	0.0380(7)
C35	0.6610(2)	0.3993(3)	-0.1911(2)	0.0427(7)
C36	0.6598(2)	0.4920(3)	-0.1523(2)	0.0449(8)
C37	0.7097(2)	0.5041(3)	-0.0753(2)	0.0450(8)
C38	0.7591(2)	0.4239(2)	-0.0396(2)	0.0422(7)
C39	0.7633(2)	0.3271(2)	-0.0791(2)	0.0379(7)
C40	0.8176(2)	0.2430(2)	-0.0447(2)	0.0402(7)

Table 5.11 Anisotropic displacement parameters for **5**

Atom	U_{11}	U_{22}	U_{33}	U_{23}	U_{13}	U_{12}
Sn1	0.03679(12)	0.03350(13)	0.03983(14)	-0.00213(9)	-0.00473(8)	0.00359(8)
S1	0.0415(4)	0.0351(4)	0.0391(4)	0.0013(3)	-0.0066(3)	-0.0018(3)
S2	0.0498(5)	0.0339(4)	0.0534(5)	-0.0032(3)	-0.0082(4)	-0.0015(3)
S3	0.0507(5)	0.0438(4)	0.0425(5)	0.0021(4)	0.0020(4)	0.0155(4)
C1	0.0372(16)	0.0442(18)	0.050(2)	-0.0049(15)	-0.0008(14)	0.0099(13)
C2	0.0346(15)	0.0424(17)	0.0442(19)	-0.0005(14)	-0.0017(13)	0.0085(13)
C3	0.0371(16)	0.0436(18)	0.047(2)	0.0034(14)	0.0027(14)	0.0066(13)
C4	0.0396(16)	0.0456(18)	0.0418(18)	0.0053(14)	0.0007(14)	0.0091(14)
C11	0.0391(16)	0.0343(16)	0.0378(18)	-0.0011(12)	-0.0082(13)	-0.0019(12)
C12	0.0367(16)	0.0387(17)	0.0405(18)	-0.0027(13)	-0.0028(13)	0.0016(12)
C13	0.0389(16)	0.0419(17)	0.0402(19)	0.0011(13)	-0.0016(14)	-0.0001(13)
C14	0.0449(18)	0.0374(16)	0.0361(18)	-0.0007(13)	-0.0028(14)	-0.0032(13)
C15	0.0540(19)	0.0409(18)	0.047(2)	0.0037(14)	-0.0004(16)	-0.0044(15)
C16	0.068(2)	0.0341(18)	0.048(2)	0.0016(14)	-0.0033(18)	0.0011(15)
C17	0.067(2)	0.0381(18)	0.046(2)	-0.0038(15)	-0.0036(17)	0.0108(16)
C18	0.053(2)	0.0444(18)	0.0413(19)	-0.0031(15)	0.0008(15)	0.0049(15)
C19	0.0442(17)	0.0366(16)	0.0345(17)	-0.0033(13)	-0.0052(14)	0.0035(13)
C20	0.0402(16)	0.0395(17)	0.0364(18)	-0.0022(13)	-0.0020(14)	-0.0022(13)
C21	0.0493(19)	0.0423(18)	0.050(2)	-0.0103(15)	-0.0078(16)	0.0045(14)
C22	0.056(2)	0.0440(19)	0.054(2)	-0.0027(16)	-0.0010(17)	-0.0021(16)
C23	0.054(2)	0.046(2)	0.058(2)	-0.0038(16)	0.0043(18)	-0.0032(16)
C24	0.0500(19)	0.0420(18)	0.042(2)	-0.0046(14)	0.0011(15)	0.0122(14)
C25	0.051(2)	0.054(2)	0.068(3)	-0.0103(19)	-0.0043(19)	0.0128(17)
C26	0.053(2)	0.059(2)	0.055(2)	-0.0184(18)	-0.0159(18)	0.0203(18)
C27	0.056(2)	0.055(2)	0.063(3)	-0.0163(19)	-0.0159(19)	0.0158(18)
C28	0.061(2)	0.051(2)	0.057(2)	-0.0059(17)	-0.0031(19)	0.0157(17)
C29	0.055(2)	0.0372(18)	0.052(2)	-0.0007(15)	0.0070(17)	0.0088(15)
C30	0.0461(19)	0.0402(18)	0.063(3)	-0.0045(16)	0.0028(17)	0.0044(14)

5.6 PhSeCl₂Sn–(CH₂)₄–SnCl₂SePh (6)

Compound **6** crystallizes as colorless blocks from a DCM/*n*-hexane mixture.

Table 5.12 Crystal data and structure refinement for **6**

Empirical formula	$C_{16}H_{18}Se_6Sn_2$
Formula weight /g·mol^{-1}	921.49
Crystal system	monoclinic
Space group	$P2_1/c$
a /Å	11.386(2)
b /Å	8.4160(17)
c /Å	11.789(2)
β /°	94.69(3)
V /Å^3	1125.9(4)
Z	2
ρ_{calc} /g·cm^{-3}	2.205
$\mu(Mo_{K\alpha})$ /mm^{-1}	5.924
2Θ range /°	4-45
Reflections measured	7527
Independent reflections	1463
R(int)	0.0672
Indepedent reflections $(I > 2\sigma(I))$	1407
Parameters	109
R_1 $(I > 2\sigma(I))$	0.0235
wR_2 (all data)	0.0574
GooF (all data)	1.151
Max. peak/hole /e$^-$·10^{-6}pm^{-3}	0.637/–789

Table 5.13 Atomic coordinates and equivalent isotropic displacement parameters for **6**

Atom	x/a	y/b	z/c	$U_{eq/iso}$
Sn1	0.17795(2)	1.22374(3)	0.95081(2)	0.02594(14)
Se1	0.35253(4)	1.04782(5)	0.98856(3)	0.03598(16)
Cl1	0.02836(9)	1.07345(11)	0.85345(8)	0.0328(2)
Cl2	0.22995(9)	1.40257(11)	0.80964(8)	0.0337(2)
C1	0.1102(3)	1.3571(5)	1.0840(3)	0.0295(9)
C2	0.0536(3)	1.5117(5)	1.0418(3)	0.0281(8)
C11	0.3547(3)	0.9809(5)	0.8314(3)	0.0300(9)
C12	0.4232(4)	1.0640(5)	0.7596(4)	0.0370(10)
C13	0.4276(4)	1.0128(5)	0.6481(4)	0.0388(10)
C14	0.3641(4)	0.8799(5)	0.6089(3)	0.0366(10)
C15	0.2962(4)	0.7994(5)	0.6819(4)	0.0345(10)
C16	0.2910(4)	0.8496(5)	0.7931(3)	0.0349(10)

Table 5.14 Anisotropic displacement parameters for **6**

Atom	U_{11}	U_{22}	U_{33}	U_{23}	U_{13}	U_{12}
Sn1	0.0294(2)	0.02482(19)	0.02395(18)	-0.00023(10)	0.00412(12)	0.00437(10)
Se1	0.0393(3)	0.0388(3)	0.0294(2)	-0.00064(17)	-0.00010(18)	0.01400(18)
Cl1	0.0383(6)	0.0335(5)	0.0274(5)	-0.0023(4)	0.0071(4)	-0.0059(4)
Cl2	0.0382(6)	0.0288(5)	0.0345(5)	0.0040(4)	0.0058(4)	-0.0007(4)
C1	0.030(2)	0.035(2)	0.0239(19)	-0.0025(17)	0.0052(16)	0.0019(17)
C2	0.030(2)	0.0276(19)	0.0270(18)	-0.0025(16)	0.0015(15)	0.0044(16)
C11	0.026(2)	0.029(2)	0.034(2)	-0.0001(18)	0.0010(17)	0.0102(17)
C12	0.033(2)	0.035(2)	0.043(2)	-0.004(2)	0.0010(18)	0.0004(18)
C13	0.032(2)	0.046(3)	0.039(2)	-0.002(2)	0.0112(18)	0.000(2)
C14	0.035(2)	0.041(2)	0.034(2)	-0.004(2)	0.0051(18)	0.0073(19)
C15	0.034(2)	0.029(2)	0.040(2)	-0.0040(19)	0.0005(19)	0.0043(17)
C16	0.036(2)	0.031(2)	0.039(2)	0.0066(19)	0.0103(18)	0.0093(18)

5.7 $(PhSe)_3Sn–(CH_2)_4–Sn(SePh)_3$ (7)

Compound **7** crystallizes as colorless blocks from a DCM/*n*-hexane mixture.

Table 5.15 Crystal data and structure refinement for **7**

Empirical formula	$C_{40}H_{38}Se_6Sn_2$
Formula weight /g·mol^{-1}	1229.84
Crystal system	triclinic
Space group	$P\bar{1}$
a /Å	9.1186(18)
b /Å	9.997(2)
c /Å	13.042(3)
α /°	70.94(3)
β /°	71.55(3)
γ /°	71.79(3)
V /Å^3	1036.6(4)
Z	1
ρ_{calc} /g·cm^{-3}	1.970
$\mu(Mo_{K\alpha})$ /mm^{-1}	6.499
2Θ range /°	5-52
Reflections measured	6871
Independent reflections	3725
R(int)	0.0498
Indepedent reflections ($I > 2\sigma(I)$)	3400
Parameters	293
R_1 ($I > 2\sigma(I)$)	0.0305
wR_2 (all data)	0.0805
GooF (all data)	0.992
Max. peak/hole /e$^-$·10^{-6}pm^{-3}	1.354/−1.224

Table 5.16 Atomic coordinates and equivalent isotropic displacement parameters for **7**

Atom	x/a	y/b	z/c	$U_{eq/iso}$
Sn1	0.50025(3)	0.46500(2)	0.219645(18)	0.02494(9)
Se1	0.50476(5)	0.65097(3)	0.03381(3)	0.03128(11)
Se2	0.25554(5)	0.35989(4)	0.29236(3)	0.03648(12)
Se3	0.71723(5)	0.23980(4)	0.18831(3)	0.03695(12)
C1	0.5296(5)	0.5531(4)	0.3398(3)	0.0310(7)
C2	0.4799(5)	0.4704(4)	0.4603(3)	0.0290(7)
C3	0.3911(4)	0.8211(3)	0.0900(3)	0.0275(7)
C4	0.2344(5)	0.8827(4)	0.0838(4)	0.0378(9)
C5	0.1567(6)	1.0115(5)	0.1148(4)	0.0459(10)
C6	0.2328(6)	1.0781(4)	0.1529(4)	0.0454(10)
C7	0.3876(5)	1.0170(4)	0.1597(3)	0.0401(9)
C8	0.4685(5)	0.8882(4)	0.1282(3)	0.0323(8)
C9	0.0952(4)	0.5368(4)	0.2627(3)	0.0338(8)
C10	0.0405(5)	0.5771(5)	0.1666(4)	0.0442(10)
C11	-0.0812(6)	0.7011(6)	0.1496(5)	0.0590(14)
C12	-0.1434(6)	0.7842(6)	0.2258(6)	0.0660(16)
C13	-0.0882(7)	0.7446(6)	0.3198(7)	0.0704(17)
C14	0.0299(6)	0.6203(5)	0.3394(5)	0.0509(11)
C15	0.7613(4)	0.1880(4)	0.3339(3)	0.0295(7)
C16	0.8618(4)	0.2527(4)	0.3516(4)	0.0351(8)
C17	0.8894(5)	0.2193(5)	0.4563(4)	0.0432(9)
C18	0.8178(5)	0.1212(5)	0.5444(4)	0.0461(10)
C19	0.7203(6)	0.0541(4)	0.5258(4)	0.0460(10)
C20	0.6906(5)	0.0875(4)	0.4219(4)	0.0383(9)

Table 5.17 Anisotropic displacement parameters for **7**

Atom	U_{11}	U_{22}	U_{33}	U_{23}	U_{13}	U_{12}
Sn1	0.03259(15)	0.02063(13)	0.02159(15)	-0.00606(9)	-0.00846(9)	-0.00342(10)
Se1	0.0474(2)	0.02187(18)	0.0221(2)	-0.00564(13)	-0.00892(15)	-0.00387(16)
Se2	0.0401(2)	0.02563(19)	0.0425(3)	-0.00590(15)	-0.00813(16)	-0.01067(16)
Se3	0.0432(2)	0.0321(2)	0.0349(2)	-0.01615(16)	-0.01567(16)	0.00652(17)
C1	0.047(2)	0.0256(17)	0.026(2)	-0.0102(13)	-0.0124(15)	-0.0081(16)
C2	0.0346(19)	0.0254(16)	0.027(2)	-0.0073(13)	-0.0087(14)	-0.0052(15)
C3	0.0405(19)	0.0202(14)	0.0200(18)	-0.0019(12)	-0.0073(13)	-0.0079(14)
C4	0.037(2)	0.0306(18)	0.046(3)	-0.0099(16)	-0.0071(16)	-0.0106(16)
C5	0.040(2)	0.035(2)	0.052(3)	-0.0117(18)	-0.0038(18)	-0.0016(18)
C6	0.065(3)	0.0244(18)	0.039(2)	-0.0107(16)	0.0009(19)	-0.0101(19)
C7	0.063(3)	0.0310(18)	0.029(2)	-0.0075(15)	-0.0095(18)	-0.0174(19)
C8	0.045(2)	0.0290(17)	0.026(2)	-0.0063(14)	-0.0100(15)	-0.0130(16)
C9	0.0321(18)	0.0311(17)	0.039(2)	-0.0087(15)	-0.0058(15)	-0.0120(15)
C10	0.048(2)	0.044(2)	0.045(3)	-0.0067(19)	-0.0149(19)	-0.017(2)
C11	0.053(3)	0.056(3)	0.070(4)	0.008(2)	-0.034(3)	-0.022(2)
C12	0.046(3)	0.042(3)	0.112(5)	-0.013(3)	-0.032(3)	-0.007(2)
C13	0.055(3)	0.060(3)	0.109(5)	-0.047(3)	-0.025(3)	0.004(3)
C14	0.045(2)	0.052(2)	0.064(3)	-0.030(2)	-0.015(2)	-0.003(2)
C15	0.0293(17)	0.0240(15)	0.032(2)	-0.0089(13)	-0.0096(14)	0.0023(14)
C16	0.0329(19)	0.0344(19)	0.035(2)	-0.0047(15)	-0.0070(15)	-0.0087(16)
C17	0.039(2)	0.053(2)	0.041(3)	-0.0131(19)	-0.0159(17)	-0.0084(19)
C18	0.048(2)	0.049(2)	0.032(3)	-0.0046(17)	-0.0157(18)	0.0022(19)
C19	0.053(2)	0.0305(19)	0.039(3)	0.0043(16)	-0.0062(19)	-0.0073(19)
C20	0.041(2)	0.0260(17)	0.043(3)	-0.0067(15)	-0.0060(16)	-0.0080(16)

5.8 (NpSe-1)₃Sn–(CH₂)₄–Sn(1-SeNp)₃ (8)

Compound **8** crystallizes in colorless blocks from a DCM/*n*-hexane mixture.

Table 5.18 Crystal data and structure refinement for **8**

Empirical formula	$C_{64}H_{50}Se_6Sn_2$
Formula weight /g·mol^{-1}	1530.18
Crystal system	triclinic
Space group	$P\bar{1}$
a /Å	11.005(2)
b /Å	12.026(2)
c /Å	12.031(2)
α /°	100.09(3)
β /°	114.29(3)
γ /°	96.93(3)
V /Å^3	1395.4(5)
Z	1
ρ_{calc} /g·cm^{-3}	1.821
$\mu(Mo_{K\alpha})$ /mm^{-1}	4.848
2Θ range /°	4-52
Reflections measured	13701
Independent reflections	5020
R(int)	0.0484
Indepedent reflections ($I > 2\sigma(I)$)	3327
Parameters	366
R_1 ($I > 2\sigma(I)$)	0.0342
wR_2 (all data)	0.0733
GooF (all data)	0.824
Max. peak/hole /e$^-$·10^{-6}pm^{-3}	1.537/–0.951

Table 5.19 Atomic coordinates and equivalent isotropic displacement parameters for **8**

Atom	x/a	y/b	z/c	$U_{eq/iso}$
Sn1	0.81257(4)	0.17008(3)	0.00131(3)	0.03341(10)
Se1	1.00294(6)	0.08793(4)	0.14418(6)	0.04509(15)
Se2	0.89972(6)	0.18930(5)	-0.16217(6)	0.04693(16)
Se3	0.81553(6)	0.37217(4)	0.11002(6)	0.04968(17)
C1	0.6088(5)	0.0684(4)	-0.0730(5)	0.0417(13)
C2	0.5749(5)	0.0228(4)	0.0240(5)	0.0393(12)
C10	0.9449(6)	0.0874(4)	0.2755(5)	0.0417(13)
C11	0.8715(6)	-0.0113(5)	0.2734(6)	0.0497(15)
C12	0.8225(7)	-0.0185(6)	0.3647(7)	0.0648(18)
C13	0.8570(7)	0.0755(6)	0.4609(7)	0.0674(19)
C14	0.9761(8)	0.2792(6)	0.5698(7)	0.073(2)
C15	1.0565(9)	0.3800(6)	0.5774(7)	0.082(2)
C16	1.1013(7)	0.3874(5)	0.4854(7)	0.0657(19)
C17	1.0654(6)	0.2943(4)	0.3863(6)	0.0502(14)
C18	0.9829(5)	0.1882(4)	0.3758(5)	0.0418(13)
C19	0.9382(6)	0.1806(5)	0.4698(6)	0.0531(15)
C20	0.7995(6)	0.3056(4)	-0.2211(6)	0.0457(14)
C21	0.8678(7)	0.4187(4)	-0.1772(7)	0.0641(18)
C22	0.7972(9)	0.5060(5)	-0.2200(8)	0.073(2)
C23	0.6660(9)	0.4800(6)	-0.3018(8)	0.081(2)
C24	0.4508(8)	0.3290(8)	-0.4370(8)	0.088(3)
C25	0.3821(9)	0.2178(9)	-0.4783(9)	0.102(3)
C26	0.4502(8)	0.1322(7)	-0.4409(8)	0.082(2)
C27	0.5861(7)	0.1567(5)	-0.3589(6)	0.0614(17)
C28	0.6626(6)	0.2752(4)	-0.3091(5)	0.0457(14)
C29	0.5914(6)	0.3624(5)	-0.3513(6)	0.0581(17)
C30	0.6158(8)	0.3503(6)	0.0439(7)	0.038(2)
C31	0.5487(13)	0.3741(9)	-0.0706(9)	0.053(3)
C32	0.4030(16)	0.3557(18)	-0.1274(13)	0.055(4)
C33	0.3313(12)	0.3166(8)	-0.0698(11)	0.061(3)
C34	0.3249(11)	0.2486(7)	0.1103(11)	0.071(4)
C35	0.3878(11)	0.2278(8)	0.2251(11)	0.065(3)
C36	0.5293(13)	0.2508(9)	0.2843(10)	0.061(3)
C37	0.6090(10)	0.2928(7)	0.2326(9)	0.051(3)
C38	0.5440(8)	0.3128(6)	0.1092(8)	0.041(2)
C39	0.3987(10)	0.2924(9)	0.0503(12)	0.045(3)
C40	0.6753(11)	0.3381(10)	0.1491(11)	0.027(3)
C41	0.7069(16)	0.3226(12)	0.2653(13)	0.043(4)
C42	0.5963(16)	0.2879(16)	0.2958(17)	0.045(5)
C43	0.4661(16)	0.2758(14)	0.2127(15)	0.052(5)
C44	0.2986(17)	0.2920(14)	0.0059(15)	0.055(5)
C45	0.2659(19)	0.3158(17)	-0.1070(17)	0.053(6).
C46	0.369(2)	0.345(5)	-0.140(3)	0.062(10)

C47	0.5029(18)	0.3521(18)	-0.0630(16)	0.041(6)
C48	0.5409(14)	0.3303(15)	0.0598(14)	0.035(5)
C49	0.4339(16)	0.302(2)	0.0948(16)	0.042(7)

Table 5.20 Anisotropic displacement parameters for **8**

Atom	U_{11}	U_{22}	U_{33}	U_{23}	U_{13}	U_{12}
Sn1	0.0385(2)	0.03172(2)	0.0370(2)	0.00981(2)	0.0224(2)	0.00930(1)
Se1	0.0577(4)	0.0541(3)	0.0401(4)	0.0182(3)	0.0302(3)	0.0300(3)
Se2	0.0544(4)	0.0605(3)	0.0509(4)	0.0286(3)	0.0364(3)	0.0307(3)
Se3	0.0506(4)	0.0372(3)	0.0590(4)	-0.0002(2)	0.0266(3)	0.0099(2)
C1	0.045(3)	0.036(3)	0.041(4)	0.004(2)	0.021(3)	0.002(2)
C2	0.041(3)	0.038(2)	0.038(4)	0.009(2)	0.017(3)	0.005(2)
C10	0.051(3)	0.044(3)	0.036(4)	0.015(2)	0.020(3)	0.021(2)
C11	0.061(4)	0.046(3)	0.049(4)	0.022(3)	0.026(3)	0.016(3)
C12	0.070(4)	0.068(4)	0.058(5)	0.028(4)	0.026(4)	0.010(3)
C13	0.073(5)	0.094(5)	0.058(5)	0.039(4)	0.040(4)	0.026(4)
C14	0.103(6)	0.085(5)	0.052(5)	0.019(4)	0.047(4)	0.044(4)
C15	0.116(7)	0.069(5)	0.055(6)	0.005(4)	0.029(5)	0.047(5)
C16	0.077(5)	0.047(3)	0.058(5)	0.005(3)	0.017(4)	0.019(3)
C17	0.058(4)	0.044(3)	0.044(4)	0.012(3)	0.017(3)	0.015(3)
C18	0.049(3)	0.048(3)	0.034(4)	0.015(2)	0.019(3)	0.023(3)
C19	0.064(4)	0.068(4)	0.040(4)	0.020(3)	0.026(3)	0.034(3)
C21	0.092(5)	0.043(3)	0.077(5)	0.015(3)	0.059(4)	0.007(3)
C22	0.114(6)	0.040(3)	0.091(6)	0.024(3)	0.065(5)	0.018(4)
C23	0.122(7)	0.074(5)	0.094(7)	0.047(4)	0.073(6)	0.060(5)
C24	0.084(6)	0.143(8)	0.081(7)	0.068(6)	0.049(5)	0.071(6)
C25	0.066(5)	0.158(9)	0.085(7)	0.051(6)	0.026(5)	0.033(6)
C26	0.065(5)	0.105(6)	0.069(6)	0.019(4)	0.024(4)	0.013(4)
C27	0.067(5)	0.069(4)	0.056(5)	0.014(3)	0.032(4)	0.024(3)
C28	0.057(4)	0.058(3)	0.040(4)	0.020(3)	0.030(3)	0.029(3)
C29	0.067(4)	0.074(4)	0.059(5)	0.036(3)	0.039(4)	0.040(3)
C30	0.049(5)	0.028(4)	0.045(6)	0.005(3)	0.030(5)	0.016(3)
C31	0.077(8)	0.036(5)	0.057(8)	0.014(4)	0.036(7)	0.020(6)
C32	0.073(9)	0.043(7)	0.038(7)	-0.002(5)	0.015(7)	0.022(8)
C33	0.052(7)	0.043(5)	0.073(9)	0.002(5)	0.014(7)	0.025(5)
C34	0.085(8)	0.042(5)	0.097(11)	-0.004(5)	0.059(8)	0.015(5)
C35	0.075(8)	0.063(6)	0.073(9)	0.008(5)	0.053(7)	0.012(5)
C36	0.092(9)	0.064(7)	0.047(8)	0.016(5)	0.046(7)	0.028(7)
C37	0.071(8)	0.037(4)	0.054(8)	0.011(4)	0.038(6)	0.014(4)
C38	0.066(7)	0.025(4)	0.041(7)	0.001(4)	0.031(5)	0.020(4)
C39	0.037(6)	0.028(5)	0.064(9)	-0.009(6)	0.026(7)	0.007(4)

5.9 (PhSe)$_3$Sn– CH$_2$–(C$_6$H$_4$)$_2$ –CH$_2$–Sn(SePh)$_3$ (9)

Compound **9** crystallizes as colorless blocks from a DCM/*n*-hexane mixture.

Table 5.21 Crystal data and structure refinement for **9**

Empirical formula	C$_{44}$H$_{38}$Se$_6$Sn$_2$
Formula weight /g·mol^{-1}	1277.88
Crystal system	monoclinic
Space group	*C*2/*c*
a /Å	17.605(4)
b /Å	7.4957(15)
c /Å	33.528(7)
β /°	97.69(3)
V /Å^3	4384.6(15)
Z	4
ρ_{calc} /g·cm^{-3}	1.936
μ(Mo$_{K\alpha}$) /mm^{-1}	6.150
2Θ range /°	5-52
Reflections measured	7231
Independent reflections	3874
R(int)	0.0687
Independent reflections ($I > 2\sigma(I)$)	2737
Parameters	235
R_1 ($I > 2\sigma(I)$)	0.0362
wR_2 (all data)	0.0836
GooF (all data)	0.869
Max. peak/hole /e$^-$·10^{-6}pm^{-3}	0.956/–0.730

Table 5.22 Atomic coordinates and equivalent isotropic displacement parameters for **9**

Atom	x/a	y/b	z/c	$U_{eq/iso}$
Sn1	0.95517(2)	0.23120(5)	0.387594(12)	0.02495(12)
Se1	1.05865(3)	0.39321(8)	0.433890(19)	0.02809(15)
Se2	1.02716(3)	0.10434(9)	0.33374(2)	0.03679(18)
Se3	0.85527(3)	0.44903(9)	0.35475(2)	0.03399(17)
C1	0.9011(3)	0.0422(8)	0.42411(19)	0.0304(14)
C2	0.9509(3)	0.0183(7)	0.4633(2)	0.0283(14)
C3	0.5031(3)	0.3789(8)	0.46900(18)	0.0281(13)
C4	0.9488(3)	0.1400(8)	0.49463(18)	0.0264(13)
C11	1.1140(3)	0.4569(8)	0.38995(18)	0.0256(13)
C12	1.1837(3)	0.3744(8)	0.38653(19)	0.0297(14)
C13	1.2224(3)	0.4125(8)	0.3543(2)	0.0316(14)
C14	1.1916(4)	0.5340(8)	0.3247(2)	0.0349(15)
C15	1.1226(4)	0.6178(8)	0.3284(2)	0.0353(15)
C16	1.0848(3)	0.5807(7)	0.36068(19)	0.0302(14)
C21	0.9381(3)	0.0380(8)	0.29675(18)	0.0276(13)
C22	0.9061(4)	0.1553(8)	0.2681(2)	0.0337(15)
C23	0.8443(4)	0.1019(9)	0.23972(19)	0.0372(16)
C24	0.8143(4)	-0.0676(9)	0.2417(2)	0.0383(16)
C25	0.8465(4)	-0.1842(8)	0.27082(19)	0.0342(15)
C26	0.9078(3)	-0.1329(8)	0.29846(19)	0.0304(14)
C31	0.8065(3)	0.4688(8)	0.40248(19)	0.0275(13)
C32	0.7347(4)	0.3891(10)	0.4036(2)	0.0444(18)
C33	0.6989(4)	0.4027(10)	0.4373(3)	0.056(2)
C34	0.7310(5)	0.4961(9)	0.4710(2)	0.0470(18)
C35	0.8018(4)	0.5744(9)	0.4702(2)	0.0426(18)
C36	0.8395(4)	0.5613(8)	0.4365(2)	0.0348(16)

Table 5.23 Anisotropic displacement parameters for **9**

Atom	U_{11}	U_{22}	U_{33}	U_{23}	U_{13}	U_{12}
Sn1	0.02413(2)	0.0227(2)	0.0279(2)	0.00138(2)	0.0030(1)	-0.0015(2)
Se1	0.0274(3)	0.0275(3)	0.0289(3)	-0.0031(3)	0.0022(2)	-0.0018(3)
Se2	0.0277(3)	0.0402(4)	0.0431(4)	-0.0156(3)	0.0068(3)	-0.0027(3)
Se3	0.0282(3)	0.0407(4)	0.0333(3)	0.0104(3)	0.0046(3)	0.0066(3)
C1	0.028(3)	0.028(3)	0.035(3)	0.008(3)	0.004(3)	-0.012(3)
C2	0.026(3)	0.017(3)	0.040(4)	0.003(3)	0.001(3)	-0.003(3)
C3	0.036(3)	0.023(3)	0.028(3)	-0.004(3)	0.014(3)	-0.006(3)
C4	0.028(3)	0.023(3)	0.030(3)	0.004(3)	0.009(3)	-0.001(3)
C11	0.027(3)	0.020(3)	0.030(3)	-0.004(2)	0.002(3)	-0.006(2)
C12	0.029(3)	0.025(3)	0.034(3)	-0.002(3)	-0.001(3)	0.003(3)
C13	0.024(3)	0.029(3)	0.042(4)	-0.004(3)	0.004(3)	0.001(3)
C14	0.042(4)	0.028(3)	0.037(4)	-0.006(3)	0.013(3)	-0.012(3)
C15	0.039(3)	0.025(3)	0.042(4)	0.007(3)	0.006(3)	0.000(3)
C16	0.026(3)	0.022(3)	0.042(4)	-0.001(3)	0.002(3)	-0.003(3)
C21	0.028(3)	0.031(3)	0.025(3)	-0.007(3)	0.010(2)	-0.001(3)
C22	0.041(3)	0.022(3)	0.041(4)	0.003(3)	0.018(3)	0.005(3)
C23	0.039(3)	0.042(4)	0.031(3)	0.008(3)	0.005(3)	0.011(3)
C24	0.036(3)	0.045(4)	0.033(3)	-0.013(3)	0.000(3)	0.005(3)
C25	0.039(3)	0.029(3)	0.035(3)	-0.003(3)	0.005(3)	-0.003(3)
C26	0.032(3)	0.032(3)	0.027(3)	0.002(3)	0.004(3)	0.002(3)
C31	0.030(3)	0.019(3)	0.034(3)	-0.004(3)	0.007(3)	0.004(3)
C32	0.031(3)	0.049(4)	0.056(5)	-0.019(4)	0.013(3)	-0.013(3)
C33	0.044(4)	0.048(5)	0.081(6)	-0.026(5)	0.028(4)	-0.017(4)
C34	0.066(5)	0.035(4)	0.046(4)	-0.004(3)	0.028(4)	0.002(4)
C35	0.050(4)	0.035(4)	0.039(4)	-0.007(3)	-0.008(3)	0.017(3)
C36	0.028(3)	0.023(3)	0.050(4)	0.003(3)	-0.004(3)	0.001(3)

5.10 (PhSe)$_3$Sn– C$_5$H$_4$–Fe–C$_5$H$_4$–Sn(SePh)$_3$ (10)

Compound **10** crystallizes as orange niddles from a DCM/*n*-hexane mixture.

Table 5.24 Crystal data and structure refinement for **10**

Empirical formula	C$_{46}$H$_{38}$Se$_6$Sn$_2$Fe
Formula weight /g·mol^{-1}	1357.75
Crystal system	monoclinic
Space group	*P*2$_1$/*n*
a /Å	13.978(3)
b /Å	9.971(2)
c /Å	16.213(3)
β /°	106.59(3)
V /Å^3	2165.5(7)
Z	2
ρ_{calc} /g·cm^{-3}	2.082
μ(Mo$_{K\alpha}$) /mm^{-1}	6.550
2Θ range /°	5-45
Reflections measured	8870
Independent reflections	2828
R(int)	0.0868
Indepedent reflections ($I > 2\sigma(I)$)	2286
Parameters	250
R_1 ($I > 2\sigma(I)$)	0.0346
wR$_2$ (all data)	0.090
GooF (all data)	0.945
Max. peak/hole /e$^-$·10^{-6}pm^{-3}	1.614/–0.820

Table 5.25 Atomic coordinates and equivalent isotropic displacement parameters for **10**

Atom	x/a	y/b	z/c	$U_{eq/iso}$
Sn1	0.20602(3)	0.23226(5)	0.03331(3)	0.01972(17)
Se1	0.33886(5)	0.33735(7)	0.15737(5)	0.0240(2)
Se2	0.29782(6)	0.09723(7)	-0.05247(5)	0.0249(2)
Se3	0.09850(6)	0.40616(8)	-0.06068(5)	0.0329(2)
Fe1	0.0000	0.0000	0.0000	0.0237(4)
C1	0.1069(5)	0.1164(8)	0.0800(4)	0.0200(16)
C2	0.1135(6)	-0.0176(8)	0.1097(5)	0.0284(19)
C3	0.0202(7)	-0.0499(10)	0.1264(5)	0.041(2)
C4	-0.0424(6)	0.0604(10)	0.1059(5)	0.036(2)
C5	0.0094(6)	0.1660(9)	0.0773(5)	0.0305(19)
C11	0.4018(5)	0.1648(8)	0.1927(4)	0.0234(17)
C12	0.3565(5)	0.0704(8)	0.2322(4)	0.0230(17)
C13	0.4023(6)	-0.0538(8)	0.2563(5)	0.0281(19)
C14	0.4904(6)	-0.0833(8)	0.2396(5)	0.032(2)
C15	0.5367(6)	0.0116(9)	0.2013(5)	0.036(2)
C16	0.4901(6)	0.1356(8)	0.1771(5)	0.0287(19)
C21	0.3403(5)	0.2501(7)	-0.1071(4)	0.0226(17)
C22	0.4255(5)	0.3174(8)	-0.0668(5)	0.0279(19)
C23	0.4594(6)	0.4205(8)	-0.1085(5)	0.0297(19)
C24	0.4057(6)	0.4563(8)	-0.1905(5)	0.0304(19)
C25	0.3190(6)	0.3906(9)	-0.2307(5)	0.033(2)
C26	0.2847(6)	0.2872(8)	-0.1897(5)	0.0286(18)
C31	0.1882(6)	0.5530(8)	-0.0213(5)	0.0295(19)
C32	0.2362(6)	0.6139(9)	-0.0756(5)	0.036(2)
C33	0.3015(5)	0.7173(8)	-0.0487(5)	0.0267(18)
C34	0.3182(7)	0.7642(8)	0.0388(6)	0.041(2)
C35	0.2684(6)	0.7011(8)	0.0925(5)	0.034(2)
C36	0.2054(6)	0.6039(9)	0.0625(5)	0.038(2)

Table 5.26 Anisotropic displacement parameters for **10**

Atom	U_{11}	U_{22}	U_{33}	U_{23}	U_{13}	U_{12}
Sn1	0.0257(3)	0.0183(3)	0.0131(3)	-0.0015(2)	0.0022(2)	-0.0035(2)
Se1	0.0289(4)	0.0193(4)	0.0195(4)	-0.0045(3)	0.0001(3)	-0.0045(3)
Se2	0.0376(4)	0.0180(4)	0.0207(4)	-0.0020(3)	0.0108(3)	-0.0039(3)
Se3	0.0395(5)	0.0255(4)	0.0274(4)	0.0028(4)	-0.0004(4)	0.0009(4)
Fe1	0.0264(8)	0.0330(9)	0.0092(7)	-0.0027(7)	0.0008(6)	-0.0111(7)
C1	0.022(4)	0.027(4)	0.011(3)	-0.003(3)	0.003(3)	-0.004(3)
C2	0.029(4)	0.035(5)	0.017(4)	-0.002(4)	-0.001(3)	-0.004(4)
C3	0.063(6)	0.049(6)	0.004(3)	-0.006(4)	-0.001(4)	-0.034(5)
C4	0.027(4)	0.062(6)	0.019(4)	-0.009(4)	0.006(3)	-0.015(5)
C5	0.033(4)	0.041(5)	0.017(4)	-0.011(4)	0.006(3)	-0.003(4)
C11	0.030(4)	0.026(4)	0.011(4)	-0.004(3)	0.000(3)	0.001(4)
C12	0.023(4)	0.027(4)	0.013(4)	-0.003(3)	-0.004(3)	-0.006(3)
C13	0.035(4)	0.029(5)	0.015(4)	0.000(4)	-0.001(3)	-0.008(4)
C14	0.041(5)	0.025(5)	0.023(4)	-0.003(4)	-0.003(4)	0.003(4)
C15	0.030(4)	0.049(6)	0.024(4)	-0.006(4)	0.000(4)	0.004(4)
C16	0.035(4)	0.032(5)	0.019(4)	0.001(4)	0.007(3)	-0.003(4)
C21	0.031(4)	0.021(4)	0.017(4)	-0.004(3)	0.008(3)	-0.006(3)
C22	0.032(4)	0.031(5)	0.016(4)	0.002(4)	0.000(3)	0.001(4)
C23	0.036(4)	0.028(4)	0.024(4)	-0.001(4)	0.006(4)	-0.013(4)
C24	0.038(5)	0.028(4)	0.028(4)	-0.003(4)	0.015(4)	-0.005(4)
C25	0.043(5)	0.037(5)	0.019(4)	0.007(4)	0.010(4)	0.002(4)
C26	0.031(4)	0.031(4)	0.023(4)	-0.001(4)	0.007(3)	-0.001(4)
C31	0.033(4)	0.026(4)	0.028(4)	0.003(4)	0.006(4)	0.007(4)
C32	0.040(5)	0.037(5)	0.028(4)	0.006(4)	0.005(4)	0.014(4)
C33	0.026(4)	0.020(4)	0.032(4)	0.013(4)	0.005(3)	-0.005(4)
C34	0.049(5)	0.022(5)	0.045(5)	-0.001(4)	0.003(4)	-0.004(4)
C35	0.054(5)	0.018(4)	0.022(4)	-0.012(4)	-0.003(4)	0.008(4)
C36	0.053(5)	0.034(5)	0.027(4)	0.007(4)	0.013(4)	0.004(5)

5.11 [Pd(SePh)(OOCCH$_3$)]$_4$ (12)

Compound **12** crystallizes as red blocks upon layering a DCM solution by *n*-hexane.

Table 5.27 Crystal data and structure refinement for **12**

Empirical formula	C$_{32}$H$_{32}$O$_8$Pd$_4$Se$_4$
Formula weight /g·mol^{-1}	1286.02
Crystal system	monoclinic
Space group	*P*2$_1$/*n*
a /Å	8.0459(8)
b /Å	11.531(2)
c /Å	19.482(2)
β /°	96.985(9)
V /Å^3	1794.1(4)
Z	2
ρ_{calc} /g·cm^{-3}	2.381
μ(Mo$_{K\alpha}$) /mm^{-1}	1.610
2Θ range /°	4-50
Reflections measured	5401
Independent reflections	2989
R(int)	0.1154
Indepedent reflections ($I > 2\sigma(I)$)	1429
Parameters	219
R_1 ($I > 2\sigma(I)$)	0.0682
wR_2 (all data)	0.1797
GooF (all data)	0.874
Max. peak/hole /e$^-$·10^{-6}pm^{-3}	1.552/–3.372

Table 5.28 Atomic coordinates and equivalent isotropic displacement parameters for **12**

Atom	x/a	y/b	z/c	$U_{eq/iso}$
Pd1	0.1355(2)	0.14100(14)	0.06018(6)	0.0296(4)
Pd2	-0.0573(2)	0.15595(14)	-0.07313(6)	0.0289(4)
O1	-0.0037(19)	0.2877(12)	0.0782(6)	0.038(3)
O2	-0.145(2)	0.3043(12)	-0.0293(6)	0.039(3)
O3	0.2998(18)	0.2342(13)	0.0089(6)	0.039(3)
O4	0.1522(19)	0.2452(13)	-0.0972(6)	0.040(3)
Se1	-0.0372(3)	0.01831(18)	0.11999(8)	0.0307(5)
Se2	0.2894(3)	-0.03399(18)	0.04997(8)	0.0315(5)
C1	0.067(3)	0.012(2)	0.2135(8)	0.039(5)
C2	0.051(3)	-0.088(2)	0.2519(9)	0.039(5)
C3	0.126(3)	-0.0943(19)	0.3197(8)	0.039(5)
C4	0.228(3)	-0.0038(17)	0.3494(9)	0.033(5)
C5	0.248(3)	0.0904(18)	0.3113(8)	0.033(5)
C6	0.168(3)	0.101(2)	0.2420(8)	0.039(5)
C7	0.433(3)	-0.0087(17)	0.1350(8)	0.032(4)
C8	0.444(3)	-0.0961(19)	0.1893(8)	0.037(5)
C9	0.552(2)	-0.0734(17)	0.2488(8)	0.028(4)
C10	0.645(3)	0.0282(18)	0.2575(9)	0.035(4)
C11	0.636(3)	0.1103(19)	0.2056(8)	0.033(4)
C12	0.527(3)	0.0895(19)	0.1434(9)	0.039(5)
C13	-0.106(3)	0.3368(16)	0.0349(8)	0.031(5)
C14	-0.192(3)	0.442(2)	0.0561(10)	0.046(6)
C15	0.284(3)	0.264(2)	-0.0558(10)	0.042(5)
C16	0.429(3)	0.3206(18)	-0.0825(10)	0.038(4)

Table 5.29 Anisotropic displacement parameters for **12**

Atom	U_{11}	U_{22}	U_{33}	U_{23}	U_{13}	U_{12}
Pd1	0.0323(9)	0.0304(8)	0.0250(6)	0.0005(6)	-0.0010(6)	0.0039(8)
Pd2	0.0324(9)	0.0313(9)	0.0226(6)	-0.0030(6)	0.0010(6)	0.0020(8)
O1	0.053(9)	0.029(6)	0.030(5)	0.007(5)	-0.007(5)	0.018(6)
O2	0.050(9)	0.035(8)	0.031(5)	0.006(5)	-0.002(5)	0.014(7)
O3	0.035(7)	0.038(7)	0.039(5)	0.005(5)	-0.008(4)	-0.004(6)
O4	0.046(7)	0.052(9)	0.023(5)	-0.002(6)	0.002(5)	-0.009(7)
Se1	0.0320(1)	0.0358(12)	0.0238(8)	-0.0026(8)	0.0010(8)	0.0037(10)
Se2	0.0339(1)	0.0356(12)	0.0243(8)	-0.0017(8)	0.0014(8)	0.0063(11)
C1	0.043(14)	0.052(12)	0.023(6)	-0.001(6)	-0.001(7)	-0.008(10)
C2	0.032(13)	0.048(10)	0.034(7)	0.008(7)	-0.005(8)	0.013(10)
C3	0.054(15)	0.042(10)	0.020(7)	-0.002(7)	0.006(8)	0.001(10)
C4	0.046(14)	0.022(9)	0.030(8)	-0.004(6)	0.003(8)	0.018(8)
C5	0.041(13)	0.033(9)	0.020(7)	-0.003(6)	-0.015(7)	0.002(9)

C6	0.048(14)	0.048(11)	0.019(6)	-0.008(7)	0.000(7)	0.000(10)
C7	0.033(12)	0.026(9)	0.035(7)	-0.006(6)	-0.001(7)	0.012(7)
C8	0.051(15)	0.033(10)	0.025(7)	-0.007(6)	-0.002(7)	0.008(9)
C9	0.028(12)	0.029(9)	0.025(7)	-0.012(6)	-0.002(7)	0.016(8)
C10	0.037(13)	0.032(10)	0.037(8)	-0.008(7)	0.006(8)	0.009(9)
C11	0.029(12)	0.039(10)	0.028(8)	-0.007(6)	-0.005(7)	0.006(8)
C12	0.044(14)	0.035(10)	0.034(8)	0.000(7)	-0.009(8)	0.002(9)
C13	0.049(13)	0.018(9)	0.026(6)	0.007(6)	0.005(7)	0.016(8)
C14	0.051(15)	0.048(13)	0.036(9)	0.001(8)	-0.005(9)	0.034(11)
C15	0.031(10)	0.051(14)	0.044(8)	0.014(9)	0.000(7)	-0.002(10)
C16	0.035(10)	0.030(12)	0.050(10)	0.000(8)	0.011(8)	0.003(9)

5.12 [(Ph₃P)₃(SePh)₂Cu₂]· 1.5THF (13·1.5THF)

Compound **13** crystallizes as yellow needles upon layering a THF solution by *n*-hexane.

Table 5.30 Crystal data and structure refinement for **13·1.5THF**

Empirical formula	$C_{72}H_{67}O_{1.5}Cu_2Se_2P_3$
Formula weight /g·mol^{-1}	1334.17
Crystal system	monoclinic
Space group	*C*2/*c*
a /Å	47.9871(18)
b /Å	10.0410(2)
c /Å	25.9708(9)
β /°	102.485(3)
V /Å^3	12217.8(7)
Z	8
ρ_{calc} /g·cm^{-3}	1.370
$\mu(Mo_{K\alpha})$ /mm^{-1}	2.012
2*Θ* range /°	4-45
Reflections measured	44562
Independent reflections	7966
R(int)	0.1196
Indepedent reflections ($I > 2\sigma(I)$)	5960
Parameters	669
R_1 ($I > 2\sigma(I)$)	0.0506
wR_2 (all data)	0.1288
GooF (all data)	0.842
Max. peak/hole /e$^-$·10^{-6}pm^{-3}	0.992/–0.889

Table 5.31 Atomic coordinates and equivalent isotropic displacement parameters for **13·1.5THF**

Atom	x/a	y/b	z/c	$U_{eq/iso}$
Se1	0.118071(19)	0.99005(10)	0.44324(3)	0.0227(3)
Se2	0.122804(19)	1.33899(10)	0.51794(3)	0.0222(3)
Cu2	0.12017(2)	1.09611(12)	0.53425(4)	0.0210(3)
Cu1	0.11605(2)	1.22685(12)	0.43307(4)	0.0233(3)
P1	0.11402(5)	1.3291(3)	0.35670(9)	0.0233(6)
P2	0.07239(5)	1.0642(3)	0.52843(9)	0.0216(6)
P3	0.14961(5)	1.0041(3)	0.60569(9)	0.0205(6)
C11	0.14825(19)	1.3338(11)	0.3357(4)	0.025(2)
C61	0.06092(18)	0.8952(10)	0.5394(3)	0.021(2)
C66	0.0765(2)	0.7918(11)	0.5226(4)	0.027(2)
C91	0.15434(19)	1.0981(11)	0.6672(4)	0.026(2)
C41	0.05184(18)	1.1005(11)	0.4617(4)	0.025(2)
C222	0.1827(2)	1.2810(12)	0.5241(4)	0.030(3)
C21	0.10340(19)	1.5054(10)	0.3518(4)	0.023(2)
C84	0.1147(2)	0.5957(11)	0.6438(4)	0.027(2)
C81	0.13726(19)	0.8408(11)	0.6237(3)	0.025(2)
C31	0.0892(2)	1.2506(11)	0.3016(4)	0.024(2)
C43	0.04001(19)	1.2572(12)	0.3886(4)	0.033(3)
C71	0.18624(18)	0.9682(9)	0.6006(3)	0.018(2)
C226	0.1702(2)	1.5087(11)	0.5100(3)	0.027(2)
C54	0.0318(2)	1.3393(11)	0.6343(4)	0.032(3)
C16	0.1507(2)	1.3086(12)	0.2840(4)	0.033(3)
C112	0.1732(2)	1.0364(11)	0.4159(4)	0.029(2)
C83	0.1384(2)	0.6000(11)	0.6215(4)	0.026(2)
C36	0.06523(19)	1.3182(11)	0.2730(4)	0.024(2)
C53	0.0150(2)	1.2932(10)	0.5871(4)	0.030(3)
C73	0.21760(19)	0.8981(10)	0.5432(4)	0.025(2)
C25	0.0807(2)	1.6899(11)	0.3854(4)	0.028(2)
C24	0.08555(19)	1.7687(12)	0.3447(4)	0.029(3)
C82	0.14977(19)	0.7231(11)	0.6116(4)	0.025(2)
C96	0.1541(2)	1.2358(12)	0.6639(4)	0.037(3)
C12	0.1723(2)	1.3674(11)	0.3734(4)	0.029(2)
C46	0.03689(18)	1.0014(11)	0.4289(3)	0.025(2)
C62	0.0379(2)	0.8649(11)	0.5621(4)	0.030(3)
C22	0.10841(19)	1.5857(10)	0.3108(4)	0.024(2)
C56	0.0716(2)	1.2179(11)	0.6175(4)	0.028(2)
C115	0.1832(2)	0.7695(14)	0.4001(4)	0.039(3)
C35	0.0458(2)	1.2538(12)	0.2324(4)	0.031(3)
C223	0.2109(2)	1.3097(13)	0.5229(4)	0.035(3)
C26	0.08953(19)	1.5563(11)	0.3887(4)	0.027(2)
C111	0.1527(2)	0.9428(12)	0.4223(4)	0.033(3)

C75	0.2363(2)	0.9377(12)	0.6347(5)	0.044(3)
C92	0.1584(2)	1.0413(12)	0.7171(4)	0.038(3)
C23	0.0996(2)	1.7170(11)	0.3079(4)	0.031(3)
C65	0.0681(2)	0.6594(12)	0.5270(4)	0.033(3)
C51	0.05541(19)	1.1711(10)	0.5699(4)	0.022(2)
C225	0.1980(2)	1.5390(12)	0.5090(4)	0.037(3)
C32	0.0931(2)	1.1198(11)	0.2888(4)	0.031(3)
C72	0.19059(19)	0.9307(11)	0.5515(4)	0.028(2)
C13	0.1985(2)	1.3766(13)	0.3602(4)	0.041(3)
C42	0.05294(19)	1.2267(12)	0.4417(4)	0.030(3)
C116	0.1583(2)	0.8078(12)	0.4140(4)	0.032(3)
C52	0.0265(2)	1.2100(10)	0.5552(4)	0.027(2)
C93	0.1626(2)	1.1151(14)	0.7622(4)	0.043(3)
C55	0.0602(2)	1.3004(11)	0.6490(4)	0.032(3)
C74	0.2405(2)	0.9043(12)	0.5856(5)	0.038(3)
C45	0.0244(2)	1.0309(13)	0.3767(4)	0.037(3)
C14	0.2012(2)	1.3509(13)	0.3094(4)	0.043(3)
C76	0.2095(2)	0.9703(10)	0.6437(4)	0.029(2)
C224	0.2187(2)	1.4382(14)	0.5152(4)	0.041(3)
C44	0.0265(2)	1.1552(13)	0.3565(4)	0.035(3)
C114	0.2034(2)	0.8653(15)	0.3944(4)	0.047(4)
C64	0.0451(2)	0.6294(12)	0.5488(4)	0.034(3)
C86	0.11303(19)	0.8335(11)	0.6448(3)	0.023(2)
C63	0.0301(2)	0.7317(12)	0.5665(4)	0.034(3)
C33	0.0742(2)	1.0574(12)	0.2489(4)	0.035(3)
C85	0.1020(2)	0.7112(11)	0.6558(4)	0.027(2)
C34	0.0505(2)	1.1248(12)	0.2207(4)	0.031(3)
C15	0.1771(2)	1.3190(13)	0.2711(4)	0.043(3)
C94	0.1629(2)	1.2498(14)	0.7594(4)	0.043(3)
C221	0.1621(2)	1.3803(11)	0.5170(3)	0.025(2)
C113	0.1980(2)	0.9966(14)	0.4013(4)	0.042(3)
C95	0.15830(14)	1.3142(7)	0.7108(3)	0.046(3)
O1	.00000(14)	0.4269(7)	0.7500(3)	0.056(3)
C1	0.97657(14)	0.3475(7)	0.7255(3)	0.048(3)
C2	0.98388(14)	0.2071(7)	0.7453(3)	0.050(3

Table 5.32 Anisotropic displacement parameters for **13·1.5THF**

Atom	U_{11}	U_{22}	U_{33}	U_{23}	U_{13}	U_{12}
Se1	0.0231(5)	0.0309(6)	0.0141(5)	-0.0014(4)	0.0042(4)	0.0023(4)
Se2	0.0237(5)	0.0285(6)	0.0141(5)	0.0012(4)	0.0031(4)	0.0019(4)
Cu2	0.0189(6)	0.0299(7)	0.0137(6)	0.0023(5)	0.0025(4)	0.0023(5)
Cu1	0.0231(6)	0.0322(8)	0.0147(6)	0.0008(5)	0.0043(5)	0.0022(5)
P1	0.0228(1)	0.0328(16)	0.0140(12)	0.0010(12)	0.0036(10)	0.0029(1)
P2	0.0177(2)	0.0314(16)	0.0154(13)	0.0013(11)	0.0030(10)	0.0006(1)
P3	0.0211(2)	0.0258(15)	0.0142(12)	0.0019(11)	0.0033(10)	0.0007(1)
C11	0.021(5)	0.035(6)	0.018(5)	-0.001(5)	0.001(4)	0.000(4)
C61	0.019(5)	0.030(6)	0.014(5)	-0.001(4)	0.004(4)	-0.004(4)
C66	0.026(5)	0.040(7)	0.015(5)	0.004(5)	0.007(4)	-0.003(5)
C91	0.024(5)	0.041(7)	0.013(5)	-0.002(5)	0.004(4)	0.001(5)
C41	0.016(5)	0.038(7)	0.022(5)	0.012(5)	0.008(4)	0.014(4)
C222	0.023(5)	0.041(7)	0.026(6)	-0.003(5)	0.004(4)	-0.003(5)
C21	0.024(5)	0.027(6)	0.017(5)	-0.003(5)	0.000(4)	0.002(4)
C84	0.031(5)	0.028(6)	0.019(5)	0.005(5)	-0.004(4)	-0.007(5)
C81	0.023(5)	0.042(7)	0.007(4)	0.002(5)	0.000(4)	-0.005(5)
C31	0.028(5)	0.032(7)	0.013(5)	0.007(5)	0.006(4)	-0.002(5)
C43	0.019(5)	0.050(8)	0.030(6)	0.014(6)	0.007(4)	0.005(5)
C71	0.019(5)	0.017(6)	0.015(5)	0.005(4)	0.002(4)	0.002(4)
C226	0.034(6)	0.032(7)	0.014(5)	-0.001(5)	0.006(4)	0.004(5)
C54	0.044(6)	0.027(6)	0.032(6)	0.001(5)	0.023(5)	0.004(5)
C16	0.024(5)	0.056(8)	0.019(5)	-0.002(5)	0.005(4)	0.003(5)
C83	0.029(5)	0.029(6)	0.019(5)	0.002(5)	0.002(4)	0.001(5)
C36	0.022(5)	0.031(6)	0.021(5)	0.001(5)	0.005(4)	0.002(4)
C53	0.032(6)	0.026(6)	0.038(6)	0.005(5)	0.016(5)	0.005(5)
C73	0.028(5)	0.022(6)	0.030(6)	0.005(5)	0.015(4)	0.001(4)
C25	0.027(5)	0.033(7)	0.021(5)	-0.005(5)	-0.001(4)	0.003(5)
C24	0.021(5)	0.039(7)	0.024(6)	-0.001(5)	-0.005(4)	0.001(5)
C82	0.019(5)	0.045(7)	0.012(5)	0.008(5)	0.005(4)	0.003(5)
C96	0.050(7)	0.044(8)	0.014(5)	-0.006(5)	0.003(5)	0.011(6)
C12	0.029(5)	0.041(7)	0.015(5)	-0.009(5)	0.005(4)	0.000(5)
C46	0.021(5)	0.038(6)	0.013(5)	-0.003(5)	-0.003(4)	-0.007(5)
C62	0.028(5)	0.039(7)	0.021(5)	0.003(5)	0.003(4)	0.009(5)
C22	0.028(5)	0.031(7)	0.015(5)	-0.002(5)	0.005(4)	-0.001(5)
C56	0.025(5)	0.042(7)	0.019(5)	0.001(5)	0.005(4)	0.008(5)
C115	0.030(6)	0.069(9)	0.018(5)	0.006(6)	0.005(4)	0.019(6)
C35	0.027(5)	0.045(8)	0.019(5)	0.005(5)	0.001(4)	-0.003(5)
C223	0.024(5)	0.057(8)	0.027(6)	0.004(6)	0.008(4)	0.001(5)
C26	0.025(5)	0.041(7)	0.013(5)	0.008(5)	-0.002(4)	-0.001(5)
C111	0.036(6)	0.050(8)	0.013(5)	-0.003(5)	0.003(4)	0.014(5)
C75	0.028(6)	0.047(8)	0.044(7)	-0.008(6)	-0.019(5)	0.000(5)
C92	0.054(7)	0.035(7)	0.023(6)	-0.001(5)	0.004(5)	-0.010(6)
C23	0.031(6)	0.034(7)	0.025(6)	0.002(5)	0.001(5)	-0.001(5)

C65	0.035(6)	0.039(7)	0.024(6)	0.002(5)	0.001(5)	0.002(5)
C51	0.028(5)	0.019(6)	0.022(5)	0.007(4)	0.010(4)	0.000(4)
C225	0.052(7)	0.041(8)	0.020(6)	-0.010(5)	0.009(5)	-0.021(6)
C32	0.025(5)	0.045(8)	0.020(5)	0.002(5)	-0.002(4)	0.002(5)
C72	0.020(5)	0.037(7)	0.023(6)	0.006(5)	0.000(4)	0.001(5)
C13	0.031(6)	0.065(9)	0.026(6)	-0.003(6)	0.005(5)	-0.009(6)
C42	0.019(5)	0.047(8)	0.024(6)	0.004(5)	0.003(4)	-0.001(5)
C116	0.027(5)	0.052(8)	0.014(5)	0.000(5)	0.001(4)	0.007(5)
C52	0.024(5)	0.036(7)	0.021(5)	0.002(5)	0.003(4)	-0.002(4)
C93	0.055(7)	0.065(10)	0.007(5)	-0.005(6)	0.006(5)	-0.020(6)
C55	0.032(6)	0.041(7)	0.023(6)	0.003(5)	0.005(4)	-0.003(5)
C74	0.019(5)	0.045(8)	0.048(7)	-0.009(6)	0.005(5)	0.001(5)
C45	0.027(6)	0.053(9)	0.030(6)	-0.009(6)	0.003(5)	0.003(5)
C14	0.032(6)	0.062(9)	0.034(7)	-0.003(6)	0.007(5)	-0.001(6)
C76	0.026(5)	0.032(7)	0.029(6)	-0.003(5)	0.006(4)	0.003(4)
C224	0.032(6)	0.064(9)	0.029(6)	-0.006(6)	0.008(5)	-0.011(6)
C44	0.025(5)	0.065(9)	0.017(5)	0.009(6)	0.007(4)	0.007(6)
C114	0.039(7)	0.081(11)	0.024(6)	0.015(6)	0.011(5)	0.032(7)
C64	0.029(6)	0.041(7)	0.029(6)	0.007(5)	0.001(5)	-0.005(5)
C86	0.022(5)	0.033(6)	0.014(5)	0.003(5)	0.002(4)	-0.001(5)
C63	0.026(5)	0.045(8)	0.030(6)	0.013(5)	0.009(5)	-0.001(5)
C33	0.048(7)	0.026(6)	0.029(6)	-0.005(5)	0.007(5)	-0.007(5)
C85	0.020(5)	0.042(7)	0.018(5)	0.002(5)	0.003(4)	-0.002(5)
C34	0.025(5)	0.044(8)	0.022(5)	0.003(5)	0.000(4)	-0.009(5)
C15	0.037(6)	0.070(9)	0.024(6)	-0.010(6)	0.012(5)	-0.005(6)
C94	0.029(6)	0.072(10)	0.024(6)	-0.024(7)	-0.001(5)	0.012(6)
C221	0.029(5)	0.039(7)	0.008(5)	-0.003(5)	0.003(4)	-0.006(5)
C113	0.024(6)	0.076(10)	0.029(6)	0.021(6)	0.012(5)	0.009(6)
C95	0.055(7)	0.054(8)	0.022(6)	0.002(6)	-0.007(5)	0.029(6)
O1	0.039(7)	0.061(9)	0.063(8)	0.000	-0.003(6)	0.000
C1	0.022(5)	0.062(9)	0.051(8)	-0.005(7)	-0.012(5)	-0.005(6)
C2	0.036(6)	0.069(10)	0.043(7)	-0.010(7)	0.006(5)	-0.007(6)

5.13 [(Ph$_3$PAg)$_8$(SePh)$_{12}$(μ_6-Se)Ag$_6$]·6THF (14·6THF)

Compound **14·6THF** crystallizes as yellow needles upon layering a THF solution by *n*-hexane.

Table 5.33 Crystal data and structure refinement for **14·6THF**

Empirical formula	C$_{240}$H$_{228}$O$_6$Ag$_{14}$Se$_{13}$P$_8$
Formula weight /g·mol^{-1}	5992.64
Crystal system	monoclinic
Space group	$P2_1/c$
a /Å	31.7987(9)
b /Å	22.9837(4)
c /Å	33.2185(8)
β /°	92.257(2)
V /Å^3	24259.0(10)
Z	4
ρ_{calc} /g·cm^{-3}	1.710
μ(Mo$_{K\alpha}$) /mm^{-1}	3.162
2Θ range /°	4-52
Reflections measured	47148
Independent reflections	47148
R(int)	0.18
Ind. reflections ($I > 2\sigma(I)$)	15371
Parameters	2724
R_1 ($I > 2\sigma(I)$)	0.0743
wR_2 (all data)	0.1625
GooF (all data)	0.780
Max. peak/hole /e$^-$·10^{-6}pm^{-3}	1.211/–1.419

Table 5.34 Atomic coordinates and equivalent isotropic displacement parameters for **14·6THF**

Atom	x/a	y/b	z/c	$U_{eq/iso}$
Ag1	0.26191(4)	0.44519(5)	0.70592(3)	0.0375(3)
Ag2	0.13916(4)	0.40677(5)	0.78851(4)	0.0438(3)
Ag3	0.23031(4)	0.34094(5)	0.90014(4)	0.0406(3)
Ag4	0.36167(4)	0.38269(5)	0.81757(4)	0.0377(3)
Ag5	0.26130(4)	0.38236(5)	0.81714(4)	0.0415(3)
Ag6A	0.21314(5)	0.53497(6)	0.76390(5)	0.0378(4)
Ag6B	0.1879(2)	0.5216(2)	0.77978(18)	0.0378(4)
Ag7	0.18668(4)	0.50236(5)	0.88562(4)	0.0382(3)
Ag8	0.31833(4)	0.47323(5)	0.87685(4)	0.0369(3)
Ag9	0.30976(4)	0.54777(5)	0.79743(4)	0.0366(3)
Ag10	0.25592(4)	0.65331(5)	0.75796(4)	0.0438(3)
Ag11	0.13945(4)	0.60313(5)	0.84786(4)	0.0419(3)
Ag12	0.23919(4)	0.53611(5)	0.95916(4)	0.0383(3)
Ag13	0.36881(4)	0.59561(5)	0.87014(3)	0.0358(3)
Ag14	0.26611(4)	0.59349(5)	0.87264(3)	0.0376(3)
Se1	0.24708(5)	0.49357(6)	0.83187(5)	0.0345(4)
Se2	0.21150(5)	0.38119(7)	0.75207(5)	0.0405(4)
Se3	0.16484(5)	0.39639(7)	0.86690(5)	0.0389(4)
Se4	0.30425(5)	0.31811(7)	0.86560(5)	0.0399(4)
Se5	0.33036(5)	0.45116(6)	0.75793(4)	0.0349(4)
Se6A	0.25148(7)	0.56473(9)	0.70210(7)	0.0400(5)
Se6B	0.2358(3)	0.5513(4)	0.7214(3)	0.0400(5)
Se7A	0.13750(7)	0.52387(9)	0.79112(6)	0.0377(5)
Se7B	0.1117(3)	0.5142(3)	0.7997(2)	0.0377(5)
Se8	0.27195(5)	0.43876(7)	0.93573(5)	0.0342(4)
Se9	0.39346(5)	0.48425(6)	0.85305(5)	0.0349(4)
Se10	0.21340(5)	0.65237(7)	0.82520(5)	0.0368(4)
Se11	0.17222(5)	0.59432(7)	0.92542(5)	0.0388(4)
Se12	0.31711(5)	0.60313(7)	0.93344(4)	0.0365(4)
Se13	0.33580(5)	0.65272(7)	0.80365(5)	0.0380(4)
P1	0.27346(14)	0.41314(17)	0.63542(12)	0.0388(10)
P2	0.07304(15)	0.35913(19)	0.76757(15)	0.0492(12)
P3	0.21722(14)	0.26222(18)	0.94838(14)	0.0414(11)
P4	0.41812(13)	0.30581(17)	0.81930(12)	0.0346(10)
P5	0.26601(16)	0.74419(18)	0.71927(13)	0.0429(11)
P6	0.07995(14)	0.67081(18)	0.85237(14)	0.0434(11)
P7	0.24024(14)	0.57288(18)	1.02931(12)	0.0384(10)
P8	0.43988(14)	0.64390(18)	0.88664(12)	0.0373(10)
O1	0.5707(5)	0.4744(5)	0.7217(5)	0.083(5)
O2	0.2982(5)	0.4177(6)	0.1727(5)	0.089(5)
O3	0.4230(7)	0.1830(11)	0.0625(7)	0.157(9)

O4	0.9362(8)	0.7607(12)	0.9385(8)	0.146(9)
O5	0.5088(7)	0.0645(9)	0.9069(7)	0.135(8)
O6	0.1890(12)	0.9007(17)	0.9781(11)	0.232(13)
O7	0.0592(10)	0.7539(14)	0.6021(8)	0.196(11)
C1	0.2075(5)	0.3074(7)	0.7237(5)	0.041(4)
C2	0.1721(6)	0.2807(7)	0.7136(5)	0.051(5)
C3	0.1699(5)	0.2296(7)	0.6914(5)	0.043(4)
C4	0.2056(8)	0.2006(8)	0.6828(5)	0.063(6)
C5	0.2469(8)	0.2255(8)	0.6935(5)	0.064(6)
C6	0.2465(6)	0.2768(7)	0.7135(5)	0.049(5)
C7	0.1143(6)	0.3721(8)	0.8927(7)	0.070(6)
C8	0.0837(5)	0.4190(8)	0.9024(6)	0.061(6)
C9	0.0457(6)	0.4034(12)	0.9182(7)	0.089(8)
C10	0.0404(7)	0.3429(13)	0.9291(7)	0.092(8)
C11	0.0687(8)	0.3020(10)	0.9207(8)	0.089(8)
C12	0.1049(6)	0.3173(7)	0.9028(6)	0.056(5)
C13	0.2935(5)	0.2408(7)	0.8470(5)	0.037(4)
C14	0.3104(6)	0.1945(7)	0.8677(5)	0.053(5)
C15	0.3053(6)	0.1355(8)	0.8578(6)	0.057(5)
C16	0.2759(8)	0.1260(8)	0.8239(7)	0.079(8)
C17	0.2567(6)	0.1718(7)	0.8040(6)	0.058(5)
C18	0.2645(5)	0.2275(7)	0.8147(5)	0.039(4)
C19	0.3723(6)	0.4636(8)	0.7188(4)	0.049(5)
C20	0.4097(7)	0.4295(13)	0.7222(8)	0.128(13)
C21	0.4368(8)	0.4325(12)	0.6881(7)	0.097(8)
C22	0.4326(6)	0.4756(8)	0.6593(6)	0.063(6)
C23	0.3960(6)	0.5051(8)	0.6581(5)	0.061(5)
C24	0.3665(5)	0.5006(7)	0.6880(4)	0.037(4)
C25	0.2094(5)	0.5703(6)	0.6600(5)	0.042(4)
C26	0.2083(7)	0.6186(8)	0.6370(6)	0.069(6)
C27	0.1838(10)	0.6231(12)	0.6010(7)	0.112(10)
C28	0.1606(10)	0.5771(10)	0.5888(7)	0.103(10)
C29	0.1588(6)	0.5280(9)	0.6134(5)	0.062(6)
C30	0.1833(5)	0.5259(6)	0.6496(4)	0.041(4)
C31	0.0941(5)	0.5446(6)	0.7520(5)	0.043(4)
C32	0.1054(5)	0.5685(7)	0.7143(6)	0.053(5)
C33	0.0777(6)	0.5806(7)	0.6841(5)	0.050(5)
C34	0.0335(6)	0.5759(6)	0.6894(6)	0.056(5)
C35	0.0214(6)	0.5584(8)	0.7274(6)	0.059(5)
C36	0.0513(6)	0.5430(6)	0.7575(5)	0.046(4)
C37	0.3038(5)	0.4138(6)	0.9832(5)	0.037(4)
C38	0.2863(6)	0.4072(6)	1.0206(5)	0.048(5)
C39	0.3094(6)	0.3906(8)	1.0530(5)	0.054(5)
C40	0.3512(6)	0.3766(8)	1.0525(6)	0.062(5)
C41	0.3688(7)	0.3842(7)	1.0150(6)	0.059(5)
C42	0.3479(5)	0.3994(7)	0.9818(5)	0.048(5)

C43	0.4288(6)	0.4678(7)	0.8998(4)	0.045(4)
C44	0.4198(5)	0.4869(6)	0.9381(5)	0.036(4)
C45	0.4467(5)	0.4731(7)	0.9706(5)	0.046(4)
C46	0.4842(5)	0.4421(7)	0.9649(5)	0.040(4)
C47	0.4936(5)	0.4246(7)	0.9257(5)	0.039(4)
C48	0.4674(5)	0.4384(7)	0.8943(5)	0.037(4)
C49	0.2063(5)	0.7318(7)	0.8368(5)	0.038(4)
C50	0.2227(5)	0.7560(7)	0.8740(5)	0.042(4)
C51	0.2180(6)	0.8162(8)	0.8805(6)	0.068(6)
C52	0.1934(6)	0.8500(8)	0.8545(6)	0.061(5)
C53	0.1773(6)	0.8270(7)	0.8216(6)	0.060(5)
C54	0.1822(6)	0.7672(8)	0.8128(6)	0.057(5)
C55	0.1273(6)	0.5756(8)	0.9617(5)	0.055(5)
C56	0.1131(5)	0.5189(7)	0.9692(5)	0.048(5)
C57	0.0806(6)	0.5110(9)	0.9948(6)	0.067(6)
C58	0.0631(6)	0.5562(9)	1.0121(6)	0.062(6)
C59	0.0745(6)	0.6116(11)	1.0051(6)	0.078(7)
C60	0.1073(6)	0.6230(7)	0.9801(5)	0.053(5)
C61	0.3240(5)	0.6856(8)	0.9449(5)	0.043(4)
C62	0.3324(5)	0.7026(9)	0.9845(4)	0.052(5)
C63	0.3380(5)	0.7613(9)	0.9928(6)	0.059(6)
C64	0.3330(5)	0.8032(6)	0.9626(5)	0.044(4)
C65	0.3239(6)	0.7865(8)	0.9246(6)	0.058(5)
C66	0.3198(5)	0.7265(6)	0.9151(5)	0.037(4)
C67	0.3865(5)	0.6550(8)	0.7727(6)	0.057(5)
C68	0.4016(5)	0.6057(9)	0.7548(5)	0.054(5)
C69	0.4357(6)	0.6073(8)	0.7300(5)	0.056(5)
C70	0.4519(6)	0.6636(8)	0.7197(5)	0.059(5)
C71	0.4366(6)	0.7118(9)	0.7356(6)	0.060(5)
C72	0.4028(6)	0.7110(7)	0.7613(5)	0.052(5)
C111	0.3029(5)	0.3464(6)	0.6335(5)	0.037(4)
C112	0.3347(5)	0.3352(7)	0.6617(5)	0.041(4)
C113	0.3594(5)	0.2862(7)	0.6611(5)	0.045(4)
C114	0.3517(7)	0.2432(8)	0.6314(6)	0.066(6)
C115	0.3202(7)	0.2546(7)	0.6026(6)	0.061(6)
C116	0.2962(6)	0.3026(7)	0.6036(5)	0.053(5)
C121	0.3023(6)	0.4594(6)	0.6019(5)	0.046(4)
C122	0.3349(6)	0.4427(8)	0.5792(5)	0.056(5)
C123	0.3540(6)	0.4825(8)	0.5546(6)	0.062(5)
C124	0.3433(6)	0.5384(8)	0.5491(6)	0.063(5)
C125	0.3106(7)	0.5535(8)	0.5704(6)	0.069(6)
C126	0.2901(6)	0.5174(7)	0.5968(5)	0.052(5)
C131	0.2244(5)	0.3976(6)	0.6065(5)	0.042(4)
C132	0.2166(7)	0.4092(9)	0.5647(5)	0.064(6)
C133	0.1799(6)	0.3946(9)	0.5455(6)	0.065(6)
C134	0.1503(6)	0.3660(9)	0.5658(6)	0.059(5)

C135	0.1565(5)	0.3525(8)	0.6065(5)	0.049(5)
C136	0.1934(5)	0.3678(7)	0.6251(5)	0.044(4)
C211	0.1100(6)	0.2566(8)	0.7946(5)	0.050(5)
C212	0.1100(8)	0.1938(9)	0.8056(6)	0.080(7)
C213	0.0731(8)	0.1657(8)	0.8012(6)	0.073(7)
C214	0.0340(7)	0.1922(9)	0.7842(6)	0.073(6)
C215	0.0365(6)	0.2498(8)	0.7772(6)	0.066(6)
C216	0.0722(6)	0.2820(8)	0.7791(5)	0.054(5)
C221	0.0226(5)	0.3862(9)	0.7856(7)	0.061(5)
C222	0.0141(5)	0.3666(8)	0.8252(7)	0.064(6)
C223	-0.0264(7)	0.3869(10)	0.8390(6)	0.075(6)
C224	-0.0523(6)	0.4236(8)	0.8172(7)	0.058(5)
C225	-0.0409(7)	0.4401(7)	0.7788(6)	0.055(5)
C226	-0.0052(6)	0.4215(7)	0.7627(6)	0.056(5)
C231	0.0627(5)	0.3617(7)	0.7127(5)	0.039(4)
C232	0.0418(7)	0.3207(11)	0.6894(7)	0.090(8)
C233	0.0353(6)	0.3295(11)	0.6481(7)	0.084(7)
C234	0.0485(6)	0.3804(10)	0.6304(6)	0.062(5)
C235	0.0677(7)	0.4221(9)	0.6521(7)	0.066(6)
C236	0.0775(6)	0.4139(8)	0.6931(6)	0.062(5)
C311	0.2624(5)	0.2201(7)	0.9648(4)	0.036(4)
C312	0.2969(6)	0.2487(7)	0.9768(5)	0.045(5)
C313	0.3334(6)	0.2203(7)	0.9928(5)	0.049(5)
C314	0.3342(6)	0.1598(8)	0.9961(5)	0.051(5)
C315	0.2995(6)	0.1311(7)	0.9839(5)	0.046(5)
C316	0.2631(6)	0.1594(7)	0.9695(5)	0.050(5)
C321	0.1807(6)	0.2059(8)	0.9332(5)	0.050(5)
C322	0.1446(6)	0.1905(8)	0.9552(6)	0.065(6)
C323	0.1170(7)	0.1439(10)	0.9449(8)	0.090(8)
C324	0.1264(11)	0.1122(11)	0.9114(8)	0.108(10)
C325	0.1619(9)	0.1281(9)	0.8875(8)	0.090(8)
C326	0.1874(7)	0.1745(9)	0.9003(7)	0.074(6)
C331	0.1994(6)	0.2919(7)	0.9945(5)	0.043(4)
C332	0.2061(6)	0.2681(8)	1.0325(6)	0.061(5)
C333	0.1964(7)	0.2950(8)	1.0675(5)	0.063(6)
C334	0.1771(6)	0.3479(9)	1.0640(6)	0.059(5)
C335	0.1691(5)	0.3733(7)	1.0290(5)	0.042(4)
C336	0.1802(5)	0.3481(7)	0.9946(6)	0.053(5)
C411	0.4735(5)	0.3229(7)	0.8196(4)	0.042(4)
C412	0.5040(5)	0.2991(7)	0.8453(5)	0.041(4)
C413	0.5449(5)	0.3171(8)	0.8465(5)	0.050(5)
C414	0.5584(6)	0.3594(7)	0.8199(5)	0.048(5)
C415	0.5307(5)	0.3809(7)	0.7918(5)	0.049(5)
C416	0.4877(6)	0.3658(7)	0.7923(6)	0.057(5)
C421	0.4096(5)	0.2538(7)	0.7801(4)	0.036(4)
C422	0.4414(6)	0.2245(7)	0.7604(5)	0.052(5)

C423	0.4316(6)	0.1786(7)	0.7329(5)	0.047(5)
C424	0.3913(6)	0.1639(6)	0.7233(4)	0.040(4)
C425	0.3589(6)	0.1932(7)	0.7427(5)	0.053(5)
C426	0.3688(5)	0.2365(6)	0.7691(4)	0.037(4)
C431	0.4157(5)	0.2616(7)	0.8663(5)	0.039(4)
C432	0.4210(5)	0.2032(7)	0.8679(4)	0.039(4)
C433	0.4245(5)	0.1755(7)	0.9048(5)	0.042(4)
C434	0.4228(5)	0.2050(8)	0.9389(6)	0.055(5)
C435	0.4202(5)	0.2662(8)	0.9374(5)	0.040(4)
C436	0.4154(5)	0.2935(8)	0.9021(5)	0.047(5)
C511	0.2965(5)	0.7986(7)	0.7450(5)	0.047(4)
C512	0.2836(7)	0.8151(7)	0.7846(5)	0.060(6)
C513	0.3061(6)	0.8580(8)	0.8041(5)	0.057(5)
C514	0.3419(6)	0.8890(10)	0.7910(7)	0.079(7)
C515	0.3526(7)	0.8725(7)	0.7543(6)	0.067(6)
C516	0.3328(6)	0.8275(7)	0.7324(5)	0.055(5)
C521	0.2229(7)	0.7864(8)	0.6995(5)	0.050(5)
C522	0.1868(7)	0.7540(11)	0.6874(6)	0.082(8)
C523	0.1525(6)	0.7810(10)	0.6670(6)	0.064(6)
C524	0.1542(8)	0.8403(11)	0.6590(6)	0.072(6)
C525	0.1862(8)	0.8721(9)	0.6685(5)	0.070(7)
C526	0.2206(9)	0.8440(10)	0.6897(6)	0.090(8)
C531	0.2948(5)	0.7300(7)	0.6739(5)	0.042(4)
C532	0.3309(6)	0.6933(7)	0.6783(6)	0.053(5)
C533	0.3530(7)	0.6753(9)	0.6454(5)	0.070(6)
C534	0.3420(6)	0.6977(7)	0.6080(5)	0.053(5)
C535	0.3053(6)	0.7333(9)	0.6032(5)	0.059(5)
C536	0.2841(6)	0.7480(7)	0.6348(5)	0.046(4)
C611	0.0788(6)	0.7211(7)	0.8943(5)	0.048(5)
C612	0.1169(5)	0.7475(7)	0.9067(5)	0.044(4)
C613	0.1168(5)	0.7877(9)	0.9382(6)	0.062(6)
C614	0.0818(6)	0.8022(9)	0.9583(6)	0.065(6)
C615	0.0429(6)	0.7707(9)	0.9485(7)	0.081(8)
C616	0.0438(6)	0.7333(9)	0.9189(7)	0.073(7)
C621	0.0773(5)	0.7208(6)	0.8100(6)	0.042(4)
C622	0.0702(6)	0.7792(8)	0.8128(5)	0.057(5)
C623	0.0700(6)	0.8141(7)	0.7795(6)	0.052(5)
C624	0.0772(6)	0.7905(8)	0.7424(6)	0.060(5)
C625	0.0832(5)	0.7325(7)	0.7398(6)	0.054(5)
C626	0.0835(6)	0.6969(8)	0.7732(6)	0.053(5)
C631	0.0277(6)	0.6337(7)	0.8473(6)	0.054(5)
C632	-0.0055(6)	0.6520(9)	0.8240(6)	0.061(5)
C633	-0.0397(6)	0.6194(8)	0.8199(7)	0.063(6)
C634	-0.0468(7)	0.5703(10)	0.8389(7)	0.077(7)
C635	-0.0142(7)	0.5508(10)	0.8635(10)	0.120(11)
C636	0.0244(6)	0.5826(8)	0.8692(7)	0.069(6)

C711	0.2209(4)	0.6480(7)	1.0298(4)	0.032(4)
C712	0.2278(4)	0.6833(6)	0.9971(5)	0.037(4)
C713	0.2131(6)	0.7396(7)	0.9949(6)	0.056(5)
C714	0.1931(8)	0.7626(8)	1.0262(6)	0.079(7)
C715	0.1833(6)	0.7299(7)	1.0608(6)	0.060(5)
C716	0.1995(5)	0.6728(7)	1.0610(5)	0.042(4)
C721	0.2929(5)	0.5795(6)	1.0533(4)	0.038(4)
C722	0.3259(5)	0.5457(6)	1.0377(5)	0.035(4)
C723	0.3665(5)	0.5481(6)	1.0555(4)	0.035(4)
C724	0.3736(5)	0.5836(6)	1.0885(5)	0.037(4)
C725	0.3419(6)	0.6188(8)	1.1052(5)	0.051(5)
C726	0.3020(5)	0.6141(7)	1.0866(4)	0.041(4)
C731	0.2092(5)	0.5379(7)	1.0673(5)	0.039(4)
C732	0.1655(6)	0.5400(8)	1.0666(5)	0.055(5)
C733	0.1410(5)	0.5110(7)	1.0941(5)	0.044(4)
C734	0.1600(6)	0.4815(10)	1.1237(6)	0.068(6)
C735	0.2031(7)	0.4741(7)	1.1264(5)	0.059(5)
C736	0.2298(7)	0.5042(8)	1.0965(5)	0.062(5)
C811	0.4520(5)	0.6673(7)	0.9384(4)	0.036(4)
C812	0.4826(6)	0.7087(7)	0.9484(5)	0.051(5)
C813	0.4909(6)	0.7259(8)	0.9873(5)	0.056(5)
C814	0.4680(6)	0.7035(9)	1.0193(6)	0.065(6)
C815	0.4382(6)	0.6620(8)	1.0103(5)	0.051(5)
C816	0.4294(4)	0.6447(6)	0.9710(5)	0.037(4)
C821	0.4475(5)	0.7138(6)	0.8606(4)	0.036(4)
C822	0.4837(6)	0.7263(7)	0.8373(5)	0.050(5)
C823	0.4908(6)	0.7771(8)	0.8187(5)	0.055(5)
C824	0.4578(5)	0.8210(7)	0.8215(5)	0.043(4)
C825	0.4228(6)	0.8079(7)	0.8444(5)	0.045(4)
C826	0.4176(6)	0.7557(7)	0.8623(5)	0.050(5)
C831	0.4857(5)	0.5976(7)	0.8742(5)	0.041(4)
C832	0.5187(5)	0.5873(7)	0.8987(5)	0.048(5)
C833	0.5508(5)	0.5507(8)	0.8847(6)	0.056(5)
C834	0.5508(6)	0.5288(8)	0.8468(6)	0.054(5)
C835	0.5146(5)	0.5388(8)	0.8230(5)	0.050(4)
C836	0.4831(5)	0.5754(7)	0.8348(5)	0.047(4)
C4E	0.0288(10)	0.7168(13)	0.6239(8)	0.114(11)
C701	0.0673(12)	0.7181(18)	0.5700(9)	0.168(17)
C703	0.0126(9)	0.6681(14)	0.5965(9)	0.124(11)
C304	0.4345(5)	0.1400(8)	0.0340(4)	0.038(4)
C702	0.0247(16)	0.6923(17)	0.5564(9)	0.19(2)
C201	0.2887(7)	0.4322(10)	0.2127(8)	0.101(10)
C202	0.2849(9)	0.4964(10)	0.2136(10)	0.115(11)
C203	0.3112(11)	0.5179(11)	0.1809(7)	0.132(14)
C303	0.4705(7)	0.1066(11)	0.0500(7)	0.092(7)
C301	0.4419(6)	0.1637(11)	0.1013(8)	0.095(8)

C302	0.4815(7)	0.1358(11)	0.0900(7)	0.086(7)
C404	0.9210(11)	0.718(2)	0.9094(15)	0.17(2)
C403	0.9320(8)	0.657(2)	0.9237(10)	0.151(17)
C402	0.9461(9)	0.6680(13)	0.9691(10)	0.124(12)
C401	0.9379(15)	0.7293(16)	0.9744(10)	0.20(2)
C501	0.5270(8)	0.1112(12)	0.8864(10)	0.124(12)
C502	0.5466(10)	0.1472(18)	0.9163(13)	0.191(19)
C503	0.5437(15)	0.1265(16)	0.9569(11)	0.181(19)
C204	0.3281(6)	0.4661(10)	0.1640(6)	0.071(6)
C504	0.5289(12)	0.0692(19)	0.9497(12)	0.164(16)
C104	0.5966(8)	0.5196(9)	0.7312(5)	0.113(11)
C103	0.6056(6)	0.5550(9)	0.6961(6)	0.086(7)
C102	0.5627(8)	0.5523(10)	0.6766(9)	0.146(15)
C101	0.5505(11)	0.4931(13)	0.6849(11)	0.24(3)
C602	0.2119(13)	0.9877(15)	0.9484(13)	0.169(16)
C604	0.2347(13)	0.9094(17)	0.9923(12)	0.179(16)
C603	0.2463(13)	0.9560(17)	0.9683(12)	0.196(18)
C601	0.1747(18)	0.953(2)	0.9575(16)	0.22(2)
O9	0.5929(17)	0.9830(17)	0.0494(14)	0.42(4)
C904	0.5820(10)	1.039(2)	0.0441(11)	0.21(2)
C903	0.5890(17)	1.0700(19)	0.0821(17)	0.52(9)
C902	0.6317(15)	1.0468(17)	0.0912(11)	0.45(7)
C901	0.6315(12)	0.9903(14)	0.0726(13)	0.172(16)
O8	0.8642(7)	0.5117(11)	0.7720(6)	0.165(10)
C801	0.8432(11)	0.4720(12)	0.7497(10)	0.19(2)
C802	0.8194(15)	0.4922(16)	0.7152(12)	0.27(3)
C803	0.831(2)	0.5541(15)	0.7165(11)	0.41(6)
C804	0.8474(10)	0.5641(10)	0.7567(9)	0.139(14)
O10	0.0611(10)	0.0182(13)	0.8548(10)	0.248(18)
C91	0.0672(18)	-0.0361(18)	0.8418(8)	0.30(4)
C92	0.0809(14)	-0.0751(11)	0.8732(14)	0.23(3)
C93	0.0588(11)	-0.0491(18)	0.9068(10)	0.22(2)
C94	0.0394(9)	0.0022(12)	0.8904(10)	0.125(11)

Table 5.32 Anisotropic displacement parameters for **14·6THF**

Atom	U_{11}	U_{22}	U_{33}	U_{23}	U_{13}	U_{12}
Ag1	0.0496(8)	0.0325(6)	0.0307(7)	-0.0013(6)	0.0037(6)	-0.0018(6)
Ag2	0.0401(8)	0.0363(7)	0.0548(8)	0.0040(6)	-0.0007(6)	-0.0043(6)
Ag3	0.0441(8)	0.0328(7)	0.0454(7)	0.0087(6)	0.0079(6)	0.0029(6)
Ag4	0.0450(8)	0.0317(6)	0.0364(7)	0.0001(6)	0.0021(6)	0.0033(5)
Ag5	0.0514(8)	0.0301(6)	0.0437(7)	0.0043(6)	0.0088(6)	0.0003(6)
Ag6A	0.0462(10)	0.0322(8)	0.0350(9)	0.0011(7)	0.0000(7)	0.0017(7)
Ag6B	0.0462(10)	0.0322(8)	0.0350(9)	0.0011(7)	0.0000(7)	0.0017(7)
Ag7	0.0392(7)	0.0354(6)	0.0400(7)	0.0010(6)	-0.0002(5)	0.0035(6)
Ag8	0.0384(7)	0.0357(7)	0.0366(7)	-0.0015(6)	0.0022(5)	-0.0004(6)
Ag9	0.0450(7)	0.0296(6)	0.0353(7)	0.0043(6)	0.0043(6)	-0.0025(5)
Ag10	0.0653(9)	0.0310(7)	0.0349(7)	0.0040(6)	-0.0001(6)	-0.0068(6)
Ag11	0.0397(7)	0.0347(7)	0.0509(8)	-0.0012(6)	-0.0040(6)	0.0050(6)
Ag12	0.0434(7)	0.0380(7)	0.0337(7)	-0.0023(6)	0.0024(5)	0.0069(6)
Ag13	0.0434(7)	0.0328(6)	0.0312(6)	0.0003(6)	0.0018(5)	-0.0002(5)
Ag14	0.0425(7)	0.0361(7)	0.0341(7)	-0.0003(6)	0.0015(6)	-0.0016(6)
Se1	0.0415(9)	0.0286(8)	0.0333(8)	0.0025(7)	-0.0014(7)	-0.0007(7)
Se2	0.0501(11)	0.0321(9)	0.0397(9)	0.0019(8)	0.0077(8)	-0.0061(8)
Se3	0.0367(10)	0.0341(9)	0.0461(10)	0.0027(8)	0.0037(8)	-0.0027(7)
Se4	0.0448(11)	0.0353(9)	0.0402(10)	-0.0008(8)	0.0076(8)	0.0018(7)
Se5	0.0433(10)	0.0314(8)	0.0301(8)	0.0007(7)	0.0048(7)	-0.0006(7)
Se6A	0.0444(14)	0.0343(11)	0.0413(14)	-0.0027(9)	0.0042(10)	0.0013(10)
Se6B	0.0444(14)	0.0343(11)	0.0413(14)	-0.0027(9)	0.0042(10)	0.0013(10)
Se7A	0.0413(14)	0.0325(11)	0.0391(12)	0.0008(9)	-0.0022(9)	-0.0012(9)
Se7B	0.0413(14)	0.0325(11)	0.0391(12)	0.0008(9)	-0.0022(9)	-0.0012(9)
Se8	0.0383(10)	0.0325(8)	0.0318(9)	0.0003(7)	0.0020(7)	0.0029(7)
Se9	0.0404(10)	0.0322(9)	0.0322(8)	0.0016(7)	0.0004(7)	0.0021(7)
Se10	0.0427(10)	0.0299(8)	0.0378(9)	0.0027(8)	0.0008(7)	-0.0028(7)
Se11	0.0401(10)	0.0373(9)	0.0394(9)	0.0006(8)	0.0045(7)	0.0050(8)
Se12	0.0431(10)	0.0371(9)	0.0296(8)	0.0000(7)	0.0032(7)	-0.0030(7)
Se13	0.0531(11)	0.0266(8)	0.0341(9)	0.0053(7)	-0.0022(8)	-0.0015(7)
P1	0.055(3)	0.033(2)	0.029(2)	-0.0020(2)	0.005(2)	0.002(2)
P2	0.043(3)	0.039(3)	0.066(3)	-0.002(2)	0.002(2)	-0.001(2)
P3	0.046(3)	0.032(2)	0.047(3)	0.013(2)	0.009(2)	0.004(2)
P4	0.038(3)	0.034(2)	0.031(2)	0.0023(19)	0.0069(19)	0.0048(18)
P5	0.068(3)	0.030(2)	0.031(2)	0.005(2)	0.003(2)	-0.007(2)
P6	0.039(3)	0.035(2)	0.055(3)	-0.003(2)	-0.004(2)	0.0063(19)
P7	0.046(3)	0.037(2)	0.032(2)	0.006(2)	0.005(2)	0.0039(19)
P8	0.044(3)	0.035(2)	0.032(2)	-0.0027(9)	0.0019(19)	-0.0081(9)
C1	0.020(9)	0.053(10)	0.050(11)	0.020(9)	0.016(8)	-0.009(8)
C2	0.064(13)	0.037(10)	0.052(11)	0.014(9)	0.011(10)	-0.002(9)
C3	0.037(10)	0.032(9)	0.059(12)	0.002(9)	0.001(9)	-0.007(8)
C4	0.114(19)	0.043(11)	0.032(10)	-0.002(9)	-0.002(11)	-0.004(12)
C5	0.12(2)	0.033(10)	0.035(11)	0.010(9)	-0.015(11)	0.007(11)

C6	0.065(13)	0.041(10)	0.041(10)	0.015(9)	-0.004(9)	-0.019(9)
C7	0.051(13)	0.054(12)	0.107(18)	0.006(12)	0.021(12)	-0.016(10)
C8	0.035(10)	0.044(11)	0.105(16)	0.012(11)	0.021(10)	-0.010(8)
C9	0.029(11)	0.12(2)	0.114(19)	0.025(17)	0.016(12)	0.000(12)
C10	0.053(14)	0.15(2)	0.076(16)	0.069(17)	0.018(12)	-0.008(16)
C11	0.064(17)	0.061(14)	0.14(2)	0.016(15)	0.005(16)	-0.016(13)
C12	0.058(13)	0.021(9)	0.087(15)	0.013(9)	-0.003(11)	-0.012(8)
C13	0.035(10)	0.036(9)	0.042(10)	0.023(8)	0.007(8)	0.004(7)
C14	0.079(14)	0.032(9)	0.050(11)	-0.008(9)	0.023(10)	-0.011(9)
C15	0.084(15)	0.042(11)	0.046(12)	0.015(9)	0.015(11)	0.017(10)
C16	0.12(2)	0.034(11)	0.086(17)	-0.008(12)	0.076(16)	0.012(12)
C17	0.091(15)	0.021(9)	0.063(13)	-0.003(9)	0.017(11)	-0.012(9)
C18	0.042(10)	0.037(9)	0.038(10)	0.010(8)	-0.007(8)	0.008(8)
C19	0.069(13)	0.057(11)	0.022(8)	0.007(9)	0.004(8)	-0.011(10)
C20	0.059(14)	0.21(3)	0.12(2)	0.13(2)	0.070(14)	0.074(17)
C21	0.093(19)	0.12(2)	0.080(17)	-0.017(16)	0.052(14)	-0.008(15)
C22	0.057(13)	0.075(14)	0.060(12)	0.037(11)	0.036(10)	0.034(11)
C23	0.064(14)	0.068(13)	0.052(12)	0.031(10)	0.011(10)	-0.016(11)
C24	0.041(10)	0.047(10)	0.025(8)	-0.008(8)	0.006(7)	0.000(8)
C25	0.060(12)	0.013(8)	0.054(11)	-0.021(8)	0.010(9)	0.002(7)
C26	0.104(18)	0.034(11)	0.070(15)	-0.012(11)	0.032(13)	-0.010(11)
C27	0.22(3)	0.061(16)	0.051(15)	0.019(14)	-0.021(18)	0.002(18)
C28	0.19(3)	0.056(14)	0.064(16)	0.010(13)	-0.012(17)	0.073(17)
C29	0.067(13)	0.073(14)	0.045(11)	0.003(11)	-0.010(9)	0.045(11)
C30	0.075(12)	0.023(8)	0.026(8)	-0.006(7)	0.004(8)	0.007(8)
C31	0.043(11)	0.029(9)	0.057(11)	0.005(8)	0.003(9)	0.010(8)
C32	0.026(10)	0.048(11)	0.086(15)	-0.015(11)	0.012(10)	-0.001(8)
C33	0.076(14)	0.050(11)	0.023(9)	-0.009(8)	-0.015(9)	0.020(10)
C34	0.069(14)	0.020(8)	0.075(14)	-0.012(9)	-0.022(11)	0.004(8)
C35	0.065(14)	0.048(11)	0.065(13)	0.007(10)	0.026(11)	0.006(10)
C36	0.083(14)	0.016(8)	0.038(10)	0.003(7)	0.007(9)	0.012(8)
C37	0.045(10)	0.022(8)	0.045(10)	0.001(7)	0.010(8)	-0.007(7)
C38	0.082(14)	0.027(9)	0.035(10)	-0.014(8)	0.004(9)	0.004(9)
C39	0.062(13)	0.073(13)	0.025(9)	-0.013(9)	-0.015(8)	-0.016(10)
C40	0.045(13)	0.061(13)	0.079(15)	0.017(11)	-0.017(11)	-0.003(10)
C41	0.086(15)	0.029(9)	0.063(13)	0.018(10)	-0.002(11)	-0.007(9)
C42	0.057(12)	0.032(9)	0.054(11)	0.027(9)	-0.015(9)	-0.004(8)
C43	0.070(13)	0.042(10)	0.024(8)	-0.016(8)	0.005(8)	-0.005(9)
C44	0.030(9)	0.033(9)	0.046(10)	0.010(8)	0.014(8)	0.009(7)
C45	0.035(10)	0.067(12)	0.035(9)	-0.011(9)	-0.006(8)	0.013(9)
C46	0.024(9)	0.057(11)	0.039(9)	0.003(8)	-0.004(7)	0.011(8)
C47	0.031(9)	0.046(10)	0.040(10)	-0.011(8)	0.020(8)	-0.011(7)
C48	0.041(10)	0.044(10)	0.025(8)	0.005(8)	0.000(7)	0.004(8)
C49	0.030(9)	0.054(10)	0.030(9)	0.019(8)	0.007(7)	-0.001(8)
C50	0.042(10)	0.029(9)	0.057(11)	0.016(8)	0.010(8)	-0.005(7)
C51	0.080(15)	0.046(11)	0.076(15)	0.019(11)	-0.021(12)	0.022(10)

C52	0.074(14)	0.039(10)	0.070(14)	-0.002(11)	0.000(11)	0.016(10)
C53	0.067(14)	0.035(10)	0.076(15)	-0.016(10)	-0.015(11)	-0.004(9)
C54	0.055(13)	0.055(12)	0.062(13)	0.003(11)	-0.005(10)	-0.006(10)
C55	0.057(12)	0.067(13)	0.044(11)	0.001(10)	0.022(9)	-0.003(10)
C56	0.058(12)	0.035(10)	0.053(11)	-0.020(8)	0.023(9)	0.003(8)
C57	0.058(13)	0.074(14)	0.072(14)	-0.033(12)	0.036(11)	-0.010(11)
C58	0.071(14)	0.057(13)	0.059(13)	0.012(11)	0.029(11)	-0.009(11)
C59	0.041(12)	0.13(2)	0.064(13)	0.014(14)	0.047(10)	0.027(12)
C60	0.060(12)	0.041(10)	0.060(12)	0.010(9)	0.003(10)	0.017(9)
C61	0.033(10)	0.063(11)	0.034(9)	0.009(9)	0.011(8)	-0.001(8)
C62	0.058(12)	0.084(15)	0.012(8)	-0.001(9)	-0.002(8)	0.000(10)
C63	0.044(11)	0.074(14)	0.060(13)	-0.049(12)	0.012(9)	-0.016(10)
C64	0.065(12)	0.014(8)	0.054(12)	-0.011(8)	0.015(9)	-0.016(8)
C65	0.051(12)	0.070(14)	0.054(12)	-0.011(11)	0.015(10)	-0.010(10)
C66	0.045(10)	0.035(9)	0.030(9)	-0.006(8)	0.006(7)	0.013(7)
C67	0.039(11)	0.056(12)	0.077(14)	-0.013(11)	-0.002(10)	-0.004(9)
C68	0.023(9)	0.078(14)	0.059(12)	0.040(11)	0.001(8)	-0.020(9)
C69	0.065(13)	0.062(13)	0.038(10)	0.008(10)	-0.017(9)	-0.007(10)
C70	0.074(14)	0.070(13)	0.035(10)	0.021(10)	0.014(9)	-0.020(11)
C72	0.066(13)	0.033(10)	0.055(12)	-0.008(9)	-0.018(10)	-0.017(9)
C111	0.043(10)	0.030(8)	0.038(9)	-0.001(8)	0.003(8)	-0.010(7)
C112	0.065(12)	0.030(9)	0.030(9)	0.020(7)	-0.002(8)	0.000(8)
C113	0.037(10)	0.036(9)	0.064(12)	-0.014(9)	0.014(9)	-0.005(8)
C114	0.088(16)	0.050(12)	0.063(14)	-0.011(11)	0.042(12)	0.000(11)
C115	0.108(18)	0.025(9)	0.051(12)	-0.013(9)	0.011(12)	0.014(10)
C116	0.065(13)	0.040(10)	0.053(12)	-0.008(9)	0.003(10)	-0.025(9)
C121	0.067(12)	0.023(8)	0.046(10)	-0.005(8)	-0.021(9)	0.008(8)
C122	0.091(15)	0.041(10)	0.036(10)	-0.011(9)	0.020(10)	0.025(10)
C123	0.079(15)	0.051(12)	0.056(12)	0.010(10)	0.011(10)	-0.006(10)
C124	0.065(14)	0.051(12)	0.074(14)	-0.004(11)	0.024(11)	-0.007(10)
C125	0.084(15)	0.032(10)	0.094(16)	0.004(11)	0.038(13)	-0.025(10)
C126	0.053(12)	0.055(12)	0.050(11)	-0.015(9)	0.017(9)	0.000(9)
C131	0.062(12)	0.022(8)	0.043(10)	-0.014(8)	0.005(8)	0.003(8)
C132	0.101(17)	0.076(14)	0.014(8)	-0.008(9)	0.001(9)	-0.013(12)
C133	0.059(14)	0.092(16)	0.043(11)	-0.039(12)	-0.012(10)	0.008(12)
C134	0.038(11)	0.082(15)	0.057(13)	-0.036(11)	-0.013(10)	-0.004(10)
C135	0.037(10)	0.064(12)	0.048(11)	-0.031(10)	0.013(8)	-0.016(9)
C136	0.034(10)	0.059(11)	0.038(9)	0.007(9)	-0.007(8)	-0.014(8)
C211	0.056(12)	0.059(12)	0.037(10)	0.010(9)	0.015(9)	0.003(9)
C212	0.13(2)	0.044(12)	0.070(15)	0.012(11)	0.031(14)	0.021(13)
C213	0.104(19)	0.037(11)	0.080(16)	0.017(11)	0.029(14)	-0.026(12)
C214	0.068(15)	0.074(15)	0.078(16)	0.026(13)	0.015(12)	-0.010(12)
C215	0.056(13)	0.043(11)	0.098(17)	0.005(11)	0.023(11)	-0.007(10)
C216	0.058(13)	0.050(11)	0.053(12)	-0.014(9)	0.009(10)	-0.018(10)
C221	0.025(10)	0.072(14)	0.088(15)	0.012(12)	0.021(10)	-0.003(9)
C222	0.020(10)	0.064(13)	0.107(18)	-0.008(12)	-0.011(10)	-0.002(9)

C223	0.077(16)	0.086(16)	0.061(13)	-0.014(13)	-0.015(12)	0.006(13)
C224	0.035(11)	0.053(12)	0.088(16)	-0.008(11)	0.010(11)	-0.007(9)
C225	0.082(15)	0.016(8)	0.068(13)	0.009(9)	-0.009(11)	-0.005(9)
C226	0.059(13)	0.028(9)	0.083(15)	-0.007(10)	0.008(11)	0.001(9)
C231	0.023(9)	0.041(9)	0.054(11)	0.003(9)	-0.006(8)	-0.003(7)
C232	0.086(18)	0.12(2)	0.059(15)	-0.004(15)	0.003(13)	-0.049(15)
C233	0.064(15)	0.12(2)	0.066(15)	-0.026(15)	-0.029(12)	-0.033(14)
C234	0.064(14)	0.076(15)	0.044(12)	0.002(12)	-0.003(10)	0.010(12)
C235	0.080(15)	0.052(12)	0.067(15)	0.022(12)	0.016(12)	0.005(11)
C236	0.069(14)	0.052(12)	0.067(14)	0.001(11)	0.011(11)	0.026(10)
C311	0.059(12)	0.035(9)	0.015(8)	0.016(7)	0.000(7)	-0.012(8)
C312	0.055(12)	0.033(9)	0.050(11)	0.010(8)	0.024(9)	0.017(9)
C313	0.081(14)	0.034(9)	0.033(9)	0.005(8)	0.021(9)	0.006(9)
C314	0.056(12)	0.048(11)	0.048(11)	0.020(9)	0.004(9)	0.011(9)
C315	0.062(13)	0.028(9)	0.051(11)	0.015(8)	0.018(9)	0.011(9)
C316	0.080(14)	0.038(10)	0.033(9)	-0.004(8)	0.027(9)	-0.012(10)
C321	0.056(12)	0.048(11)	0.044(11)	-0.001(9)	-0.004(9)	-0.002(9)
C322	0.058(13)	0.063(13)	0.071(14)	0.025(11)	-0.025(11)	-0.036(10)
C323	0.096(19)	0.083(17)	0.090(19)	0.066(16)	-0.003(15)	-0.025(14)
C324	0.18(3)	0.075(18)	0.060(16)	0.017(15)	-0.049(18)	-0.030(19)
C325	0.14(2)	0.051(14)	0.081(17)	0.016(13)	-0.021(17)	0.005(14)
C326	0.078(16)	0.073(15)	0.069(15)	-0.008(13)	-0.014(12)	-0.024(12)
C331	0.072(13)	0.031(9)	0.025(9)	0.012(8)	-0.005(8)	-0.016(8)
C332	0.053(13)	0.039(10)	0.092(16)	0.003(11)	0.007(11)	0.001(9)
C333	0.111(18)	0.058(12)	0.021(9)	-0.003(9)	0.030(10)	0.007(12)
C334	0.050(12)	0.067(13)	0.060(13)	-0.029(12)	-0.005(10)	0.009(10)
C335	0.055(11)	0.034(9)	0.036(10)	-0.013(8)	0.008(8)	0.003(8)
C336	0.032(10)	0.048(11)	0.081(14)	0.011(11)	0.013(9)	0.013(8)
C411	0.049(11)	0.050(10)	0.027(9)	-0.005(8)	0.012(8)	0.034(8)
C412	0.047(11)	0.040(9)	0.035(9)	0.008(8)	0.000(8)	-0.012(8)
C413	0.027(10)	0.087(14)	0.036(10)	0.029(10)	-0.001(8)	0.008(9)
C414	0.055(12)	0.054(11)	0.035(10)	-0.036(9)	0.008(9)	-0.015(9)
C415	0.034(10)	0.060(11)	0.054(11)	0.000(10)	0.027(9)	-0.004(9)
C416	0.044(12)	0.042(10)	0.086(15)	0.019(10)	-0.004(10)	0.007(8)
C421	0.039(10)	0.043(9)	0.027(8)	0.017(8)	-0.002(7)	0.018(8)
C422	0.074(14)	0.052(11)	0.031(10)	0.003(9)	0.012(9)	0.010(10)
C423	0.078(15)	0.042(10)	0.023(9)	0.006(8)	0.011(9)	0.005(10)
C424	0.078(14)	0.020(8)	0.021(8)	0.002(7)	0.008(8)	0.002(8)
C425	0.067(13)	0.051(11)	0.043(11)	-0.013(9)	0.011(9)	-0.022(10)
C426	0.052(11)	0.034(9)	0.025(8)	-0.007(7)	0.001(7)	0.008(8)
C431	0.022(9)	0.047(10)	0.046(10)	0.005(9)	-0.015(7)	0.007(7)
C432	0.063(12)	0.037(9)	0.017(8)	-0.009(7)	0.002(7)	0.018(8)
C433	0.069(13)	0.022(8)	0.035(10)	0.008(8)	0.004(9)	0.010(8)
C434	0.049(12)	0.067(13)	0.048(12)	0.021(11)	-0.003(9)	0.028(10)
C435	0.024(9)	0.065(12)	0.030(9)	-0.008(9)	0.009(7)	-0.002(8)
C436	0.030(10)	0.058(11)	0.055(12)	0.001(10)	0.020(8)	0.013(8)

C511	0.050(11)	0.038(9)	0.053(11)	-0.008(9)	0.001(9)	-0.018(8)
C512	0.101(16)	0.038(10)	0.042(11)	-0.019(9)	0.029(10)	-0.028(10)
C513	0.075(14)	0.066(13)	0.029(10)	-0.012(9)	-0.010(9)	-0.016(11)
C514	0.051(13)	0.109(19)	0.077(15)	-0.045(14)	0.005(11)	0.008(12)
C515	0.116(18)	0.033(10)	0.050(12)	0.002(9)	-0.011(12)	-0.046(11)
C516	0.084(14)	0.055(12)	0.028(9)	0.009(9)	0.025(9)	-0.017(10)
C521	0.075(14)	0.043(11)	0.034(10)	0.001(9)	0.004(9)	-0.008(10)
C522	0.062(15)	0.113(19)	0.075(15)	0.018(14)	0.039(13)	0.047(15)
C523	0.030(11)	0.102(17)	0.061(13)	-0.010(13)	0.011(9)	-0.013(11)
C524	0.073(16)	0.078(17)	0.067(15)	0.031(13)	0.013(12)	0.011(13)
C525	0.13(2)	0.051(12)	0.028(10)	0.027(10)	0.029(12)	0.035(14)
C526	0.15(2)	0.075(16)	0.050(13)	0.020(13)	0.024(14)	0.039(16)
C531	0.037(10)	0.038(9)	0.051(11)	-0.006(8)	0.009(8)	-0.020(8)
C532	0.059(13)	0.047(11)	0.053(12)	-0.003(10)	-0.008(10)	0.008(9)
C533	0.107(18)	0.076(14)	0.026(10)	-0.002(10)	-0.006(10)	0.046(13)
C534	0.062(13)	0.049(11)	0.049(11)	-0.020(9)	0.024(10)	0.025(9)
C535	0.073(14)	0.083(15)	0.020(9)	-0.007(10)	-0.008(9)	-0.014(11)
C536	0.061(12)	0.038(10)	0.038(10)	0.021(8)	0.002(9)	0.010(8)
C611	0.051(12)	0.042(10)	0.051(11)	0.003(9)	0.005(9)	0.009(9)
C612	0.023(9)	0.044(10)	0.066(12)	-0.020(9)	0.012(8)	0.002(7)
C613	0.023(10)	0.088(15)	0.077(14)	0.010(12)	0.016(9)	0.012(9)
C614	0.051(13)	0.067(13)	0.076(14)	-0.019(11)	0.001(11)	0.030(10)
C615	0.054(13)	0.096(16)	0.096(16)	-0.064(14)	0.054(12)	-0.025(12)
C616	0.040(12)	0.061(13)	0.12(2)	-0.002(13)	0.026(12)	-0.012(10)
C621	0.041(10)	0.012(7)	0.071(13)	0.000(8)	-0.020(9)	0.014(7)
C622	0.062(13)	0.074(14)	0.035(10)	0.015(10)	-0.008(9)	0.007(10)
C623	0.059(13)	0.033(10)	0.065(13)	-0.012(10)	0.003(10)	0.000(8)
C624	0.067(14)	0.044(11)	0.068(14)	0.009(11)	0.006(11)	0.009(10)
C625	0.053(12)	0.044(11)	0.067(13)	0.008(10)	0.020(10)	0.011(9)
C626	0.057(13)	0.043(11)	0.061(13)	-0.001(10)	0.018(10)	-0.009(9)
C631	0.056(13)	0.038(10)	0.068(13)	-0.019(10)	0.022(10)	-0.004(9)
C632	0.039(11)	0.066(13)	0.078(14)	0.003(12)	0.016(10)	0.009(10)
C633	0.037(11)	0.039(10)	0.113(18)	-0.016(12)	-0.006(11)	-0.016(9)
C634	0.040(13)	0.086(17)	0.106(18)	0.029(14)	0.001(12)	0.005(11)
C635	0.038(13)	0.076(16)	0.25(4)	0.04(2)	0.010(17)	-0.040(12)
C636	0.061(14)	0.052(12)	0.095(17)	0.010(12)	0.005(12)	-0.015(10)
C711	0.030(9)	0.047(9)	0.021(8)	0.003(7)	0.005(6)	-0.004(7)
C712	0.028(9)	0.036(9)	0.047(10)	0.002(8)	0.015(7)	0.009(7)
C713	0.076(14)	0.043(11)	0.051(12)	-0.018(9)	0.030(10)	-0.005(10)
C714	0.14(2)	0.032(11)	0.063(14)	-0.016(11)	-0.013(14)	-0.007(12)
C715	0.078(14)	0.045(11)	0.059(13)	-0.008(10)	0.033(11)	0.023(10)
C716	0.067(12)	0.034(9)	0.026(9)	0.002(7)	-0.003(8)	0.004(8)
C721	0.060(11)	0.034(9)	0.021(8)	-0.004(7)	0.007(8)	0.003(8)
C722	0.050(10)	0.019(8)	0.036(9)	0.008(7)	0.011(8)	0.000(7)
C723	0.037(10)	0.042(9)	0.025(8)	-0.001(7)	0.010(7)	0.009(7)
C724	0.029(9)	0.043(9)	0.039(9)	-0.013(8)	0.001(7)	0.007(7)

C725	0.056(12)	0.061(12)	0.036(10)	-0.002(9)	0.009(9)	0.017(10)
C726	0.060(12)	0.037(9)	0.025(8)	0.007(8)	-0.005(8)	0.017(8)
C731	0.052(11)	0.035(9)	0.030(9)	0.006(8)	0.002(8)	0.010(8)
C732	0.067(14)	0.051(11)	0.049(11)	-0.001(10)	0.010(10)	0.002(10)
C733	0.037(10)	0.051(11)	0.043(10)	0.025(9)	0.001(8)	0.000(8)
C734	0.044(13)	0.103(18)	0.058(13)	-0.021(13)	-0.001(10)	-0.017(12)
C735	0.099(17)	0.039(10)	0.036(10)	0.012(9)	-0.023(10)	-0.020(10)
C736	0.091(16)	0.047(11)	0.048(11)	-0.017(10)	0.011(11)	-0.023(11)
C811	0.028(9)	0.055(10)	0.025(8)	0.017(8)	0.006(7)	0.017(8)
C812	0.068(13)	0.059(12)	0.024(9)	-0.005(8)	-0.006(8)	-0.034(10)
C813	0.051(12)	0.065(12)	0.052(12)	0.022(10)	-0.016(9)	-0.022(9)
C814	0.062(14)	0.078(14)	0.053(12)	0.025(11)	0.006(10)	0.033(12)
C815	0.063(13)	0.057(12)	0.032(10)	0.005(9)	0.008(9)	-0.025(10)
C816	0.024(9)	0.037(9)	0.051(10)	-0.007(8)	0.005(7)	-0.021(7)
C821	0.068(12)	0.015(7)	0.026(8)	-0.007(7)	0.007(8)	0.005(7)
C822	0.062(12)	0.042(10)	0.047(11)	0.006(9)	0.020(9)	-0.009(9)
C823	0.063(13)	0.071(13)	0.032(10)	0.002(10)	0.003(9)	-0.035(11)
C824	0.042(10)	0.048(10)	0.039(10)	0.013(8)	0.008(8)	-0.015(8)
C825	0.072(13)	0.035(9)	0.029(9)	-0.007(8)	0.011(9)	0.010(9)
C826	0.077(14)	0.033(9)	0.042(10)	-0.003(8)	0.031(9)	-0.025(9)
C831	0.034(10)	0.049(10)	0.040(10)	0.024(9)	0.004(8)	-0.008(8)
C832	0.034(10)	0.053(11)	0.056(11)	0.027(9)	-0.009(8)	-0.007(8)
C833	0.013(9)	0.067(13)	0.088(15)	0.020(12)	-0.009(9)	0.008(8)
C834	0.041(11)	0.053(11)	0.069(14)	0.011(11)	-0.002(10)	-0.007(9)
C835	0.042(11)	0.056(11)	0.052(11)	0.016(10)	0.012(9)	0.003(9)
C836	0.046(11)	0.057(11)	0.039(10)	0.000(9)	0.004(8)	-0.011(9)

All the solvent THF molecules were refined isotropically.

5.14 [(Ph$_3$PAg)$_8$(SePh)$_{12}$(μ$_6$-Se)$_{0.5}$Ag$_6$][Ph$_3$SnCl$_2$]·6THF (15·6THF)

Compound **15** crystallizes as yellow hexagonal thin plates from THF/hexane..

Table 5.33 Crystal data and structure refinement for **15·6THF**

Empirical formula	C$_{258}$H$_{243}$Ag$_{14}$Se$_{12.5}$P$_8$O$_6$Cl$_2$Sn
Formula weight /g·mol^{-1}	6374.05
Crystal system	monoclinic
Space group	*I2/a*
a /Å	24.7467(19)
b /Å	26.8921(15)
c /Å	36.722(3)
β /°	95.356(10)
V /Å^3	24332.0(3)
Z	4
ρ_{calc} /g·cm^{-3}	1.740
μ(Mo$_{K\alpha}$) /mm^{-1}	3.199
2Θ range /°	4-52
Reflections measured	114389
Independent reflections	23468
R(int)	0.0637
Indepedent reflections ($I > 2\sigma(I)$)	14508
Parameters	1380
R_1 ($I > 2\sigma(I)$)	0.0443
wR_2 (all data)	0.1073
GooF (all data)	0.892
Max. peak/hole /e$^-$·10^{-6}pm^{-3}	2.983/–2.697

Table 5.34 Atomic coordinates and equivalent isotropic displacement parameters for **15·6THF**

Atom	x/a	y/b	z/c	$U_{eq/iso}$
Sn1	0.7500	0.25416(3)	0.0000	0.04776(18)
Ag1	0.255690(17)	0.373892(18)	0.173349(13)	0.03441(12)
Ag2	0.392818(16)	0.235604(19)	0.191862(12)	0.03582(12)
Ag3	0.093254(16)	0.250537(18)	0.165328(13)	0.03441(12)
Ag4	0.269305(15)	0.394726(17)	0.312860(12)	0.02960(11)
Ag5	0.34795(2)	0.30331(2)	0.253260(15)	0.03938(15)
Ag5A	0.3257(3)	0.3218(3)	0.25099(19)	0.03938(15)
Ag6	0.23033(2)	0.22632(2)	0.175053(15)	0.04075(15)
Ag6A	0.2570(3)	0.2487(3)	0.17831(18)	0.04075(15)
Ag7	0.17544(4)	0.32872(4)	0.23728(5)	0.0903(5)
Ag7A	0.1786(6)	0.3171(6)	0.2280(7)	0.0903(5)
Se1	0.15447(2)	0.33324(3)	0.16834(4)	0.0822(4)
Se2	0.29762(3)	0.38585(3)	0.243317(19)	0.03145(17)
Se2A	0.2844(3)	0.4082(4)	0.2394(3)	0.03145(17)
Se3	0.30650(3)	0.28572(3)	0.163026(17)	0.03174(17)
Se3A	0.3332(4)	0.3040(3)	0.1608(2)	0.03174(17)
Se4	0.34563(3)	0.33154(3)	0.346346(18)	0.03256(17)
Se4A	0.3199(3)	0.3122(3)	0.3416(2)	0.03256(17)
Se5	0.43150(3)	0.24983(3)	0.262800(18)	0.03218(16)
Se5A	0.4079(4)	0.2678(4)	0.2603(2)	0.03218(16)
Se6	0.33108(2)	0.14675(3)	0.19707(3)	0.0753(3)
Se7	0.2500	0.2500	0.2500	0.0266(3)
Cl1	0.83825(8)	0.25385(9)	0.04190(6)	0.0712(6)
P1	0.26085(6)	0.43792(6)	0.12643(5)	0.0350(4)
P2	0.47097(5)	0.22322(6)	0.15550(4)	0.0305(3)
P3	0.00629(5)	0.25284(6)	0.12616(4)	0.0270(3)
P4	0.28224(5)	0.47887(6)	0.34199(4)	0.0294(3)
C512	0.5368(5)	0.3951(6)	0.9727(4)	0.131(5)
C1	0.6604(3)	0.2299(4)	0.0501(3)	0.082(3)
C2	0.6350(4)	0.2055(5)	0.0765(3)	0.105(4)
C3	0.6583(4)	0.1654(4)	0.0930(3)	0.086(3)
C4	0.7074(4)	0.1495(4)	0.0844(3)	0.086(3)
C5	0.7341(3)	0.1743(3)	0.0592(2)	0.066(2)
C6	0.7103(3)	0.2144(3)	0.0405(2)	0.0547(19)
C7	0.7500	0.3339(4)	0.0000	0.056(3)
C8	0.7520(4)	0.3606(4)	0.0324(2)	0.072(2)
C9	0.7517(4)	0.4119(4)	0.0320(3)	0.085(3)
C10	0.7500	0.4372(5)	0.0000	0.082(4)
C11	0.1049(2)	0.3889(3)	0.1617(3)	0.054(2)
C12	0.0889(3)	0.4051(3)	0.1267(3)	0.069(2)
C13	0.0558(4)	0.4456(4)	0.1217(3)	0.083(3)

C14	0.0382(3)	0.4701(4)	0.1514(3)	0.083(3)
C15	0.0531(3)	0.4549(3)	0.1858(3)	0.068(2)
C16	0.0865(3)	0.4133(3)	0.1918(3)	0.062(2)
C21	0.3564(2)	0.4337(2)	0.24539(16)	0.0320(13)
C22	0.3609(3)	0.4677(3)	0.2181(2)	0.0507(18)
C23	0.4043(3)	0.5017(3)	0.2209(2)	0.065(2)
C24	0.4412(3)	0.5018(3)	0.2511(2)	0.0516(19)
C25	0.4350(2)	0.4698(3)	0.27883(19)	0.0425(16)
C26	0.3929(2)	0.4354(2)	0.27616(17)	0.0349(14)
C31	0.3126(2)	0.2808(2)	0.11065(16)	0.0340(14)
C32	0.3557(3)	0.3031(3)	0.09586(18)	0.0426(16)
C33	0.3610(3)	0.2990(3)	0.0585(2)	0.0510(18)
C34	0.3240(3)	0.2717(3)	0.03689(19)	0.0493(18)
C35	0.2811(3)	0.2497(3)	0.05188(19)	0.0509(18)
C36	0.2750(3)	0.2548(3)	0.08874(17)	0.0417(15)
C41	0.3337(3)	0.3413(2)	0.39714(16)	0.0376(15)
C42	0.3758(4)	0.3334(3)	0.4238(2)	0.068(3)
C43	0.3695(4)	0.3461(4)	0.4596(2)	0.088(3)
C44	0.3222(4)	0.3669(4)	0.4693(2)	0.070(3)
C45	0.2808(3)	0.3754(3)	0.4422(2)	0.0546(19)
C46	0.2854(3)	0.3621(3)	0.40668(17)	0.0400(15)
C51	0.5421(3)	0.2792(3)	0.2637(2)	0.060(2)
C52	0.5845(3)	0.3116(3)	0.2599(3)	0.073(3)
C53	0.5753(3)	0.3601(3)	0.2500(2)	0.060(2)
C54	0.5242(3)	0.3774(3)	0.2437(2)	0.0538(19)
C55	0.4801(3)	0.3456(3)	0.2470(2)	0.0456(17)
C56	0.4895(2)	0.2971(3)	0.25767(17)	0.0387(15)
C61	0.3686(2)	0.0836(2)	0.2027(2)	0.0447(18)
C62	0.3501(2)	0.0471(2)	0.2250(2)	0.0457(18)
C63	0.3739(2)	0.0005(2)	0.2263(2)	0.0431(16)
C64	0.4164(2)	-0.0099(3)	0.2053(2)	0.0447(17)
C65	0.4353(2)	0.0266(3)	0.1841(2)	0.0516(19)
C66	0.4113(2)	0.0736(3)	0.1824(2)	0.0493(19)
C111	0.3282(3)	0.4462(3)	0.11040(19)	0.0428(16)
C112	0.3371(3)	0.4709(3)	0.0785(2)	0.063(2)
C113	0.3892(4)	0.4749(4)	0.0676(2)	0.079(3)
C114	0.4327(4)	0.4545(4)	0.0892(3)	0.084(3)
C115	0.4243(3)	0.4297(4)	0.1201(3)	0.072(3)
C116	0.3725(3)	0.4256(3)	0.1309(2)	0.0498(18)
C121	0.2256(3)	0.3846(3)	0.0652(2)	0.065(2)
C122	0.1970(4)	0.3741(4)	0.0320(3)	0.076(3)
C123	0.1588(3)	0.4071(3)	0.0176(2)	0.065(2)
C124	0.1498(4)	0.4500(3)	0.0358(2)	0.077(3)
C125	0.1803(3)	0.4607(3)	0.0687(2)	0.062(2)
C126	0.2186(2)	0.4277(2)	0.08320(18)	0.0380(15)
C131	0.2394(2)	0.4990(2)	0.14054(18)	0.0399(15)

C132	0.2647(3)	0.5430(3)	0.1332(2)	0.056(2)
C133	0.2441(4)	0.5884(3)	0.1437(3)	0.074(3)
C134	0.1975(4)	0.5900(3)	0.1613(3)	0.071(3)
C135	0.1725(3)	0.5466(3)	0.1695(3)	0.068(2)
C136	0.1935(3)	0.5015(3)	0.1599(2)	0.0539(19)
C211	0.5040(2)	0.2771(2)	0.13658(17)	0.0360(14)
C212	0.5276(3)	0.3120(3)	0.1601(2)	0.061(2)
C213	0.5528(4)	0.3535(4)	0.1478(3)	0.075(3)
C214	0.5549(4)	0.3609(4)	0.1116(3)	0.075(3)
C215	0.5304(4)	0.3276(4)	0.0872(3)	0.081(3)
C216	0.5050(3)	0.2852(3)	0.1002(2)	0.062(2)
C221	0.5270(2)	0.1919(2)	0.18246(17)	0.0363(14)
C222	0.5812(3)	0.1974(3)	0.1768(2)	0.060(2)
C223	0.6204(3)	0.1708(4)	0.1980(3)	0.078(3)
C224	0.6060(5)	0.1399(4)	0.2245(3)	0.089(3)
C225	0.5524(4)	0.1339(3)	0.2301(3)	0.080(3)
C226	0.5140(3)	0.1604(3)	0.2095(2)	0.0537(19)
C231	0.4559(2)	0.1825(2)	0.11582(16)	0.0322(13)
C232	0.4961(3)	0.1576(3)	0.09950(19)	0.0495(18)
C233	0.4827(3)	0.1279(3)	0.0689(2)	0.057(2)
C234	0.4297(3)	0.1225(3)	0.0554(2)	0.058(2)
C235	0.3898(3)	0.1468(3)	0.0720(2)	0.057(2)
C236	0.4024(3)	0.1766(3)	0.10219(19)	0.0428(16)
C311	-0.0375(2)	0.3067(2)	0.13188(17)	0.0326(13)
C312	-0.0299(3)	0.3332(3)	0.1637(2)	0.0519(19)
C313	-0.0604(4)	0.3750(3)	0.1685(3)	0.077(3)
C314	-0.0985(3)	0.3906(3)	0.1423(2)	0.067(2)
C315	-0.1068(3)	0.3645(3)	0.1102(2)	0.056(2)
C316	-0.0758(2)	0.3230(3)	0.1044(2)	0.0442(16)
C321	-0.0363(2)	0.1981(2)	0.13082(16)	0.0310(13)
C322	-0.0919(2)	0.1977(3)	0.12228(18)	0.0390(15)
C323	-0.1210(2)	0.1537(3)	0.1247(2)	0.0503(19)
C324	-0.0950(3)	0.1105(3)	0.1359(2)	0.055(2)
C325	-0.0401(3)	0.1112(3)	0.1451(2)	0.061(2)
C326	-0.0106(2)	0.1542(3)	0.1421(2)	0.0433(16)
C331	0.0157(2)	0.2549(2)	0.07710(16)	0.0319(13)
C332	-0.0165(3)	0.2294(3)	0.05069(19)	0.0514(19)
C333	-0.0060(3)	0.2321(4)	0.0148(2)	0.066(2)
C334	0.0365(4)	0.2597(4)	0.0048(2)	0.069(2)
C335	0.0673(4)	0.2855(3)	0.0305(2)	0.069(2)
C336	0.0580(3)	0.2832(3)	0.0670(2)	0.0488(18)
C411	0.2472(2)	0.4879(2)	0.38289(17)	0.0363(14)
C412	0.1944(3)	0.4714(3)	0.3822(2)	0.0519(19)
C413	0.1643(3)	0.4774(3)	0.4123(3)	0.070(2)
C414	0.1876(4)	0.4990(4)	0.4431(3)	0.087(3)
C415	0.2408(4)	0.5164(4)	0.4448(3)	0.093(3)

C416	0.2701(3)	0.5106(3)	0.4142(2)	0.062(2)
C421	0.2597(2)	0.5319(2)	0.31293(17)	0.0327(13)
C422	0.2323(2)	0.5722(2)	0.3254(2)	0.0443(16)
C423	0.2176(3)	0.6116(3)	0.3020(2)	0.058(2)
C424	0.2304(3)	0.6110(3)	0.2667(2)	0.0535(19)
C425	0.2576(3)	0.5710(3)	0.2542(2)	0.0524(19)
C426	0.2715(2)	0.5314(3)	0.27740(19)	0.0436(16)
C431	0.3524(2)	0.4954(2)	0.35749(17)	0.0336(14)
C432	0.3771(2)	0.5388(3)	0.34817(19)	0.0428(16)
C433	0.4299(3)	0.5496(3)	0.3612(2)	0.059(2)
C434	0.4586(3)	0.5169(3)	0.3846(2)	0.056(2)
C435	0.4355(3)	0.4738(3)	0.3936(2)	0.062(2)
C436	0.3824(3)	0.4623(3)	0.3804(2)	0.0487(17)
C511	0.5105(5)	0.4257(6)	0.9996(4)	0.140(6)
C513	0.6003(5)	0.4120(5)	1.0206(4)	0.118(4)
C514	0.5876(6)	0.3793(6)	0.9904(4)	0.134(6)
C517	0.7243(6)	0.2675(6)	0.1560(5)	0.138(6)
C518	0.7741(6)	0.2626(6)	0.1438(4)	0.130(5)
C519	0.8148(5)	0.2715(5)	0.1727(4)	0.118(4)
C521	0.6175(12)	0.0766(12)	0.0072(9)	0.217(12)
C522	0.7862(6)	0.2856(7)	0.2044(4)	0.172(8)
C523	0.5562(8)	0.0886(9)	-0.0331(6)	0.187(9)
C524	0.5929(12)	0.0418(12)	0.0142(6)	0.225(15)
C525	0.6029(9)	0.1105(7)	-0.0157(6)	0.183(9)
O1	0.5539(8)	0.0403(9)	-0.0211(8)	0.303(11)
O2	0.5538(4)	0.4399(4)	1.0259(3)	0.149(4)
O3	0.7312(4)	0.2894(4)	0.1930(3)	0.151(4)

Table 5.35 Anisotropic displacement parameters for **15·6THF**

Atom	U_{11}	U_{22}	U_{33}	U_{23}	U_{13}	U_{12}
Sn1	0.0396(3)	0.0574(5)	0.0449(4)	0.000	-0.0030(3)	0.000
Ag1	0.0333(2)	0.0313(3)	0.0378(3)	0.0037(2)	-0.00123(19)	0.0014(2)
Ag2	0.0252(2)	0.0534(3)	0.0289(2)	-0.0013(2)	0.00253(17)	0.0018(2)
Ag3	0.0293(2)	0.0379(3)	0.0352(3)	-0.0012(2)	-0.00154(18)	0.0016(2)
Ag4	0.02560(19)	0.0296(3)	0.0335(2)	0.0001(2)	0.00232(17)	0.0018(2)
Ag5	0.0316(3)	0.0487(4)	0.0378(3)	-0.0051(3)	0.0031(2)	-0.0063(2)
Ag5A	0.0316(3)	0.0487(4)	0.0378(3)	-0.0051(3)	0.0031(2)	-0.0063(2)
Ag6	0.0425(3)	0.0434(4)	0.0361(3)	-0.0015(3)	0.0023(2)	0.0064(3)
Ag6A	0.0425(3)	0.0434(4)	0.0361(3)	-0.0015(3)	0.0023(2)	0.0064(3)
Ag7	0.0327(3)	0.0268(6)	0.2047(16)	-0.0096(5)	-0.0250(6)	0.0010(3)
Ag7A	0.0327(3)	0.0268(6)	0.2047(16)	-0.0096(5)	-0.0250(6)	0.0010(3)
Se1	0.0210(3)	0.0263(4)	0.1979(12)	-0.0184(5)	0.0031(4)	0.0005(3)
Se2	0.0277(3)	0.0392(5)	0.0276(3)	-0.0062(3)	0.0034(3)	-0.0105(3)
Se2A	0.0277(3)	0.0392(5)	0.0276(3)	-0.0062(3)	0.0034(3)	-0.0105(3)
Se3	0.0361(4)	0.0333(4)	0.0251(3)	-0.0016(3)	-0.0008(3)	0.0116(3)
Se3A	0.0361(4)	0.0333(4)	0.0251(3)	-0.0016(3)	-0.0008(3)	0.0116(3)
Se4	0.0318(3)	0.0373(4)	0.0290(4)	0.0043(3)	0.0046(3)	0.0120(3)
Se4A	0.0318(3)	0.0373(4)	0.0290(4)	0.0043(3)	0.0046(3)	0.0120(3)
Se5	0.0348(4)	0.0373(4)	0.0238(3)	0.0005(3)	-0.0011(3)	-0.0104(3)
Se5A	0.0348(4)	0.0373(4)	0.0238(3)	0.0005(3)	-0.0011(3)	-0.0104(3)
Se6	0.0208(3)	0.0235(4)	0.1785(10)	0.0258(5)	-0.0067(4)	-0.0005(3)
Se7	0.0247(7)	0.0295(9)	0.0256(8)	-0.0004(7)	0.0025(6)	0.0020(6)
Cl1	0.0486(10)	0.0913(17)	0.0692(14)	0.0021(12)	-0.0183(9)	-0.0036(1)
P1	0.0381(8)	0.0306(9)	0.0347(9)	0.0037(7)	-0.0061(7)	-0.0018(7)
P2	0.0244(6)	0.0389(9)	0.0288(8)	-0.0015(7)	0.0048(6)	0.0002(6)
P3	0.0243(6)	0.0308(8)	0.0256(7)	0.0006(7)	0.0001(5)	0.0006(6)
P4	0.0262(7)	0.0280(9)	0.0343(9)	-0.0032(7)	0.0039(6)	0.0011(6)
C512	0.098(9)	0.165(14)	0.130(12)	-0.067(11)	0.007(8)	-0.011(9)
C1	0.061(5)	0.096(8)	0.095(8)	0.014(6)	0.029(5)	0.012(5)
C2	0.085(7)	0.126(11)	0.112(9)	0.023(8)	0.053(7)	0.003(7)
C3	0.088(7)	0.090(8)	0.084(7)	0.015(6)	0.032(6)	-0.014(6)
C4	0.096(7)	0.067(7)	0.093(8)	0.029(6)	0.007(6)	-0.004(5)
C5	0.065(5)	0.067(6)	0.066(6)	0.014(5)	0.002(4)	0.007(4)
C6	0.046(4)	0.060(5)	0.059(5)	0.004(4)	0.011(3)	-0.003(3)
C7	0.059(6)	0.045(7)	0.061(7)	0.000	-0.004(5)	0.000
C8	0.095(6)	0.069(7)	0.051(5)	-0.003(5)	0.007(5)	-0.014(5)
C9	0.117(8)	0.059(6)	0.077(7)	-0.018(5)	-0.001(6)	-0.002(6)
C10	0.104(10)	0.057(9)	0.083(11)	0.000	-0.003(8)	0.000
C11	0.025(3)	0.039(4)	0.098(7)	-0.020(4)	0.004(4)	0.000(3)
C12	0.057(5)	0.066(6)	0.084(7)	-0.025(5)	0.001(4)	-0.001(4)
C13	0.085(6)	0.073(7)	0.085(7)	-0.009(6)	-0.026(5)	0.022(5)
C14	0.063(5)	0.067(6)	0.113(9)	-0.013(6)	-0.027(5)	0.036(5)
C15	0.053(4)	0.065(6)	0.084(7)	-0.010(5)	-0.002(4)	0.028(4)

C16	0.035(3)	0.051(5)	0.098(7)	0.000(5)	-0.004(4)	0.013(3)
C21	0.032(3)	0.032(3)	0.033(3)	-0.005(3)	0.008(2)	0.000(2)
C22	0.060(4)	0.047(5)	0.043(4)	-0.004(4)	-0.008(3)	-0.010(3)
C23	0.091(6)	0.044(5)	0.059(5)	0.013(4)	0.007(4)	-0.028(4)
C24	0.055(4)	0.039(4)	0.060(5)	-0.005(4)	0.009(4)	-0.026(3)
C25	0.029(3)	0.049(4)	0.049(4)	-0.017(4)	0.000(3)	-0.010(3)
C26	0.029(3)	0.038(4)	0.038(4)	-0.001(3)	0.005(2)	-0.003(2)
C31	0.043(3)	0.037(4)	0.021(3)	-0.002(3)	0.001(2)	0.014(3)
C32	0.047(4)	0.039(4)	0.040(4)	-0.002(3)	-0.003(3)	0.010(3)
C33	0.056(4)	0.042(4)	0.056(5)	0.013(4)	0.013(4)	0.006(3)
C34	0.074(5)	0.050(5)	0.026(3)	0.002(3)	0.011(3)	0.008(4)
C35	0.070(5)	0.045(4)	0.036(4)	0.001(3)	-0.006(3)	-0.001(4)
C36	0.048(3)	0.047(4)	0.030(3)	0.006(3)	0.001(3)	0.001(3)
C41	0.057(4)	0.036(4)	0.021(3)	0.003(3)	0.010(3)	0.007(3)
C42	0.083(5)	0.076(6)	0.043(5)	-0.010(4)	-0.013(4)	0.042(5)
C43	0.104(7)	0.109(8)	0.046(5)	-0.019(5)	-0.022(5)	0.044(6)
C44	0.083(6)	0.091(7)	0.037(4)	-0.013(4)	0.006(4)	0.020(5)
C45	0.063(4)	0.054(5)	0.050(5)	-0.007(4)	0.021(4)	0.000(4)
C46	0.047(3)	0.049(4)	0.027(3)	-0.002(3)	0.013(3)	0.004(3)
C51	0.041(4)	0.054(5)	0.080(6)	0.013(4)	-0.018(4)	-0.005(3)
C52	0.037(4)	0.070(6)	0.109(8)	0.004(5)	-0.016(4)	-0.016(4)
C53	0.042(4)	0.055(5)	0.084(6)	-0.015(4)	0.009(4)	-0.027(4)
C54	0.052(4)	0.034(4)	0.077(6)	-0.017(4)	0.015(4)	-0.012(3)
C55	0.037(3)	0.038(4)	0.064(5)	-0.011(4)	0.015(3)	-0.008(3)
C56	0.042(3)	0.047(4)	0.027(3)	-0.006(3)	0.003(3)	-0.017(3)
C61	0.019(3)	0.027(4)	0.086(5)	0.010(4)	-0.006(3)	0.000(2)
C62	0.026(3)	0.033(4)	0.078(5)	0.006(4)	0.005(3)	0.002(3)
C63	0.037(3)	0.030(4)	0.061(5)	0.008(3)	0.001(3)	0.001(3)
C64	0.039(3)	0.034(4)	0.061(5)	0.006(3)	0.001(3)	0.014(3)
C65	0.029(3)	0.053(5)	0.073(5)	0.006(4)	0.003(3)	0.012(3)
C66	0.029(3)	0.044(4)	0.074(5)	0.021(4)	-0.001(3)	-0.004(3)
C111	0.049(4)	0.035(4)	0.044(4)	-0.008(3)	0.002(3)	-0.011(3)
C112	0.072(5)	0.068(6)	0.046(5)	0.004(4)	0.000(4)	-0.020(4)
C113	0.088(6)	0.102(8)	0.051(5)	-0.017(5)	0.023(5)	-0.053(6)
C114	0.057(5)	0.107(8)	0.092(8)	-0.046(7)	0.023(5)	-0.038(5)
C115	0.046(4)	0.085(7)	0.087(7)	-0.020(6)	0.016(4)	-0.015(4)
C116	0.044(4)	0.050(5)	0.056(5)	-0.007(4)	0.004(3)	-0.001(3)
C121	0.062(5)	0.041(5)	0.084(6)	-0.014(4)	-0.026(4)	0.008(4)
C122	0.079(6)	0.066(6)	0.077(6)	-0.028(5)	-0.029(5)	0.004(5)
C123	0.078(5)	0.064(6)	0.049(5)	-0.004(4)	-0.021(4)	-0.012(4)
C124	0.098(6)	0.052(5)	0.070(6)	0.004(5)	-0.045(5)	0.012(5)
C125	0.080(5)	0.040(5)	0.058(5)	0.001(4)	-0.027(4)	0.005(4)
C126	0.042(3)	0.031(4)	0.039(4)	0.004(3)	-0.009(3)	-0.008(3)
C131	0.045(3)	0.033(4)	0.039(4)	0.000(3)	-0.010(3)	-0.002(3)
C132	0.057(4)	0.037(4)	0.072(6)	0.001(4)	-0.004(4)	-0.006(3)
C133	0.076(6)	0.035(5)	0.107(8)	0.003(5)	-0.010(5)	-0.007(4)

C134	0.083(6)	0.038(5)	0.085(7)	-0.015(5)	-0.017(5)	0.011(4)
C135	0.060(5)	0.054(6)	0.087(7)	-0.020(5)	0.000(4)	0.012(4)
C136	0.068(5)	0.037(4)	0.056(5)	-0.005(4)	-0.001(4)	-0.011(4)
C211	0.030(3)	0.042(4)	0.037(4)	0.009(3)	0.008(3)	0.000(3)
C212	0.081(5)	0.054(5)	0.050(5)	-0.007(4)	0.018(4)	-0.025(4)
C213	0.089(6)	0.070(6)	0.068(6)	-0.007(5)	0.016(5)	-0.035(5)
C214	0.081(6)	0.066(6)	0.082(7)	0.014(5)	0.021(5)	-0.026(5)
C215	0.104(7)	0.083(7)	0.057(6)	0.030(5)	0.016(5)	-0.018(6)
C216	0.076(5)	0.066(6)	0.043(4)	0.006(4)	0.004(4)	-0.023(4)
C221	0.034(3)	0.040(4)	0.033(3)	-0.006(3)	-0.003(3)	0.007(3)
C222	0.034(3)	0.086(6)	0.060(5)	0.006(5)	0.001(3)	0.009(4)
C223	0.041(4)	0.116(9)	0.074(6)	-0.005(6)	-0.013(4)	0.027(5)
C224	0.112(8)	0.083(8)	0.063(6)	-0.008(6)	-0.035(6)	0.052(6)
C225	0.099(7)	0.054(6)	0.083(7)	0.018(5)	-0.009(6)	0.026(5)
C226	0.062(4)	0.040(4)	0.059(5)	0.010(4)	0.003(4)	0.004(3)
C231	0.033(3)	0.034(4)	0.028(3)	0.003(3)	-0.002(2)	-0.001(2)
C232	0.039(3)	0.069(5)	0.041(4)	-0.006(4)	0.009(3)	0.009(3)
C233	0.068(5)	0.068(6)	0.037(4)	-0.008(4)	0.011(4)	0.013(4)
C234	0.078(5)	0.056(5)	0.037(4)	-0.005(4)	-0.007(4)	0.010(4)
C235	0.054(4)	0.056(5)	0.056(5)	-0.014(4)	-0.014(4)	0.006(4)
C236	0.041(3)	0.039(4)	0.047(4)	-0.007(3)	-0.002(3)	0.005(3)
C311	0.026(3)	0.035(4)	0.037(3)	-0.001(3)	0.004(2)	0.000(2)
C312	0.049(4)	0.055(5)	0.049(4)	-0.010(4)	-0.013(3)	0.026(3)
C313	0.086(6)	0.072(6)	0.068(6)	-0.031(5)	-0.019(5)	0.037(5)
C314	0.061(5)	0.060(6)	0.077(6)	-0.025(5)	-0.007(4)	0.028(4)
C315	0.050(4)	0.052(5)	0.064(5)	0.002(4)	-0.008(4)	0.016(3)
C316	0.039(3)	0.044(4)	0.048(4)	-0.006(3)	-0.001(3)	0.012(3)
C321	0.027(3)	0.037(4)	0.029(3)	0.000(3)	0.003(2)	0.000(2)
C322	0.034(3)	0.041(4)	0.041(4)	0.004(3)	0.000(3)	0.001(3)
C323	0.029(3)	0.060(5)	0.063(5)	0.011(4)	0.005(3)	-0.009(3)
C324	0.047(4)	0.047(5)	0.072(5)	0.014(4)	0.004(4)	-0.010(3)
C325	0.049(4)	0.043(5)	0.093(6)	0.027(4)	0.014(4)	0.006(3)
C326	0.029(3)	0.042(4)	0.059(5)	0.012(3)	0.002(3)	-0.003(3)
C331	0.029(3)	0.039(4)	0.029(3)	0.007(3)	0.005(2)	0.006(2)
C332	0.039(3)	0.078(6)	0.037(4)	0.000(4)	0.000(3)	-0.010(3)
C333	0.067(5)	0.095(7)	0.036(4)	-0.006(4)	0.004(4)	-0.014(5)
C334	0.078(5)	0.099(7)	0.033(4)	0.001(4)	0.016(4)	0.002(5)
C335	0.079(5)	0.071(6)	0.060(6)	0.002(5)	0.029(5)	-0.021(5)
C336	0.057(4)	0.046(5)	0.046(4)	-0.006(3)	0.017(3)	-0.011(3)
C411	0.042(3)	0.032(4)	0.036(4)	0.000(3)	0.012(3)	0.005(3)
C412	0.042(4)	0.057(5)	0.060(5)	-0.012(4)	0.021(3)	0.000(3)
C413	0.060(5)	0.068(6)	0.087(7)	0.000(5)	0.040(5)	0.001(4)
C414	0.101(7)	0.091(8)	0.080(7)	-0.010(6)	0.062(6)	0.006(6)
C415	0.105(7)	0.122(10)	0.058(6)	-0.040(6)	0.034(5)	-0.016(7)
C416	0.066(5)	0.077(6)	0.046(5)	-0.020(4)	0.023(4)	-0.013(4)
C421	0.025(3)	0.031(3)	0.042(4)	-0.001(3)	0.002(2)	0.001(2)

C422	0.043(3)	0.034(4)	0.056(5)	-0.003(3)	0.004(3)	0.005(3)
C423	0.056(4)	0.035(4)	0.082(6)	-0.003(4)	-0.001(4)	0.013(3)
C424	0.045(4)	0.042(5)	0.072(6)	0.019(4)	-0.002(4)	0.002(3)
C425	0.042(4)	0.060(5)	0.055(5)	0.020(4)	0.005(3)	0.002(3)
C426	0.037(3)	0.044(4)	0.050(4)	0.002(3)	0.006(3)	0.008(3)
C431	0.031(3)	0.035(4)	0.034(3)	-0.006(3)	0.001(2)	0.002(3)
C432	0.035(3)	0.045(4)	0.049(4)	-0.003(3)	0.006(3)	-0.003(3)
C433	0.039(4)	0.059(5)	0.077(6)	-0.004(4)	0.006(4)	-0.015(3)
C434	0.032(3)	0.073(6)	0.061(5)	-0.010(4)	-0.005(3)	-0.007(3)
C435	0.043(4)	0.072(6)	0.068(5)	-0.003(5)	-0.013(4)	0.011(4)
C436	0.046(4)	0.044(4)	0.054(5)	0.003(4)	-0.006(3)	-0.007(3)
C511	0.086(8)	0.178(15)	0.151(13)	-0.073(12)	-0.015(8)	0.017(9)
C513	0.073(7)	0.128(11)	0.155(13)	-0.011(10)	0.014(7)	-0.003(7)
C514	0.142(12)	0.152(14)	0.101(10)	-0.057(10)	-0.020(9)	0.050(10)
C516	0.125(7)	0.176(10)	0.158(10)	0.006(8)	0.054(7)	0.044(7)
C517	0.114(10)	0.125(12)	0.173(16)	-0.049(11)	-0.004(10)	-0.038(9)
C518	0.109(10)	0.179(15)	0.103(10)	-0.044(10)	0.010(8)	0.035(9)
C519	0.099(8)	0.139(12)	0.119(11)	-0.012(9)	0.032(8)	0.012(8)
C522	0.137(12)	0.25(2)	0.121(12)	-0.062(13)	-0.024(10)	0.104(14)
C523	0.167(16)	0.20(2)	0.180(19)	0.071(17)	-0.061(14)	-0.046(16)
C524	0.24(2)	0.31(3)	0.134(16)	0.15(2)	0.091(16)	0.16(2)
C525	0.22(2)	0.103(12)	0.21(2)	0.043(13)	-0.071(16)	-0.041(12)
O1	0.234(18)	0.28(2)	0.40(3)	0.03(2)	0.043(19)	-0.126(18)
O2	0.129(7)	0.145(9)	0.170(10)	-0.083(8)	0.000(7)	0.002(6)
O3	0.120(7)	0.178(10)	0.152(9)	-0.004(8)	0.048(6)	0.037(7)

5.15 $[(Ph_3PAg)_8(SePh)_{12}(\mu_6\text{-}Se)_{0.5}Ag_6][Cy_3SnCl_2]$ (16)

Compound **16** crystallizes as yellow hexagonal thin plates from THF/hexane.

Table 5.36 Crystal data and structure refinement for compound **16**

Empirical formula	$C_{234}H_{195}Ag_{14}Se_{12.5}P_8Cl_2Sn$
Formula weight /g·mol^{-1}	5941.43
Crystal system	trigonal
Space group	$R\bar{3}$
a /Å	20.3517(4)
b /Å	20.3517(4)
c /Å	99.087(3)
V /Å^3	35542.5(15)
Z	6
ρ_{calc} /g·cm^{-3}	1.665
$\mu(Mo_{K\alpha})$ /mm^{-1}	3.276
2Θ range /°	4-52
Reflections measured	71446
Independent reflections	14706
R(int)	0.1337
Indepedent reflections ($I > 2\sigma(I)$)	7518
Parameters	619
R_1 ($I > 2\sigma(I)$)	0.083
wR_2 (all data)	0.1919
GooF (all data)	0.895
Max. peak/hole /e$^-$·10^{-6}pm^{-3}	1.566/–0.881

Table 5.37 Atomic coordinates and equivalent isotropic displacement parameters for compound **16**

Atom	x/a	y/b	z/c	$U_{eq/iso}$
Ag1	0.44060(7)	0.15382(7)	0.847792(15)	0.0446(4)
Ag2	0.6667	0.3333	0.87519(3)	0.0466(6)
Ag3	0.53371(7)	0.20275(7)	0.821134(16)	0.0453(4)
Ag3A	0.6250(15)	0.2167(14)	0.8532(3)	0.0453(4)
Se1	0.40923(10)	0.24992(9)	0.83452(2)	0.0415(5)
Se1A	0.4606(19)	0.2845(19)	0.8425(4)	0.0415(5)
Se2	0.56985(9)	0.20582(10)	0.86165(2)	0.0421(5)
Se2A	0.5329(19)	0.2119(18)	0.8710(4)	0.0421(5)
Se3	0.6667	0.3333	0.8333	0.047(2)
Ag4	0.0000	0.0000	0.95803(3)	0.0535(6)
Ag5	-0.12835(10)	0.11666(9)	1.013710(18)	0.0695(5)
Ag6	-0.04552(15)	0.07315(14)	0.98171(3)	0.0622(6)
Ag6A	-0.0958(3)	0.0456(3)	0.98825(5)	0.0622(6)
Se4	-0.1768(2)	0.02134(19)	0.99208(3)	0.0610(8)
Se4A	-0.2279(4)	0.0018(4)	0.99719(7)	0.0610(8)
Se5	0.09527(17)	-0.05719(19)	0.96495(3)	0.0585(8)
Se5A	0.1067(3)	-0.0098(4)	0.97114(7)	0.0585(8)
Se6	0.0000	0.0000	1.0000	0.0379(18)
P1	0.3164(2)	0.0512(2)	0.85590(5)	0.0460(11)
P2	0.2079(4)	-0.1688(4)	0.97909(8)	0.088(2)
P3	0.0000	0.0000	0.93295(8)	0.0455(19)
P4	0.6667	0.3333	0.89967(9)	0.0465(19)
Sn1	0.3333	0.6667	0.89925(2)	0.0492(6)
Cl1	0.3333	0.6667	0.87329(10)	0.064(2)
Cl2	0.359(3)	0.664(4)	0.9275(4)	0.23(3)
C6	0.3346(10)	0.2550(10)	0.8465(2)	0.049(5)
C7	-0.0199(11)	-0.1436(11)	0.9320(3)	0.072(7)
C8	0.2641(11)	0.7190(10)	0.9007(2)	0.059(5)
C9	0.2623(12)	0.2272(10)	0.8422(2)	0.057(5)
C10	0.3016(9)	-0.0458(9)	0.85649(18)	0.042(4)
C11	0.1971(13)	0.6864(14)	0.8920(3)	0.098(9)
C12	0.2331(16)	0.2664(14)	0.8621(3)	0.080(8)
C13	0.3477(11)	-0.1264(12)	0.8635(2)	0.058(5)
C14	0.2588(11)	0.0523(9)	0.8305(2)	0.050(5)
C15	0.3543(10)	-0.0574(10)	0.8631(2)	0.055(5)
C16	0.5325(9)	0.1221(9)	0.8739(2)	0.049(5)
C17	0.0121(10)	-0.0761(11)	0.92527(19)	0.048(4)
C19	0.0495(13)	-0.0689(12)	0.9137(2)	0.071(6)
C20	0.1202(13)	0.0214(15)	0.8391(4)	0.090(9)
C21	0.5518(12)	0.0645(13)	0.8727(3)	0.078(7)
C22	0.3076(12)	0.8025(10)	0.9000(2)	0.062(5)

C24	0.5720(11)	0.2986(11)	0.9067(2)	0.054(5)
C25	0.2297(12)	-0.1792(12)	0.8514(2)	0.060(5)
C27	0.2372(9)	-0.1078(8)	0.85073(18)	0.040(4)
C28	0.1371(14)	0.0338(11)	0.8259(4)	0.091(10)
C29	0.2848(10)	-0.1886(10)	0.8580(2)	0.051(5)
C31	0.5206(15)	0.317(2)	0.8994(4)	0.146(16)
C33	0.2583(13)	0.8391(12)	0.9007(3)	0.084(8)
C34	0.3561(12)	0.2895(13)	0.8595(2)	0.068(6)
C35	0.0219(13)	-0.1978(13)	0.9151(2)	0.068(6)
C36	0.3041(16)	0.2956(18)	0.8665(3)	0.103(9)
C37	0.2421(12)	0.0193(14)	0.8956(2)	0.069(6)
C38	0.1705(11)	0.0249(11)	0.8489(3)	0.075(7)
C39	0.2429(10)	0.0405(8)	0.8441(2)	0.048(5)
C40	0.5440(14)	0.2533(14)	0.9172(3)	0.094(8)
C42	0.2119(12)	0.2314(12)	0.8506(2)	0.061(5)
C43	0.1936(13)	0.8057(14)	0.8921(3)	0.086(8)
C45	-0.0158(15)	-0.2049(13)	0.9267(3)	0.085(7)
C46	0.2865(12)	0.0616(10)	0.8724(2)	0.061(5)
C47	0.0552(15)	-0.1276(15)	0.9080(2)	0.081(7)
C69	0.1460(15)	0.7213(15)	0.8935(4)	0.105(10)
C4X	0.2048(14)	0.0442(11)	0.8215(3)	0.068(6)
C64	0.4915(13)	0.1217(12)	0.8850(3)	0.079(7)
C68	0.2602(13)	0.0059(14)	0.8827(3)	0.084(8)
C65	0.4619(15)	0.0631(12)	0.8950(2)	0.084(7)
C66	0.4819(14)	0.0050(15)	0.8933(3)	0.082(7)
C67	0.5220(12)	0.0054(12)	0.8823(3)	0.079(8)
C63	0.2453(19)	0.0829(15)	0.8984(3)	0.110(11)
C60	0.4759(16)	0.230(2)	0.9236(3)	0.134(14)
C62	0.268(3)	0.1371(17)	0.8888(4)	0.21(3)
C5	0.427(2)	0.241(2)	0.9176(6)	0.19(3)
C61	0.294(3)	0.1254(16)	0.8762(4)	0.22(3)
C57	0.450(2)	0.288(3)	0.9058(7)	0.26(4)
C1	0.192(3)	-0.246(2)	0.9931(9)	0.263(14)
C1A	0.184(3)	-0.277(4)	1.0059(7)	0.316(17)
C1B	0.200(3)	-0.335(4)	1.0080(6)	0.37(2)
C1C	0.225(3)	-0.361(3)	0.9973(10)	0.42(2)
C1D	0.234(3)	-0.330(4)	0.9845(8)	0.37(2)
C1E	0.217(3)	-0.272(4)	0.9824(5)	0.316(17)
C2	0.3097(18)	-0.094(2)	0.9778(4)	0.179(9)
C2A	0.370(3)	-0.109(2)	0.9783(4)	0.215(10)
C2B	0.442(2)	-0.054(3)	0.9741(4)	0.251(12)
C2C	0.4537(19)	0.016(2)	0.9695(4)	0.287(14)
C2D	0.394(3)	0.0304(18)	0.9690(4)	0.251(12)
C3	0.190(3)	-0.2020(19)	0.9606(3)	0.185(9)
C3A	0.116(2)	-0.228(2)	0.9561(5)	0.222(11)
C3B	0.094(2)	-0.261(2)	0.9434(5)	0.259(12)

C3C	0.145(3)	-0.267(2)	0.9351(4)	0.296(14)
C3D	0.219(3)	-0.242(2)	0.9396(5)	0.259(12)
C3E	0.2412(18)	-0.209(2)	0.9523(5)	0.222(11)
C4E	0.2337(14)	0.0645(13)	0.9553(2)	0.131(5)
C4	0.1760(11)	-0.0100(13)	0.9535(2)	0.109(4)
C4A	0.1782(13)	-0.0514(11)	0.9425(3)	0.131(5)
C4B	0.2381(16)	-0.0182(15)	0.9334(2)	0.175(7)
C4C	0.2958(13)	0.0563(16)	0.9352(2)	0.153(6)
C4D	0.2936(12)	0.0976(11)	0.9462(3)	0.153(6)
C5A	-0.220(3)	0.063(4)	0.9803(4)	0.243(13)
C5B	-0.187(2)	0.142(4)	0.9805(5)	0.292(16)
C5C	-0.223(4)	0.176(2)	0.9743(6)	0.340(19)
C5D	-0.292(4)	0.132(5)	0.9679(6)	0.39(2)
C5E	-0.326(2)	0.054(4)	0.9677(5)	0.340(19)
C5F	-0.289(4)	0.019(2)	0.9739(5)	0.292(16)

Table 5.38 Anisotropic displacement parameters for compound **16**

Atom	U_{11}	U_{22}	U_{33}	U_{23}	U_{13}	U_{12}
Ag1	0.0371(7)	0.0378(7)	0.0554(9)	0.0020(6)	0.0015(6)	0.0162(6)
Ag2	0.0438(8)	0.0438(8)	0.0522(15)	0.000	0.000	0.0219(4)
Ag3	0.0408(8)	0.0366(7)	0.0585(10)	0.0006(7)	0.0056(7)	0.0193(6)
Ag3A	0.0408(8)	0.0366(7)	0.0585(10)	0.0006(7)	0.0056(7)	0.0193(6)
Se1	0.0364(9)	0.0362(9)	0.0517(12)	0.0019(8)	0.0026(8)	0.0181(8)
Se1A	0.0364(9)	0.0362(9)	0.0517(12)	0.0019(8)	0.0026(8)	0.0181(8)
Se2	0.0349(9)	0.0353(9)	0.0529(12)	-0.0002(8)	-0.0020(8)	0.0150(8)
Se2A	0.0349(9)	0.0353(9)	0.0529(12)	-0.0002(8)	-0.0020(8)	0.0150(8)
Se3	0.046(3)	0.046(3)	0.050(6)	0.000	0.000	0.0228(15)
Ag4	0.0577(9)	0.0577(9)	0.0453(15)	0.000	0.000	0.0288(5)
Ag5	0.0809(11)	0.0588(10)	0.0558(10)	-0.0009(8)	0.0033(9)	0.0251(9)
Ag6	0.0798(17)	0.0676(14)	0.0515(15)	-0.0054(11)	-0.0073(11)	0.0460(14)
Ag6A	0.0798(17)	0.0676(14)	0.0515(15)	-0.0054(11)	-0.0073(11)	0.0460(14)
Se4	0.074(2)	0.0744(19)	0.056(2)	-0.0141(15)	-0.0114(15)	0.0531(19)
Se4A	0.074(2)	0.0744(19)	0.056(2)	-0.0141(15)	-0.0114(15)	0.0531(19)
Se5	0.0521(15)	0.070(2)	0.058(2)	0.0124(15)	0.0081(14)	0.0338(16)
Se5A	0.0521(15)	0.070(2)	0.058(2)	0.0124(15)	0.0081(14)	0.0338(16)
Se6	0.039(3)	0.039(3)	0.036(5)	0.000	0.000	0.0194(13)
P1	0.038(2)	0.037(2)	0.059(3)	0.002(2)	0.010(2)	0.016(2)
P2	0.072(4)	0.077(4)	0.107(6)	-0.001(4)	-0.016(4)	0.033(3)
P3	0.047(3)	0.047(3)	0.042(5)	0.000	0.000	0.0237(14)
P4	0.044(3)	0.044(3)	0.051(5)	0.000	0.000	0.0222(13)
Sn1	0.0454(7)	0.0454(7)	0.0567(15)	0.000	0.000	0.0227(4)
Cl1	0.063(3)	0.063(3)	0.064(6)	0.000	0.000	0.0317(16)

Cl2	0.19(4)	0.16(3)	0.25(3)	0.01(3)	0.09(3)	0.02(3)
C6	0.045(10)	0.048(10)	0.068(14)	0.005(9)	-0.012(9)	0.034(9)
C7	0.055(12)	0.054(12)	0.105(19)	0.017(12)	0.038(12)	0.026(10)
C8	0.049(11)	0.049(11)	0.072(15)	-0.004(10)	0.015(10)	0.019(9)
C9	0.098(16)	0.047(11)	0.050(12)	0.022(9)	0.007(11)	0.053(11)
C10	0.046(10)	0.032(8)	0.056(12)	0.005(8)	0.003(8)	0.025(8)
C11	0.068(15)	0.070(15)	0.17(3)	-0.004(17)	-0.007(17)	0.048(13)
C12	0.11(2)	0.091(17)	0.077(18)	0.002(14)	0.042(16)	0.079(16)
C13	0.061(12)	0.081(15)	0.056(13)	0.012(11)	0.013(10)	0.053(12)
C14	0.056(11)	0.032(9)	0.064(14)	0.002(9)	-0.003(10)	0.022(8)
C15	0.035(9)	0.044(10)	0.085(15)	-0.006(10)	0.009(9)	0.020(8)
C16	0.023(8)	0.028(8)	0.084(15)	-0.021(9)	-0.007(9)	0.005(7)
C17	0.046(10)	0.070(12)	0.041(11)	-0.005(9)	0.006(8)	0.039(10)
C19	0.089(16)	0.070(14)	0.082(17)	0.013(12)	0.012(13)	0.062(13)
C20	0.050(13)	0.10(2)	0.14(3)	-0.029(19)	-0.036(17)	0.046(13)
C21	0.062(13)	0.067(14)	0.097(19)	0.015(13)	0.016(13)	0.027(12)
C22	0.074(13)	0.042(10)	0.080(16)	0.007(10)	-0.002(11)	0.036(10)
C24	0.053(11)	0.058(11)	0.063(14)	0.000(10)	0.007(10)	0.035(10)
C25	0.068(13)	0.077(13)	0.063(14)	-0.024(11)	-0.014(10)	0.057(11)
C27	0.044(9)	0.035(9)	0.054(11)	0.006(8)	0.008(8)	0.028(8)
C28	0.069(17)	0.031(11)	0.16(3)	-0.029(15)	-0.065(19)	0.019(11)
C29	0.045(10)	0.037(9)	0.069(14)	0.001(9)	0.015(9)	0.019(8)
C31	0.068(17)	0.16(3)	0.22(4)	0.11(3)	0.04(2)	0.058(19)
C33	0.079(16)	0.052(12)	0.13(2)	-0.006(14)	0.006(16)	0.039(12)
C34	0.056(12)	0.090(16)	0.074(16)	-0.027(13)	-0.008(11)	0.048(12)
C35	0.091(16)	0.083(16)	0.054(14)	-0.021(12)	-0.015(12)	0.062(14)
C36	0.077(18)	0.15(3)	0.09(2)	-0.034(18)	0.017(15)	0.056(18)
C37	0.077(15)	0.080(16)	0.059(15)	0.000(12)	0.021(12)	0.046(13)
C38	0.048(12)	0.042(11)	0.12(2)	0.013(12)	0.019(13)	0.014(9)
C39	0.047(10)	0.022(8)	0.076(15)	0.005(8)	0.005(10)	0.018(7)
C40	0.073(16)	0.080(17)	0.11(2)	0.030(16)	-0.006(16)	0.026(14)
C42	0.067(13)	0.079(14)	0.058(14)	0.008(12)	0.016(11)	0.052(12)
C43	0.073(16)	0.083(17)	0.12(2)	-0.016(16)	-0.008(15)	0.054(14)
C45	0.12(2)	0.064(14)	0.10(2)	0.000(13)	0.015(16)	0.062(15)
C46	0.070(13)	0.038(10)	0.058(13)	0.018(9)	0.003(11)	0.014(9)
C47	0.108(19)	0.12(2)	0.061(15)	-0.007(14)	0.006(13)	0.095(18)
C69	0.083(18)	0.09(2)	0.16(3)	0.004(19)	-0.012(18)	0.060(16)
C4X	0.089(16)	0.049(11)	0.085(17)	-0.014(11)	-0.027(13)	0.050(12)
C64	0.079(15)	0.042(11)	0.10(2)	0.009(12)	0.003(15)	0.022(11)
C68	0.069(15)	0.072(15)	0.12(2)	0.034(15)	0.014(14)	0.038(13)
C65	0.103(18)	0.054(13)	0.065(16)	-0.002(12)	-0.018(14)	0.016(13)
C66	0.074(16)	0.089(18)	0.088(19)	0.011(15)	-0.002(14)	0.046(14)
C67	0.052(12)	0.059(13)	0.12(2)	0.018(14)	-0.025(14)	0.022(11)
C63	0.19(3)	0.077(17)	0.064(17)	0.039(14)	0.064(19)	0.06(2)
C60	0.072(19)	0.23(4)	0.08(2)	0.04(2)	0.028(16)	0.07(2)
C62	0.40(7)	0.065(19)	0.13(3)	0.02(2)	0.11(4)	0.09(3)

C5	0.13(3)	0.17(4)	0.34(7)	0.15(4)	0.16(4)	0.12(3)
C61	0.43(7)	0.058(17)	0.14(3)	0.028(19)	0.17(4)	0.09(3)
C57	0.15(3)	0.21(4)	0.52(10)	0.21(6)	0.21(5)	0.16(4)

5.16 $\frac{1}{\infty}$ [SnS$_2$·en] (17)

Compound **17** crystallizes as colorless blocks from under solvothermal condition from methanol.

Table 5.36 Crystal data and structure refinement for compound **17**

Empirical formula	C$_4$H$_{16}$N$_4$S$_4$Sn$_2$
Formula weight /g·mol^{-1}	485.83
Crystal system	monoclinic
Space group	*C2/c*
a /Å	15.317(3)
b /Å	10.443(2)
c /Å	12.754(3)
β /°	93.62(3)
V /Å^3	2036.1(7)
Z	6
ρ_{calc} /g·cm^{-3}	2.377
μ(Mo$_{K\alpha}$) /mm^{-1}	4.268
2Θ range /°	10-55
Reflections measured	6179
Independent reflections	1771
R(int)	0.0946
Indepedent reflections ($I > 2\sigma(I)$)	903
Parameters	96
R_1 ($I > 2\sigma(I)$)	0.0648
wR_2 (all data)	0.1023
GooF (all data)	1.246
Max. peak/hole /e$^-$·10^{-6}pm^{-3}	1.488/−1.885

Table 5.37 Atomic coordinates   and equivalent isotropic displacement parameters for compound **17**

Atom	x/a	y/b	z/c	$U_{eq/iso}$
Sn1	0.33458(6)	0.19136(8)	0.58464(8)	0.0146(2)
Sn2	0.5000	0.32226(15)	0.7500	0.0168(3)
S1	0.4985(2)	0.1789(4)	0.5986(3)	0.0222(8)
S2	0.3380(2)	0.3441(4)	0.7335(3)	0.0197(8)
S3	0.1724(2)	0.1717(4)	0.5729(3)	0.0207(8)
N1	0.3398(8)	0.0295(12)	0.7037(10)	0.024(3)
N2	0.3327(8)	0.0129(15)	0.4803(10)	0.033(4)
N3	0.4996(8)	0.5042(11)	0.6452(10)	0.024(3)
C1	0.3657(10)	-0.0966(14)	0.6555(13)	0.032(4)
C2	0.3148(9)	-0.1048(15)	0.5470(15)	0.034(4)
C3	0.4765(12)	0.618(2)	0.699(2)	0.095(12)

Table 5.38 Anisotropic displacement parameters for compound **17**

Atom	U_{11}	U_{22}	U_{33}	U_{23}	U_{13}	U_{12}
Sn1	0.0110(4)	0.0231(4)	0.0099(3)	0.0035(4)	0.0018(2)	0.0065(4)
Sn2	0.0162(6)	0.0247(8)	0.0098(6)	0.000	0.0038(4)	0.000
S1	0.0128(15)	0.036(2)	0.0174(16)	-0.0024(15)	-0.0008(12)	0.0092(14)
S2	0.0146(15)	0.026(2)	0.0191(16)	-0.0064(13)	0.0078(12)	0.0086(13)
S3	0.0149(15)	0.034(2)	0.0132(15)	0.0190(15)	0.0014(11)	0.0077(14)
N1	0.032(6)	0.009(6)	0.032(6)	0.012(5)	0.008(5)	-0.008(5)
N2	0.013(6)	0.054(10)	0.031(7)	-0.009(6)	0.000(5)	-0.024(6)
N3	0.025(6)	0.002(6)	0.048(7)	0.019(5)	0.026(5)	-0.001(4)
C1	0.030(7)	0.012(7)	0.054(9)	0.033(7)	0.009(6)	0.010(6)
C2	0.007(6)	0.011(7)	0.086(12)	-0.033(7)	0.008(6)	0.001(5)
C3	0.031(13)	0.067(16)	0.20(3)	-0.009(16)	0.076(15)	0.026(10)

5.17 [*en*H]₄[Sn₂S₆]·*en* (18)

Compound **18** crystallizes as colorless blocks from under solvothermal condition from *en*.

Table 5.39 Crystal data and structure refinement for compound **18**

Empirical formula	$C_{10}H_{44}N_{10}S_6Sn_2$
Formula weight /g·mol^{-1}	734.29
Crystal system	triclinic
Space group	$P\bar{1}$
a /Å	9.8777
b /Å	9.934
c /Å	15.423
α /°	72.63
β /°	86.22
γ /°	81.38
V /Å^3	1427.6
Z	2
ρ_{calc} /g·cm^{-3}	1.708
μ(Mo$_{K\alpha}$) /mm^{-1}	2.207
2Θ range /°	10-52
Reflections measured	15399
Independent reflections	6015
R(int)	0.0523
Indepedent reflections ($I > 2\sigma(I)$)	5178
Parameters	257
R_1 (I > 2$\sigma(I)$)	0.0321
wR_2 (all data)	0.1138
GooF (all data)	1.111
Max. peak/hole /e$^-$·10^{-6}pm^{-3}	1.071/–1.916

Table 5.40 Atomic coordinates and equivalent isotropic displacement parameters for compound **18**

Atom	x/a	y/b	z/c	$U_{eq/iso}$
Sn1	-0.126105(17)	0.115820(18)	-0.223478(11)	0.01140(9)
Sn2	0.118117(17)	-0.114206(18)	-0.279307(11)	0.01125(9)
S1	-0.23228(7)	0.04514(8)	-0.07897(5)	0.01449(16)
S2	-0.18700(7)	0.34284(8)	-0.32104(5)	0.01582(16)
S3	-0.12985(7)	-0.06475(7)	-0.30168(5)	0.01422(16)
S4	0.12175(7)	0.06788(7)	-0.20219(5)	0.01403(16)
S5	0.18209(7)	-0.33580(7)	-0.17493(5)	0.01493(16)
S6	0.22878(7)	-0.04981(8)	-0.42147(5)	0.01493(16)
N1	0.0348(3)	0.7976(3)	-0.01568(17)	0.0162(5)
N2	0.1268(3)	0.4622(3)	0.17717(17)	0.0167(5)
N3	0.4118(2)	0.8381(2)	-0.08970(15)	0.0162(5)
N4	0.6182(2)	0.6842(2)	-0.25602(15)	0.0158(5)
N5	0.5196(2)	0.5587(2)	0.23627(15)	0.0168(5)
N6	0.5395(2)	0.8746(2)	0.16797(15)	0.0150(4)
N7	0.4188(2)	0.1983(2)	0.44343(15)	0.0177(5)
N8	0.4002(2)	0.2070(3)	0.64556(16)	0.0194(5)
N9	0.0403(3)	0.7931(3)	0.48322(17)	0.0165(5)
N10	0.1603(3)	0.4580(3)	0.66949(18)	0.0218(6)
C1	0.0083(3)	0.6747(3)	0.0637(2)	0.0154(6)
C2	0.1408(3)	0.5728(3)	0.0911(2)	0.0167(6)
C3	0.5202(3)	0.7408(3)	-0.11674(19)	0.0174(6)
C4	0.5387(3)	0.7935(3)	-0.21901(18)	0.0160(5)
C5	0.5457(3)	0.6389(3)	0.14172(18)	0.0163(5)
C6	0.6185(3)	0.7672(3)	0.12748(18)	0.0151(5)
C7	0.4497(3)	0.3121(3)	0.47798(19)	0.0205(6)
C8	0.5011(3)	0.2634(4)	0.5747(2)	0.0230(6)
C9	0.0209(3)	0.6682(3)	0.5628(2)	0.0170(6)
C10	0.1588(3)	0.5745(3)	0.5854(2)	0.0197(6)

Table 5.41 Anisotropic displacement parameters for compound **18**

Atom	U_{11}	U_{22}	U_{33}	U_{23}	U_{13}	U_{12}
Sn1	0.00856(13)	0.01216(14)	0.01191(14)	-0.00208(9)	0.00059(9)	0.0003(9)
Sn2	0.00861(13)	0.01132(14)	0.01245(14)	-0.00205(9)	0.00083(9)	-0.0004(9)
S1	0.0105(3)	0.0171(3)	0.0134(3)	-0.0022(3)	0.0018(3)	0.0000(3)
S2	0.0161(3)	0.0131(3)	0.0155(3)	-0.0018(3)	-0.0011(3)	0.0021(3)
S3	0.0098(3)	0.0150(3)	0.0181(3)	-0.0053(3)	-0.0005(3)	-0.0014(3)
S4	0.0093(3)	0.0151(3)	0.0181(3)	-0.0057(3)	-0.0007(3)	-0.0010(3)
S5	0.0137(3)	0.0123(3)	0.0163(3)	-0.0016(3)	-0.0011(3)	0.0010(3)
S6	0.0119(3)	0.0169(4)	0.0149(3)	-0.0033(3)	0.0035(3)	-0.0031(3)
N1	0.0139(11)	0.0158(12)	0.0157(12)	-0.0012(10)	0.0001(9)	0.0005(9)
N2	0.0153(11)	0.0123(11)	0.0192(12)	-0.0005(9)	-0.0018(9)	0.0007(9)
N3	0.0166(11)	0.0164(11)	0.0125(10)	-0.0015(9)	0.0010(8)	0.0008(9)
N4	0.0177(11)	0.0132(11)	0.0139(10)	-0.0024(9)	0.0015(8)	0.0014(9)
N5	0.0166(11)	0.0154(12)	0.0178(11)	-0.0027(9)	0.0012(9)	-0.0057(9)
N6	0.0137(10)	0.0128(11)	0.0170(11)	-0.0029(9)	0.0003(8)	-0.0006(8)
N7	0.0176(11)	0.0192(12)	0.0141(11)	-0.0015(9)	0.0005(9)	-0.0028(9)
N8	0.0184(11)	0.0257(13)	0.0132(11)	-0.0028(10)	-0.0014(9)	-0.0053(10)
N9	0.0165(12)	0.0151(12)	0.0153(12)	-0.0016(10)	-0.0002(9)	-0.0004(9)
N10	0.0191(12)	0.0176(12)	0.0228(13)	0.0005(10)	0.0024(10)	0.0014(10)
C1	0.0135(13)	0.0149(13)	0.0156(13)	-0.0015(11)	0.0007(10)	-0.0013(10)
C2	0.0120(12)	0.0173(14)	0.0177(14)	-0.0019(11)	0.0004(10)	0.0007(11)
C3	0.0180(13)	0.0169(13)	0.0154(13)	-0.0035(11)	-0.0002(10)	0.0007(11)
C4	0.0149(12)	0.0138(13)	0.0155(12)	-0.0013(10)	0.0026(10)	0.0021(10)
C5	0.0157(12)	0.0136(13)	0.0187(13)	-0.0036(10)	0.0002(10)	-0.0014(10)
C6	0.0130(11)	0.0146(13)	0.0160(12)	-0.0027(10)	0.0015(10)	-0.0007(10)
C7	0.0229(14)	0.0196(14)	0.0181(13)	-0.0031(11)	0.0040(11)	-0.0070(11)
C8	0.0201(14)	0.0308(17)	0.0199(14)	-0.0082(13)	0.0021(11)	-0.0090(12)
C9	0.0170(14)	0.0153(14)	0.0158(14)	-0.0014(11)	0.0006(11)	-0.0001(11)
C10	0.0167(14)	0.0197(15)	0.0183(14)	-0.0012(12)	0.0025(11)	0.0009(11)

5.18 [(Ph$_3$PCu^I)$_6${$cyclo$-(CH$_2$)$_4$Sn^{IV}S$_2$}$_6$Cu$^I_4$Sn^{II}] (19)

Compound **19** crystallizes as orange-yellow blocks under solvothermal condition from methanol.

Table 5.42 Crystal data and structure refinement for compound **19**

Empirical formula	C$_{132}$H$_{138}$Cu$_{10}$P$_6$S$_{12}$Sn$_7$
Formula weight /g·mol^{-1}	3761.19
Crystal system	Monoclinic
Space group	$P2_1/n$
a /Å	17.6227(5)
b /Å	22.6814(4)
c /Å	18.8353(5)
β /°	115.099(2)
V /Å^3	6817.7(3)
Z	2
ρ_{calc} /g·cm^{-3}	1.832
μ(Mo$_{K\alpha}$) /mm^{-1}	3.081
2Θ range /°	4-52
Reflections measured	38108
Independent reflections	14367
R(int)	0.0514
Indepedent reflections ($I > 2\sigma(I)$)	8789
Parameters	794
R_1 ($I > 2\sigma(I)$)	0.0377
wR_2 (all data)	0.0734
GooF (all data)	0.834
Max. peak/hole /e$^-$·10^{-6}pm^{-3}	0.676/–0.644

The structure was solved by direct methods and refined against all F^2 data with full-matrix least squares methods to residuals wR_2 = 0.0768 for all 14367 independent reflections, corresponding to R_1 = 0.0377 for 8789 F_o data > $3\sigma(F)$. All heavier atoms were refined using anisotropic displacement parameters, the H-atoms were kept riding on calculated positions with isotropic displacement parameters set to $1.2U_{eq}$ of their bonding partners. The structure shows disorder of the inner cluster core over the center of symmetry (Sn4, Cu4-7 half occupied). There is no choice for an ordered description in a non-centrosymmetric space group as no violation of the extinction rules of $P2_1/n$ is observed within the 3σ limit. In addition, a small contribution of disorder by rotation of about 20° around the Sn4-Cu7 axis is found for Cu4-6 in a 91.2(1):8.8(1) ratio, and Sn1 is disordered over three close positions in a 84.7(7):11.6(6):3.2(3) ratio. Strongly anisotropic displacement parameters of one phenyl ring (C49-C54) suggest disorder by rotation around the P–C axis. As by refinement of a split-atom model the results could not be improved, the description with large anisotropy was retained. Figure 5.1 shows a thermal ellipsoid diagram (50% probability) of the Cu/Sn/P/S cluster core considering the inversion disorder of the inner Cu_4Sn unit (Cu4'-Cu6', green spheres; Cu7' ruby sphere Sn7', orange sphere), the additional rotational disorder of Cu4-Cu6 (Cu4A-Cu6A, pink spheres; Cu4'A-Cu6'A, turquise spheres), and the disorder of Sn1.
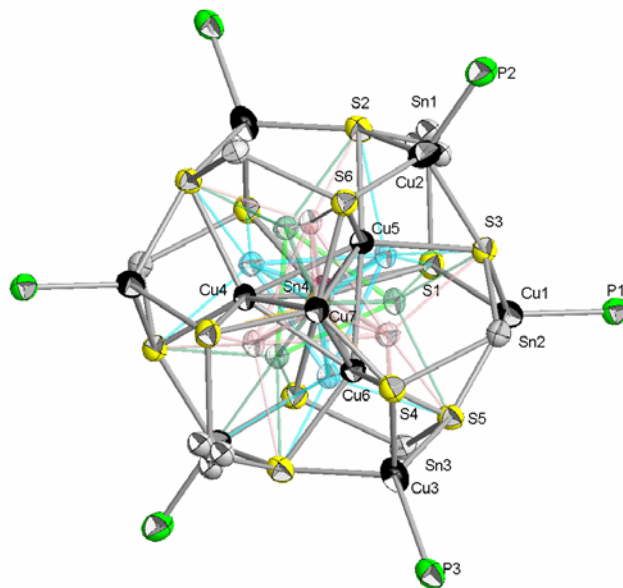

Figure 5.1 Thermal ellipsoid diagram (50% probability) of the Cu/Sn/P/S cluster core considering the inversion disorder of Cu4-Cu7, Sn4 and the rotational disorder of Cu4-Cu6.

Table 5.43 Atomic coordinates and equivalent isotropic displacement parameters for compound **19**

Atom	x/a	y/b	z/c	$U_{eq/iso}$
Sn1	0.17086(11)	0.98347(5)	0.74859(4)	0.0298(3)
Sn1A	0.1454(6)	0.9851(3)	0.7542(3)	0.0298(3)
Sn1B	0.1604(10)	1.0110(13)	0.7524(7)	0.0298(3)
Sn2	0.19912(2)	0.918013(16)	0.451303(18)	0.03166(9)
Sn3	-0.10486(2)	0.827480(15)	0.522714(18)	0.03171(8)
Sn4	0.04992(4)	0.94125(3)	0.54518(3)	0.02550(14)
Cu1	-0.07826(4)	0.95392(3)	0.66057(3)	0.03489(15)
Cu2	-0.04146(4)	0.87205(3)	0.35060(3)	0.04242(17)
Cu3	0.24218(5)	1.03859(3)	0.60110(3)	0.04108(17)
Cu4	0.02639(9)	1.01786(6)	0.43283(6)	0.0280(3)
Cu4A	-0.0211(9)	0.9931(6)	0.4073(7)	0.0280(3)
Cu5	0.01467(8)	1.05201(5)	0.55867(6)	0.0274(3)
Cu5A	0.0615(9)	1.0588(6)	0.5352(6)	0.0274(3)
Cu6	-0.10025(8)	0.98514(6)	0.46084(6)	0.0276(3)
Cu6A	-0.0847(8)	1.0045(6)	0.5125(7)	0.0276(3)
Cu7	-0.08673(8)	1.09518(5)	0.42430(6)	0.0293(3)
S1	0.05603(8)	0.91568(6)	0.67805(6)	0.0334(3)
S2	-0.15643(8)	0.93445(6)	0.33432(6)	0.0337(3)
S3	0.06103(8)	0.94310(5)	0.35857(6)	0.0305(3)
S4	0.20636(8)	0.93474(6)	0.58029(6)	0.0337(3)
S5	0.16239(8)	1.07778(5)	0.47161(6)	0.0302(3)
S6	0.00736(8)	0.84100(5)	0.48347(6)	0.0321(3)
P1	-0.11208(8)	0.93396(6)	0.75917(6)	0.0309(3)
P2	-0.06453(10)	0.79710(7)	0.26936(8)	0.0443(4)
P3	0.37889(10)	1.05429(6)	0.66677(7)	0.0380(3)
C1	0.2823(4)	0.9320(3)	0.7944(3)	0.0538(16)
C2	0.2904(4)	0.9167(3)	0.8762(4)	0.0675(19)
C3	0.2767(4)	0.9701(4)	0.9174(3)	0.070(2)
C4	0.1910(4)	0.9995(3)	0.8681(3)	0.0614(18)
C5	0.2498(3)	0.8341(2)	0.4386(3)	0.0431(13)
C6	0.3409(4)	0.8509(3)	0.4593(4)	0.0624(18)
C7	0.3482(4)	0.9083(3)	0.4220(4)	0.0635(19)
C8	0.3026(3)	0.9601(3)	0.4392(3)	0.0471(14)
C9	-0.1891(4)	0.7562(3)	0.4602(3)	0.0479(14)
C10	-0.1869(4)	0.7171(3)	0.5288(3)	0.0566(17)
C11	-0.1031(5)	0.7146(3)	0.5968(3)	0.0588(18)
C12	-0.0696(4)	0.7749(2)	0.6280(3)	0.0425(13)
C13	-0.1745(3)	0.8687(2)	0.7539(3)	0.0413(12)
C14	-0.2261(4)	0.8453(3)	0.6835(4)	0.0549(16)
C15	-0.2714(5)	0.7929(4)	0.6822(5)	0.079(2)
C16	-0.2625(6)	0.7688(3)	0.7525(5)	0.075(2)

C17	-0.2170(5)	0.7939(3)	0.8221(5)	0.077(2)
C18	-0.1704(5)	0.8420(3)	0.8230(4)	0.075(2)
C19	-0.1667(3)	0.9931(2)	0.7855(2)	0.0357(12)
C20	-0.2397(4)	0.9846(3)	0.7930(3)	0.0583(16)
C21	-0.2807(4)	1.0341(4)	0.8071(4)	0.070(2)
C22	-0.2490(4)	1.0884(3)	0.8125(3)	0.0586(18)
C23	-0.1756(5)	1.0974(3)	0.8055(3)	0.0555(17)
C24	-0.1367(4)	1.0501(2)	0.7901(3)	0.0437(14)
C25	-0.0181(3)	0.9194(2)	0.8490(2)	0.0315(11)
C26	0.0103(3)	0.9536(2)	0.9169(2)	0.0389(13)
C27	0.0841(4)	0.9392(3)	0.9809(3)	0.0477(15)
C28	0.1315(4)	0.8912(3)	0.9785(3)	0.0455(14)
C29	0.1046(3)	0.8574(2)	0.9114(3)	0.0401(12)
C30	0.0319(3)	0.8718(2)	0.8473(3)	0.0375(12)
C31	-0.0083(4)	0.7314(3)	0.3173(3)	0.0494(15)
C32	0.0748(5)	0.7344(3)	0.3613(6)	0.099(3)
C33	0.1220(5)	0.6873(4)	0.4047(5)	0.096(3)
C34	0.0847(5)	0.6352(3)	0.4028(4)	0.070(2)
C35	-0.0008(5)	0.6313(3)	0.3632(3)	0.0645(19)
C36	-0.0481(5)	0.6801(3)	0.3209(3)	0.0574(16)
C37	-0.0402(4)	0.8086(2)	0.1849(3)	0.0432(13)
C38	-0.0015(5)	0.7689(3)	0.1583(4)	0.0637(18)
C39	0.0078(5)	0.7795(3)	0.0894(4)	0.069(2)
C40	-0.0206(4)	0.8298(3)	0.0483(3)	0.0527(15)
C41	-0.0555(5)	0.8719(3)	0.0773(3)	0.068(2)
C42	-0.0644(5)	0.8615(3)	0.1464(3)	0.0632(19)
C43	-0.1734(4)	0.7730(2)	0.2216(3)	0.0455(14)
C44	-0.2096(4)	0.7488(3)	0.1476(3)	0.0535(16)
C45	-0.2913(4)	0.7286(3)	0.1170(3)	0.0577(17)
C46	-0.3359(4)	0.7308(3)	0.1621(3)	0.0551(16)
C47	-0.3014(4)	0.7553(3)	0.2350(3)	0.0542(16)
C48	-0.2212(4)	0.7773(3)	0.2645(3)	0.0526(15)
C49	0.4229(4)	1.1206(2)	0.6431(3)	0.0420(13)
C50	0.3856(5)	1.1428(4)	0.5690(4)	0.094(3)
C51	0.4204(6)	1.1905(5)	0.5491(6)	0.137(5)
C52	0.4896(6)	1.2177(3)	0.6018(5)	0.074(2)
C53	0.5253(6)	1.1976(3)	0.6750(4)	0.094(3)
C54	0.4910(6)	1.1493(4)	0.6949(4)	0.096(3)
C55	0.4172(4)	1.0609(2)	0.7733(3)	0.0387(12)
C56	0.3719(4)	1.0975(3)	0.8006(3)	0.0464(14)
C57	0.3993(4)	1.1073(3)	0.8813(3)	0.0566(17)
C58	0.4702(5)	1.0795(3)	0.9332(3)	0.0613(18)
C59	0.5142(4)	1.0423(3)	0.9069(3)	0.0607(18)
C60	0.4888(4)	1.0335(3)	0.8270(3)	0.0485(15)
C61	0.4442(4)	0.9959(2)	0.6567(3)	0.0420(13)
C62	0.5038(4)	1.0041(3)	0.6297(4)	0.0600(17)

Atom						
C63	0.5492(5)	0.9572(3)	0.6212(4)	0.074(2)		
C64	0.5380(4)	0.9017(3)	0.6433(4)	0.0632(17)		
C65	0.4775(5)	0.8925(3)	0.6690(4)	0.0647(18)		
C66	0.4299(4)	0.9386(3)	0.6752(3)	0.0520(15)		

Table 5.44 Anisotropic displacement parameters for compound **19**

Atom	U_{11}	U_{22}	U_{33}	U_{23}	U_{13}	U_{12}
Sn1	0.0294(6)	0.0351(5)	0.02278(19)	0.00190(19)	0.0091(2)	-0.0014(3)
Sn1A	0.0294(6)	0.0351(5)	0.02278(19)	0.00190(19)	0.0091(2)	-0.0014(3)
Sn1B	0.0294(6)	0.0351(5)	0.02278(19)	0.00190(19)	0.0091(2)	-0.0014(3)
Sn2	0.02953(19)	0.0352(2)	0.03287(16)	-0.0022(14)	0.0158(14)	-0.0015(1)
Sn3	0.0342(2)	0.02854(18)	0.03348(16)	-0.0010(14)	0.0154(14)	-0.0037(1)
Sn4	0.0262(4)	0.0272(4)	0.0235(3)	0.0021(3)	0.0109(3)	-0.0006(3)
Cu1	0.0357(4)	0.0356(4)	0.0305(3)	0.0003(2)	0.0112(3)	0.0000(3)
Cu2	0.0359(4)	0.0446(4)	0.0426(3)	0.0061(3)	0.0126(3)	-0.0083(3)
Cu3	0.0532(4)	0.0399(4)	0.0325(3)	0.0020(3)	0.0205(3)	0.0071(3)
Cu4	0.0312(8)	0.0310(7)	0.0243(6)	0.0027(5)	0.0143(5)	-0.0006(6)
Cu4A	0.0312(8)	0.0310(7)	0.0243(6)	0.0027(5)	0.0143(5)	-0.0006(6)
Cu5	0.0278(7)	0.0298(7)	0.0242(5)	0.0000(5)	0.0108(5)	-0.0035(6)
Cu5A	0.0278(7)	0.0298(7)	0.0242(5)	0.0000(5)	0.0108(5)	-0.0035(6)
Cu6	0.0259(7)	0.0289(7)	0.0267(6)	0.0007(5)	0.0098(5)	-0.0015(6)
Cu6A	0.0259(7)	0.0289(7)	0.0267(6)	0.0007(5)	0.0098(5)	-0.0015(6)
Cu7	0.0301(7)	0.0311(7)	0.0271(5)	0.0011(5)	0.0126(5)	-0.0007(6)
S1	0.0327(7)	0.0401(7)	0.0278(5)	0.0053(5)	0.0133(5)	-0.0001(6)
S2	0.0359(7)	0.0366(7)	0.0266(5)	-0.0011(5)	0.0113(5)	-0.0005(6)
S3	0.0331(7)	0.0305(7)	0.0296(5)	0.0002(5)	0.0150(5)	-0.0034(6)
S4	0.0325(7)	0.0380(7)	0.0302(5)	-0.0012(5)	0.0130(5)	0.0030(6)
S5	0.0327(7)	0.0302(6)	0.0262(5)	0.0003(5)	0.0110(5)	-0.0015(6)
S6	0.0339(7)	0.0301(7)	0.0344(6)	-0.0003(5)	0.0165(5)	-0.0023(6)
P1	0.0315(7)	0.0295(7)	0.0312(6)	0.0024(5)	0.0128(5)	-0.0009(6)
P2	0.0423(9)	0.0440(9)	0.0469(7)	-0.0004(6)	0.0190(7)	-0.0107(7)
P3	0.0480(9)	0.0364(8)	0.0281(6)	0.0019(5)	0.0147(6)	0.0007(7)
C1	0.040(3)	0.060(4)	0.052(3)	0.017(3)	0.010(3)	-0.005(3)
C2	0.050(4)	0.087(5)	0.061(4)	0.027(4)	0.018(3)	0.015(4)
C3	0.052(4)	0.100(6)	0.045(3)	0.013(4)	0.009(3)	-0.013(4)
C4	0.069(5)	0.075(5)	0.038(3)	-0.002(3)	0.021(3)	-0.009(4)
C5	0.039(3)	0.045(3)	0.045(3)	-0.001(2)	0.017(2)	0.008(3)
C6	0.050(4)	0.070(5)	0.070(4)	-0.012(3)	0.029(3)	0.011(4)
C7	0.041(4)	0.100(6)	0.060(4)	0.007(4)	0.032(3)	0.004(4)
C8	0.034(3)	0.066(4)	0.042(3)	0.004(3)	0.017(2)	-0.016(3)
C9	0.052(4)	0.047(3)	0.050(3)	-0.011(3)	0.026(3)	-0.015(3)
C10	0.070(5)	0.051(4)	0.055(3)	-0.004(3)	0.033(3)	-0.021(3)

C11	0.088(5)	0.044(4)	0.048(3)	0.007(3)	0.032(3)	-0.008(4)
C12	0.040(3)	0.046(3)	0.047(3)	0.011(2)	0.024(3)	0.007(3)
C13	0.027(3)	0.037(3)	0.060(3)	0.001(3)	0.020(2)	0.001(3)
C14	0.062(4)	0.053(4)	0.069(4)	-0.021(3)	0.046(3)	-0.017(3)
C15	0.058(5)	0.089(6)	0.102(6)	-0.054(5)	0.045(4)	-0.021(4)
C16	0.100(7)	0.037(4)	0.111(6)	0.002(4)	0.067(5)	-0.004(4)
C17	0.067(5)	0.073(5)	0.091(5)	0.022(4)	0.035(4)	-0.014(4)
C18	0.055(4)	0.077(5)	0.079(4)	0.041(4)	0.016(3)	-0.015(4)
C19	0.034(3)	0.040(3)	0.028(2)	0.001(2)	0.008(2)	0.007(3)
C20	0.041(4)	0.063(4)	0.068(4)	-0.018(3)	0.020(3)	-0.004(3)
C21	0.032(4)	0.103(6)	0.073(4)	-0.016(4)	0.020(3)	0.005(4)
C22	0.048(4)	0.066(5)	0.043(3)	-0.012(3)	0.001(3)	0.020(4)
C23	0.078(5)	0.049(4)	0.036(3)	0.007(3)	0.021(3)	0.022(4)
C24	0.064(4)	0.039(3)	0.032(2)	0.002(2)	0.024(3)	0.009(3)
C25	0.033(3)	0.035(3)	0.033(2)	0.009(2)	0.020(2)	0.006(2)
C26	0.043(3)	0.048(3)	0.026(2)	0.000(2)	0.014(2)	0.007(3)
C27	0.053(4)	0.062(4)	0.029(2)	-0.001(2)	0.018(2)	0.007(3)
C28	0.049(4)	0.057(4)	0.030(2)	0.004(2)	0.016(2)	0.009(3)
C29	0.039(3)	0.043(3)	0.042(3)	0.006(2)	0.021(2)	0.011(3)
C30	0.046(3)	0.035(3)	0.036(2)	0.004(2)	0.022(2)	0.002(3)
C31	0.057(4)	0.037(3)	0.053(3)	0.000(3)	0.021(3)	-0.008(3)
C32	0.049(5)	0.048(5)	0.171(8)	0.025(5)	0.018(5)	0.001(4)
C33	0.050(5)	0.066(5)	0.142(7)	0.038(5)	0.011(5)	-0.004(4)
C34	0.078(6)	0.055(4)	0.066(4)	0.013(3)	0.020(4)	0.000(4)
C35	0.085(6)	0.047(4)	0.058(4)	0.007(3)	0.027(4)	-0.009(4)
C36	0.065(4)	0.051(4)	0.055(3)	0.003(3)	0.026(3)	-0.009(4)
C37	0.037(3)	0.044(3)	0.050(3)	0.003(3)	0.020(3)	0.001(3)
C38	0.076(5)	0.049(4)	0.089(4)	0.020(3)	0.056(4)	0.017(4)
C39	0.073(5)	0.071(5)	0.085(5)	0.003(4)	0.054(4)	0.011(4)
C40	0.061(4)	0.054(4)	0.048(3)	-0.003(3)	0.028(3)	-0.008(3)
C41	0.106(6)	0.051(4)	0.054(3)	0.005(3)	0.041(4)	-0.008(4)
C42	0.092(6)	0.049(4)	0.055(3)	-0.004(3)	0.038(4)	0.005(4)
C43	0.055(4)	0.041(3)	0.043(3)	-0.011(2)	0.024(3)	-0.016(3)
C44	0.050(4)	0.059(4)	0.058(3)	-0.014(3)	0.029(3)	-0.011(3)
C45	0.053(4)	0.064(4)	0.055(3)	-0.022(3)	0.023(3)	-0.018(4)
C46	0.044(4)	0.063(4)	0.063(3)	-0.018(3)	0.027(3)	-0.012(3)
C47	0.048(4)	0.058(4)	0.062(3)	-0.008(3)	0.028(3)	-0.023(3)
C48	0.056(4)	0.050(4)	0.052(3)	-0.008(3)	0.024(3)	-0.016(3)
C49	0.055(4)	0.042(3)	0.036(3)	0.004(2)	0.027(3)	0.005(3)
C50	0.047(4)	0.140(8)	0.083(5)	0.073(5)	0.016(4)	-0.002(5)
C51	0.065(6)	0.189(11)	0.136(8)	0.127(8)	0.024(6)	-0.009(7)
C52	0.091(6)	0.047(4)	0.120(6)	0.033(4)	0.079(5)	0.015(4)
C53	0.174(9)	0.063(5)	0.067(4)	-0.023(4)	0.074(5)	-0.065(6)
C54	0.146(8)	0.093(6)	0.041(3)	-0.015(3)	0.032(4)	-0.078(6)
C55	0.042(3)	0.038(3)	0.034(2)	0.002(2)	0.014(2)	-0.006(3)
C56	0.049(4)	0.054(4)	0.033(2)	0.000(2)	0.014(2)	-0.009(3)

C57	0.062(4)	0.073(5)	0.039(3)	-0.011(3)	0.026(3)	-0.016(4)
C58	0.071(5)	0.077(5)	0.032(3)	-0.004(3)	0.018(3)	-0.012(4)
C59	0.061(4)	0.073(5)	0.030(3)	0.010(3)	0.003(3)	0.001(4)
C60	0.051(4)	0.057(4)	0.038(3)	0.002(3)	0.019(3)	-0.003(3)
C61	0.042(3)	0.046(3)	0.033(2)	0.000(2)	0.012(2)	-0.001(3)
C62	0.058(4)	0.049(4)	0.085(4)	-0.005(3)	0.042(4)	-0.008(3)
C63	0.066(5)	0.066(5)	0.117(6)	-0.004(4)	0.064(5)	-0.007(4)
C64	0.050(4)	0.061(4)	0.085(4)	-0.005(4)	0.035(4)	0.006(4)
C65	0.082(5)	0.050(4)	0.075(4)	0.004(3)	0.046(4)	0.005(4)
C66	0.061(4)	0.048(4)	0.056(3)	0.009(3)	0.033(3)	0.010(3)

# Chapter 6

Conclusion and Outlook

In the preceding work, some topics of organotin chalcogenide chemistry were added to this field regarding the following four aspects: i) the synthesis of new bis[tris(arylchalcogenolato)stannyl]organyls; ii) the potential physical and chemical applications of the newly synthesized bis[tris(arylchalcogenolate)stannyl]organyl compounds; iii) the reactivity of bis(trichlorostannyl)organyls or triorganotin chloride towards coinage metal complexes in the presence of PhSeSiMe$_3$; and iv) the reactivity of bis(trichlorostannyl)organyls towards chalcogenide or/and transition metal complexes under solvothermal condition. This way, the work intended to a) explore whether arylchlcogenolato complexes of bis(trichlorostannyl)organyls are possible precursors for thermolysis for the synthesis of tin chalcogenide materials or serve as donor ligands for linkage of transition metal ions or for the formation of metal chalcogenolate complexes b) explore whether the reactivity of bis(trichlorostannyl)organyls toward chalcogenide or chalcogenolate and transition metals lead to the formation of organo-clad or organo-bridged complexes or clusters.

Bis(trichlorostannyl)organyl compounds (Cl$_3$Sn−R−SnCl$_3$) were reacted with sodium thiophenolate in methanol or with 2-thionaphthol in toluene in the presence of triethylamine as a base to end up with the formation of bis[tris(arylthiolato)stannyl]organyls of the general type [(R'S)$_3$Sn−R−Sn(SR')$_3$] (**1-5**). The selenium analogue of compounds **1-5** were synthesized by reaction of bis(trichlorostannyl)organyl compounds with diaryl diselenide in presence of a reducing agent (NaBH$_4$) in ethanol. These reactions gave rise for the synthesis of compounds **6-11**. All compounds were characterized by means of NMR spectroscopy and X-ray diffraction. According to the orientations of the arylchalcogenolate groups at the tin atoms, they were classified into three different categories, Type I, Type II and Type III. Quantum chemical calculations were undertaken in order to rationalize the experimental observations regarding the different orientations of the arylchalcogenolate groups.

$$Cl_3Sn-R-SnCl_3$$

6 NaSPh   3 Ph_2Se_2 or Np_2Se_2

or 6 NpSH + Et_3N 6 $NaBH_4$

Ph_2Se_2
2 $NaBH_4$

$(R'S)_3Sn-R-Sn(SR')_3$ $Cl_2(PhSe)Sn-R-Sn(SePh)Cl_2$ $(R'Se)_3Sn-R-Sn(SeR')_3$

R = Bu, R' = Ph   **1**   **6**   R = Bu, R' = Ph   **7**

R = 1,4-Dimethylbenzene, R' = Ph   **2**   R = Bu, R' = 1-Naphthyl   **8**

R = 4,4'-Dimethylbiphenyl, R' = Ph   **3**   R = 1,4-Dimethylbenzene, R' = Ph   **9**

R = Bu, R' = 2-Naphthyl   **4**   R = Ferrocene, R' = Ph   **10**

R = 1,4-Dimethylbenzene, R' = 2-Naphthyl   **5**   R = Ferrocene, R' = 1-Naphthyl   **11**
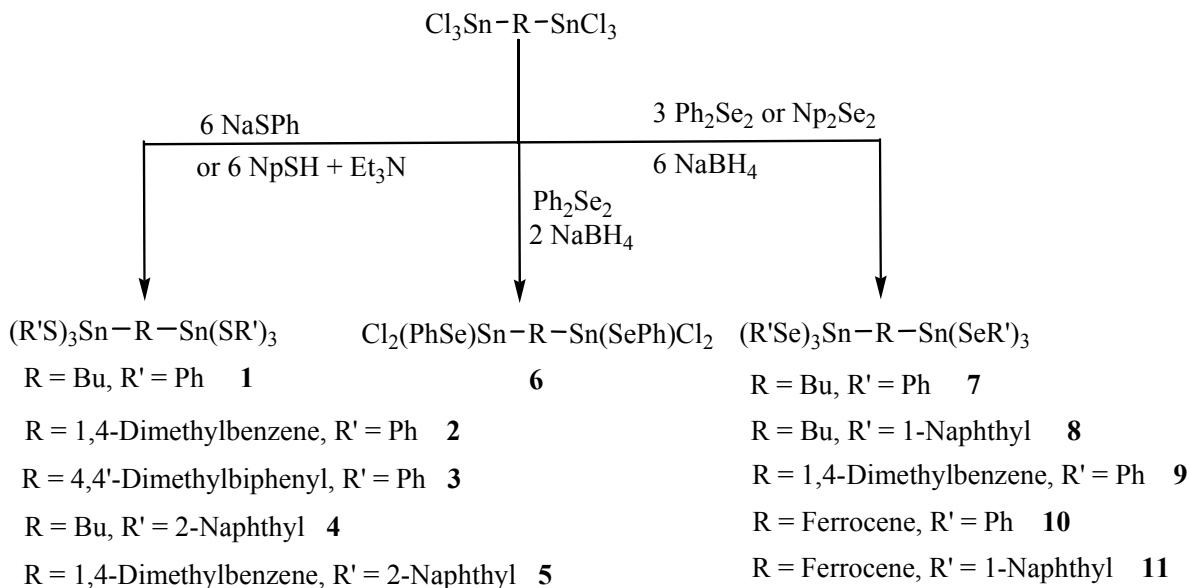
Type I and Type II are the preferable ones, as far as thermodynamic preferences of isolated molecules are considered that seem to be overcompensated by intermolecular interactions in the crystal lattice of one of the compounds (**4**).

In ensuing studies, the bis[tris(arylchalcogenolato)stannyl]organyl compounds prepared as discussed above were used as synthons for the synthesis of tin chalogenide materials or metal-arylchalcogenolato clusters. Thermolysis of $(PhS)_3Sn–Bu–Sn(SPh)_3$ and $(PhSe)_3Sn–Bu–Sn(SePh)_3$ lead to the formation of binary SnS_2 and $SnSe_2$ at 375 and 335 ºC. $(PhSe)_3Sn–Bu–Sn(SePh)_3$ was reacted with palladium acetate in dichloromethane to end up with a tetrameric complex of palladium and selenophenolate, $[Pd(SePh)(OAc)]_4$ (**12**).

$$SnE_2 \ (E = S, Se)$$

TGA

$$(PhE)_3Sn-Bu-Sn(EPh)_3$$

E = Se
+ 2 $Pd(OAc)_2$
in DCM

$$[Pd(SePh)(OAc)]_4 \ \ \mathbf{12}$$
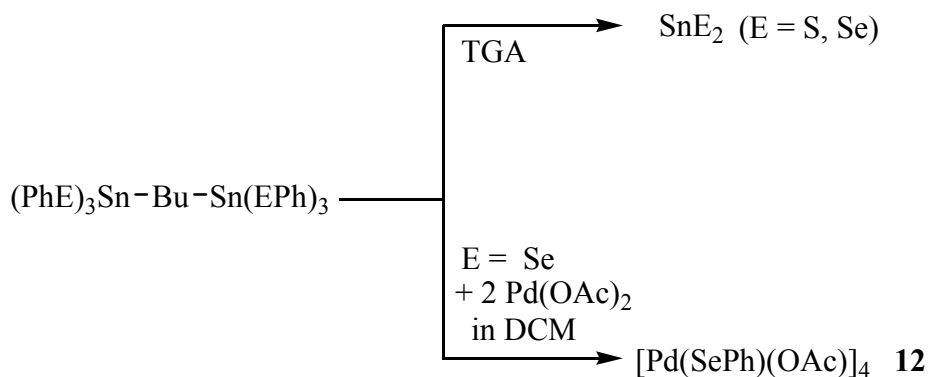
Compound **12** possesses rectangular Pd_4 arrangement. Quantum chemical calculations showed the existence of Pd-Pd interaction and also indicated that the experimentally observed isomer to be the most favorable one out of nine possible conformers. Thermal treatment of compound **12** ends up with a material with nominal composition $Pd_{10}Se_7$.

In order to explore the reactivity, bis(trichlorostannyl)organyl compounds were reacted with $PhSeSiM_3$ and triphenyl phosphine complexes of coinage metals (Cu, Ag). The reaction of bis(trichlorostannyl)organyl with $(PPh_3)_3CuCl$ in THF resulted in the formation of a dimeric copper selenophenolate complex, $[(Ph_3P)_3(SePh)_2Cu_2]\cdot 1.5THF$ (**13**); with $(PPh_3)_3AgNO_3$ a neutral tetradecanuclear silver cluster, $[(Ph_3PAg)_8(SePh)_{12}(\mu_6\text{-}Se)Ag_6]\cdot 6THF$ (**14**) was obtained. In both cases, bis(trichlorostannyl)organyl compounds were not incorporated into the products. The reaction of triphenyltin chloride or tricyclohexyltin chloride instead of bis(trichlorostannyl)organyls with $PhSeSiM_3$ and $(PPh_3)_3AgNO_3$ resulted in an ionic silver selenide cluster, $[(Ph_3PAg)_8(SePh)_{12}(\mu_6\text{-}Se)_{0.5}Ag_6][Ph_3SnCl_2]\cdot 6THF$ (**15**) or $[(Ph_3PAg)_8(SePh)_{12}(\mu_6\text{-}Se)_{0.5}Ag_6][Cy_3SnCl_2]$ (**16**). Here, cationic $Ag_{14}Se_{12.5}$ cluster cores covered by an organic blanket. The pecularty of these latter compounds is the s.o.f. = 0.5 at the central μ_6–Se ligand. Thus, half of the clusters in **15, 16** contain a central Se ligand, whereas the other half exhibits an empty cluster center. The structures of the statistically distributed neutral and +2 charged clusters in **15, 16** are averaged over the crystal. The potentially free site within the 14 silver atoms rationalize the highgrade of disorder of the cluster atoms and correlate with the facts that some coinage metal chalcogenide clusters are able to capture E^{2-} ions.

Since the reactions of bis(trichlorostannyl)organyls in solution do not seem to come along with the formation tin containing compound due to the formation of insoluble, amorphous products beside tin-free compounds, further investigations were performed under solvothermal conditions. An according reaction of bis(trichlorostannyl)butane with elemental sulfur in ethylenediamine under solvothermal condition resulted in the formation of a polymeric compound $^1_\infty[SnS_2\cdot en]$ (**17**), containing a neutral *en* ligated tin sulfide chain with exceptional six-coordination at the Sn atoms. In order to compare the reactivity of the bis(trichlorostannyl)butane precursor with metallic tin, metallic tin and elemental sulfur were reacted under the indentical reaction condition as for the synthesis

of compound **17**. The latter ended up with the formation of a thiostannate salt, [*en*H]$_4$[Sn$_2$S$_6$]·*en* (**18**).

Methanothermal (solvothermal) reaction of bis(trichlorostannyl)butane with Na$_2$S·9H$_2$O and (PPh$_3$)$_3$CuCl finally led to the formation of an organyl-clad Sn/Cu/S cluster, [(Ph$_3$PCu)$_6${*cyclo*-(CH$_2$)$_4$SnS$_2$}$_6$Cu$_4$Sn] (**19**), combining three peculiarities at once: being (a) mixed-metallic, (b) mixed-valent, and (c) walnut-type with a metalloid core, a metal sulfide shell and an organic surface. DFT calculations rationalized the electronic situation and showed that the observed intramolecular cyclization of *n*-butyl groups at the Sn atoms is thermodynamically not favored. Hence, the formation should be driven mainly by the reductive sulfidic conditions that led to the observed formation of elemental sulfur and reduction of Sn^{IV}Cl$_4$ to Sn^{II}Cl$_2$. Future investigations may lead to the generation of ternary mixed valence chalcogenide film by CVD of **19** and the synthesis of further heterometallic compounds of the presented type including further transition metal atoms or organo-bridged clusters using the reductive solvothermal technique.
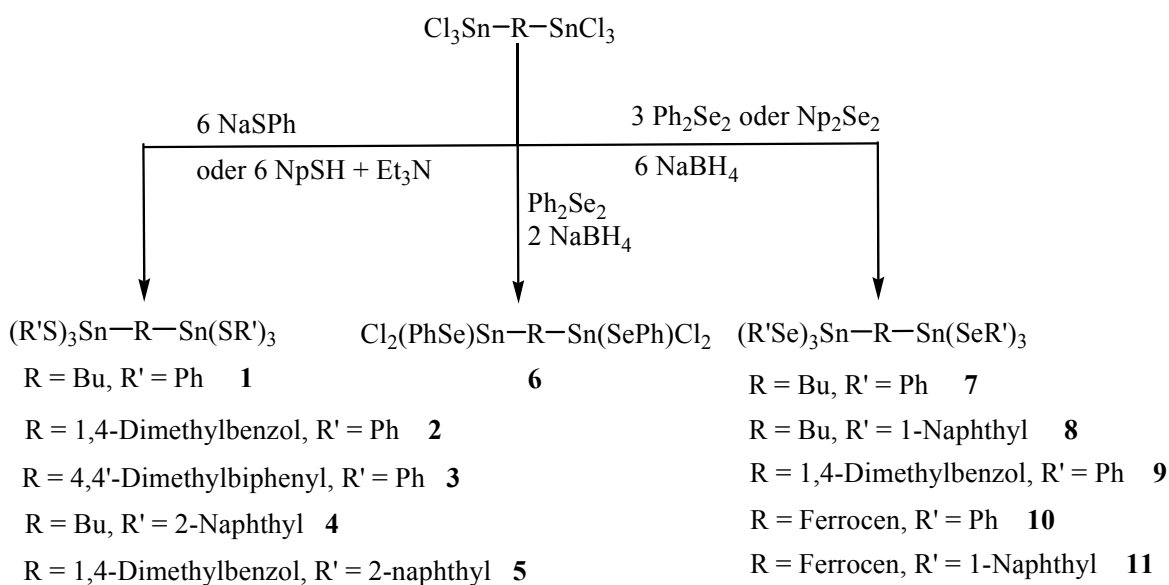
Kapitel 6

Zusammenfassung und Ausblick

Die vorgestellte Arbeit zeigt einige neue Themenfelder auf dem Gebiet der Organozinnchalkogenidchemie auf; dies betrifft folgende Aspekte: i) die Synthese neuer Bis[tris(arylchalkogenato)stannyl]organyle; ii) potentielle physikalische und chemische Anwendungen dieser Verbindungen; iii) die Reaktivität von Bis(trichlorostannyl)-organylen oder Triorganozinnchlorid gegenüber Münzmetallkomplexen in Gegenwart von PhSeSiMe$_3$; und iv) die Reaktivität von Bis(trichlorostannyl)organylen gegenüber Chalkogeniden und/oder Übergangsmetallkomplexen unter solvothermalen Bedingungen.

Es war das Ziel dieser Arbeit a) die Anwendbarkeit von Arylchalkogenolatokomplexen von Bis(trichlorostannyl)organylen als potentielle Prekursoren für die Synthese von Zinnchalkogenidverbindungen mittels thermischer Zersetzung und als Donorliganden für die Verbrückung von Übergangsmetallionen oder für die Bildung von Metallchalkogenolatokomplexen zu untersuchen und b) einen Einblick in die Reaktivität von Bis(trichlorostannyl)organylen gegenüber Chalkogeniden oder Chalkogenolaten und Übergangsmetallen zu erhalten und herauszufinden, ob auf diesem Wege die Synthese von ligandgeschützten oder organoverbrückten Komplexen und Clustern möglich ist.

Bis(trichlorostannyl)organylverbindungen des Typs (Cl$_3$Sn−R−SnCl$_3$) wurden mit Natriumthiophenolat in Methanol oder 2-Thionaphthol in Toluol unter Zusatz von Triethylamin als Base zur Reaktion gebracht. Dies resultierte in der Bildung von Bis[tris(arylthiolato)stannyl]organylen der allgemeinen Form [(R'S)$_3$Sn−R−Sn(SR')$_3$] (**1-5**). Die Selenanaloga der Verbindungen **1-5** wurden über die Reaktion von Bis(trichlorostannyl)organylverbindungen mit Diaryldiselenid in Gegenwart von NaBH$_4$ als Reduktionsmittel dargestellt. Auf diesem Wege konnten Verbindungen **6-11** erhalten werden. Alle Verbindungen wurden mittels NMR-Spektroskopie und Einkristall-strukturanalyse charakterisiert. Anhand der Orientierung der Arylchalkogenolatgruppen am Zinnatom konnten diese Verbindungen in drei verschiedene Kategorien, Typ I, Typ II und Typ III eingeordnet werden. Durch quantenchemische Untersuchungen wurden die experimentellen Befunde hinsichtlich einer unterschiedlichen Orientierung erklärt.

$$Cl_3Sn{-}R{-}SnCl_3$$

6 NaSPh   3 Ph_2Se_2 oder Np_2Se_2

oder 6 NpSH + Et_3N 6 $NaBH_4$

Ph_2Se_2
2 $NaBH_4$

$(R'S)_3Sn{-}R{-}Sn(SR')_3$ $Cl_2(PhSe)Sn{-}R{-}Sn(SePh)Cl_2$ $(R'Se)_3Sn{-}R{-}Sn(SeR')_3$

R = Bu, R' = Ph **1**   **6**   R = Bu, R' = Ph **7**

R = 1,4-Dimethylbenzol, R' = Ph **2**   R = Bu, R' = 1-Naphthyl **8**

R = 4,4'-Dimethylbiphenyl, R' = Ph **3**   R = 1,4-Dimethylbenzol, R' = Ph **9**

R = Bu, R' = 2-Naphthyl **4**   R = Ferrocen, R' = Ph **10**

R = 1,4-Dimethylbenzol, R' = 2-naphthyl **5**   R = Ferrocen, R' = 1-Naphthyl **11**

Typ I und Typ II sind, für ein einzelnes Molekül betrachtet, die thermodynamisch bevorzugten Konformationen. In Verbindung **4** wird dies durch intermolekulare Wechselwirkungen im Kristallgitter überkompensiert.

In nachfolgenden Studien wurden die oben diskutierten Bis[tris(arylchalkogenolato)stannyl]organylverbindungen als Synthon für die Synthese von Zinnchalkogenidmaterialien oder Metallarylchalkogenolatoclustern verwendet. Die thermische Behandlung von $(PhS)_3Sn{-}Bu{-}Sn(SPh)_3$ und $(PhSe)_3Sn{-}Bu{-}Sn(SePh)_3$ führt zur Bildung von binärem SnS_2 und $SnSe_2$ bei 375 °C respektive 335 °C. Bei der Umsetzung von $(PhSe)_3Sn{-}Bu{-}Sn(SePh)_3$ mit Palladium(II)acetat in Dichlormethan erhält man einen tetrameren Komplex aus Palladium und Selenophenolat, $[Pd(SePh)(OAc)]_4$ (**12**).

TGA → SnE_2 (E = S, Se)

$(PhE)_3Sn{-}Bu{-}Sn(EPh)_3$ ⟶

E = Se
+ 2 $Pd(OAc)_2$
in DCM

→ $[Pd(SePh)(OAc)]_4$ **12**
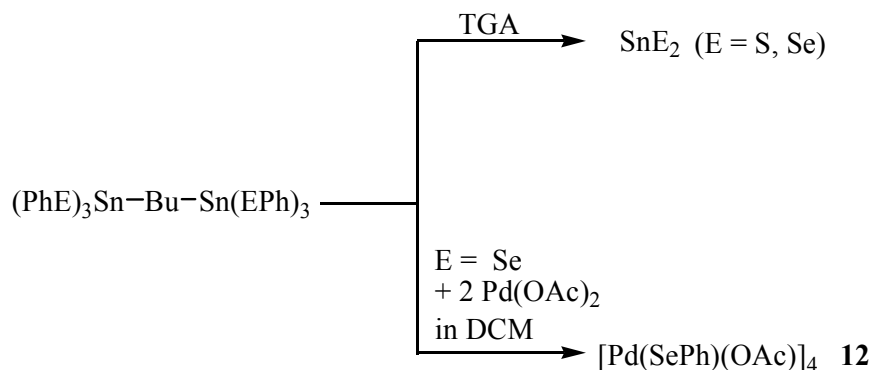
Verbindung **12** zeigt eine rechteckige Pd_4 Anordnung. Quantenchemische Untersuchungen belegen die Existenz einer Pd-Pd Wechselwirkung und weisen das experimentell beobachtbare Isomer als das thermodynamisch günstigste unter neun möglichen Konformeren aus. Die thermische Zersetzung von Verbindung **12** führt zu einem Material der nominellen Zusammensetzung $Pd_{10}Se_7$.

Um einen Einblick in ihre Reaktivität zu erhalten, wurden Bis(trichlorostannyl)organylverbindungen mit $PhSeSiMe_3$ und Triphenylphosphinkomplexen von Münzmetallen (Cu, Ag) zur Reaktion gebracht. Durch Reaktion von Bis(trichlorostannyl)organylen mit $(PPh_3)_3CuCl$ in THF gelingt die Darstellung eines dimeren Kupferselenolatkomplexes, $[(Ph_3P)_3(SePh)_2Cu_2]\cdot THF$ (**13**); mit $(PPh_3)_3AgNO_3$ erhält man einen neutralen tetradecanuklearen Silbercluster, $[(Ph_3PAg)_8(SePh)_{12}(\mu_6\text{-}Se)Ag_6]\cdot 6THF$ (**14**). In beiden Fällen sind die Bis(trichlorostannyl)organylverbindungen kein Bestandteil der isolierten Produkte. Die Reaktion von Triphenylzinnchlorid oder Tricyclohexylzinnchlorid mit $PhSeSiMe_3$ und $(PPh_3)_3AgNO_3$ resultiert in einem ionischen Silberselenidcluster, $[(Ph_3PAg)_8(SePh)_{12}(\mu_6\text{-}Se)_{0.5}Ag_6][Ph_3SnCl_2]\cdot 6THF$ (**15**) or $[(Ph_3PAg)_8(SePh)_{12}(\mu_6\text{-}Se)_{0.5}Ag_6][Cy_3SnCl_2]$ (**16**). In diesen Verbindungen tragen die $Ag_{14}Se_{12.5}$ Clusterkerne eine organische Hülle. Eine Besonderheit zeigt sich in einem s.o.f. von 0.5 am zentralen μ_6-Se-Liganden. Dies bedeutet, dass die Hälfte aller Cluster in **15** und **16** einen zentralen Se-Liganden tragen, während die andere Hälfte ein leeres Zentrum besitzt. Die neutralen und mit +2 geladenen Cluster in **15** und **16** sind statistisch innerhalb der Kristallstruktur verteilt. Diese potentiell unbesetzten Positionen innerhalb des Käfigs aus vierzehn Silberatomen erklären den Befund einer hochgradigen Fehlordnung der Clusteratome und korrelieren mit der Tatsache, dass manche Münzmetallchalkogenidcluster E^{2-}-Ionen einfangen können.

Da Reaktionen von Bis(trichlorostannyl)organylen in Lösung aufgrund der Bildung unlöslicher, amorpher Niederschläge und zinnfreier Reaktionsprodukte nicht zu den den angestrebten komplexen Organozinnverbindungen führten, wurden weitere Reaktionen unter solvothermalen Bedingungen durchgeführt. Durch die Reaktion von Bis(trichlorostannyl)butan mit elementarem Schwefel in Ethylendiamin unter

solvothermalen Bedingungen lässt sich die polymere Verbindung $\frac{1}{\infty}$[SnS$_2$·*en*] (**17**) darstellen, welche eine neutrale, *en*-koordinierte Zinnsulfidkette mit einer außergewöhnlichen sechsfachen Koordination am Zinn enthält. Um einen Vergleich der Reaktivitäten von Bis(trichlorostannyl)butan und metallischem Zinn zu erhalten, wurde die Reaktion ausgehend von den Elementen unter identischen Reaktionsbedingungen wie für **17** durchgeführt. Das Reaktionsprodukt war in diesem Fall das Thiostannatsalz [*en*H]$_4$[Sn$_2$S$_6$]·*en* (**18**).

Schließlich führte die solvothermale Umsetzung von Bis(trichlorostannyl)butan mit Na$_2$S·9H$_2$O und (PPh$_3$)$_3$CuCl in Methanol zur Bildung eines organisch umhüllten Sn/Cu/S-Clusters, [(Ph$_3$PCu)$_6${*cyclo*-(CH$_2$)$_4$SnS$_2$}$_6$Cu$_4$Sn] (**19**), welcher drei Besonderheiten in sich vereint: er ist a) heterometallisch b) gemischtvalent und c) zwiebelartig aufgebaut, mit einem metalloiden Kern, einer Metallsulfidschale und einer organischen Hülle. DFT-Rechnungen halfen bei der Erklärung der elektronischen Situation und zeigen, dass die beobachtete intramolekulare Zyklisierung der *n*-Butylgruppen am Zinnatom thermodynamisch nicht begünstigt ist. Dies lässt darauf schließen, dass die Triebkraft der Bildung von Verbindung **19** in den reduktiven, sulfidischen Reaktionsbedingungen liegt, die zu der beobachteten Bildung von elementarem Schwefel und der Reduktion von Sn^{IV}Cl$_4$ zu Sn^{II}Cl$_2$ führten.

Gegenstand zukünftiger Untersuchungen kann die gezielte Herstellung ternärer, gemischtvalenter Chalkogenidfilme mittels CVD von **19** und die Synthese weiterer heterometallischer Verbindungen des vorgestellten Typs mit weiteren Übergangsmetallatomen oder organoverbrückten Clustern durch Anwendung der reduktiven Solvothermaltechnik sein.

7 Appendices

A.1 Directory of abbreviations

A.1.1 General

Ar	Aryl group	
Me	Methyl	$-CH_3$
n-Bu	n-Butyl	$-CH_2CH_2CH_2CH_3$
Et	Ethyl	$-CH_2CH_3$
Cp	Cyclopentadienyl	$\eta_5\text{-}C_5H_5$
Cy	Cyclohexyl	$-C_6H_{11}$
Ph	Phenyl	$-C_6H_5$
Np	Naphthyl	$-C_{10}H_7$
Fc	Ferrocene	$Fe(C_5H_5)_2$
THF	Tetrahydrofuran	C_4H_8O
DCM	Dichloromethane	CH_2Cl_2
DMF	Dimethylformamide	$(CH_3)_2NCHO$
DMSO	Dimethyl sulfoxide	$(CH_3)_2SO$
en	Ethylenediamine	$H_2NCH_2CH_2NH_2$
TMEDA	Tetramethylethylenediamine	$Me_2NCH_2CH_2NMe_2$
R	Organic group	
X	Halogen/halide	
M	Metal atom	
HOMO	Highest occupied molecular orbital	
LUMO	Lowest unoccupied molecular orbital	
NMR	Nuclear magnetic resonance	

EI-MS	Electron-ionization mass spectrometry
IR	Infrared

A.1.2 NMR Abbreviations

δ	Chemical shift
ppm	Parts per million
s	singlet
d	doublet
t	triplet
m	multiplet

A.1.3 IR Abbreviations

br	broad
w	weak
m	medium
s	strong
vs	very strong
sh	shoulder

A.2 Directory of Compounds

1	$(PhS)_3Sn–(CH_2)_4–Sn(SPh)_3$
2	$(PhS)_3Sn– CH_2–C_6H_4–CH_2–Sn(SPh)_3$
3	$(PhS)_3Sn– CH_2–(C_6H_4)_2–CH_2–Sn(SPh)_3$
4	$(NpS)_3Sn–(CH_2)_4–Sn(SNp)_3$
5	$(NpS)_3Sn– CH_2–C_6H_4–CH_2 –Sn(SNp)_3$
6	$PhSeCl_2Sn–(CH_2)_4–SnCl_2SePh$
7	$(PhSe)_3Sn–(CH_2)_4–Sn(SePh)_3$
8	$(NpSe-1)_3Sn–(CH_2)_4–Sn(1-SeNp)_3$
9	$(PhSe)_3Sn– CH_2–C_6H_4–CH_2–Sn(SePh)_3$
10	$(PhSe)_3Sn– C_5H_4–Fe–C_5H_4–Sn(SePh)_3$
11	$(NpSe)_3Sn– C_5H_4–Fe–C_5H_4–Sn(SeNp)_3$
12	$[Pd(SePh)(OOCCH_3)]_4$
13	$[(Ph_3P)_3(SePh)_2Cu_2]·1.5THF$
14	$[(Ph_3PAg)_8(SePh)_{12}(\mu_6\text{-}Se)Ag_6]·6THF$
15	$[(Ph_3PAg)_8(SePh)_{12}(\mu_6\text{-}Se)_{0.5}Ag_6][Ph_3SnCl_2]·6THF$
16	$[(Ph_3PAg)_8(SePh)_{12}(\mu_6\text{-}Se)_{0.5}Ag_6][Cy_3SnCl_2]$
17	$^1_\infty [SnS_2·en]$
18	$[enH]_4[Sn_2S_6]·en$
19	$[(Ph_3PCu^I)_6\{(CH_2)Sn^{IV}S_2\}_6Cu^I_4Sn^{II}]$

A.3 Literature Cited

[1]   M. Gielen, A. G. Davies, K. Pannell, E. Tiekink, *Tin Chemistry: Fundamentals, Frontiers and Applications* **2008**.

[2]   Carlin, Jr., James F. *"Mineral Commodity Summary* **2008***: Tin", United States Geological.*

[3]   *"Advanced Inorganic Chemistry" 4*[th] *Ed. Cotton & Wilkinson.*

[4]   *http://sn-tin.info/isotopes.html*

[5]   C. L. Bowes, G. A. Ozin, *Adv. Mater.* **1996**, 8, 13.

[6]   J. Llanos, C. Mujica, V. S_anchez, O. Pena, *J. Solid State Chem.* **2003**, 173, 78.

[7]   C. R. Evenson IV, P. K. Dorhout, *Z. Anorg. Allg. Chem.* **2001**, 627, 2178.

[8]   U. Simon, F. Schueth, S. Schunk, X. Wang, F. Liebau, *Angew. Chem. Int. Ed. Eng.* **1997**, 36, 1121.

[9]   R. L. Glitzendanner, F. L. Di Salvo, *Inorg. Chem.* **1996**, 35, 2623.

[10]   R. R. Chianelli, T. A. Pecoraro, T. R. Halber, W. H. Pan, E. I. Stiefel, *J. Catal.* **1984**, 86, 226.

[11]   J. B. Parise, Y. Ko, J. Rijssenbeek, D. M. Nellis, K. Tan, S. Koch, *J. Chem. Soc. Chem. Commun.* **1994**, 527.

[12]   S. Dehnen, M. Melullis, *Coordination Chemistry Reviews*, **2007**, 251, 1259–1280.

[13]   B. Krebs, *Angew. Chem. Int. Edit.* **1983**, 22, 113-134.

[14]   C. Zimmermann, S. Dehnen, *Z. Allg. Anorg. Chem.* **1999**, 625, 1963.

[15]   S. Dehnen, C. Zimmermann, C. E. Anson, *Z. Anorg. Allg. Chem.* **2002**, 628, 279.

[16]   S. Dehnen, C. Zimmermann, *Z. Anorg. Allg. Chem.* **2002**, 628, 2463.

[17]   J. B. Parise, Y. Ko, J. Rijssenbeek, D. M. Nellis, K. Tan, S. Koch, *J. Chem. Soc. Chem. Commun.* **1994**, 527.

[18]   J. Li, H. Kessler, *Micropor. Mesopor. Mater*. **1999**, 27, 57.

[19]   T. Jiang, A. Lough, G.A. Ozin, *Adv. Mater.* **1998**, 10, 42.

[20]   H. Ahari, O. Dag, S. Petrov, G. A. Ozin, *J. Phys. Chem. B*, **1998**, 102, 2356.

[21]   Y. Ko, K. Tan, D. M. Nellis, S. Koch, J.B. Parise, *J.* Solid State Chem. **1995**, 114, 506.

[22]   G. A. Marking, M. Evain, V. Petricek, M. G. Kanatzidis, *J. Solid State Chem.* **1998**, 141, 17.

[23]   J. Liao, C. Varotsis, M. G. Kanatzidis, *Inorg. Chem.* **1993**, 32, 2453.

[24]   Y. Ko, K. Tan, D. M. Nellis, S. Koch, J. B. Parise, *J. Solid State Chem.* **1995**, 114, 506.

[25]   G. A. Marking, M. Evain, V. Petricek, M. G. Kanatzidis, *J. Solid State Chem.* **1998**, 141, 17.

[26]   D. Jia, J. Dai, Q. Zhu, Y. Zhang, X. Gu, *Polyhedron*, **2004**, 23, 937–942.

[27]   T. Jiang, A. Lough, G. A. Ozin, R. L. Bedard, R. Broach, *J. Mater. Chem.,* **1998**, *8*, 721.

[28]   T. Jiang, A. Lough, G. A. Ozin, R.L. Bedard, *J. Mater. Chem*. **1998**, *8*, 733.

[29]   W. S. Sheldrick, H. G. Braunbeck *Z. Anorg. Allg. Chem.* **1993**, *619*, 1300.

[30]   M.K. Brandmayer, R. Clerac, F. Weigend, S. Dehnen, *Chem. Eur. J*. **2004**, 10, 147.

[31]   E. Ruzin, A. Fuchs, S. Dehnen, *Chem. Commun.* **2006**, doi:10.1039/B610833D.

[32]   C. Zimmermann, C.E. Anson, F. Weigend, R. Clerac, S. Dehnen, *Inorg. Chem.* **2005**, 44, 5686.

[33]   S. Bag, P. N. Trikalitis, P. J. Chupas, G. S. Armatas, M. G. Kanatzidis, *Science*, **2007**, 317, 490-493.

[34]   K. Tsamourtzi, J. Song, T. Bakas, A. J. Freeman, P. N. Trikalitis, M. G. Kanatzidis, *Inorg. Chem.* **2008**, 47, 11920-11929.

[35]   S. Haddadpour, M. Melullis, H. Staesche, C. R. Mariappan, B. Roling, R.
         Clerac, S. Dehnen, *Inorg. Chem.* **2009**, 48, 1689-1698.

[36]   C. Lowich, Liebigs *Ann. Chem.* **1852**, 84, 308.

[37]   E. Frankland, Liebigs *Ann. Chem.* **1849**, 71, 171.

[38]   Editorial, *J. Orgmetall. Chem.* **2006**, 691, 1435-1436.

[39]   S. H. L. Thoonen, B. Deelman, G. Koten, *J. Orgnometal. Chem.* **2004**, 689,
         2145-2157.

[40]   M. Gingras, T. H. Chan, D. N. Harpp, *J. Org. Chem. Vol.* **1990**, 55, 2079.

[41]   O. R. Flöck, M. Dräger, *Organometallics*, **1993**, 12, 4623-4632.

[42]   D. Dakternieks, K. Jurkschat, H. Wu, *Organometallics*, **1993**,12, 2788-2793.

[43]   U. Herzog, U. Böhme, E. Brendler, G. Rheinwald, *J. Organometal. Chem.* **2001**,
         630, 139–148.

[44]   C. Dorfelt, A. Janeck, D. Kobelt, E. F. Paulus, H. Scherer, *J. Organometal.
         Chem.* **1968**, 14, P22-P24.

[45]   H. Schumann, M. Schmidt, *Angew. Chem. Int. Ed.* **1965**, 4, 1007-1013.

[46]   Z. Hassanzadeh Fard, C. Müller, T. Harmening, R. Pöttgen, S. Dehnen, *Angew.
         Chem.* **2009**, *Angew. Chem. Int. Ed.*, **2009**, DOI: 10.1002/anie.200805719.

[47]   Z. Hassanzadeh Fard, L. Xiong, C. Müller, M. Holynska, S. Dehnen, *Chem. Eur.
         J.* **2009** (VIP), *in the print*.

[48]   R. Hauser, K. Merzweiler, *Z. Anorg. Allg. Chem.* **2002**, *628*, 905-906.

[49]   T. Matsumoto, Y. Matsui, M. Ito, K. Tatsumi, *Chem. Asian J.* **2008**, 3, 607–
         613.

[50]   T. Matsumoto, Y. Matsui, M. Ito, K. Tatsumi, *Inorg. Chem.* **2008**, 47, 1901–
         1903.

[51]   L. Wang, T. Sheng, X. Wang, D. Chen, S. Hu, R. Fu, S. Xiang, X. Wu, *Inorg.
         Chem.* **2008**, 47, 4054–4059.

[52]   X. Wang, T. Sheng, R. Fu, S. Hu, S. Xiang, L. Wang, X. Wu, *Inorg. Chem.* **2006**, 45, 5236–5238.

[53]   T. Matsumoto, Y. Nakaya, K. Tatsumi, *Angew. Chem. Int. Ed.* **2008**, 47, 1913–1915.

[54]   Y. Ohki, M. Sakamoto, K. Tatsumi, *J. Am. Chem. Soc.* **2008**, *130*, 11610–11611.

[55]   T. Matsumoto, Y. Nakaya, N. Itakura, K. Tatsumi, *J. Am. Chem. Soc.* **2008**, *130*, 2458–2459.

[56]   B. Zobel, A. Duthie, D. Dakternieks, *Organometallics*, **2001**, *20,* 2820-2826.

[57]   B. Jousseaume, H. Riague, T. Toupance, *Organometallics* **2002**, *21*, 4590-4594.

[58]   B. Jousseaume, H. Riague, T. Toupance, H. Allouchi, *Organometallics* **2007**, *26*, 3908-3917.

[59]   M. Herberhold, W. Milius, U. Steffl, K. Vitzithum, B. Wrackmeyer, R. H. Herber,   M. Fontani, P. Zanello, *Eur. J. Inorg. Chem.* **1999**, 145-151.

[60]   R. Kumar, H. E. Mabrouk, D. G. Tuck, *J. Chem. Soc. Dalton Trans.* **1988**, 1445-1446.

[61]   R. C. Mehrotra, V. D. Gupta, D. Sukhani, *J. Inorg. Nucl. Chem.* **1967**, 29, 1577-1580.

[62]   K. C. Kumara Swamy, R. O. Day, R. R. Holmes, *J. Am. Chem. Soc.* **1988**, 110, 7543-7544.

[63]   Kalsoom, M. Mazhar, S. Ali, M. F. Mahon, K. C. Molloy, M. I. Chaudry, *Appl. Organomet. Chem.* **1997**, 11, 47-55.

[64]   D. Dakternieks, K. Jurkschat, H. Wu, E. R. T. Tiekink, *Organometallics*, **1993**, 12*, 2788-2793.*

[65]   M. Gielen, K. Jurkschat, *J. Organomet. Chem.* **1984**, 273, 303-312.

[66]   D. Dakternieks, K. Jurkschat, D. Schollmeyer, H. Wu. *Organometallics* **1994**, 13, 4121-4123.

[67]   Dakternieks, K. Jurkschat, D. Schollmeyer, H. Wu*., J .Organomet. Chem.* **1995***, 492, 145-250.

[68]   Y. Azuma, M. Newcomb, *Organometallics* **1984**, 3, 9-14.

[69]   N. Belai, M. T. Pope, *Polyhedron* **2006**, 25, 2015-2020.

[70]   R. Hauser, K. Merzweiler, *Z. Anorg. Allg. Chem.* **2002**, 628, 905-906.

[71]   J. Otera, T. Mizutani, H. Nozaki, *Organometallics* **1989**, 8, 2063-2065.

[72]   G. Barone, T. G. Hibbert, M. F. Mahon, K. C. Molloy, L. S. Price, I. P. Parkin, A. M. E. Hardy, M. N. Field, *J. Mater. Chem.* **2001**, *11*, 464-468.

[73]   G. Barone,T. Chaplin, T. G. Hibbert, A. T. Kana, M. F. Mahon, K. C. Molloy, I. D. Worseley, I. P. Parkin, L. S. Price, *J. Chem. Soc., Dalton Trans.* **2002**, 1085-1092.

[74]   T. Sato, J. Otera, H. Nozaki, *Tetrahedron*, **1989**, *45* (4), 1209-1218.

[75]   R. G. Parr, W. Yang, *Density Functional Theory of Atoms and Molecules*, Oxford University Press, New York 1988; b) T. Ziegler, *Chem. Rev.* **1991**, *91*, 651–667.

[76]   K. Eichkorn, O. Treutler, H. Öhm, M. Häser, R. Ahlrichs, *Chem. Phys. Lett.* **1995**, *242*, 652–660.

[77]   K. Eichkorn, F. Weigend, O. Treutler, R. Ahlrichs, *Theor. Chem. Acc.* **1997**, *97*, 119–124.

[78]   A. I. Stash, T. I. Perepelkova, Y. G. Noskov, T. M. Buslaeva, I. P. Romm, *Russ. J. Coord. Chem.* **2001**, 27, 585-590.

[79]   A.C. Albniz, P. Espinet, Y.-S. Lin, A.G. Orpen, A. Martn, *Organometallics*, **1996**, 15, 5003-5009.

[80]   T. Murahashi, H. Kurosawa, *Coord. Chem. Rev.*, **2002**, 231, 207-228.

[81]   S. Dey, V.K. Jain, A. Knoedler, A. Klein, W. Kaim, S. Zalis, *Inorg. Chem.*, **2002**, 41, 2864-2870.

[82]   S. Jing, C. P. Morley, C.A. Webster, M.D. Vaira, *Dalton Trans.*, **2006**, 4335–4342.

[83]   S. Dey, V.K. Jain, B. Varghese, T. Schurr, M. Niemeyer, W. Kaim, R.J. Butcher, *Inorg. Chim. Acta*, **2006**, 359, 1449-1457.

[84]   S. Dey, V.K. Jain, S. Chaudhury, A. Knoedler, F. Lissner, W. Kaim. *J. Chem. Soc., Dalton Trans.*, **2001**, 5, 723-728.

[85]   L.B. Kumbhare, V.K. Jain, B. Varghese, *Inorg. Chim. Acta*, **2006**, 359, 409-416.

[86]   R. H. Crabtree, *The Organometallic Chemistry of the Transition Metals*, 4th ed., **2005**, Wiley-VCH, 119.

[87]   S. Dehnen, D. Fenske, *Chem. Eur. J.* **1996***, 2, 1407-1416.

[88]   S. Dehnen, D. Fenske, *Angew. Chem. Int. Ed. Engl.* **1994**, 33, 2287-2289.

[89]   T. Langetepe, D. Fenske, *Angew. Chem. Int. Ed. Engl.* **2002**, 41, 300-303.

[90]   C. Nitschke, A. I. Wallbank, D. Fenske, J. F. Corrigan, *J. Clus.Sci.* **2007**, 18, 131-141

[91]   J. Kampf, R. Kumar, J. P. Oliver, *Inorg. Chem.* **1992**, 31, 3626-3629.

[92]   A. Bondi, *J. Phys. Chem.* **1964**, 68, 441.

[93]   D. F. Lewis, S. J. Lippard, P. S. Welcker, *J. Am. Chem.* Soc. **1970**, 92, 3805.

[94]   I. G. Dance, P. J. Guerney, A. D. Rae, M. L. Scudder, *Inorg. Chem.* **1983,** 22, 2883.

[95]   J. Cusick, M. L. Scudder, D. C. Craig, I. G. Dance, *Polyhedron*, **1989**, 8, 1139.

[96]   U. Müller, M. L. Ha-Eierdanz, G . Kräuter, K. D ehnicke, Z. *Nufurforsch.* **1990**, 458, 1128.

[97]   M. Kubicki, S. K. Hadjikakou, M. N. Xanthopoulou, *Polyhedron*, **2001**, 20, 2179.

[98]   J. Chen, Q. Xu, Y. Zhang, Z. Chen, J. Lang, *J. Organomet. Chem.* **2004**, 689, 1071-1077.

[99]   J. Zhou, J. Dai, G. Bian, C. Li, *Coord. Chem. Rev.* **2008** doi:10.1016/j.ccr.2008.08.015.

[100]   W. S. Sheldrick, H. G. Braunbeck *Z. Anorg. Allg. Chem.* **1993**, *619*, 1300

[101]   S. Dehnen, C. Zimmermann, *Z. Anorg. Allg. Chem.* **2002**, 628, 2463.

[102]   a) K. Eichkorn, O. Treutler, H. Öhm, M. Häser, R. Ahlrichs, *Chem. Phys. Lett.* **1995**, *242*, 652–660; b) K. Eichkorn, F. Weigend, O. Treutler, R. Ahlrichs, *Theor. Chem. Acc.* **1997**, *97*, 119–124.

[103]   a) A.D. Becke, *Phys. Rev. A* **1988**, *38*, 3098-3109; b) S.H. Vosko, L. Wilk, M. Nusair, *Can. J. Phys.* **1980**, *58*, 1200–1205; c) J.B. Perdew, *Phys. Rev. B* **1986**, *33*, 8822–8837.

[104]   a) F. Weigend, R. Ahlrichs, *Phys. Chem. Chem. Phys.* **2005**, *7*, 3297-3305; b) F. Weigend, *Phys. Chem. Chem. Phys.* **2006**, *8*, 1057-1065.

[105]   B. Metz, H. Stoll, M. Dolg, *J. Chem. Phys.* **2000**, *113*, 2563-2569.

[106]   A. E. Reed, R. B. Weinstock, F. Weinhold. *J. Chem. Phys.* **1985**, *83*, 735–746.

[107]   R.S. Mulliken, *J. Chem. Phys.* **1955**, *23*, 1833-1840.

[108]   Y. Azuma, M. Newcomb, *Organometallics*, **1984**, *3*, 9-14.

[109]   J. A. Fernandes, S. Lima, S. S. Braga, P. Ribeiro-Claro, J. E. Rodriguez-Borges, C. Teixeira, M. Pillinger, J. J. C. Teixeira-Dias, I. S. Goncalves, *J. Organomet. Chem.* **2005**, 690, 4801-4808.

[110]   N. Lenze, B. Neumann, A. Salmon, A. Stammler, H. Stammler, P. Jutzi, *J. Organomet. Chem.* **2001**, 619, 74-87.

[111]   J. V. Verma, S. E. Boyd, P. C. Healy, G. A. Bowmaker, B. W. Skelton, A. H. White, *Dalton Trans.* **2005**, 2547-2556.

[112]   P. F. Barron, J. C. Dyason, P. C. Healy, L. M. Engelhardt, B. W. Skelton, A. H. White, *Dalton Trans.* **1986**, 1965-1970.

[113]   Sheldrick, G.M. *SHELXS97, program for the solution of crystal structures*, University of Göttingen, **1997**.

[114]   Sheldrick, G.M. *SHELXL97, program for refinement of crystal structures*, University of Göttingen, **1997**.

Curriculum Vitae

Name	Mr. Hari Pada Nayek
Date of Birth	May 1st, 1983
Place of Birth	Howrah, West Bengal, India
Sex	Male
Marital Status	Single
Nationality	Indian

Education

Ph.D. in Chemistry:	(2006-present): Department of Chemistry, Philipps Universität Marburg, Germany.
Thesis Supervisor:	Prof. Dr. Stefanie Dehnen
Thesis Title:	Investigations of the Reactivity of Bis(trichlorostannyl)organyl Compounds
Master of Science:	(2004-2006) Department of chemistry, Indian Insitute of Technology Kanpur, India.
Thesis Supervisor:	Prof. Dr. Jitendra K. Bera
Thesis Title:	Study of Charge Transfer Complex using Tetrazine as Potential Electron Acceptor and Different Inorganic Metal Complex as Electron Donor
Bachelor of Science:	(2001-2004) Chemistry (Honors), University of Calcutta, Kolkata, India.

Publications

1.   A Heterometallic, Heterovalent $Cu^I/Sn^{II/IV}/S$ Cluster with an Unprecedented Cu_4Sn Core and Stannacyclopentane Units

H. P. Nayek, W. Massa, S. Dehnen, *Inorg. Chem.* **2008**, *47* (20), 9146-9148.

2.   Preparation and Conformation of Organo-Bridged Bis[tris(arylchalcogenolato)tin] Compounds: An Experimental and Quantum Chemical Study

H. P. Nayek, H. Niedermeyer, S. Dehnen, *Z. Anorg. Allg. Chem.* **2008**, *634*, 2805-2810.

3.   Transformation of a Layered Zinc Phosphite to a Three-Dimensional Open-Framework Structure with Intersecting 16- and 12-Ring Channels

Z. Lin, H. P. Nayek, S. Dehnen, *Inorg. Chem.* **2009**, *48* (8), 3517-3519.

4.   Synthesis and Structure of a Tetranuclear Palladium Chalcogenolate Acetate Complex $[Pd_4(SePh)_4(OOCCH_3)_4]$: An Experimental and Theoretical Study

H. P. Nayek, H. Niedermeyer, S. Dehnen, *Dalton Trans.* **2009**, *21*, 4208-4212.

5.   A Cubic Coordination Framework Constructed from Benzobistriazole Ligands and Zinc Ions Having Selective Gas Sorption Properties

S. Biswas, M. Grzywa, H. P. Nayek, S. Dehnen, D. Volkmer, *Dalton Trans.* **2009**, DOI: 10.1039/ b904280f. (Cover page).

6.   Synthesis, Crystal Structures and Properties of $[SnS_2.en]_\infty$ and $[enH]_4[Sn_2S_6].en$

H. P. Nayek, Z. Lin, S. Dehnen, *Z. Anorg. Allg. Chem.* **2009**, *in the print*.

7.   Flux synthesis of three-dimensional open-framework zinc phosphite and manganese phosphite-oxalate with 12-ring channels

Z. Lin, H. P. Nayek, S. Dehnen, *Microporous and Mesoporous Materials,* **2009**, *10.1016/j.micromeso.2009.05.025*

8.   Structural Transformation of Three-Dimensional Bimetallic Phosphites Containing Corner-Sharing 4-Ring Chains

Z. Lin, H. P. Nayek, S. Dehnen, *submitted*

9. Presence or Absence of a Central Se Atom in Silverselenide Clusters with Halite-Topology: Synthesis and Properties of $[(Ph_3PAg)_8Ag_6(\mu_6{-}Se)_{1-x/2}(SePh)_{12}]^{x+}$ (x = 0, 1; R = Ph, Cy)

H. P. Nayek, S. Dehnen, *in preparation*

10. Synthesis and Characterization of Ferrocene-Bridged bis[tris(arylselenolato) stannyl] Compounds

H. P. Nayek, S. Dehnen, *in preparation*